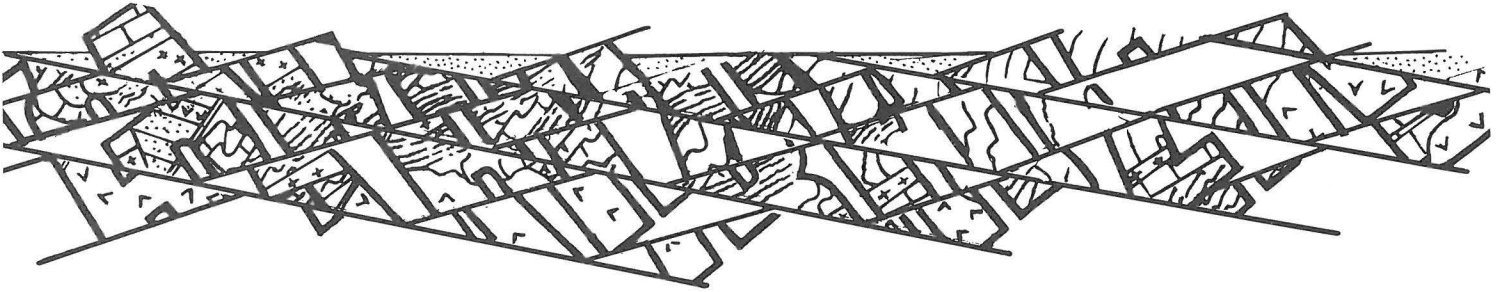


WESTERN



Paleoecology and Taphonomy of Recent to Pleistocene Intertidal Deposits, Gulf of California

Karl W. Flessa
Department of Geosciences
University of Arizona
Tucson, Arizona 85721

A. A. Ekdale
Department of Geology and Geophysics
University of Utah
Salt Lake City, Utah 84112

INTRODUCTION

The purpose of this field trip is to examine sedimentary environments, fauna, and Pleistocene deposits in the northeastern Gulf of California. The coastal area experiences tides of up to 8 meters in amplitude, the Gulf harbors a rich invertebrate fauna, especially molluscs, crustaceans, and echinoderms, and the arid climate of the region makes for a distinctive sedimentary regime. Adjacent fossiliferous Pleistocene deposits provide a glimpse into both ancient habitats and taphonomic processes. In short, the area is an excellent natural laboratory -- a laboratory for the study of Recent animal-sediment relations, sedimentary processes, and taphonomy.

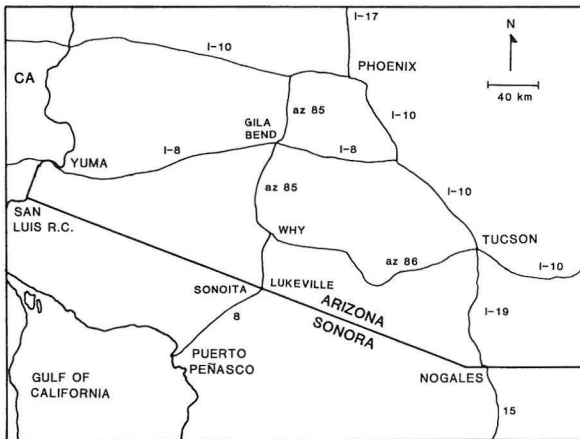


Figure 1. Major highways and towns in the vicinity of field-trip route.

From Phoenix, we will travel west along Interstate 10 to Buckeye, then south past the Palo Verde nuclear power plant, on Arizona Highway 85 past the towns of Gila Bend, Ajo (a declining copper-mining and smelter town), and Why to the U.S. border town of Lukeville (sometimes called Gringo Pass). From Why to Lukeville, the highway passes through Organ Pipe Cactus National Monument. We will stop in Lukeville for fuel and then cross the border into Sonoita, Sonora, Mexico (Figure 1).

From Sonoita to Puerto Peñasco, Mexican Highway 8 passes to the south of the Pinacates, an extensive complex of Plio-Pleistocene volcanoes. Puerto Peñasco is 100 km from the U.S. border.

For a resume of the geology along the way, see Halka Chronic's (1983) Roadside Geology of Arizona.

Crossing the Border

Non-Mexicans need a visa to enter Mexico. American citizens can obtain the necessary forms at the border. Proof of U.S. citizenship is required by the Mexican authorities. Such proof may be a voter registration card, passport, birth certificate, or notarized affidavit of U.S. citizenship (U.S. driver's licenses are not acceptable). There is no charge for a tourist visa.

Non-U.S. citizens MUST obtain a visa from a Mexican consulate BEFORE reaching the border. There are consulates in Tucson, Phoenix, Los Angeles, San Diego, and many other cities. The visa application process takes only a few minutes.

After having your visa stamped, keep it. The Mexican authorities may require its return when you return to the U.S.

Upon reentering the United States, the U.S. immigration authorities will inquire about your citizenship or birthplace. If you are not a U.S. citizen or were born in a foreign country, you may be asked to provide a passport with a valid visa, or, if naturalized, proof of citizenship (passport or naturalization certificate).

There are certain regulations concerning what you may bring back into the U.S. from Mexico. Sea shells and marine sediment (not soil!) are permitted, although live animals and plants are not. If you have any questions, please ask a field-trip leader, or inquire with U.S. Customs before you depart.

The Puerto Peñasco Area

Puerto Peñasco (also known as "Rocky Point") is a rapidly growing town of approximately 40,000 inhabitants. It has grown from a small village in the 1950's to a bustling community whose economy principally depends on shrimp-fishing and tourism.

The very large influx of tourists from the U.S. makes Puerto Peñasco something like a border town. U.S. money is accepted in the shops and restaurants, although change may be given in pesos. A slightly better exchange rate can be gained by changing money at a bank beforehand, but a rapidly fluctuating exchange rate may make American cash the currency of choice. Bring small denominations: singles and fives.

Our base of operations is the Edificio Agustín

Cortes of CEDO (Centro de Estudios de Desiertos y Océanos -- the "Center for the Study of Deserts and Oceans"). CEDO is an autonomous marine station managed by marine biologists Peggy Turk and Rick Boyer. CEDO plays host to numerous school and university classes, museum groups, and individual researchers.

The Edificio Agustín Cortés is a large, two-story building (sometimes called "the castle") atop a large dune and overlooks the Gulf of California. It is equipped with several sleeping rooms, two bathrooms, a large, fully-equipped kitchen, a small library and museum, and a laboratory with marine aquaria. THERE ARE NO BEDS, so bring some sort of mattress with your sleeping bag. Running water is available for washing, and bottled drinking water is available in the kitchen.

The Puerto Peñasco area is shown in Figure 2. Bahía la Choya is a 5-square-kilometer complex of coastal habitats located 7 km to the west of Puerto Peñasco. Punta Pelicano is a promontory that defines the southern flank of Bahía la Choya. The promontory is a granitic intrusive body that predates the basaltic extrusions of Punta Peñasco and Cerro Prieto, but perhaps not by much. Estero Morua is a large estuary/tidal inlet complex 7 km east of Puerto Peñasco.

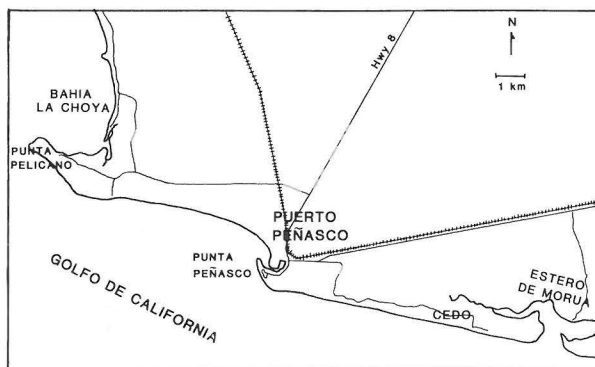


Figure 2. Map of the Puerto Peñasco region.

GEOLOGIC SETTING OF THE NORTHERN GULF OF CALIFORNIA

The 1100-km-long Gulf of California is a rifted basin, which opened approximately 3.5 to 4.5 million years ago (Larsen and others, 1968; Moore and Curray, 1982). At its southern end the Gulf links with the East Pacific Rise at a triple junction, which passes northward into a series of short spreading centers offset by transform faults (Figure 3). At its northern end the Gulf reflects the submarine extension of a regional tectonic system that links with the Imperial Valley and San Andreas Fault in southern California (Anderson, 1971). Thus, the longitudinal axis of the Gulf represents the complexly faulted boundary between the North American and Pacific Plates in northwestern Mexico.

Deep-sea drilling in the southern and central parts of the Gulf on DSDP Leg 64 revealed that sedimentation rates have been high. For example, in the Guaymas Basin near the middle of the Gulf, where the water is now up to 2 km deep, pelagic sediment accumulation rates for the late Pleistocene and Holocene are estimated to exceed 2 m per 1000 years in places (Curray and others, 1982). This rate is higher than that at the mouth of the Gulf but is much lower than the extremely high sediment accumulation rate in the northern end, where the Colorado River has prograded rapidly out into the Gulf. Within the past 50 years, however, the construction of Hoover Dam and large-

scale irrigation projects in the Imperial Valley have greatly restricted the flow of the lower Colorado River, and now little or no river sediment enters the northern Gulf (Brusca, 1980).

In the vicinity of Puerto Peñasco, sedimentary rocks of late Pleistocene age rim the coastline, often lapping onto slightly older volcanic and plutonic rocks that apparently formed at the time this portion of the Gulf opened up. The igneous bodies include Punta Peñasco ("Rocky Point") and Cerro Prieto ("Black Mountain"), which are basaltic in composition and have been dated radiometrically as 15 Ma (Lynch, 1981), and Punta Pelicano ("Pelican Point"), which is granitic in composition. The Pleistocene sedimentary rocks include terrigenous arkosic sandstones and conglomerates (derived locally), limestones (calcarenes and shell coquinas), and mixed carbonate-clastic rocks.

Modern dunes, principally composed of fine carbonate sand, typify the coastal terrain. Although most are stabilized by vegetation, some large dunes (especially around the margin of Estero Morua) are largely unvegetated and are actively moving. Predominant wind direction is from the northwest, and long-shore drift has caused eastward migration of beach sands and construction of spits (especially at the mouth of Estero Morua).

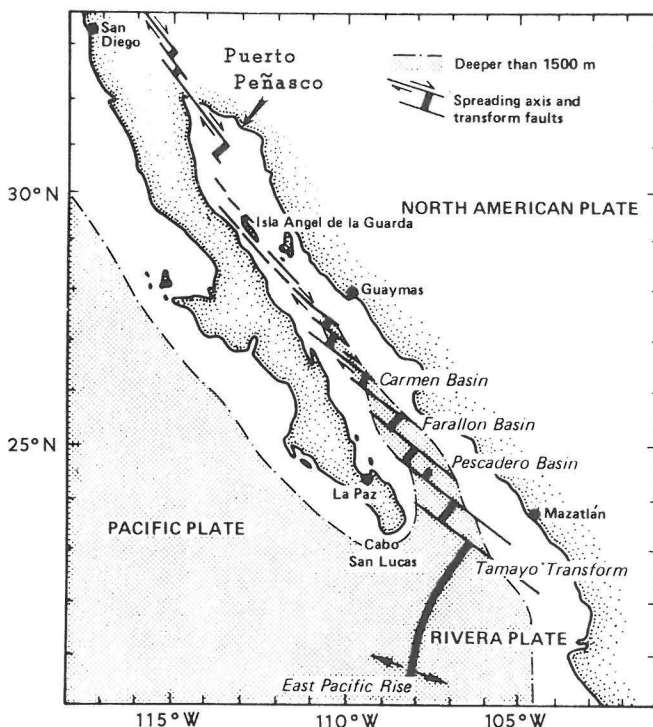


Figure 3. Tectonic features of the Gulf of California (modified after Moore and Curray, 1982, Fig. 3).

ENVIRONMENTAL SETTING OF THE PUERTO PEÑASCO AREA

Puerto Peñasco, at 31°N latitude, lies about 850 km north of the Tropic of Cancer. The climate is arid, with annual rainfall less than 10 cm. Surface water temperatures are rather mild (ranging from 30–32°C in the summer to 10–14°C in the winter). During occasional winter cold snaps, the water temperature may drop to 8°C or less and a massive mortality

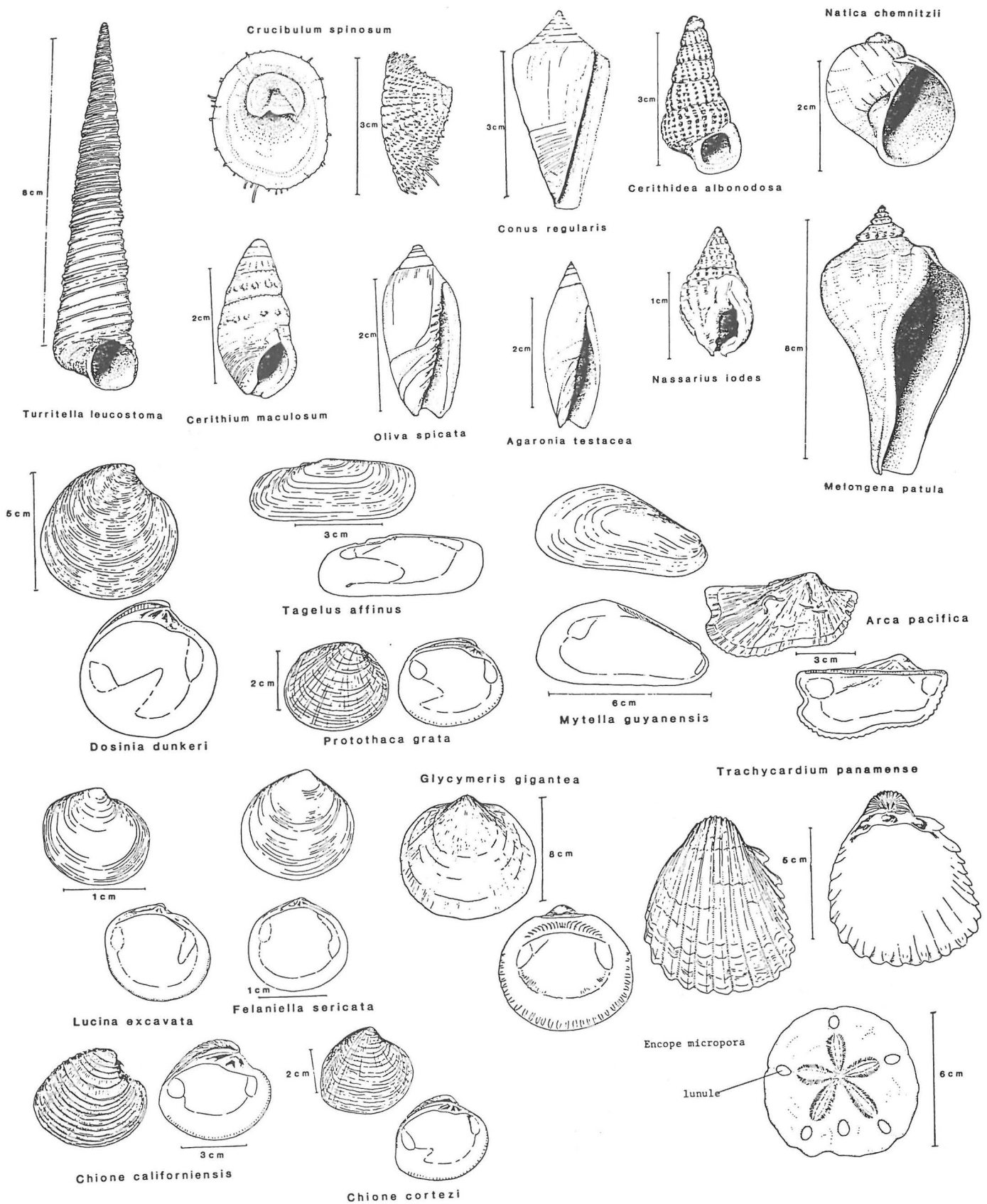


Figure 4. Common shelly invertebrates of the Puerto Peñasco area. Drawings by Richard Norris.

of macroscopic algae and stenothermal ("tropical") invertebrates may occur. In fact, most marine organisms inhabiting the area appear to be limited by winter temperatures (Brusca, 1980).

Salinity of the Gulf of California in general is higher than that in the open Pacific Ocean. In the northern Gulf near Puerto Peñasco, offshore surface-water salinities are 35 to 36‰, whereas salinities in shallow coastal waters are 36 to 39‰.

Evaporation markedly exceeds precipitation (by as much as 250 cm/year) in this region, so the coastline is quite arid and is characterized by Sonoran desert vegetation (especially cholla cactus and various desert grasses). Most streams are ephemeral, and estuaries (called "esteros") are negative in the sense that evaporation significantly exceeds runoff, so salinity and temperature of the water typically increase from the mouth of the estero up to its head (Brusca, 1980).

Of particular interest in the northern Gulf is the extremely high tidal range. Spring tides in the Puerto Peñasco area, which occur during new and full moon phases, commonly reach 8 or 9 m of vertical displacement. The tides are "mixed semidiurnal," meaning that there are two unequal high tides and two unequal low tides per day. The 0-tide level ("zero datum") in the northern Gulf is defined as the average position of the low tideline during the spring tides of a given year. Because the tidal flats in the area have such a gentle slope and low topographic relief, the tides that flood and drain them twice a day move quite rapidly. Thus, when out walking on the flats, be careful not to get cut off from land by the incoming tide. We have clocked the incoming tide in Bahía la Choya traveling horizontally across the tidal flat at a rate of 10 m per minute.

The extreme tidal range allows for intertidal zonation of organism communities to be displayed dramatically. On rocky shores this zonation is manifested in a vertical sense, often with knife-sharp boundaries between different communities; on tidal flats the zones are spread out laterally in broad bands that parallel the shoreline, usually with very diffuse, gradational boundaries between communities. In many cases, the intertidal zonation of animal communities is discernible in the Pleistocene record. Zoned communities and habitats are discussed specifically in the sections describing each field trip stop.

FAUNA OF THE PUERTO PEÑASCO REGION

The fauna of the Gulf of California falls within the Panamic Province, a largely tropical province that ranges from the northern Gulf and the tip of Baja California southward to Panama. Thus, the Gulf fauna has more in common with the truly tropical faunas to the south than it does with the faunas on the Pacific coast of Baja California.

The high faunal diversity and limited space here preclude lengthy discussion, so we list and illustrate (Table 1; Figure 4) only the most common species of shelly invertebrates. We have identified more than 228 species of molluscs alone. Beckvar and others (1985) have written a key to their identification. Keen (1971) is a comprehensive guide to the molluscs of the area, while Brusca (1980) is a guide to the identification of the intertidal invertebrates of the Gulf.

STOP 1. BAHIA LA CHOYA

Bahía la Choya is a 5-square-kilometer complex of tidal flats, channels, and salt marshes (Figure 5).

TABLE 1
Common shelly invertebrates

bivalve molluscs	gastropod molluscs
<u>Arca pacifica</u>	<u>Crucibulum spinosum</u>
<u>Glycymeris gigantea</u> P*	<u>Turbo fluctuosus</u>
<u>Mytella guyanensis</u>	<u>Theodoxus luteofasciatus</u>
<u>Saccostrea palmula</u> P*	<u>Turritella leucostoma</u> P*
<u>Cardita affinis</u>	<u>Cerithium stercusmuscarum</u> P*
<u>Lucina excavata</u>	<u>Cerithidea albonodosa</u> P*
<u>Felaniella sericata</u>	<u>Hipponix pilosus</u>
<u>Trachycardium</u>	<u>Calyptraea mamillaris</u>
<u>panamense</u> P*	<u>Crepidula striolata</u>
<u>Chione californiensis</u> P*	<u>Natica chemnitzii</u> P*
<u>Chione cortezi</u>	<u>Muricanthus nigrilus</u>
<u>Dosinia ponderosa</u> P*	<u>Melongena patula</u>
<u>Megapitaria squalida</u>	<u>Nassarius iodes</u>
<u>Protothaca grata</u>	<u>Agaronia testacea</u>
<u>Tagelus affinis</u> P*	<u>Oliva spicata</u> P*
	<u>Conus regularis</u> P*
scaphopod	crustaceans
<u>Dentalium semipolium</u>	<u>Balanus</u>
	<u>Cthamalus</u>
echinoderms	<u>Callinectes</u>
<u>Encope micropora</u>	<u>Callianassa</u>
<u>Encope grandis</u> P*	<u>Upogebia</u>
	<u>Uca</u>
brachiopod	<u>Eurytium</u>
<u>Glottidea palmeri</u>	<u>Eriphea</u>
	<u>Tetraclita</u>

P* indicates species is also common in Pleistocene deposits

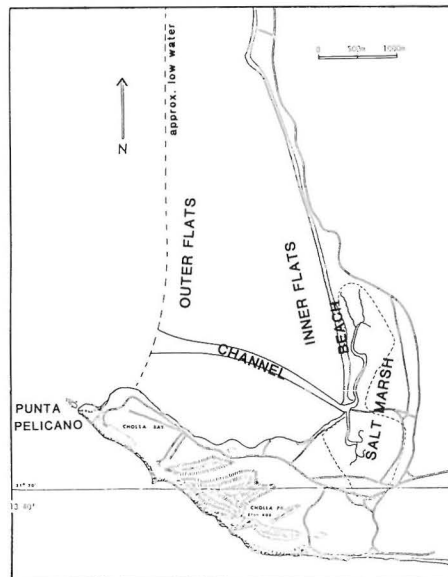


Figure 5. Map of Bahía la Cholla showing major habitats. Course of channel is highly schematic.

We will park in the largely American village of Bahía la Choya and walk north, past exposures of a Pleistocene terrace, across the main tidal channel to the low tide line. From there, we will walk due east toward the beach and salt marsh, where we will meet one of the vehicles that will shuttle us back to the parking area. The walking tour will take approximately four hours. There is no danger of being caught by the incoming tide.

We recognize six habitats within the Bahía la Choya complex: outer flats, inner flats, beach, salt marsh, tidal channel, and hardgrounds of Pleistocene coquina. Each habitat is characterized by a distinctive assemblage of organisms, bedforms, and biogenic structures.

We will walk from the outer flats to the inner flats just north of the main tidal channel, cross the barrier beach to examine "subfossil" shell-beds exposed by local gravel mining, and examine the salt marsh and channel behind the beach.

Outer Flats

The outer flats constitute the low intertidal zone, an area exposed only during spring tides, and then for only a rather short period of time during the tidal cycle. The area is characterized by medium to coarse-grained quartz, feldspar, and carbonate sand. The topography of the outer flats is dominated by linear, long-wavelength, flood-oriented sand waves. Superimposed on these large-scale bedforms are smaller ripples, either ebb-oriented (at low tide, at any rate), or oriented according to the late-stage drainage of the sand waves. The outer flats contain a diverse and abundant fauna of shelly remains of molluscs and echinoids. The troughs are often very shell-rich, containing tests of the sand dollar Encope, and disarticulated valves of Dosinia, Trachycardium, Megapitaria, and Chione. Live animals are much rarer, but include the infaunal venerid bivalve Chione and the predatory gastropods Natica and Conus. Common traces in the outer flats include the shallow, circular depressions and adjacent "spoil piles" made by the burrowing activities of rays, the vertical burrows constructed by infaunal sea anemones (Calamactis), numerous polychaete (Diopatra, Onuphis) burrows, and the surface trails of gastropods.

Inner Flats

The outer flats grade into the inner flats. The inner flats are characterized by a smaller grain size, a decrease in sedimentary carbonate, an absence of large-scale bedforms, and a lower diversity of shelly fauna (both live and dead). Ripple marks, principally ebb-oriented (though often modified by winds and late-stage drainage), are ubiquitous. The inner flats are characterized by a topography consisting of interconnected, flat-topped firmgrounds of fine sand (apparently produced by algal binding), interrupted by shallow (a few cm) depressions of pellet-rich, soupy, fine sand. Shells are rather rare on the surface. Typical members of the live fauna include the infaunal razor clam Tagelus and the scavenging gastropod Nassarius. We have occasionally found live Glottidea, a burrowing lingulid brachiopod. Common traces include ray feeding burrows, gastropod trails, the tracks and feeding traces of shore birds, and the extensive burrow systems of the ghost shrimp Callinassa and Upogebia. Often present at depth over much of the inner flats is a shell-rich layer. Located at depths ranging from 1 to 40 cm, this layer appears to be the result of biogenic stratification -- the concentration of coarse-grained material, at

depth, by the sediment-sorting activities of deposit-feeding animals.

Beach and Spit

The beach and spit include the highest intertidal zone as well as areas that are reached by tides only during the most severe storms. Sediments range in size from the fine, windblown sands on the surface, to the very coarse, shelly debris that is exposed in the gravel pits. Most of the sediment is comprised of medium-grained quartz sands and molluscan debris. The higher parts of the spit are modified into aeolian dunes displaying wind ripples. The landward portion of the spit consists of shell-rich spillover lobes, formed during storm events. The accretionary ridges on the southern tip of the spit suggest a southerly longshore drift.

Salt Marsh

Areas of salt marsh form principally behind the shelter of the spit. These mid- to high intertidal habitats are composed of fine sands that are bound by a dense network of roots of the marsh grasses Salicornia, a succulent, and Distichlis, spike grass. The high-spired, herbivorous gastropod Cerithidea is particularly abundant, and the endobyssate bivalve Modiolus can often be found in grassy areas. The galleried burrows of fiddler crabs (Uca) and salt marsh crabs (Eurytium) are ubiquitous.

Channel

The tidal channels connect all the other habitats and often share features of the adjacent habitats. Sediments range in size from fine sands to very coarse shelly and pebbly gravels. Current-aligned shells are common along the banks of the main tidal channel. High-amplitude sand waves occur in the faster-flowing parts of the main channels. An ebb-tidal delta of coarse sand is located immediately to the west of the inlet. The deeper portions of the principal channels are always flooded. Where a firm substrate is available, these areas support an abundant fauna of the grazing gastropods Cerithium and Theodoxus. The infaunal bivalve Chione and the ill-tempered blue crab Callinectes are common. The banks of the tidal channels within the salt marsh are riddled with the burrows of fiddler crabs, while the shell pavement of the main channel as it crosses the flats restricts burrowing.

Hardgrounds

Areas near spring low water and much of the northern parts of the bay are underlain by a hardground consisting of Pleistocene coquina. These hardgrounds form an uneven surface that, where exposed, is readily colonized by algae and a variety of boring organisms. The herbivorous gastropod Cerithium is particularly abundant. The hardgrounds are encrusted with sponges and colonial tunicates. Crevice nestlers include the bivalve Cardita, and the boring infauna include sipunculid worms and mytilid bivalves (Lithophaga).

STOP 2. ESTERO MORUA

Southeast of the town of Puerto Peñasco is a large embayment, known as Estero Morua, where several ephemeral streams join to meet the sea. Unlike Bahía la Choya, which is a broad, open, baylike tidal flat that floods and drains during the tidal cycle without

deeply incised channels, Estero Morua has a relatively narrow mouth (constricted by spits) and a prominent, permanent channel that serves to funnel the incoming and outgoing tides. Thus, primary sedimentary structures and bedforms in Estero Morua testify to much higher-energy depositional and erosional conditions than can be seen in Bahia la Choya. Also, as might be expected, the benthic fauna of Estero Morua is patchier and less diverse than that in Bahia la Choya, although marine animals are locally quite abundant.

The various intertidal subenvironments of Estero Morua represent five major habitats for animals and plants: muddy salt marsh, sand flats, sandy tidal channel, sandy mud firmgrounds, and calcarenite/coquina hardgrounds. The subaerial dunes surrounding the estero represent a sixth major habitat (Figure 6).

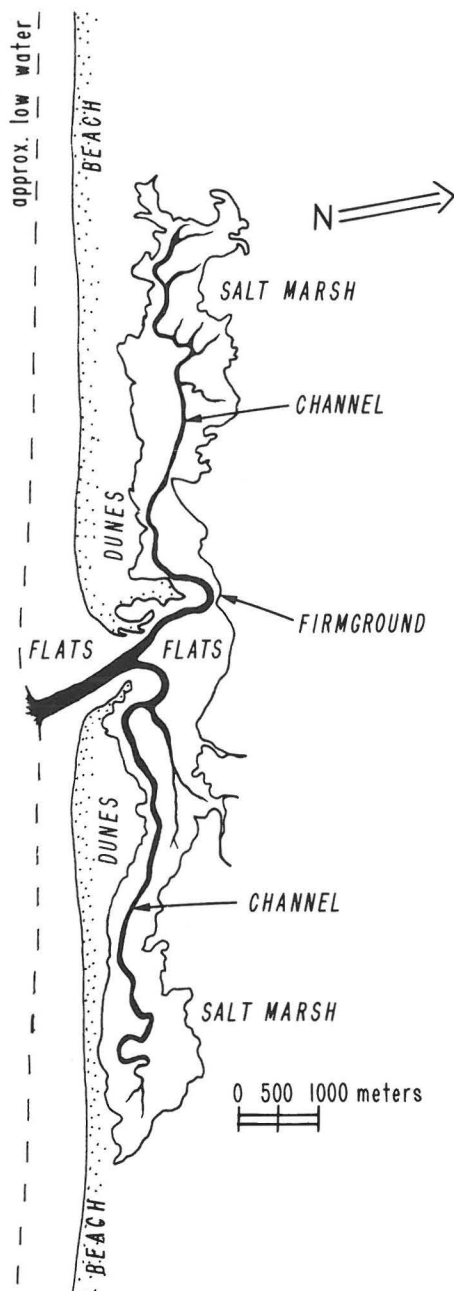


Figure 6. Locality map of Estero Morua.

Salt Marsh

The salt marsh in the upper reaches of the estero floods only during high tide and is floored with terrigenous mud and clay. Thick stands of angiosperm halophytes (salt marsh plants) stabilize the muddy substrate; these include pickleweed (*Salicornia*), spike grass (*Distichlis*), saltbush (*Atriplex*), and saltwort (*Batis*).

Invertebrates, including mainly gastropods, crabs, and various insects, are quite abundant in the salt marsh. Especially characteristic are cerithid gastropods (*Cerithidea mazatlanica*), fiddler crabs (*Uca princeps*, *U. musica* and *U. crenulata*), and white-fingered xanthid crabs (*Eurytium albidigitum*). The crabs are all active burrowers; *Uca* creates an unbranched but often rather deep burrow, whereas *Eurytium* constructs a shallow "Thalassinoides-like" Y-branched burrow system. The substrate is thoroughly bioturbated by rooted plants and burrowing crustaceans, so no primary stratification or sedimentary structures remain.

Flats

The flats of Estero Morua are composed mostly of well-sorted fine to medium-grained sand. A wide variety of primary sedimentary structures occur here, and numerous types of ebb-oriented current ripple marks can be seen on the tops of well-formed mega-ripples.

Biogenic structures are common on the flats but not nearly as abundant here as at Bahia la Choya. Typically they are dominated by resting/feeding traces of sting rays and crawling trails of various gastropods. Dense but highly localized populations of deep-burrowing bivalves (*Tagelus affinis*) are present in the upper flats, and flamboyantly decorated tubes of the polychaete annelid *Diopatra splendidissima* are quite common in the high-energy, unrippled sand at the mouth of the estero. Throughout the whole estero, in small patches of very shallow standing water during low tide, tiny green polychaete annelids (*Phyllodoce tuberculosa*) actively inscribe the sand surface with a scribbled network of crawling trails; these delicate traces are ephemeral and disappear when the tide returns and the worms burrow back into the sand. Agglutinated tubes of well-sorted sand are constructed by some burrowing polychaetes, including *Onuphis microcephala*, and piles of coiled fecal strings are excreted onto the sand surface by other burrowing worms, including the annelid *Arenicola* sp. and the hemichordate *Balanoglossus* sp.

At places where a thin layer of sand covers a flat pavement of shells or rock, enormous numbers of epifaunal herbivorous and detritivorous gastropods (*Cerithium stercusmuscarum* and *Theodoxus luteofasciatus*) congregate. We have observed local population densities of *C. stercusmuscarum* as high as 1500 individuals/m² in such situations.

Channel

The sand flats of Estero Morua are cut by a main tidal channel, which splits into divergent subsidiary channels in the upper reaches of the estero. The channel never fully drains during low tide, although during a low spring tide it is possible to wade across even at the mouth of the estero. This may be a hazardous venture, however, because of the large sting rays that commonly inhabit it.

Although lag deposits of empty mollusc shells are abundant in the channel, particularly on the inside of meanders, few molluscs actually inhabit the channel,

perhaps owing to the high-energy shifting substrate. Rapidly burrowing bivalves (*Donax* sp.) and shallow-burrowing venerid bivalves (*Chione* spp., *Protothaca grata*, etc.) are patchily distributed, and gastropod predators (*Melogenia patula*, *Natica chemnitzii*, etc.) commonly are seen prowling along the margins of the channel.

Firmgrounds

In some parts of the upper margin of Estero Morua's sand flats, usually adjacent to the salt marsh, a firm (but uncemented) substrate of muddy sand provides a distinctive habitat for burrowing crustaceans. These include small fiddler crabs (*Uca musica* and *U. crenulata*), which come out of their burrows to feed at the sediment surface, and ghost shrimp (*Upogebia* sp.), which are deposit feeders that never leave their burrows.

Hardgrounds

Pleistocene/Holocene calcarenite and shell coquina outcrop at several isolated places within the intertidal zone of Estero Morua. Attached epifauna include barnacles, such as the large *Tetraclita squamosa*, which prefers to sit atop the outcrops exposed to maximum wave energy, and the small *Chthamalus fissus*, which usually sits at a lower, adjacent position on the outcrop relative to *Tetraclita*. The distinct zonation of barnacles is especially apparent at the very mouth of Estero Morua, where the combined action of bioerosion, wave energy, and substrate stabilization by barnacles has produced a spectacular microtopography of sharp pinnacles covered with barnacles. Epifaunal gastropods include the herbivorous *Nerita funiculata*, which congregates in large numbers in the tide pools, and the carnivorous *Acanthina angelica*, which pries open and preys upon barnacles by using its distinctive apertural spine. Crabs are abundant on and under the rocks; they include the colorful and belligerent *Eriphia squamata* and the small, black *Petrolisthes armatus*. Inside the rock itself are many boring animals, including sponges (*Cliona* spp.), bivalves (*Lithophaga* spp., etc.), and both annelid and sipunculid worms, each producing a distinctive boring to serve as its domicile.

Dunes

The modern subaerial sand dunes that surround Estero Morua provide habitat for terrestrial organisms. Numerous trace-making organisms populate the dunes. These include insects, rodents, and reptiles (mostly lizards, rattlesnakes, and gopher snakes) that create extensive trackways across the dune surfaces, as well as burrow systems within the sand. Beetles may produce horizontal meniscate burrows just beneath the sand surface, and some wasps dig rather deep burrows. Unidentified rodents construct extensive branched burrow systems in the vegetated, stabilized portions of dunes, but no detailed study has been accomplished on these to date.

STOP 3. THE PLEISTOCENE AND PUNTA PELICANO

Fossiliferous marine deposits of Pleistocene age are common on both coasts and on islands in the Gulf of California. Hertlein and Emerson (1956) provide faunal lists for many localities in the Puerto Peñasco area. Stump (1975) and Beckvar (1986) discuss the paleoecology of Pleistocene deposits approximately 300 km south of the Puerto Peñasco region, and Ortleib

(1981a,b) reports on the geochronology and tectonic implications of Pleistocene terraces along the Sonoran coast.

We have identified approximately 40 species of marine invertebrates from the Pleistocene deposits flanking Bahia la Choya. The most common species are listed in Table 1.

All of the fossils found in the Pleistocene are present in the area today.

Hertlein and Emerson (1956) assigned the Puerto Peñasco deposits to a late Pleistocene age. Bernat and others (1980) report a U/Th age of 180 ka from a *Dosinia ponderosa* shell from the deposits at Puerto Libertad (300 km to the south). The deposits at Puerto Peñasco have not been dated radiometrically. They are beyond the range of Carbon-14 (Rose, 1975). They may represent deposition during a highstand of sea level approximately 120 ka (Ortleib, 1981b).

Lithologies present range from cobble conglomerates to coquinas to fine-grained sandstones. Micritic coatings of carbonate grains are ubiquitous and both aragonitic and high-magnesium calcite cements are common (Jones, 1975).

A generalized stratigraphic section of the Bahia la Choya Pleistocene is shown in Figure 7. The Pleistocene deposits rest unconformably on mid-Tertiary(?) granites or basalts. Fractures in these "basement" rocks are often filled with Pleistocene shell-rich sandstones. The basal 20 to 60 cm of the Pleistocene often consists of a cobble conglomerate with rare fossils. The cobble lithologies are usually the same as the underlying igneous rock. Above this horizon are richly fossiliferous (typically with abundant *Chione*) sandstones, ranging from 60 to 80 cm in thickness. In many areas near Bahia la Choya, a distinct storm bed, 10 to 20 cm thick, unconformably overlies the fossiliferous sandstone. The bed is poorly sorted and pebble-rich, and contains large articulated bivalves oriented with their planes of commissure parallel to bedding. Though exposures are rare, the sequence is capped by unfossiliferous, presumably nonmarine sandstone.

Biofacies and lithofacies vary laterally within the Pleistocene deposits. Deposits near the rocky

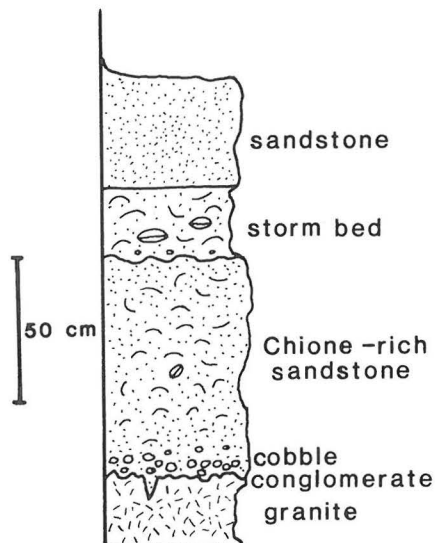


Figure 7. Generalized stratigraphic column of Pleistocene rocks of Bahia la Choya region.

headlands of Punta Pelicano typically contain abundant cobbles, pebbles, and a rocky intertidal fauna, whereas those on the northeastern flank of Bahía la Choya have fewer pebbles and cobbles, are generally better sorted, and contain a fauna typical of an outer sand-flat habitat.

We will examine two outcrops: a terrace along the northeastern flank of Bahía la Choya; and a section at Punta Pelicano, along the southern margin of the bay.

Stop 3a. The Bahía la Choya Terrace

The Pleistocene forms an extensive terrace along the northeastern margin of Bahía la Choya. A 1.5-m section is exposed at low and mid-tides. The basal one meter consists of poorly sorted sandstone with abundant, randomly oriented shells of the bivalve *Chione*. Unconformably overlying this layer is a 20- to 30-cm-thick bed of very poorly sorted coarse sandstone, with abundant, large, articulated bivalves (principally *Dosinia*, *Glycymeris*, and *Trachycardium*) that are frequently oriented with their planes of commissure parallel to the bedding surface. Other common faunal elements in this bed include the echinoid *Encope* and the gastropods *Natica* and *Conus*. The unconformable lower contact, the poor sorting, and the articulated but displaced bivalves suggest that this bed represents a storm event. Above the storm bed and capping the sequence is a 20- to 30-cm-thick bed of largely unfossiliferous, well-sorted, carbonate-rich sandstone. The faunal composition of the basal two units is similar to that found today on the outer flats of the bay. The Pleistocene terrace deposits probably represent a shallow subtidal or low intertidal zone.

Stop 3b. The Punta Pelicano Outcrop

One outcrop on the northwestern tip of Punta Pelicano exposes a section of approximately three meters thickness. The sediments are dominantly poorly sorted sandstones and conglomerates. The cobbles are composed of locally derived granite. The basal portion of the section represents deposition in a rocky intertidal habitat. The sediments are very poorly sorted and cobbles are frequently encrusted with bryozoa, barnacles, and oysters (*Saccostrea*). The sequence grades upward into unfossiliferous, presumably nonmarine conglomerates and sandstones.

The most common fossils in this exposure are calcitic in composition. Aragonitic forms tend to be represented by only casts and molds. Thus, a taphonomic bias toward calcitic hard parts has caused a significant change in faunal composition.

Other Punta Pelicano Pleistocene

Other discontinuous, small outcrops of loosely cemented sandstone occur high in the supertidal on the seaward side of Punta Pelicano. Its position (several meters to tens of meters above the current high-tide line) and the absence of marine fossils indicate that its origin was nonmarine. High-angle cross-stratification suggests aeolian deposition, and large branching burrow systems (resembling modern rodent burrows) and small meniscate burrows (resembling modern beetle burrows) testify to the terrestrial conditions.

On the landward side of Punta Pelicano, huge sandstone outcrops extend almost to the 100-m summit. Aeolian deposition is certain, as indicated by the presence of high-angle, wedge-planar and tabular-planar cross-strata, aeolian ripple marks (with

high R.I. and low R.S.I.), rhizcretions, and meniscate (beetle?) burrows. The height and extent of these aeolian sandstones suggest that Pleistocene wind velocities were much stronger and that Pleistocene wind direction was more northerly than at present.

STOP 4. PUNTA PELICANO ROCKY SHORE

The granitic shoreline of Punta Pelicano provides an opportunity to view vertical zonation of animal communities in the modern rocky intertidal zone, although, of course, the fossilization potential of such communities is lower than for those inhabiting the soft sediments in Estero Morua and Bahía la Choya. The plutonic rock prevents bioerosion by endolithic organisms, so only epifauna inhabit the shore. Tide pools are deep, and many at even high-tide levels remain wet throughout the tidal cycle.

Crawling over the rocks in the uppermost intertidal zone are large isopods (*Ligia*) that superficially resemble cockroaches. Clinging to the sides of high intertidal pools are the barnacles *Tetraclita squamosa* and *Chthamalus fissus*, as well as abundant herbivorous gastropods (*Nerita funiculata* and *N. scabricosta*). Lower in the intertidal, diversity and abundance of tide-pool life increases dramatically, and dozens of invertebrate taxa are common. Molluscs of all types (including octopus) are very prominent, but they do not overshadow numerous taxa of sponges, anthozoan coelenterates, polyclad flatworms, bryozoans, crustaceans, annelids, ascidean tunicates, and echinoderms. Various ophiuroids (*Ophioderma teres*, *Ophiocoma aethiops*, *Ophioneries annulata*, etc.) and holothuroids (*Selenkothuria lubrica*, etc.) are quite common in the middle intertidal zone, and asteroids (*Othilia tenuispina* and *Nidorellia armata*) and echinoids (*Echinometra vanbrunti*) are common in the lower intertidal zone.

Modern intertidal plants at Punta Pelicano are nonvascular. Several species of calcareous red algae can be seen in the tide pools, and fleshy brown algae cover the lower intertidal rocks, rendering them slippery and treacherous for walking.

TAPHONOMY

The effects of the taphonomic processes at work in the Puerto Peñasco area will be seen in the field and are briefly discussed below.

Physical Destruction

Physical destruction of hard parts occurs as a consequence of wave action (especially during storms) and tidal currents. The low sediment accumulation rates at Bahía la Choya allow physical destructive processes to operate on exposed shells for extended periods of time. Disarticulation, abrasion, and breakage of many hard parts can result from purely physical means as well as in combination with other forms of hard-part destruction. The outer flats and tidal channels are areas in which wave and current energy are highest and are habitats characterized by an abundance of disarticulated, abraded, and broken shell material.

Biological Destruction

Prolonged surface exposure due to low sedimentation rates makes hard parts especially prone to destruction by bioeroding sponges, polychaetes, bivalves, and algae. The predatory activities of birds, rays, gastropods, and crabs also cause shell

destruction. Repair scars on such gastropods as Melongena and Natica suggest that predation by crabs is a common source of shell breakage. The outer flats and the tidal channels contain abundant shell material and are the habitats most often covered by the tides. Rates of biological destruction here are probably very high. Rates of biological destruction are also very high on the hardgrounds of Pleistocene coquina. The hardgrounds support an abundant and diverse boring infauna.

Chemical Destruction

Chemical destruction's principal effect is the dissolution of carbonate shell material. Using specimens from Bahia la Choya, Flessa and Brown's (1983) laboratory experiments documented the effects of surface area to volume ratios and carbonate mineralogy on relative rates of dissolution. In the field, dissolution occurs over many time frames: from the partial dissolution of the beak region in live specimens of Mytella in salt-marsh sediments, to the acquisition of a chalky surface texture in empty shells buried within fine-grained salt-marsh sediments, to the dissolution of Pleistocene shells in uplifted terraces. Though some Pleistocene exposures, such as those in the northern part of the bay, contain hard parts composed of aragonite, calcite, and high-magnesium calcite, other exposures, such as at Punta Pelicano, are dominated by the more solution-resistant calcitic hard parts of oysters, barnacles, and bryozoans, and originally aragonitic species are represented by either very chalky shells or casts and molds. Chemical destruction's effects are most severe within salt-marsh sediments and Pleistocene coquinas. Dissolution within the coarse sediments of the tidal flats, even at depth, appears to be insignificant.

Transportation

The 6-m mean tidal range produces strong and persistent tidal currents, and transportation might be expected to be an effective taphonomic process. However, with the exception of the main tidal channel, surprisingly little mixing occurs between habitats. Exotics may appear in some death assemblages, but when the relative abundance of species is considered, the correspondence between life and death assemblages is quite good (Watson, 1979). The main channel appears to be the only habitat characterized by significant transport.

Recycling

Recycling is the reintroduction of older, once-buried, shell material back into one of the active sedimentary environments. Recycling in Bahia la Choya occurs when shells from the spit deposits are washed out from either the seaward part of the spit by wave action or from the landward side of the spit by lateral migration of the tidal channel. Many of the exotic species found within the salt-marsh channels are probably due to recycling. Unless the habitat preferences of the species are known, it is very difficult to recognize recycling over this time scale. Recycling also occurs over a longer time frame. Pleistocene shells are eroded from hardgrounds or adjacent terraces and reenter active sedimentary environments. Such shells are often easy to recognize by their chalky appearance and by the small amounts of matrix still attached to the shells.

Time-Averaging

Time-averaging is an important process in Bahia la Choya because of the very low rate of sediment accumulation. Most species, such as the bivalves Lucina and Protothaca, are abundant among the dead shells, but rare among the living. Time-averaging also is suggested by the great range in preservation quality among specimens of the same species. The most direct evidence for time-averaging comes from radio-carbon dates. Meldahl (1987) reports a carbon-14 date of 3230 ± 75 y.b.p. for a shell recovered from the surface, and 2260 ± 75 , 4250 ± 80 and 2600 ± 145 y.b.p. for shells recovered from 50-, 60-, and 125-cm depth respectively. (The shell of a live specimen yielded a date of 15 ± 65 y.b.p., indicating that contamination is not a problem.) Not only do these dates indicate time-averaging on the scale of thousands of years, the lack of correspondence between depth and relative age suggests extensive vertical mixing and exhumation of once-buried shells. Much of this vertical mixing may be due to biogenic mixing.

Biogenic Stratification

Biogenic stratification is manifested by the subsurface concentration of coarse, shelly material by the deposit-feeding activities of polychaetes and burrowing shrimp (Meldahl, 1987). Such organisms frequently feed at depth and transport fine-grained sediment to the surface either through the gut or by water currents. Material too large to ingest or too cumbersome to transport remains at depth. In areas of very low rates of sedimentation, such coarse material becomes concentrated at depth, forming a shell bed within the sediment. In Bahia la Choya, such intra-stratal shell beds occur where deposit-feeding polychaetes and shrimp are most abundant.

Lateral Shearing

Lateral shearing is a late-stage taphonomic process that remains a minor mystery. Storm beds in some of the Pleistocene deposits contain articulate bivalves, oriented with the plane of commissure parallel to bedding. In many such specimens, one valve is laterally displaced 1 or 2 cm past the other. The processes responsible for this lateral shearing are not known.

INTERTIDAL SEDIMENTOLOGY

In spite of the extensive intertidal exposures and the wealth of sedimentary structures and bedforms, very few sedimentologic studies of the modern tidal flats at Bahia la Choya and Estero Morua have been accomplished. The most detailed sedimentologic analyses are unpublished University of Arizona master's theses by Sandusky (1969) on Estero Morua and Rose (1975) on Bahia la Choya.

Sediment Type and Texture

Sandusky (1969) reports that the sediments of Estero Morua are composed of quartz (42 to 59%), calcium carbonate shell fragments (8 to 30%), feldspar (3 to 10%), heavy minerals (1 to 17%), and igneous rock fragments (7 to 20%). Shells are mostly molluscan; foraminifera (Buccella, Elphidium, and Quinqueloculina) and ostracods are common but comprise less than 1%. The heavy mineral component includes (in decreasing order) epidote, sphene, hornblende, tourmaline, lamprobolite, garnet, and zircon. The high epidote content (epidote/amphibole ratio of 1 or

more) places the assemblage within Van Andel's (1964) "Rio Concepción Province."

Sediment grain size in Estero Morua increases from clay and silt (greater than 4 phi) in the salt marshes to fine sand (3.3 to 2 phi) on the sand flats and medium to coarse sand (2 to -0.5 phi) in the main tidal channel (Sandusky, 1969). In areas of high current velocity, the sediment tends to be coarser grained and skewed to the coarse end of the scale. Velocities during flood tide (up to 0.2 m/second) are sufficient to transport bivalve shells 15 cm in diameter in traction along the bottom.

Primary Sedimentary Structures

When McKee (1957, 1965) briefly described the extensively rippled tidal flat of Bahia la Choya, he noted that the widespread ripple marks were not preserved beneath the sediment surface as ripple cross-laminae. Instead, peels and x-ray radiographs from trenches revealed an irregular horizontal lamination within the sediment. He concluded that the constant shifting back and forth of the sand during ebb and flood tides produced this crude lamination and that superposed ripple or climbing ripple structures were precluded by the lack of input of new sand during ripple migration.

Sandusky (1969) used SCUBA to study the formation of ripple marks in Estero Morua. He noted that current ripples increase in size with water depth and that asymmetry of current ripples increases with current velocity. As the flood tide enters the estero and the water level rises, the current velocity increases and current ripples are destroyed by the formation of larger, second-order bedforms. These large megaripples can be seen at low tide along the main channel and at the mouth of the estero. Typically, they have wavelengths of 2 to 4.5 m and amplitudes of 15 to 25 cm. The crests of the megaripples may be straight or sinuous, and commonly there is a high concentration of shell material in the troughs.

Several types of current ripples form in Estero Morua and Bahia la Choya. Asymmetrical parallel ripples are common throughout. Typically, they have wavelengths averaging 9 cm and amplitudes of less than 1 cm. Symmetrical parallel ripples are common in the mid flats and along the high intertidal beach, generally in long, slightly sinuous rows. Often they bifurcate to resemble tuning forks. Wavelengths may be 7 to 16 cm, and amplitudes may be 2 to 4 cm. Linguoid ripples, which form in fairly turbid water with sinuous flow lines, are tongue-shaped structures oriented with the "tongue" pointing down-current. Wavelengths range from 2.5 to 10 cm, and amplitudes range from 3 to 4.5 cm. Lunate ripples are crescent-shaped structures that commonly occur in association with linguoid ripples. They are oriented with the concave side pointing down-current in such a way that the pointed tips intersect the middle of the next lunate ripple down-current. Wavelengths are 2.5 to 8 cm, and amplitudes are 3 to 5 cm. Rhomboid ripples occur at the mouth of Estero Morua, where waves cause water to wash over the sand bar. They also point down-current, and range from 5 to 12 cm long and 1 to 6 cm wide, with amplitudes of about 1 cm. Double-crested ripples, which form during falling water levels, may be oriented parallel, subparallel, or normal to the shoreline. Wavelengths are 8 to 25 cm, and amplitudes are 2.5 to 4.5 cm. Flat-topped ripples likewise form during falling water levels, as water action planes off the top of preexisting ripples. Wavelengths are 7 to 15 cm, and amplitudes are 1.5 to 4 cm.

Interference ripple patterns, with wind-generated

wave ripples superimposed on larger tide-generated current ripples of a different (often perpendicular) orientation, are very common on sand flats throughout Estero Morua and Bahia la Choya. Ripples occurring in the troughs of large tidal current-generated sand waves are often oriented perpendicular to the sand waves, reflecting shifting drainage direction during late-stage emergence. Also common in Estero Morua are small current ripples of various geometries superimposed on the stoss sides of second-order bedforms (megaripples).

Anoxic Horizons

In the tidal flats of both Estero Morua and Bahia la Choya, surface sediments are thoroughly oxidized, but sediment permeability immediately below the surface is low enough that interstitial waters are depleted in oxygen. The horizon separating brown oxidized sediment from black, stinking, anoxic layers is abrupt, but the depth of this anoxic boundary in the sediment is quite variable from place to place. In the inner flats of Bahia la Choya and Estero Morua, where the fine fraction percentage is great and the sand contains some mud, the anoxic horizon may be only a millimeter or two below the sediment surface. In contrast, along the main tidal channel in Estero Morua the anoxic zone may be several decimeters below the sediment surface. In Bahia la Choya, the greatest concentrations of organic carbon and hydrogen sulfide in the sediment occur in the upper reaches of the tidal flat and decrease seaward (P. Buettner, pers. comm.).

Many infaunal organisms, particularly crustaceans and annelid worms, burrow beneath the oxidized zone and penetrate the anoxic layers. They feed on the rich organic detritus accumulating in the oxygen-depleted sediment, but they breathe oxygenated water brought down from above via open shafts. These vertical shafts typically are enclosed by a brown halo of oxidized sediment immediately adjacent to them.

Storm Deposition

Winter winds in the Puerto Peñasco region are from the north and northwest; summer winds are from the south and southwest. Average wind speed in the region is about 12 km/hour, with the strongest winds typically occurring in the late summer. Major storms are not infrequent. When major storm surges with strong onshore winds accompany a high spring tide, extensive deposition of large shells, cobbles, and miscellaneous debris occurs along the high tideline. Spectacular transgressive storm deposits of late Pleistocene age are preserved discontinuously around the interior margin of Bahia la Choya (see discussion of Pleistocene outcrops at Stop 3). Unlithified "subfossil" shell beds in the sandy spit along the eastern margin of Bahia la Choya represent storm spillover lobes.

INTERTIDAL ICHNOLOGY

The ichnology (animal-sediment relations and biogenic sedimentary structures) of the Puerto Peñasco intertidal realm is fascinating, but little detailed study has been accomplished to date (Ekdale, 1978; Ekdale and others, 1984; Stearley and Ekdale, 1984, 1986). Two uncompleted master's theses at the University of Utah have focused on bioturbation of soft sediments (P. Buettner, in prep.) and bioerosion of hard substrates (R. Stearley, in prep.) in the intertidal zone of this region. Common biogenic structures are illustrated in Figure 8.

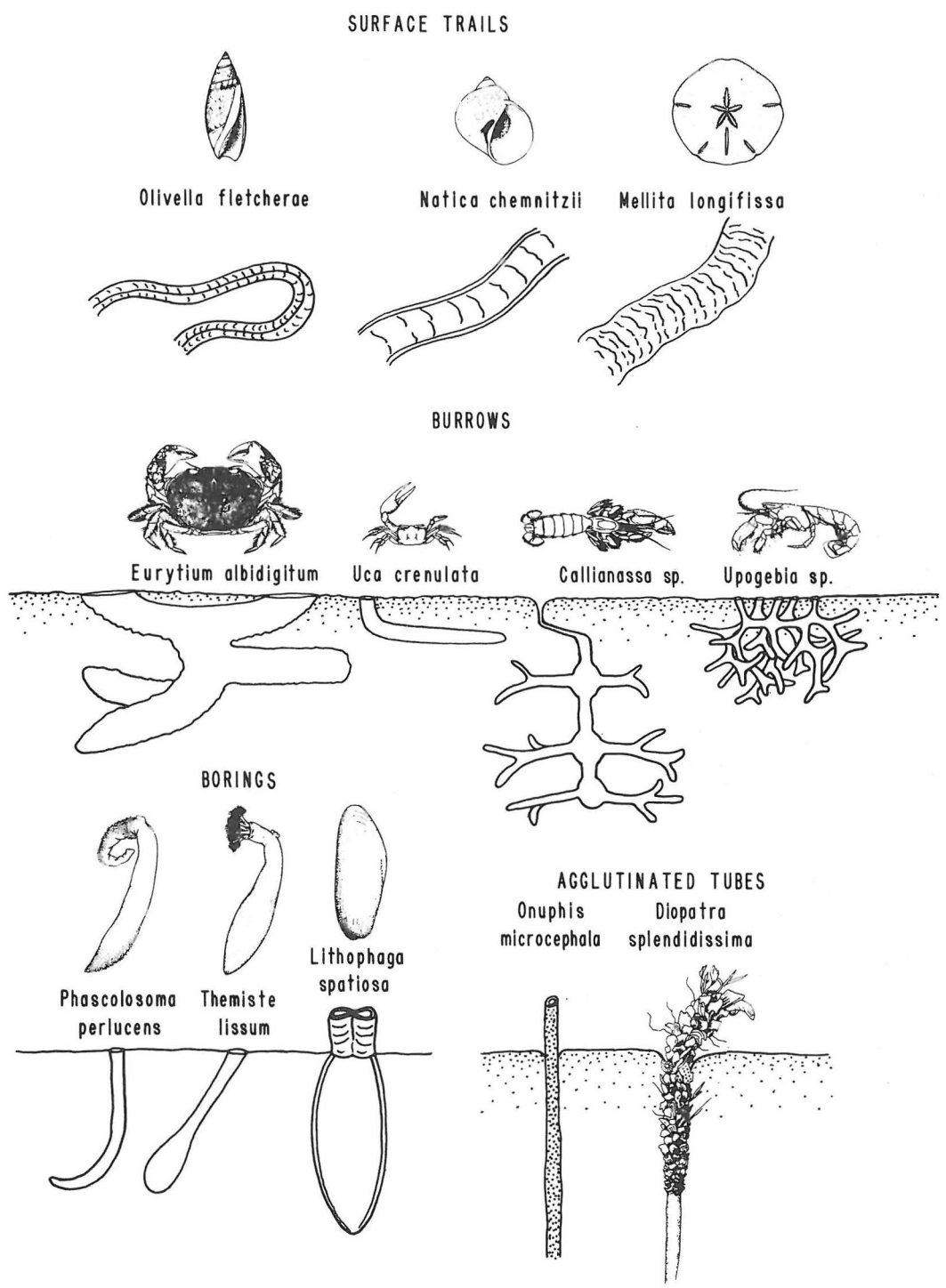


Figure 8. Common biogenic sedimentary structures and bioerosion structures in the Puerto Peñasco area (adapted from various sources).

Surface Tracks and Trails

The surface of the tidal flats, especially Bahia la Choya, contains countless tracks and trails of mobile epifauna. The vast majority are gastropod locomotion and grazing trails, which meander irregularly across the flats. In most cases the sediment is wet enough to allow production of smooth, continuous, double-ridged trails, resembling the trace fossil Aulichnites. Often, however, the sediment is sufficiently dry and cohesive that lumpy or ragged trails are formed. Numerous gastropod taxa, including the grazing cerithids and predatory olivids, are responsible for creating both such trails. Other species, like the predatory Natica chemnitzii, glide along on a broad foot which spreads over a wide layer of mucus, producing a flat trail with short, marginal ridges. The vast majority of gastropod trails are destroyed by the rising tide.

Trackways of various crabs are common on the flats, but not nearly as abundant as the gastropod trails. Crab trackways are composed of imprints of the ten podia (or eight, in the case of the swimming crabs) as the crab scuttles sideways across the sediment. These trackways require that substrate cohesiveness be just right for preservation. The most active crabs are fiddlers (Uca spp.), which typically inhabit sand too dry for tracks to be preserved. However, Uca creates other types of biogenic structures on the surface as they feed. Loosely joined sand pellets of two sizes are common around the entrance to Uca burrows; the larger ones are excavation pellets, composed of sediment carried up from depth in the burrow, and the smaller ones are feeding pellets, produced as the crabs feed on algae that grow on surface sand grains. Associated with the feeding pellets are distinctive, delicate, scratch traces on the sand flats. Neither the pellets nor the scratch traces survive submergence by the rising tide.

Trails resembling tire treadmarks are produced by small sand dollars (Mellita longifissa) that plow around the tidal flats just below the sediment surface, presumably grazing on algae on sand grains.

Worms of various types are abundant, but few produce surface traces. Tiny, green, phyllodocid polychaetes create ephemeral trails in shallow pools of standing water at low tide, but these are too delicate to be preserved throughout a tidal cycle. Burrowing arenicolid polychaetes and balanoglossid hemichordates excrete long, coiled strings of feces, and certain holothurroids excrete distinctive, knotted strings of feces. Such fecal strings occasionally will persist through a tidal cycle if wave energy is not too high.

In general, surface tracks and trails have a low preservation potential, as do pellets and fecal material strewn about the tidal flats.

Burrows and Dwelling Tubes

Biogenic structures created by infaunal organisms have an excellent preservation potential. Dwelling and feeding burrows are produced mainly by crustaceans, worms, and bivalves. The salt-marsh crabs all are active burrowers; Uca creates an unbranched but often rather deep burrow, whereas Eurytium constructs a large, shallow, "Thalassinoides-like" Y-branched burrow system (P. Buettner, pers. comm.).

In the muddy-sand firmgrounds of the high intertidal zone, Uca makes straight or curved, unbranched burrows, as it does in the salt marsh. Upogebia, on the other hand, constructs highly branched burrow systems that are perfect Thalassinoides boxworks (i.e., dense networks of Y-branched burrows three-

dimensionally oriented). Countless tiny openings link the burrows with the sediment surface and create a "squishy" sound when one trods upon the sediment.

In clean, fine sand of the high intertidal sand flats, other ghost shrimp (Callianassa sp.) create branched burrow systems that differ geometrically from those of Upogebia. Callianassa burrows are predominantly vertical in orientation, with some horizontal tunnels branching off the main shaft at enlarged nodes. A narrow shaft at the upper end connects the main part of the burrow system with the water-sediment interface. On the sediment surface, conical mounds mark excurrent openings from the burrow, and these typically are littered with rodlike fecal pellets produced by Callianassa. Incurrent openings to the burrow are marked by shallow conical pits. Unlike Callianassa burrows along other coasts, those here are unpebbled and thus are not similar to the trace fossil Ophiomorpha as are the burrows of C. major along the U.S. Atlantic coast, for example.

Burrowing bivalves are not as common in Bahia la Choya and Estero Morua as in other intertidal faunal provinces. Various Chione species are shallow burrowers in sand, often in sand-filled tidal channels. Their burrows resemble the trace fossil Pelecypodichnus (=Lockeia). Deep-burrowing Tagelus create straight vertical burrows several times their shell length. Paired openings at the sediment surface testify to the presence of Tagelus burrows.

Burrowing worms, including mostly annelids but also nemertines and enteropneusts, are abundant and diverse in the Puerto Penasco tidal flats, but there has been no detailed study of their traces. Some worms, such as the large polychaete Arenicola sp., build U-shaped burrows with paired openings at the sediment surface. A tongue-shaped mucus-feeding trap may be found at the incurrent opening to an Arenicola burrow, and a distinctively coiled pile of fecal strings typically occurs at the exit from the burrow.

Other worms construct agglutinated dwelling tubes, which have a good potential for preservation. The polychaete Onuphis microcephala, for example, builds straight, vertical, soda-straw-like tubes from well-sorted fine sand; these are common along point bars of sandy tidal channels. Its close relative Diopatra splendidissima, which lives in higher energy subenvironments where tidal currents are strongest, constructs distinctive vertical tubes from coarse bits of flat shell debris and even blades of grass. Construction of identical tubes by the related species D. cuprea along the U.S. Atlantic coast has been described in detail by Myers (1970, 1972).

Bioerosion and Borings

Bioerosion structures are abundant and diverse in the intertidal realm in the Puerto Penasco region. Surficial rasping traces produced by the radulas of algal-grazing epifaunal gastropods and, to a much lesser extent, chitons are common on exposed limestone; granite and basalt, of course, are unbioeroded. Dwelling structures created by infaunal borers are much more prominent than surface bioerosion traces.

Boring sponges are common throughout the area; only Cliona celata and C. vestifia have been identified with certainty, but several other clionid species probably are present as well (R. Stearley, pers. comm.). Cliona creates a spectacular geometric network of tiny chambers in calcareous substrates (mostly mollusc shells). Such sponge borings in the trace-fossil record are known as Entobia. Bioerosion proceeds as the sponge sends exploratory filaments into the calcareous substrate and then excavates chambers

by chemically isolating and mechanically removing minute chips. The surface of a sponge-infested shell may appear to be covered with countless tiny (1- to 2-mm-diameter) yellow or orange spots; actually these are portions of a single clionid sponge that protrude from the many external apertures to an extensive network of chambers inside the shell.

Numerous worms bore into calcareous substrates, but only a few species of endolithic sipunculids and polychaete annelids in this area have been studied. All apparently excavate long, finger-shaped or club-shaped borings resembling the trace fossil Trypanites. Stearley (in prep.) studied bioerosion by the common intertidal sipunculids Phascolosoma perlucens and Themiste lissum. The former produced J-shaped borings oriented perpendicular to the substrate surface; the latter creates club-shaped borings oriented oblique to the substrate surface. Pepe (1983) observed the boring habits of the intertidal polychaete Eunice afra, and he estimated an annual bioerosion rate of more than 100 cm³ of material removed per m² of exposed substrate by this one species.

Perhaps the greatest magnitude of bioerosion in this region is accomplished by boring bivalves. Various species of the siphonate mytilid Lithophaga (L. aristata, L. attenuata, and L. spatiosa) are the most prominent and abundant, although other endolithic bivalves (e.g., Gastrochaena ovata) also are locally common (R. Stearley, pers. comm.). These are primarily chemical borers in pure calcareous substrates, producing flask-shaped borings that resemble the trace fossil Gastrochaenolites. The borings are lined with an aragonitic sheath that is secreted by the siphonal tissues of the animal. In situations where shifting sand commonly buries the bivalve-infested rock under a thin blanket of sediment, the Lithophaga or Gastrochaena may build a hard siphonal chimney that extends for several millimeters (or even centimeters) above the rock surface, so that the animal's siphons do not become clogged.

Petricola denticulata and Pholas chiloensis are mechanically boring bivalves that use their coarse shell sculpture to excavate flask-shaped borings in loosely cemented calcarenite and coquina. Like the borings of Lithophaga and Gastrochaena, these structures morphologically resemble the trace fossil Gastrochaenolites, but they lack the aragonitic sheath and external chimney of the chemical borers' dwelling structures.

Some common endolithic bivalves, such as Cardita affinis and Diplodonta subquadrata, are not true borers because they do not excavate their own dwellings (R. Stearley, pers. comm.). Rather, they are nestlers that live in crevices beneath the surface of the rock or in borings created by other bivalves. Sometimes they modify the crevices or borings in which they live by mechanical abrasion or simple shell growth, but they are not considered to be active borers.

ACKNOWLEDGMENTS

We thank Keith Meldahl for his review of the manuscript, Jo Ann Overs for the speedy application of her word-processing skills, and Peggy Turk and Rick Boyer for their continuing hospitality. K.W.F. is grateful to Franz Fürsich and all the Geos. 470 students for sharing their ideas and observations. A portion of the work was supported by a University of Utah Research Committee grant (to A.A.E.).

REFERENCES CITED

- Anderson, D.L., 1971, The San Andreas Fault: Scientific American, v. 225, no. 5, p. 52-68.
- Beckvar, N., 1986, Stratigraphy, taphonomy, and fauna-substrate associations in a Gulf of California Pleistocene marine terrace near Punta Chueca, Sonora, Mexico [M.S. prepublication manuscript]: Tucson, University of Arizona, 98 p.
- Beckvar, N., Norris, R., and Suter, S., 1985, Keys to the shells of Bahia Cholla, Sonora: University of Arizona, unpublished manuscript, 46 p.
- Bernat, M., Gaven, C., and Ortleib, L., 1980, Datation de dépôts littoraux du dernier Interglaciaire (Sangamon) sur la cote orientale du Golfe de Californie, Mexique: Société Géologique de France Bulletin, ser. 7, v. 22, no. 2, p. 219-224.
- Brusca, R.C., 1980, Common intertidal invertebrates of the Gulf of California: Tucson, University of Arizona Press, 513 p.
- Chronic, H., 1983, Roadside geology of Arizona: Missoula, Montana Press, 314 p.
- Curry, J.R., Moore, D.G., Aguayo, J.E., Aubry, M. P., Einsele, G., Fornari, D., Gieskes, J., Guerrero-Garcia, J., Kastner, M., Kelts, K., Lyle, M., Matoba, Y., Molina-Cruz, A., Niemitz, J., Saunders, A., Schrader, H., Simonett, B.R.T., and Vacquier, V., 1982, Guaymas Basin: Sites 477, 478, and 481, in Curry, J.R., and others, Initial reports of the Deep Sea Drilling Project, v. 64, pt. 1: Washington, U.S. Government Printing Office, p. 211-415.
- Ekdale, A.A., 1978, Holocene ichnofacies from the northern Gulf of California and possible analogues in the Cretaceous of Utah [abs.]: American Association of Petroleum Geologists and Society of Economic Paleontologists and Mineralogists -- Rocky Mountain Section, Annual Meeting, Salt Lake City, p. 24.
- Ekdale, A.A., Bromley, R.G., and Pemberton, S.G., 1984, Ichnology -- trace fossils in sedimentology and stratigraphy: Society of Economic Paleontologists and Mineralogists Short Course Notes 15, 317 p.
- Flessa, K.W., and Brown, T., 1983, Selective solution of macroinvertebrate calcareous hard parts -- a laboratory study: Lethaia, v. 16, p. 193-205.
- Hertlein, L.G., and Emerson, W.K., 1956, Marine Pleistocene invertebrates from near Puerto Peñasco, Sonora, Mexico: Transactions of the San Diego Society of Natural History, v. 12, p. 154-175.
- Jones, P.L., 1975, Petrology and petrography of beach-rock (Pleistocene?), Sonoran coast, northern Gulf of California [M.S. thesis]: Tucson, University of Arizona, 47 p.
- Keen, A.M., 1971, Seashells of tropical west America, 2nd ed.: Palo Alto, Stanford University Press, 1064 p.
- Larson, R.L., Menard, H.W., and Smith, S.M., 1968, Gulf of California; a result of ocean-floor spreading and transform faulting: Science, v. 161, p. 781-784.
- Lynch, D.J., II., 1981, Genesis and geochronology of alkaline volcanism in the Pinacate volcanic field, northwestern Sonora, Mexico [Ph.D. thesis]: Tucson, University of Arizona, 248 p.
- McKee, E.D., 1957, Primary structures in some recent sediments (U.S. and Mexico): American Association of Petroleum Geologists Bulletin, v. 41, p. 1704-1747.
- _____, 1965, Experiments on ripple lamination, in Middleton, G.V., ed., Primary sedimentary struc-

- tures and their hydrodynamic interpretation: Society of Economic Geologists and Mineralogists Special Publication 12, p. 66-83.
- Meldahl, K.H., 1987, Sedimentologic, stratigraphic, and taphonomic implications of biogenic stratification: *Palaios*, v. 2 (in press).
- Moore, D.G., and Curray, J.R., 1982, Objectives of drilling on young passive continental margins; application to the Gulf of California, in Curray, J.R., and others, Initial reports of the Deep Sea Drilling Project, v. 64, pt. 1: Washington, U.S. Government Printing Office, p. 27-34.
- Myers, A.C., 1970, Some ichnological observations on the tube of *Diopatra cuprea* (Bosc.); Polychaeta, Onuphidae, in Crimes, T.P., and Harper, J.C., eds., Trace fossils: Liverpool, Seel House Press, p. 331-334.
- _____ 1972, Tube-worm-sediment relationships of *Diopatra cuprea* (Polychaeta: Onuphidae): *Marine Biology*, v. 11, p. 255-261.
- Ortleib, L., 1981a, Recent investigations on Quaternary geology of the coast of central Sonora, Mexico, in Ortleib, L., and Roldan, J., eds., *Geology of northwestern Mexico and southern Arizona, field guides and papers: Hermosillo, Mexico*, Instituto Geologia, Universidad Nacional Autónoma de México, p. 137-149.
- _____ 1981b, Pleistocene interglacial high stands of sea level in the Gulf of California: *Geological Society of America Abstracts with Programs*, v. 13, p. 99.
- Pepe, P., 1983, Bioerosion by a polychaete annelid, *Eunice afra* Peters, at Puerto Penasco, Gulf of California, Mexico [Ph.D. thesis]: Los Angeles, University of Southern California, 179 p.
- Rose, M.W., 1975, Sedimentology of Estero la Cholla, northwest coast of Sonora, Mexico [M.S. thesis]: Tucson, University of Arizona, 99 p.
- Sandusky, C.L., 1969, Sedimentology of Estero Marua, Sonora, Mexico [M.S. thesis]: Tucson, University of Arizona, 84 p.
- Stearley, R.F., and Ekdale, A.A., 1984, Bioerosion in the rocky intertidal zone of the northern Gulf of California [abs.]: American Association of Petroleum Geologists and Society of Economic Paleontologists and Mineralogists -- Rocky Mountain Section, Annual Meeting, Salt Lake City, p. 20.
- _____ 1986, Effects of periodic burial and exhumation by storms on endolithic communities, northern Gulf of California [abs.]: American Association of Petroleum Geologists and Society of Economic Paleontologists and Mineralogists, Annual Meeting, Atlanta, p. 651-652.
- Stump, T.E., 1975, Pleistocene molluscan paleoecology and community structure of the Puerto Libertad region, Sonora, Mexico: *Palaeogeography, Palaeoclimatology, Palaeoecology*, v. 17, p. 177-226.
- Van Andel, T.H., 1964, Recent marine sediments of the Gulf of California, in Van Andel, T.H., and Shor, G.G., Jr., eds., *Marine geology of the Gulf of California: American Association of Petroleum Geologists Memoir 3*, p. 216-310.
- Watson, M.E., 1979, Post-mortem effects on molluscan assemblages in a tidal flat environment [M.S. prepublication manuscript]: Tucson, University of Arizona, 31 p.

Volcanic Structures and Alkaline Rocks in the Pinacate Volcanic Field of Sonora, Mexico

Daniel J. Lynch II
Laboratory of Isotope Geochemistry
Department of Geosciences
University of Arizona
Tucson, Arizona 85721

James T. Gutmann
Department of Earth and Environmental Sciences
Wesleyan University
Middletown, Connecticut 06457

INTRODUCTION

Pinacate is a typical continental alkali basalt cinder-cone field (Figure 1) that has an exceptionally diverse assemblage of volcanic landforms. Two alkalic rock series make up the field; one constitutes the more than 500 Pinacate monogenetic volcanoes and the other forms the Santa Clara composite volcanic mountain. The purpose of this field trip is to examine some of the landforms and structures and the rocks of which they are made. The first full day entails a climb to the top of the Santa Clara trachyte shield volcano for a view of the entire volcanic field and the surrounding desert. The second day involves transit to Crater Elegante maar volcano and a hike part way into its interior where normally hidden volcanic features are exposed in the walls. Day three will include visits to the intriguing Tecolote cinder cone and to the Cerro Colorado tuff cone.

Volcanoes have been active sporadically here for the past 2-3 million years (Lynch, 1981). Santa Clara rock ages range from 1.7 ± 0.1 to 1.1 ± 0.1 Ma; volcanism on the shield is extinct. The Pinacate monogenetic basalt-hawaiite volcanism began earlier than 1.2 Ma and is only dormant. Volcanism in Pinacate has been coeval with generation of sea-floor basalt at spreading centers in the nearby Gulf of California, but there is no obvious link between them.

The rocks of Volcan Santa Clara constitute an entire alkaline differentiation series. Basalt, hawaiite, mugearite, benmoreite, and trachyte occur in that stratigraphic order. Compositions of olivine, clinopyroxene, Ti-magnetite, and plagioclase found in gabbro nodules dredged up by Pinacate cinder-cone eruptions on the Santa Clara summit can be subtracted in magma-mixing programs to show the possible derivation of the successive rock compositions.

Santa Clara appears to have been derived from a large batch of magma as it differentiated mainly by fractional crystallization, producing a series of eruptions through a central conduit system. The magma body was tapped at various stages in its history to yield the Santa Clara series of alkaline rocks in nearly ideal stratigraphic order.

Basalts and hawaiites of the Pinacate monogenetic volcanoes mantle most of Santa Clara and extend out into the surrounding desert. The Pinacate rocks are typically porphyritic; many contain conspicuously large megacrysts of labradorite, augite, and olivine. Their compositions form tighter groupings on variation

diagrams (Figure 2) than do those of the Santa Clara rocks. Each Pinacate cone may represent eruption from one of hundreds of discrete, small magma bodies that formed at different times and places beneath the field.

Pinacate lacks well-defined cone-group alignments. Although the long axis of the field is north-south and the majority of eruptive centers lie within 8 km either side of this axis, cone placement appears to be random.

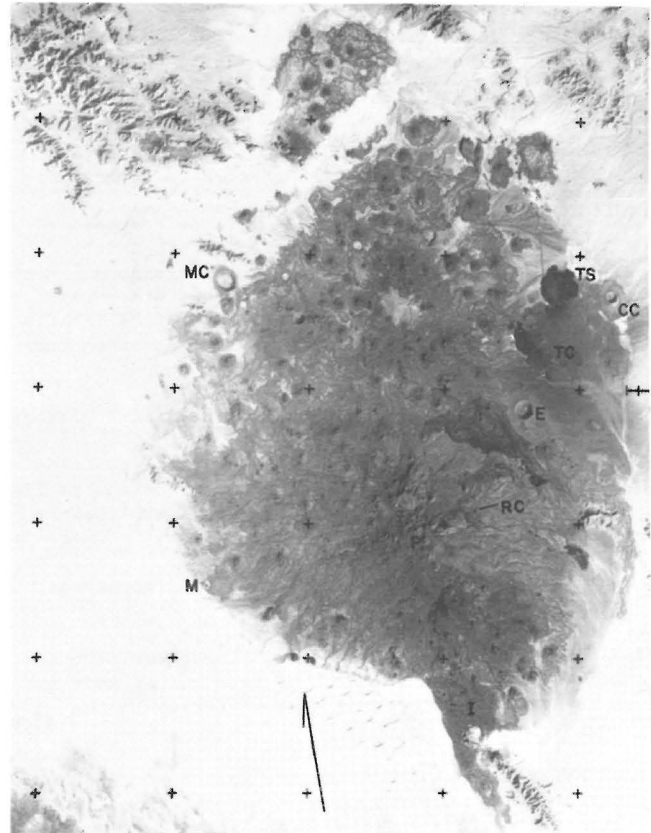


FIGURE 1. PINACATE FROM EARTH ORBIT. Lighter tones near "P" are rocks of Volcan Santa Clara. I- Ives flow, M- Moon Crater, P- Pinacate Peak, RC- Red Cone Camp, E- Crater Elegante, TC- Tecolote, CC- Cerro Colorado, TS- Tesonle, MC- MacDougal Maar. North arrow is 10 km long. Image courtesy NASA.

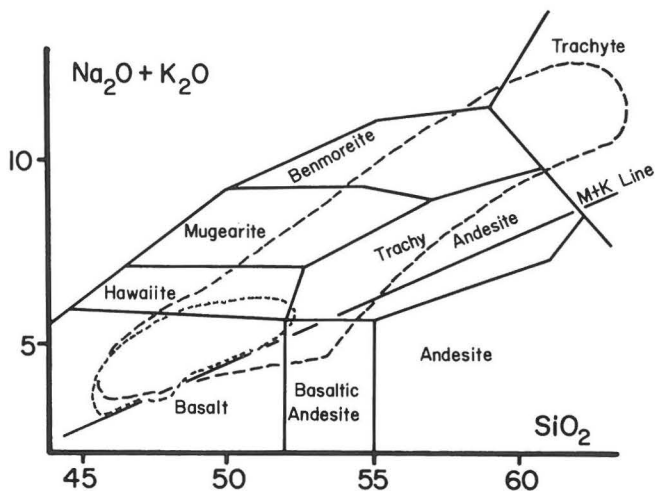


FIGURE 2. ALKALI-SILICA DIAGRAM OF PINACATE VOLCANIC FIELD ROCKS. Long dashes surround the compositional field of Santa Clara rocks, short dashes enclose rocks of Pinacate monogenetic volcanoes. Rock names from LeBas and others (1986), data from Lynch (1981 and unpub.), some Pinacate analyses from Donnelly (1974).

ACCESS TO PINACATE

This field trip will depart Phoenix late in the afternoon and most of the drive to camp will be in the dark. This road log identifying features between Sonoyta and Red Cone Camp (Figure 3) is for later users. Road-log distances are in miles.

- 0.0 Highway 2 bridge over Rio de Sonoyta. Check in with the ranger before taking Rt. 8 to Pinacate.
- 11.1 The Sierra Cipriano on the left is composed of a leucogranite apophysis of the batholith in the aerial gunnery range of southwestern Arizona. Rocks collected at this site and in various other parts of the batholith yield K-Ar ages around 53 Ma (Shafiqullah and others, 1980), an age of intrusion corroborated by Rb-Sr isochrons (Damon, unpub.).
- 13.0 The shield of Volcan Santa Clara is at 2 o'clock.
- 20.4 North end of the Sierra de San Francisco. The dunes on both sides of the road here contain aeolian dust from the far side of Pinacate, stabilized by desert plants.
- 25.4 Road to Micro-ondas San Pedro. The uppermost flow has an age of 12.6 ± 0.3 Ma.
- 31.3 Rio de Sonoyta - 2 bridges. The river occupies a well-defined channel north of here but spreads into a series of anastomosing distributaries to the south.
- 31.8 Ejido Nayarit and Ejido Los Nortenos. The agriculture that supports these communities east of Pinacate depends on water pumped from deep wells in the sediment of the valleys. The paved road goes on to Puerto Peñasco. Turn north onto the dirt "East Side" road. This road connects with Highway 2 at "El Pinacate" 30 miles west of Sonoyta.
- 32.1 Road fork, bear left.

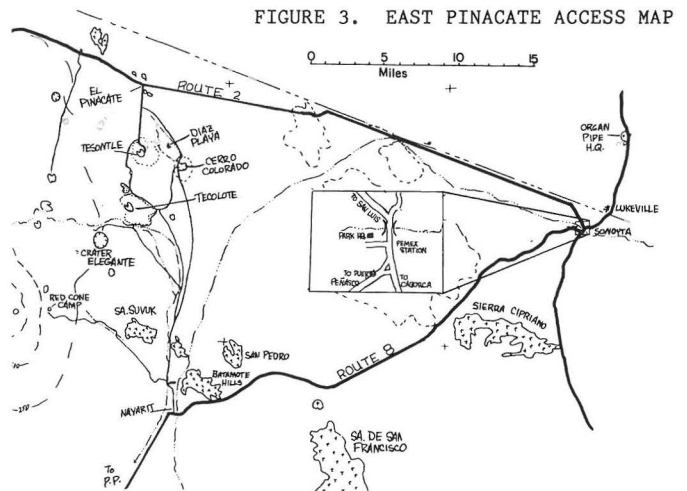


FIGURE 3. EAST PINACATE ACCESS MAP

- 33.5 Outcrop of Mid-Tertiary basalt possibly contemporaneous with the basalt of Micro-ondas San Pedro. "Diaz Wash," the main drainage for northeastern Pinacate, lies at its western end. This wash never joins with Rio de Sonoyta.
- 33.7 Cross the wash.
- 33.8 Summit road intersection, turn west. Drive directly toward the mountain; do not make any major turns until you are on a lava surface.
- 34.5 West edge of basalt flow designated #452 on Donnelly's (1974) geologic map.
- 38.5 Road intersection at a large ironwood tree; turn right, up the wash. The road follows segments of wash from here to the lava flow, and it can be wiped out by heavy runoff. It may be necessary to walk to the lava flow on the north, find the road there, and backtrack to your vehicle.
- 38.9 Edge of the lava north of the wash.
- 40.0 Cross a deep, possibly soft, 5-m-wide wash.
- 46.6 Red Cone, the base camp. An alluvial fan of Carnegie cinder here provides a comfortable place to sleep. Scramble up the cone or the flow edge to see a spectacular panorama; the best time is just after sunrise. Pinacate Peak can't be seen from camp.

DAY 1 - HIKE TO THE SUMMIT

Pinacate Peak, a cinder cone on the top of Volcan Santa Clara, can be reached in about 5 hours from Red Cone Camp. Direct hiking distance is 6 km with a total elevation gain of 780 m (2500 ft) from the campsite to the summit. This direct route, which passes many key outcrops of the Santa Clara rock series, is almost entirely on lavas and cinder of the young Carnegie volcano. The hike is not easy; most steep hillslopes are loose soft cinder and many slabs on the young lava surfaces are precariously balanced. WARNING: 2 liters of water may be barely enough if the day gets hot!

Climb up the road ramp in the cliff above the fan, follow the road about 50 m, cross the wash, and climb south onto the edge of the lava flow. Find a convenient place to view the flank of the mountain.

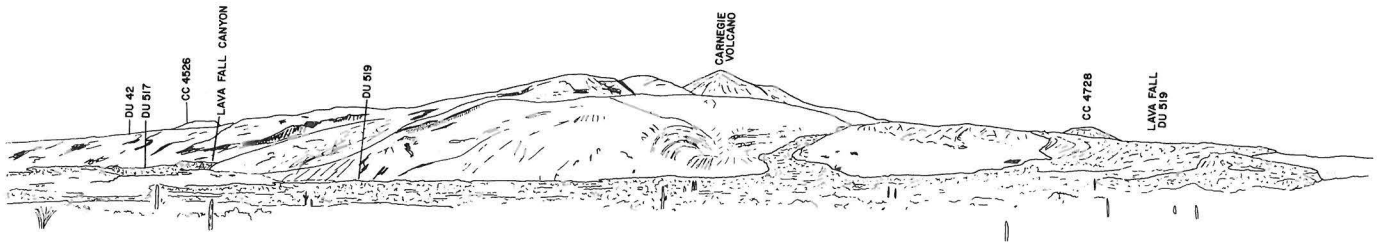


FIGURE 4. EAST FLANK PANORAMA. A slope break between "lower" and "upper" Santa Clara (foreground) occurs on both east and west flanks of the mountain. "DU" numbers are from Donnelly's (1974) geologic map. Drawn from photographs by DJL.

Stop 1

Two major elements of Pinacate geology are obvious (Figure 4): the shield massif of Volcan Santa Clara, and the young lavas and tephra from Carnegie cone, the highest point on the horizon.

The camp at Red Cone is on "Lower Santa Clara," which extends from the desert floor at 150-m altitude to the slope break ahead at 500 m. Its slopes constitute a piedmont to the steeper and more deeply dissected "Upper Santa Clara." Santa Clara flow units dip less than 10° , a principal characteristic of the trachyte shield volcano type (Webb and Weaver, 1976). Note the difficulty of tracing individual rock units across the face of the mountain from ridge to ridge.

The same deep erosion that presently cuts the mountain flanks existed during the construction of Santa Clara; lavas flowed down canyons, creating geometrically complex contacts between units. As an example, a trachyte of 1.14 ± 0.03 Ma age crops out on the piedmont in the foreground, topographically below outcrops of the oldest exposed members of the series.

Erosion appears to be slow. The mountain flank to the south is covered with Donnelly's unit 42, a basalt of 0.87 ± 0.03 Ma age (Figures 5 and 6). The topography beneath this flow is preserved and has not changed in that considerable period of time.

Carnegie volcano sits atop the western end of a 2-km-long, N70W fissure, the source of several basalt flows. The extensive cinder blanket that covers the summit platform and extends down the northern and eastern flanks of Santa Clara appears to have originated at Carnegie (Figure 5). The three flows that extruded after the main cone-building phase of eruption cross this cinder and are not covered by it. These flows have both aa and pahoehoe surface structures that are described at the next few stops.

The relationships between flow units shown in Figure 5 are complex. The youngest rocks are the darkest. The flow from the "Pahoehoe Jungle" vent (Stop 2) forms the prominent broad lava fall on the flank (left). A separate dark flow extends out from the mouth of Lava Fall Canyon in the distance (our next goal). These two flow units coalesced on the piedmont and poured into

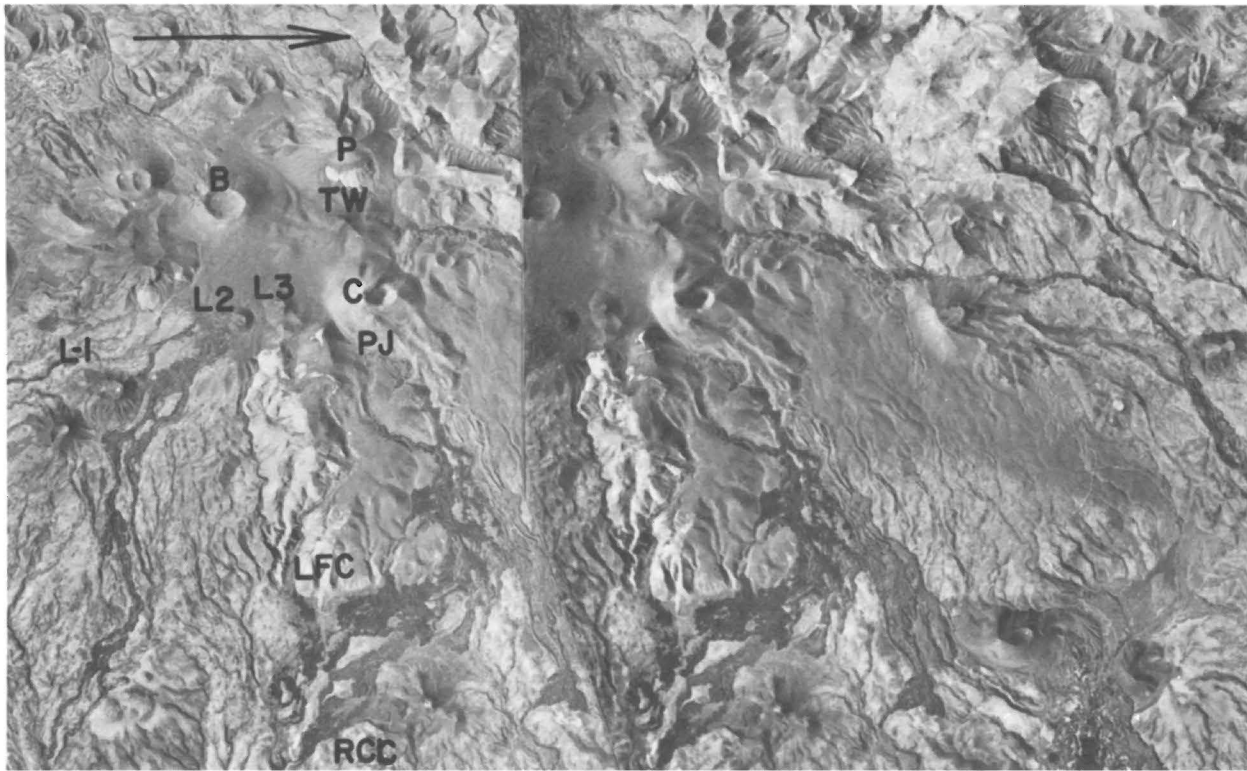


FIGURE 5. STEREO PHOTOGRAPH OF THE EAST FLANK. P- Pinacate Peak, TW- Trachyte Wall, B- Bonillas, L-1,2,3 - Vents on the Lumholtz N20W fissure, C- Carnegie, PJ- pahoehoe jungle, LFC- Lava Fall Canyon, RCC- Red Cone Camp. Distribution of cinder around the summit area, including the NNE feather, is obvious. North arrow is 2 km long.



FIGURE 6. SOUTHEAST FLANK OF VOLCAN SANTA CLARA. Santa Clara rocks are the lightest tones (top right). The gray lava below them is DU 42, which mantled the topography $0.87 \pm .03$ Ma. Three vents on the Lumholtz fissure are visible at the source of the youngest (darkest) lavas; a fourth vent is just out of the picture on the lower left.

an arroyo cut in lower Santa Clara. The magma, insulated by the arroyo walls, was able to flow an additional 10 km out to the desert floor. Another dark unit from the west base of Carnegie extends west and north, 7 km down an arroyo.

The basalt at Stop 1 is gray in Figure 5 and appears on close examination to be more weathered than the darker basalt; points and corners are not as sharp. The appearance of the lava at stop 1 is similar to that of the extensive flows with prominent lava levees (Figure 7) that also seem to have come from Carnegie. Unfortunately, neither the black nor the gray lavas have accumulated sufficient aeolian material to permit use of soil development as a clue to relative age.

The north wall of Carnegie collapsed during the eruption in a debris-flow avalanche down the flank of Santa Clara (Figure 7) and was then partially rebuilt. The failure occurred directly above the lava-leveed gray flow units, suggesting that they might have been involved. Cone-wall breachment is common in Pinacate cinder cones (Gutmann, 1979), but this debris avalanche is unique. If the gray flows are older than Carnegie and came possibly from Bonillas cone to the southwest, the juxtaposition is coincidental.

Choose your own route across the upper piedmont to Lava Fall Canyon. Between this flow and the canyon flow is an alluvial surface littered with hard, pedogenic carbonate and detritus from Santa Clara deposited atop both Carnegie basalt and Santa Clara trachytes. As you walk across nearly any Pinacate land surface, you may notice fragments of phenocrysts that look like pieces of broken glass.

The lava surface at the mouth of Lava Fall Canyon is all accretionary balls, a common aa surface type. A short segment of Indian trail is visible crossing the lava here. Boulders fallen from the walls litter the lava surface and a mound of alluvial detritus covers the center of the flow in the lower part of the canyon.

The south canyon wall contains three Santa Clara units. The oldest and most primitive rock so far discovered in the series, a basalt of 1.70 ± 0.04 Ma age, crops out at the base of the lowest lava fall. The massive flow unit above it is a mugearite of 1.45 ± 0.03 Ma age. Above that, the ridge-crest unit is a trachyte of 1.26 ± 0.03 Ma age. All the dates are from Lynch (1981).

As you climb the young basalt of the lava fall, note the shear structures and the large accretionary balls welded into the slope. The old lava channel is now an abraded runoff chute, an easy place to climb.

A line of spatter cones (Figure 8) was built on the canyon wall where the Carnegie fissure intersected the surface. The considerable flow of basalt that effused from this vent can be traced onto the piedmont to a place about 1.5 km from the canyon mouth where it coalesced with the flow at lower left in Figure 7.

The best route from the vents is up the opposite (north) side of the canyon, not directly toward Carnegie. Look south from this canyon edge to see the massive trachyte flow/dome that forms the ridge. This is the youngest dated Santa Clara rock with an age of 1.1 ± 0.1 Ma. Climb the cinder-covered slope headed toward Carnegie.

Many Pinacate volcanic units contain megacrysts of labradorite, augite, olivine, and rarely titanomagnetite. The labradorite megacrysts can contain tubular voids up to several millimeters long. These voids are primary inclusions (Gutmann, 1974) representing fluid either exsolved from boundary-layer liquid or, more probably, derived by coalescence of CO_2 -rich bubbles. Many phenocrysts in Pinacate lavas were resorbed, whereas many others exhibit skeletal textures. Skeletal morphologies occur among megacrysts more than 1 cm long. The labradorite megacrysts typically are rounded by resorption, but others are perfectly euhedral and riddled with inclusions of basaltic glass. Pinacate megacrysts evidently have various histories. You may find megacrysts in the cinders between here and the peak and in many other places in Pinacate.

Stop 2 - The Pahoehoe Jungle

Basalt effused from a segment of fissure marked by another line of spatter cones (Figure 9) as well as from the side of the cone. Discontinuous sections of lava-tube cave are open through apertures that are rimmed with smooth pahoehoe spatter. Some of them have large bee nests under lava slabs. The stop is at "Iitoi's Cave," a place of worship for the indigenous peoples until the 1930's (Ives, 1942). The trail encountered lower down leads to this place.



FIGURE 7. CARNEGIE CONE AND THE LAVA FALL. The dark, cinder-free lavas in the foreground issued from the fissure at the east cone base. Adjacent on the right are the cinder-covered flows with the prominent lava levees that may have contributed to failure of the cone wall in the prominent debris flow.

Unusual features that Lynch (1981) called "pahoehoe spatter tubes" extend down the sides of some hornitoes. Small blobs of magma spattered off the surfaces of narrow streams flowing down the flanks of the hornitoes and welded to form thin, parallel walls on the sides of the streams. The walls built upward and some joined overhead to enclose the tubes. Similar structures are found on the Ives and Baroque flows.

The route from here is northwest, around the base of Carnegie over the debris flow. Climb diagonally to the right, up the cinder wall above the pahoehoe. Move westward atop the debris flow toward the opposite steep cone wall. On reaching the western edge of the debris flow, traverse across the slope of the cone, climbing slightly upward along the developing trail. Go through the pass to the complex fissure-vent source of the Carnegie-west lava at the west base of the cone wall (Figure 10). You will find superb slab-chaos pahoehoe above the slope break where this flow tumbled over the lip of the hill, changing to aa. Follow the wash westward toward the saddle north of the peak cone. It looks high because you have 220 m more to climb.

Ascent is easier hopping across the boulders on the north side of the valley rather than by slogging through the cinder on the south. On the ridge crest above, flow laminations in trachyte change dip from vertical to horizontal. This ridge might be on the north side of a main Santa Clara vent. The crystalline rock of this wall grades into vitrophyre on Big Horn Ram Ridge to the north.

Climb toward the summit after reaching the saddle. This part of Pinacate Peak cone is littered with gabbro nodules that are probably fragments of the cumulate that resulted from fractional crystallization in the Santa Clara magma body (Lynch, 1981).

Stop 3 - The Summit

At your feet are the more than 500 cinder-cone volcanoes of Pinacate (Figure 11). The range of their ages is obvious from the widely differing erosional morphologies they display. North is toward the prominent contact between the light "Gunnery Range" granite and dark Precambrian rocks of the Sierra Pintada (actual azimuth 359) 60 km away. Below that is the sand belt of MacDougal Pass (25-30 km), which separates the northern section of the field in Arizona from the main part in Sonora. Baboquivari Peak, 180 km due east of



FIGURE 8. SPATTER CONES EAST OF CARNEGIE. A 25-m-long fissure was the source of DU 517. These spatter cones have a wealth of pahoehoe vent features. DJL



FIGURE 9. SOUTHEAST BASE OF CARNEGIE VOLCANO. Thick deposits of cinder lie atop the lava-levees and another fresh flow apparently from Carnegie (lower right). The route down is through the pass on the left of the cone.

Pinacate Peak, can be seen to the right of Carnegie summit only on the best of days. The black area out on the desert flat above the Lumholtz cones is the distal end of the Carnegie flow. The adjacent white area is sediment it has impounded.

The Lumholtz cones, about 1500 m distant on the east edge of the summit platform, are two of four vents on a 1200-m, N20W fissure. These cones are of the same erosional state as Carnegie but appear to be older because Carnegie cinder lies on their lavas (Figure 6).

Ives (1966) reconstructed Kino's travels and reported that he or his companion Manje claimed to have seen the Colorado-Gila River junction from some point in the field and to have determined from this observation that Baja California is not an island. The river junction is 142 km from the summit on the same azimuth as La Jarapena and behind the Sierra del Viejo, neither visible from here nor from the Hornaday Mountains, Ives' deduced location of Manje's vantage point. The mouth of the Colorado River is 133 km from the summit, exactly on the horizon. Kino thought he could see these things, but the geometry precludes it.

Back Down The Hill

The easiest path off the summit is toward the south; aim first for the summit of Bonillas cone and curve left while descending. This avoids the upper parts of the Trachyte wall making the descent a quick, easy cinder slide. The direct route down is eastward, up across the ridge that extends between the "cliffy," eroded cone (0.41 ± 0.04 Ma age) and Bonillas cone. Bear sharply to the left after reaching the saddle, going toward Carnegie, to avoid crossing a cholla-choked cinder flat. Leave the summit platform through the pass east of Carnegie cone.

If time and ambition permit, Carnegie cone can be climbed from the west by ascending the north ridge, thence directly up the side of Carnegie. Getting off Carnegie is the same in any direction, loose and dangerous. Alternatively, one may climb the slopes of Bonillas for a view into its crater or go to the top of the closest Lumholtz cone.



FIGURE 10. BIG HORN RAM RIDGE AND WEST CARNEGIE. The west Carnegie flow may have come from the fissure or from beneath the cinder wall; a mound of tephra lies atop its proximal end. The prominent ridge top is a vitrophyre, the most evolved Santa Clara lava, that rests atop an agglomerate wedge. The horizontal unit beneath it is a benmoreite of 1.15 ± 0.03 Ma age.

The pass leads down to the hornito chain at the fissure above the Pahoehe Jungle (Figure 8). Cross the lava there and follow its south edge into the canyon. The agglutinate rim cliff above Red Cone

can be seen from high in this canyon. Use that, Sierra Suvuk, and the Batamote Hills as guides to find camp. Descend the series of slopes and benches; stay out of canyon bottoms below the highest bench. You will be able to see the lava chaos on the upper piedmont from the top of the last slope and you can adjust your route to avoid crossing it if you so desire.

=====

DAY 2 - TO CRATER ELEGANTE

- 46.6 From Red Cone Camp, return to Diaz Wash.
- 59.4 Diaz Wash intersection; turn left (north).
- 60.0 Chain-fruit cholla forest.
- 63.1 Bear left at fork; straight is to Cerro Colorado.
- 66.3 Bear left at fork; straight is to Tecolote.
- 67.0 "Semplaya," an extensive area of anastomosing distributary channels in a creosote flat on Salvatierra Wash.
- 68.9 Dos Mujeres cones on the left.
- 72.0 Intersection at Salvatierra Wash crossing - continue straight ahead.
- 73.3 Elegante parking area. Walk to the rim.

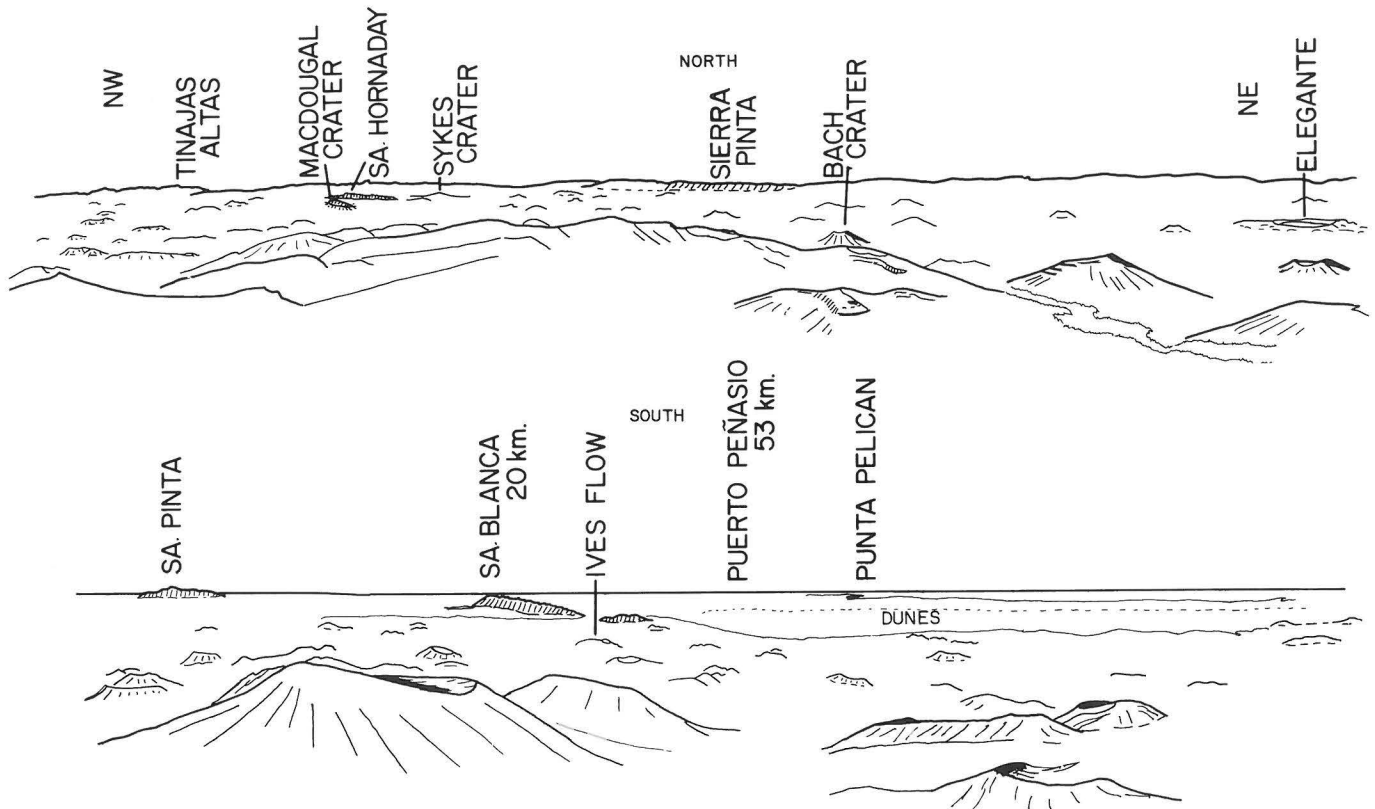


FIGURE 11. PANORAMIC DIAGRAM OF THE PINACATE VOLCANIC FIELD FROM THE SUMMIT. Drawn from photographs by DJL.

Stop 1 - Crater Elegante

Crater Elegante (Figure 12) is the largest of nine maars in Pinacate. It is 1600 m in diameter and 244 m deep. Gutmann (1976) described the geology of Crater Elegante and included geologic maps of the crater and of its walls; copies will be distributed to participants. The crater originated by collapse attendant upon hydromagmatic eruptions that deposited tuff breccia from pyroclastic-surge clouds.

The oldest lava flow exposed in the crater wall is a hawaiite of 0.5 ± 0.1 Ma age (all dates from Lynch, 1981). This flow and others above it come from unknown sources. Upon these is a flow from the largely buried cinder cone just south of the crater. Cinders from that cone appear in the southern crater walls resting on this flow, deformed by its motion, and overlain by similar, younger flows.

The cinder cone displayed in cross section in the eastern and southern walls of the crater (far wall in Figure 12) is above these flows. Two units from this cone yield K-Ar ages of 0.46 ± 0.05 and 0.43 ± 0.06 Ma. Up-dip projections of its layering indicate that its principal vent lay in the southeastern part of the maar, about where the floor meets the foot of the talus. The first unit erupted from this vent was a flow that baked and/or deformed the overlying cinders. This cone was breached on the southeast following emplacement of sills within the cone and along its base. Renewed eruptions then produced phenocryst-rich cinders, flows, and dikes.

Several more volcanic units were erupted prior to the cataclysmic eruption that produced the maar. A thick dike fed a shallow, sill-like intrusion and small flows (unit dp of Gutmann, 1976, Figure 3) that rest on the crystal-rich cinders in the breach of the cone. In the southeastern wall of the crater, a dike fed a tiny cinder cone with a lobate sill at its base.

Resting on these are younger cinders from a cone centered in the southern part of what is now the maar. Like their predecessors, these cinder eruptions were immediately preceded by effusion of a lava flow.

The maar-forming eruption began with effusion of a lava flow from a vent probably located near or somewhat northeast of the center of the crater. The age of this flow is 0.15 ± 0.02 Ma. Minor eruption of cinder may have followed this, but groundwater soon gained access to the conduit and the hydromagmatic eruptions began.

Chief constituents of the tuff breccia at the crater rim are vesicular pellets of glassy, juvenile ash rich in tiny crystals, accessory blocks of basalt torn from the vent walls, and quartzofeldspathic sand, silt, and clay from beneath the volcanic section. Accessory ejecta decrease rapidly in abundance with distance from the crater rim, whereas the abundance of silt and clay increases in that direction.

Unless the space into which collapse occurred was made by evacuation of a shallow magma chamber, the volume of ejecta originally deposited outside the crater must be at least as great as the volume of missing material. Thickness variation of the tuff breccia with distance from the rim indicates that ejecta equal to about one-third of crater volume were deposited between the rim and 1.3 km away from the rim. The trends of compositional change out to 1.3 km indicate that the distal parts of the deposit were chiefly fine-grained sediment and that this sediment was by far the most abundant constituent ejected from the crater. Evidently, the space into which collapse occurred was made chiefly by ejection of large quantities of unconsolidated sediment from beneath the volcanic section.

The estimated volume of accessory ejecta between the crater rim and 1.3 km away is 9 percent of the volume of the crater below the base of the tuff breccia. The tuff breccia contains abundant blocks petrographically unlike rocks exposed in the crater walls,

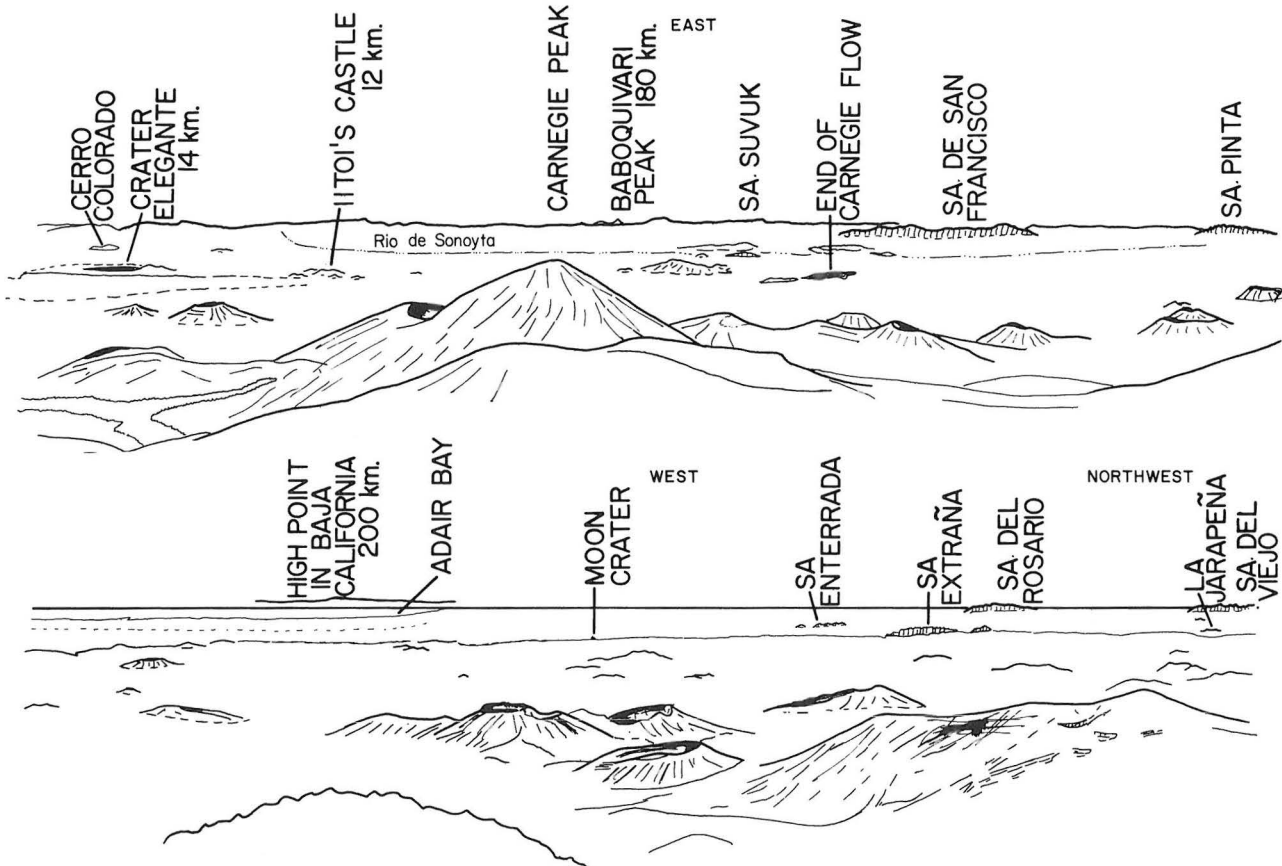




FIGURE 12. CRATER ELEGANTE FROM THE WEST. The blanket of tuff breccia forming the rim of the collapse depression partly buried the old cone on the right edge of the photo. Strata from that cone and two others are exposed in the crater walls. Salvatierra Wash is in the upper left.

suggesting that the thickness of the volcanic section is considerably greater than exposed. This thickness is not known, however, so the diameter of a hypothetical cylindrical vent cannot be calculated. In addition, many large volcanic blocks probably crumbled into the vent as it developed. Nevertheless, the position and structure of a large hill of tuff breccia cropping out on the crater floor deny the former existence of a vent more than 600–700 m in diameter. Furthermore, the paucity of accessory debris derived from the cinder cones indicates that the vent pierced only thin sections of cinder and places a comparable upper limit on vent size. Rather than crumbling piece-meal into a gigantic maw, the rocks of the crater and much overlying tuff breccia probably subsided more or less *en masse* as support was removed from beneath the volcanic section. Details of the process cannot be known, although subsidence doubtless was accompanied by extensive fracturing, and the inner parts of the pile may have begun to subside earlier than those near the crater walls.

The strata around the margins of the crater up to about 60 m above its floor are topset- and foreset-like deposits of sediment that accumulated in a pluvial lake.

Walk counterclockwise along the rim to a point due north from the center of the crater and descend to the base of the rim-bed section. AVOID THE EDGE OF THE CLIFFS – ESPECIALLY IN GROUPS.

Stop 2

Relationships between the lava flow and tuff breccia deposited on it while it was still mobile are well exposed at the base of the section here. Note the dike projecting up into and baking the tuff, the wavelike

bulge of the flow top and its peculiar shark-tooth texture (Figure 13), and the folds and faults in the lower 10 m of tuff breccia. Scattered quartzofeldspathic xenocrysts in the flow suggest that admixture of sediment with magma had already begun.

Return to the rim and walk clockwise to a point on azimuth 063 from the center of the crater.

Stop 3

Descend toward the base of the rim beds. According to Wohletz and Sheridan (1983), these thinly bedded tuff deposits with their abundant sandwave bed forms represent the relatively dry surges typical of basaltic tuff rings. Gray lapilli tuff about half way down through the section suggests that the supply of meteoric water and sediment temporarily diminished during the eruption. Excellent exposures occur further down the slope. A lens of breccia resting on cinders at the base of the section represents initial, vent-clearing explosions.

Walk south about 200 m along the base of the gray cinder section to a prominent dike.

Stop 4

This vertical dike was injected horizontally from the vent region of the cinder cone. Its horizontal crest is about 33 m above you and its keel is exposed just below you. Pulses of magma through the dike are recorded as successive chilled zones. These enclose a porphyritic zone exceptionally rich in labradorite megacrysts. This zone also contains numerous xenoliths; both they and the megacrysts may have been concentrated by flow differentiation. Rock comparably rich in coarse materials is absent from the upper parts

of the dike. It is possible that gravitational settling contributed to their concentration in the lower part. The core of the dike is occupied by an intrusion of chilled basalt that widens upward. PLEASE DO NOT MINE THE DIKE ANY FURTHER; SAMPLE THE LOOSE ROCKS INSTEAD.

Note the tan, tuffaceous layers in the cinder section here. These contain slightly palagonitized juvenile ash together with accidental sand and silt. They suggest incipient hydromagmatic activity that failed to lead to a major tuff eruption.

Return northward 50 m and ascend the first gully to the upper parts of the dike. These contain sheetlike megavesicles more than 1 m long with magma drips on their walls. The vesicles may be gravity-driven gas accumulations in the top of the dike. Note also the bifurcations of the dike crest in the cinder.

Return to the crater rim and continue clockwise to the edge of the scallop-shaped depression about 100 m beyond the highest point on the crater rim. Note the narrow dike feeding a sill and tiny cinder cone atop the south wall of the crater. Descend gradually into the Scallop to the upper parts of the cinder section on a 110° azimuth from the center of the crater (see Gutmann, 1976, Figure 3).

Stop 5

This depression began as a breach in the wall of the cinder cone. Masses of cinder were carried from the breach on a flow exposed on the flats east of the crater. Following breachment, the breach was partially filled as renewed eruptions produced phenocryst-rich, relatively dense bombs. A small flow of similar lava is exposed high in the northeastern part of the Scallop, and another flow occurs outside the crater southeast of the Scallop. Large, gem-quality labradorite crystals occur in these cinders as do rare clinopyroxene megacrysts. Clinopyroxene crystals from this locality as much as 1.8 cm long can exhibit sector zoning.



FIGURE 13. SHARK-TOOTH OR CORDUROY TEXTURE. This distinctive texture forms at the interface between fluid basalt and unconsolidated material like fresh tuff breccia or cinder. Grass clump is 15 cm high.

Return to the rim, continue clockwise to azimuth 167°, and descend through the tuff breccia and underlying cinders to the top of the highest flow.

Stop 6

These gray cinders were derived from a vent located out in what is now the crater. The flow beneath them carries the same phenocryst assemblage and rests on cinders from the old cone to the northeast. Where flow-top breccia is absent, the base of the overlying cinders is oxidized and indurated to form a resistant, red ledge a few centimeters thick. These cinders were baked by the underlying flow, effusion of which must have immediately preceded the cinder production.

Climb down over the flow, traverse a few meters westward, and descend the gully through the older cinders to the top of the cliffs. Exposed in this gully is a dike that is the upturned end of a sill emplaced along the base of the gray cinder cone. The cinders are deformed over the flow at the top of the cliffs here; this flow immediately preceded pyroclastic eruptions and is petrographically identical to a flow that bakes the base of the cinder section in the northern walls of the crater.

Return to the rim, walk back eastward to the 145° azimuth, and turn southward into the gully dissecting the outer slopes of the tuff breccia.

Stop 7

Displayed in the walls of this gully within a few hundred meters from the rim is a variety of pyroclastic-surge bed forms. Wohletz and Sheridan (1979) mapped the transition from sandwave facies through massive beds to planar bed facies progressing outward from the rim in this area. Look for low-angle cross-stratification, soft-sediment deformation features, and deflation structures in the tuff beds.

Return to the rim; walk counterclockwise along the rim to the road and down the road to the new camp.

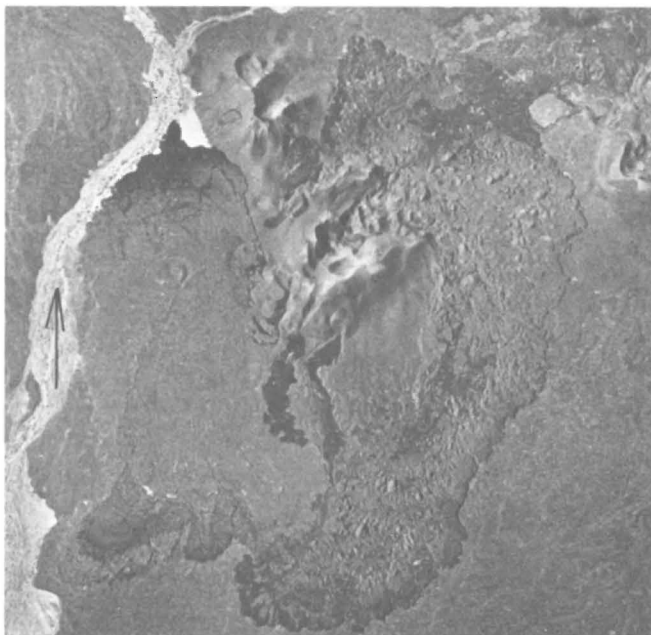


FIGURE 14. TECOLOTE VOLCANO. Flow S blocked Salvatierra Wash (bottom), diverting the water and trapping sediment in the white area on the left. The adjacent black lava appears to have flowed out from under the cinder deposited earlier atop the flow.



FIGURE 15. TECOLOTE FROM THE SOUTH. Mayo cone, slightly older, is 1 km to the north; Tesontle cone, possibly younger, is 5 km beyond that. The arrow points to the "Bus" bomb. Note the faults, the gullies inboard of flows A and B, the valley separating the cinder wedge from the main cone, two collapse depressions on the east rim, and an enigmatic "crater" on the slope in front of flow R (foreground). Peter Kresan copyright 1987.

DAY 3 - TECOLOTE VOLCANO

Tecolote Volcano is one of the youngest cones in Pinacate and is certainly one of the most complex of the small eruptive centers. A wealth of lava surface types and pyroclasts, including bombs of astounding size, are concentrated within its small area - most can be visited in an easy morning walk.

The volcano consists of a complex cone, six lava flows, and a cinder blanket (Figure 14). Contacts between adjacent flow units and between lava and cinder permit development of a crude eruption chronology. Tecolote cinder lies atop Mayo, the adjacent cone on the north, but the aa lavas from each volcano are nearly indistinguishable at their contact.

Tecolote "cone" is not conical. The main edifice is U-shaped and open to the northwest. An irregular group of tephra hills lies west of the south horn, and a wedge-shaped mass of cinder is attached on the southeast. Four of the six Tecolote flows originated from the base of this wedge; flows A, B, and C effused from distinct boccas in its eastern wall. The origin of flow S is not as clear, but at least some of S came from the base of an amphitheater on the southwestern end of the wedge (foreground in Figure 15). Broad

cinder blankets extend both northward and south-eastward from Tecolote.

The tops of both horns of the cone are cut by arcuate, semiparallel fault scarps that are most numerous on the north horn (clearly visible in Figures 15 and 16). Where the tephra was cemented by fumarolic activity, the scarps are vertical and show downward relative motion of the side nearer the crest. The crest appears to have subsided as a complex graben. No other cone in Pinacate is known to have such faults. Gutmann and Sheridan (1978) described faults at Tesontle cone that they attributed to motion in the underlying lava, but they were cone-flank faults.

Tecolote cone is composed of various tephra types. The wedge appears to be entirely well-sorted, non-indurated cinder. Material exposed in the walls of the interior craters, including the high inner wall of the south horn, is a heterogeneous mixture of cinder, scoria, agglomerate, and agglutinate. The tephra deposits are variously indurated from tightly welded agglutinate, compacted agglomerate to loose material. Similar mixed tephra constitute the mounds of wall material that litter the surface of flow Q.

Most striking is the distinctive layer of large bombs that covers the south and east rims and mantles

the outer southern cone slope. Few are smaller than 20 cm in diameter. Most were spherical but many are broken. Accessory blocks derived from older volcanic units and accidental fragments of quartzofeldspathic rock occur loose in the deposit and also constitute cores in some of these bombs. The juvenile bombs are dense and relatively crystal-rich, with tiny vesicles. Many have cauliflower surfaces; others are more fluidal. These characteristics suggest that the magma was degassed and somewhat stiff and pasty.

The tephra mounds on the west are rich in notably large bombs, many having major axes longer than 1 m. These large bombs are generally spindle shaped with stretch-striated surfaces. The largest found so far is shown in Figure 17.

Cinder blankets extend from Tecolote in two directions. The plume on the north covers and fills a section of the aa surface of flow Q (Figures 14-16), mantles the slopes of Mayo, and extends almost to Tesontle. On the south, flow S is nearly completely covered with cinder and only the distal edges on east and west show more than the ends of flow-top projections. Irregularities in the cinder blanket caused by postdepositional flow within S are visible in Figures 14 and 16. Baked zones of red cinder can be seen in crevasses developed in S and the basal cinder is reddened adjacent to some of the flow-top projections.

Features of the Tecolote Flow Lavas

Aa is the major surface type. Roughness exists on scales ranging from micrometer spines on rock surfaces to meter-tall projections above flow surfaces. Surface blocks range from decimeter to multimeter, irregular to slab, locked in place to precariously balanced. The surface material is usually highly scoriaceous with irregular vesicles. Pahoehoe is present on B at various places starting about 100 m from the bocca.

The A flow is noteworthy in being composed entirely of "anosma," squeeze-ups of viscous magma with scrape and chattermarks attributable to plastic to



FIGURE 17. THE "BUS" BOMB. This pyroclast, 4.5 x 3.1 x 2.5 m, is 200 m from the nearest craterlet and 400 m from the center of the cone.

brittle deformation. Striated slabs project out of fractures in many other Pinacate flow surfaces, but this unit is unusual because the slabs are stacked one against the next like plates in a dishwasher rack (Figure 18). The A flow excavated a canyon in the outer wall of the wedge and its distal end is covered with piles of the cinder it removed.

Flow B effused from a bocca on the outer face of the wedge. The B magma appears to have been highly gas-charged and of low viscosity. Some of the surface structures near the B bocca resemble shelly pahoehoe but are, nonetheless, spiny aa. B has dendritic structures (Figure 19) on the edges of some slabs about 100 m east of its vent.

Flow C, the most northerly small flow on the east side of the wedge, emerged from a broadly excavated amphitheatre much like the source of S. A short lava tube near its source is a cool refuge on a hot day. The surface of C near the proximal end is slab aa, much less scoriaceous than the aa of B. For much of its length, C is flanked by a series of cinder "dunes" of unknown origin.

Flow R emerged on the ridge between Tecolote and the older cone to the southwest. This flow split: one tongue spilled eastward down the ridge toward S and the other westward down the ridge toward Q. The exact source of R is not clear; it may have emerged from beneath the closest of the western tephra hills. A mass of tephra was rafted outward along the ridgecrest by R. R and Q did not meet; a space of about 1 m separates the two flow fronts north of the ridge.

Flow Q is the largest and most complex of the Tecolote flows. It can be traced directly to the center of the cone, the presumed main vent. Where not buried beneath tephra, the surface is free-clast aa, slab in some places and irregular in others. To the northwest, Q overlies the edge of a nearly identical aa flow that originated from Mayo.

The surface of Q is littered with debris from the breached cone wall both in clearly defined, blocky masses and in rubbly piles (Figure 16). Tall mounds of bedded tephra are a distinctive feature of Q. The layers of solid basalt seen on the sides of some of these mounds were emplaced as dikes at an acute angle to the bedding when liquid basalt welled into opening fissures as the cone wall failed. The tall mounds of bedded tephra near the eastern distal end are far too large to have been simply rafted along the top of the flow as material is normally transported by aa. They may have slid along a lubricating basalt layer.

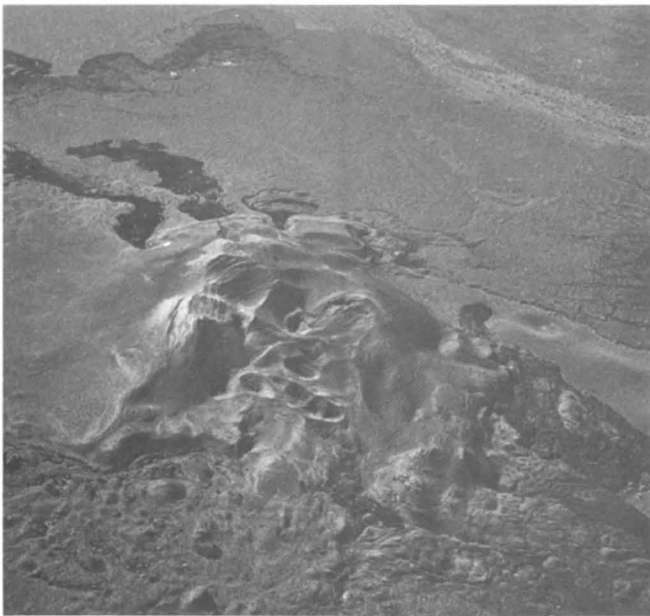


FIGURE 16. TECOLOTE VOLCANO. This photograph shows the faults, the central craterlets, the tephra mound atop R (lower right) and its near contact with Q, and the assorted tephra mounds atop Q (left and bottom) detached from the cone wall. © - Peter Kresan, 1987.



FIGURE 18. ANOSMA ON THE "A" FLOW. The bocca of A is in a canyon cut in the cinder of the wedge. People on the right show the size of these large slabs.

Flow Q effused from the center of the crater after having breached the northwest segment of wall. The five other flows emerged from various places beneath the walls. Nearly parallel gullies extend inward from the boccas of A and B across both the wedge and the cone. Another gully extends inward from R through the outer tephra hills. These gullies appear to have been excavated from beneath by block caving of tephra into voids created by removal of the cinder as magma flowed beneath.

A Possible Scenario for the Eruption

Relationships between the geologic features at this exceptionally complex eruptive center do not permit inference of a complete eruption chronology and the origin of many of the features is not understood. Flow S is apparently the oldest flow. Its thick, deformed mantle of locally baked cinder suggests that its effusion immediately preceded most or all of the pyroclastic eruptions that built the central cone. However, at least part of flow S appears to have emerged from an amphitheater at the base of the wedge after the cinders of the wedge had been deposited. It seems possible that the wedge, and perhaps the tephra hills west of the south horn, could be remnants of a cone built just prior to the large central cone.

Effusion of Q was contemporaneous with the last part of construction of the central cone. Flow Q removed a large section of cone wall and carried substantial pieces of it nearly 6 km out onto the desert. The apparently undisturbed band of cinder atop Q suggests that it had stopped moving prior to the end of cinder eruptions at this locality. Some of the giant bombs are on tephra that rest atop Q (Figure 17).

Eruption of large bombs followed all major cinder eruptions and evidently was not accompanied by significant cinder production. The remarkable size of these bombs demands a powerful eruptive force. One possible driving mechanism is a gas jet described as a "gas blast" by Budnikov and others (1983) from the eruption of Gorshkov cone on Tol'bachik. Such a jet entrains large blobs of magma and blocks of wall rock during "throat clearing." The source of the gas is

problematic. Eruptions of cinder can have large gas-to-magma ratios, but little if any cinder appears to have accompanied these bombs. Relatively fluidal bombs on the south rim contain more abundant phenocrysts (especially microphenocrysts) than do the earlier, cone-building cinders. Crystallization of vapor-saturated melt held beneath the volcano would have been accompanied by resurgent boiling. Accumulation of the evolved gas beneath a plug of pasty magma could have contributed to high gas/magma ratios; and the volume increase associated with such boiling could have led to cracking of the conduit walls, access of ground water to the system, and consequent hydromagmatic gas production. Whatever the driving mechanism, some of these bombs are of extraordinary size.

The large bombs are absent from the surfaces of flows A and B, but are present on the cinder adjacent to their boccas. Effusion of these small-volume flows appears to have followed the bomb eruption. The bombs on the surface of flow R, also a small-volume unit, could have been carried along after it disaggregated the tephra hill above its source.

Some bombs on the rim have yellowish surfaces altered by fumarolic activity. This activity also cemented tephra of the main cone locally, and the cemented zones are cut by faults of the cone-rim fault system. Also among the last events is formation of the craterlets within the debris on the floor and at the breach of the central crater. Some of these evidently represent local collapse, whereas a few near the breach appear to reflect minor explosions that produced small amounts of relatively crystal-rich scoria. Except for the relationship between the faults and the fumarole-cemented tephra, most of the sequence of events following eruption of flow Q is unclear. The complexity of relationships on Tecolote almost assures a future of lively conjecture.

Return to the vans for the drive to the lunch stop at Cerro Colorado.

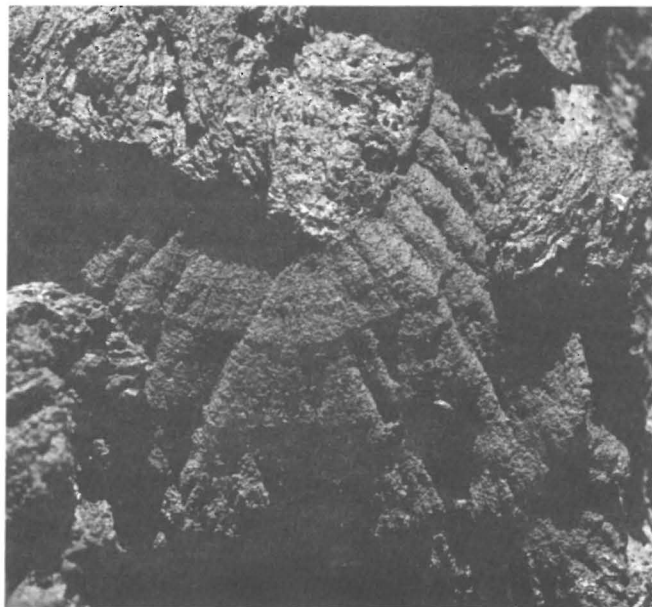


FIGURE 19. DENDRITIC OR ARBORESCENT STRUCTURE ON "B." This structure appears to have grown as two pahoehoe slabs pulled apart.



FIGURE 20. CERRO COLORADO TUFF CONE. This view looks southwest across Cerro Colorado toward the shield of Volcan Santa Clara (top left) and the dunes of the Desierto de Altar beyond Pinacate (top right). Tecolote is directly above the high crest of the tuff cone and Crater Elegante is above and to the left of that. Note the dark, inward-dipping tuff layers on the south wall of the crater, the broad apron of detritus shed from the cone, and abrupt termination of gullies draining its outer slopes. Cerro Colorado blocked a major drainageway creating Diaz Playa, which is out of this view on the right. Peter Kresan copyright 1987.

74.6 Salvatierra Wash Crossing.

77.3 Bear right at the road fork (the left fork passes Mayo and Tesontle cones and exits via the cinder mine road - 9 miles). Bear left at the next fork about 30 m beyond.

81.6 Rim of Cerro Colorado Crater.

Lunch Stop - Cerro Colorado Crater

Cerro Colorado is a reddish tuff cone with a crater about 1000 m in diameter. The cone was mapped by Jahns (1959) and its stratigraphy described by Wohletz and Sheridan (1983). Playa deposits in the northern and eastern walls of the crater are overlain by thin-bedded and then massively bedded surge deposits capped by air-fall tuff. Compared to the rim beds at Elegante, those here are rich in gravel, attain steeper dips, are thicker and more massive, exhibit more palagonitization of juvenile clasts, and contain accretionary lapilli and mud-armored clasts. Cerro Colorado is a tuff cone built by relatively wet pyroclastic surges (Wohletz and Sheridan, 1983). Its form suggests the presence of several centers of eruption and collapse. Its original rim is preserved on the south side where beds can be traced up from the crater floor over collapse-

truncated older layers and finally over the rim of the crater. Normally graded air-fall deposits rich in accretionary lapilli are well exposed on the path to the highest point on the north rim of the crater.

Follow the road to the west and north to exit Pinacate.

86.2 Broad cinder-haul road; turn right.

88.0 Highway 2; turn right. Sonoyta is 32 miles away.

ACKNOWLEDGMENTS

Financial support for some of the aerial photography came through a grant to D.J. Lynch from the Tucson Gem and Mineral Society.

Aerial oblique photographs in Figures 15, 16, and 20 are copyrighted by Peter Kresan; all other oblique and ground photographs are by D.J. Lynch.

REFERENCES CITED

- Budnikov, V.A., Markhinin, Ye.K., and Ovsyannikov, A.A., 1983, Quantity, distribution and petrochemical features of pyroclasts of the Great Tolbachik Fissure Eruption, in Fedotov, S.A., and Markhinin, Ye.K., eds., *The Great Tolbachik fissure eruption*: Cambridge, U.K., Cambridge University Press, p. 41-56.
- Donnelly, M.F., 1974, *Geology of the Sierra del Pinacate volcanic field in northern Sonora, Mexico, and southern Arizona, U.S.A.* [Ph.D. thesis]: Stanford, Stanford University, 722 p.
- Gutmann, J.T., 1974, Tubular voids within labradorite phenocrysts from Sonora, Mexico: *American Mineralogist*, v. 59, p. 666-672.
- _____, 1976, *Geology of Crater Elegante, Sonora, Mexico*: Geological Society of America Bulletin, v. 87, p. 1718-1729.
- _____, 1979, Structure and eruptive cycle of cinder cones in the Pinacate volcanic field and the controls of Strombolian activity: *Journal of Geology*, v. 87, p. 448-454.
- Gutmann, J.T., and Sheridan, M.F., 1978, *Geology of the Pinacate volcanic field*, in Pewe, T., and Burt, D., eds., *Guidebook to the geology of central Arizona*: Arizona Bureau of Geology and Mineral Technology Special Paper 2, p. 47-59.
- Ives, R.L., 1942, The discovery of Pinacate volcano: *The Scientific Monthly*, v. 54, p. 230-237.
- _____, 1966, Kino's explorations at Pinacate: *Journal of Arizona History*, v. 7, p. 59-75.
- Jahns, R.H., 1959, Collapse depressions of the Pinacate volcanic field, Sonora, Mexico, in Heindl, L.A., ed., *Southern Arizona Guidebook II*: Arizona Geological Society, p. 165-184.
- LeBas, M.J., LeMaitre, R.W., Streckeisen, A., and Zanettin, B., 1986, A chemical classification of volcanic rocks based on the total alkali-silica diagram: *Journal of Petrology*, v. 27, p. 745-750.
- Lynch, D.J., 1981, *Genesis and geochronology of alkaline volcanism in the Pinacate volcanic field of northwestern Sonora, Mexico* [Ph.D. thesis]: Tucson, University of Arizona, 248 p.
- Shafiqullah, M., Damon, P.E., Lynch, D.J., Reynolds, S.J., Rehrig, W.A., and Raymond, R.H., 1980, K-Ar geochronology and geologic history of southwestern Arizona and adjacent areas: *Arizona Geological Society Digest*, v.12, p. 201-260.
- Webb, P.K., and Weaver, S.D., 1976, Trachyte shield volcanoes; a new volcanic landform from South Turkana, Kenya: *Bulletin Volcanologique*, v. 39, p. 294-312.
- Wohletz, K.H., and Sheridan, M.F., 1979, A model of pyroclastic surge, in Chapin, C.E., and Elston, W.E., eds., *Ash flow tuffs*: Geological Society of America Special Paper 180, p. 177-194.
- _____, 1983, Hydrovolcanic explosions II; evolution of basaltic tuff rings and tuff cones: *American Journal of Science*, v. 283, p. 385-413.



Frontispiece: Oblique aerial view of the Picacho mine showing the multiple pits, which are the disrupted pieces of a once continuous orebody. Volcanic rocks in the background overlie the deposit and show little of the detachment-related deformation.



The Mesquite and Picacho Gold Mines: Epithermal Mineralization Localized Within Tertiary Extensional Deformation

Eric G. Frost
California Consortium for Crustal Studies
Department of Geological Sciences
University of California, Santa Barbara
Santa Barbara, California 93106

Stanley N. Watowich
Gold Fields Mining Corporation
1201 West 9th Street
Yuma, Arizona 85364

INTRODUCTION

Exploration for large-tonnage, low-grade gold deposits has been strongly stimulated by the opening of the Picacho and Mesquite mines in southeasternmost California. These two deposits form the focus of this field trip and should provide the participants with an overall view of the mines themselves, as well as the geologic setting in which they occur. The Mesquite deposit is operated by Gold Fields Mining Corporation and has been officially in production since February 1986. Little previous production had occurred on the Mesquite claims, although a significant number of small workings dot nearly all the outcrops of gneissic rocks protruding from the alluvium. The Picacho mine is currently operated by Chemgold, Inc., and has had a long history of sporadic development dating back more than a century. Near the turn of the century, Picacho was a major underground mine, which closed in 1908 because of a major mechanical failure at its 450-ton mill (Odens, 1973). Both Mesquite and Picacho are largely within shattered Jurassic gneiss and represent a different type of ore deposit than was widely recognized before these mines came into production. Their exact genesis is still not completely known, but both appear to have had a similar origin. This field trip is designed to point out the similarities between the deposits, information that should help those seeking to find similar gold deposits.

GENERAL STRUCTURAL SETTING

Both deposits occur along the southwestern limb of the regional Chocolate Mountains antiform (Figure 1), an elongate structure that exposes the Orocochia Schist in western Arizona and southeastern California. The early Mesozoic Orocochia Schist represents the structurally deepest recognized basement within southern California and has long been a key to unravelling the complex history of the region. Offset of the Orocochia Schist and some of the distinctive overlying gneisses formed part of the early basis for proving major offset on the San Andreas fault (e.g., Crowell and Walker, 1962). Work by UCSB Ph.D. students Bruce Crowe, John Dillon, Gordon Haxel, and Dick Tosdal (all working with John Crowell) has provided the basis for much of our understanding of the overall geologic history of the region. Their work on the Mesozoic tectonics of the region, in particular, has formed the basis for most of what is known of the Mesozoic magmatism and deformation in the area (Haxel and Dillon,

1978; Haxel and others, 1985; Haxel and Tosdal, 1986). Major regional synthesis of the magmatic and deformational development of this region has also been done by Stan Keith (Keith, 1986; Keith and Wilt, 1986), providing many thought-provoking alternatives to previous ideas.

Overprinted on the Mesozoic magmatic and deformational history is crustal-scale extension of mid-Tertiary age. One component of this extensional system is a regionally developed low-angle normal fault, or detachment fault. A detachment fault is well exposed just north of the Picacho mine (Frost and others, 1986) and was reported in some of the early workings in the Picacho open pit (Wilkins, 1984). The genetic relationship between detachment faulting and gold mineralization has sparked much recent work on the region, as well as in the vicinity of other detachment faults in the western United States. Mineralization within the overall detachment system appears to occur within the zone of shattering near the low-angle fault, along the high-angle normal faults that feed downward into the detachment fault, and within placers and talus breccias produced by the erosion of the deposits.

How the Picacho and Mesquite mines fit into the combined history of Mesozoic magmatism-deformation and mid-Tertiary extension will be the theme of this trip. Most observers of the geological setting related to the gold mineralization at Mesquite and Picacho are generally impressed with the following major features:

- 1) intense deformation of the host rock,
- 2) intense cataclasis associated with this deformation,
- 3) restriction of the mineralization to metamorphic rocks,
- 4) favorable host dominance by the more quartzofeldspathic units,
- 5) lack of significant veining and silicification,
- 6) relatively minor alteration of the host rock, and
- 7) persistence of gold mineralization even in relatively unaltered gneiss.

As the gold potential at Mesquite and Picacho were uncovered by mining, several different genetic models for the mineralization were proposed, based on differing experiences, biases, and interpretations of diverse data. The most widely proposed models include the following:

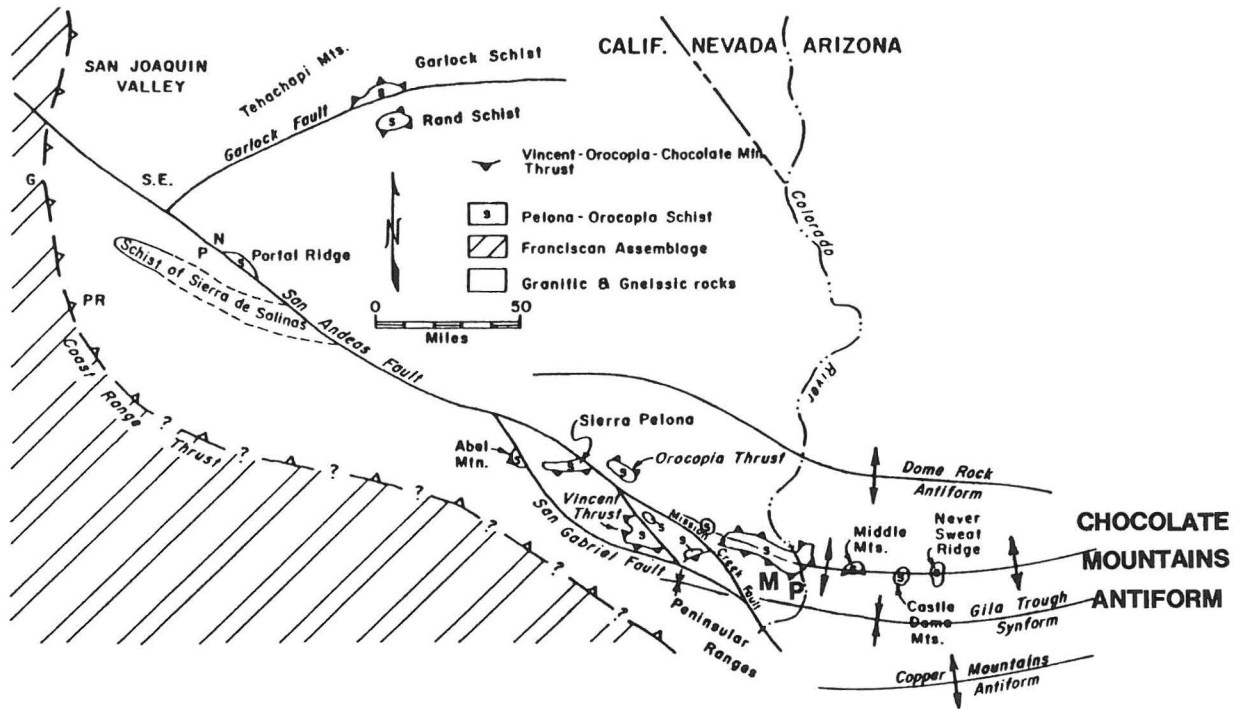


Figure 1. Regional geologic map of southern California and western Arizona in a pre-San Andreas reconstruction by Dillon (1975). Large-scale antiforms and synforms produced during mid-Tertiary crustal extension are drawn on Dillon's base map. Both the Mesquite mine (M) and Picacho mine (P) are on the southwestern limb of the major Chocolate Mountains regional antiform.

- 1) a syngenetic model related to exhalative processes that predated metamorphism. Such a syngenetic model seemed especially attractive because of the low dip of the deposit, similar to that in the apparently Precambrian host gneisses.
- 2) a Cretaceous - Paleocene structural model related to the formation of the Chocolate Mountains thrust, which served as a hydrothermal conduit that fed the fluid-receptive, upper-plate gneisses. The proximity of the thrust, the strong structural control of mineralization, and the similar shattered character of some mapped occurrences of the thrust made this interpretation attractive.
- 3) a magmatic source related to hydrothermal solutions derived from a felsic (peraluminous) intrusive body in the vicinity of the mineralization. The regional association of peraluminous rocks with gold mineralization made this interpretation promising as the original source for the gold, if not for the current mineralization.
- 4) a detachment-fault model in which crustal extension produced the ground preparation for localizing the ore fluids and continued to deform, progressively offsetting the early-formed faults and mineralization. The shattered character of the ore and proximity of the detachment fault at Picacho made this interpretation seem inviting.
- 5) a hot-spring model related to the early development of the San Andreas transform or to volcano-plutonic, heat-driven fluid. The proximity of the San Andreas to the Mesquite mine and the nature of mineralizing fluids in the Salton Sea geothermal wells made this interpretation seem appealing.

All of the above models have been variously advocated by different individuals on the basis of a variety of data. As more work has been done on these deposits, several of the above hypotheses have lost their attractiveness. A goal of this trip will be to elucidate the appropriate information that will allow each participant to see what is currently known about these deposits, their genesis, and their subsequent deformation.

DAY ONE: MESQUITE MINE AND ITS GEOLOGIC SETTING

Leave Yuma and drive west on Interstate 8 to the Ogilby Road turnoff. Continue north on the Ogilby Road past the Cargo Muchacho Mountains to the intersection with State Highway (SH) 78. Pull off the highway onto the dirt road that is the northward continuation of the Ogilby Road. From this vantage point, the overall form of the Chocolate Mountains and the setting of the Mesquite and Picacho deposits can be seen.

STOP 1: REGIONAL STRUCTURAL SETTING

The high portion of the Chocolate Mountains is composed of the rather uniformly dark-colored Orocopia Schist, which is deformed into an elongate NW-SE-trending antiform. From this view point, the short axis of the antiform is visible with dips of the foliation to the SW and NE. At the center of the antiform is the mid-Tertiary Mount Barrow granodiorite, which is well exposed just to the north (Gables Road), especially in morning light. Most of the low, maroon-colored rocks to the west of this vantage point are volcanic rocks whose genetic relationship to the Mount Barrow granodiorite is not well known. However, their K-Ar ages are nearly the same, and it was the feeling of Dillon (1975) that the volcanics represented a caldera sequence intruded by its own plutonic

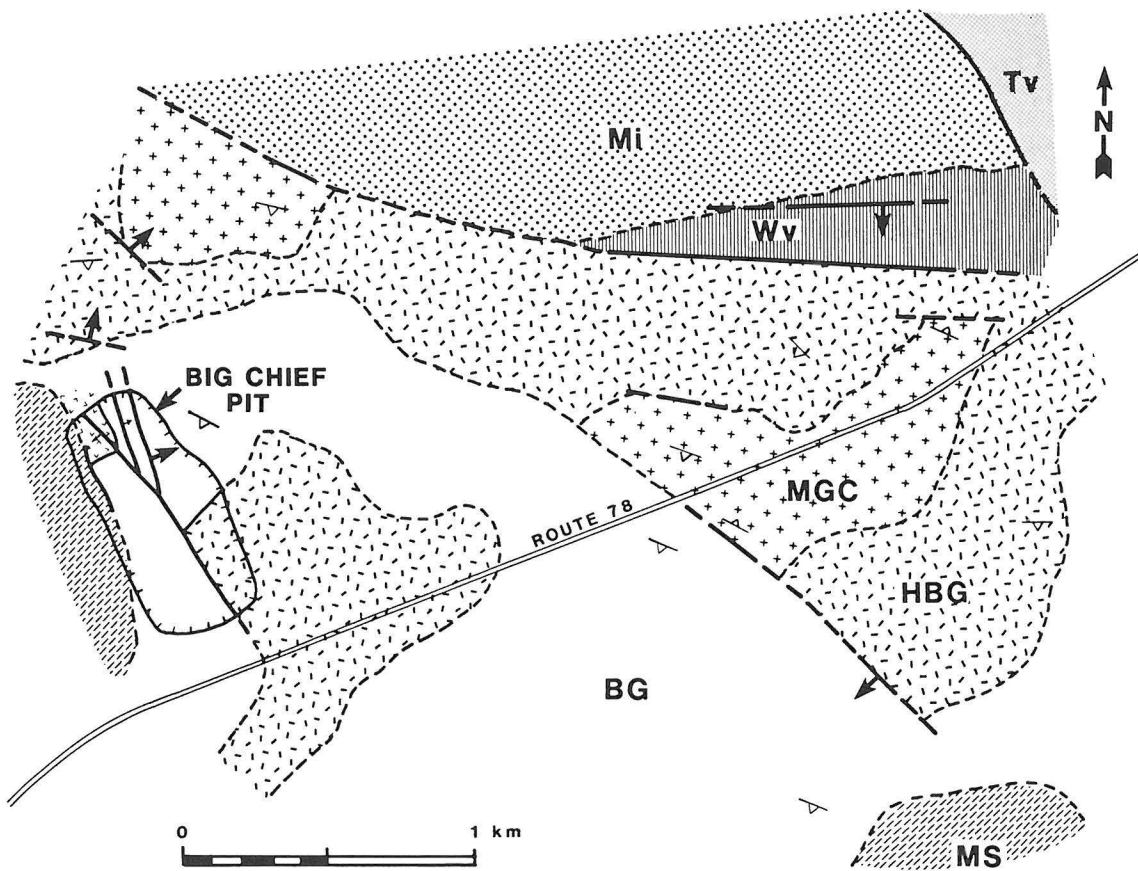


Figure 2. Large-scale geologic map of the Mesquite mine area as deduced from geologic mapping and extensive drilling (from Manske and others, 1987). Outline of the Big Chief pit is shown; several other pits are planned for this same area. Ore deposits occur largely within Jurassic gneiss with minor Cretaceous leucogranite. Abbreviations: BG = Biotite Gneiss, HBG = Hornblende-Biotite Gneiss, MS = Muscovite Schist, MGC = Mafic Gneiss Complex, Wv = Winterhaven Formation, Mi = Mesozoic intrusive rocks, and Tv = Tertiary volcanic rocks. From: Manske and others (1987).

root. These volcanic and interbedded sedimentary rocks overlie the relatively low-relief gneisses that sit structurally above the Orocopia Schist. The contact between the schist and the gneiss is defined as the Chocolate Mountains thrust, a regional fault system that appears to have moved in Late Cretaceous time (87–74 Ma) based on work done in the San Gabriel Mountains (Haxel and others, 1985).

The dip of the thrust has little relationship to its orientation during Mesozoic deformation; it has been tilted to its present position by deformation related to mid-Tertiary extension. The intermediate to steep dip of both the thrust and foliation within the Orocopia Schist indicates that major, postthrust deformation has affected this terrane. In contrast, the volcanic rocks visible along the road and forming the low foothills to the range are only gently tilted, indicating that a significant amount of the postthrust deformation was over prior to the extrusion of these late Oligocene–early Miocene volcanic rocks (Dillon, 1975; Crowe, 1978). Evidence of a similar deformational history is apparent over much of SE California and SW Arizona along the flanks of the Chocolate Mountains antiform (Figure 1). Similar geometries are also present on the west side of the San Andreas fault system, which has offset the regional antiforms and synforms, beginning in late Miocene time.

The change from regional extension to transform motion associated with the San Andreas system was marked by the extrusion of black basalts such as those that form most of the Black Mesa skyline to the SE. Regionally, these flows yield similar ages of about 12 Ma and generally have low strontium initial isotopic ratios, indicating a large component derived from mantle sources. North-south feeder dikes characterize this system, indicating a major change in stress orientation at this time. Microplate rotations, such as those described just to the north by Carter and others (1987), also characterize the region during this time period.

Proceed west along SH 78 to the Mesquite mine for Stop 2. Along the drive from Stop 1 to the mine, the Tertiary andesites occupy most of the area on either side of the road. These deposits actually form only a thin veneer over the gneissic rocks that host the mineralization at Mesquite and Picacho. When the mine comes into view, note the low outcrops north of the road—they are good examples of the various gneissic units in the Mesquite mine. The pseudostratigraphic section that forms the deposit can be seen along the road (Figure 2), with a basal mafic complex overlain by biotite gneiss, hornblende-biotite gneiss, and muscovite schist, all of which are intruded by several generations of aplite, pegmatite, and leucogranite.

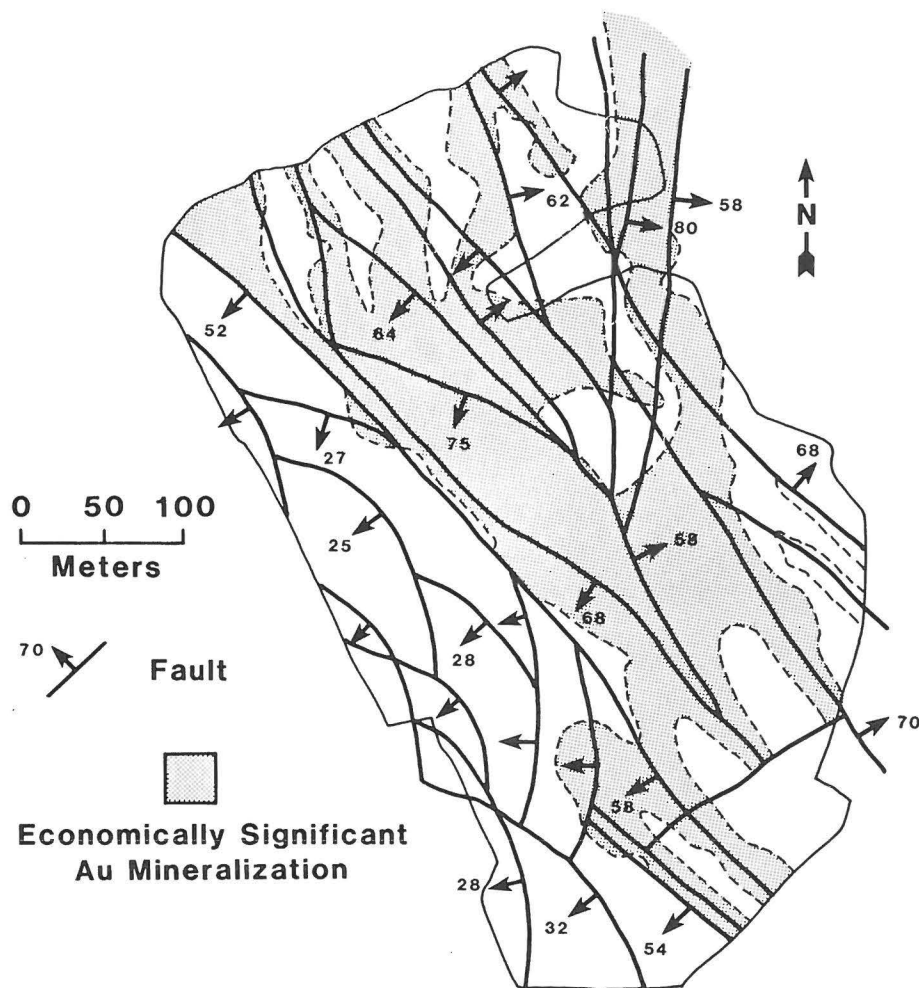


Figure 3. Map of the Big Chief pit showing the relationship between large-scale faults and gold mineralization. Faults on the southwest side of the pit are scoop shaped and appear to be related to gravitational motion toward the Salton Trough, significantly after mineralization occurred. These low-angle faults are unmineralized and cut the high-angle faults, which localize the most significant gold mineralization. Modified from Willis and Holm (1987).

These gneisses generally dip to the SW off the Chocolate Mountains antiform. They are repeated by several major normal faults that dip to the NE, thus tilting the gneisses back toward the Salton Trough. On a large scale, the entire Chocolate Mountains are tilted to the SW, probably as a response to crustal-scale extension. Most of the gneissic rocks that host the mineralization are on the SW limb of the antiform, with the deeper crustal Orocopia Schist and postdetachment volcanic rocks forming much of the NE limb of the antiform.

STOP 2: MESQUITE MINE OVERLOOK

At the northeastern corner of the pit, the overall character of the deposit can be seen. Most of the gneissic rocks dip to the SW and are cut by numerous generations of normal faults (Figure 3). These faults offset the rocks exposed on the NE side of the pit to the NE and the rocks on the SW side to the SW, producing a central horst and an adjoining series of half grabens. The high-angle normal faults strike $N40^{\circ}-50^{\circ} W$ and are relatively steep and planar on the scale

of the pit. In detail, the fault surfaces are highly convoluted because of the complexity of the faulting and their obvious development through a significant amount of progressive deformation. Mineralization is strongly localized along these high-angle faults (Figure 3), indicating the profound structural control that has localized the deposit.

Cutting these high-angle faults are a number of spoon-shaped, low-angle faults, which place unmineralized muscovite schist over the mineralized gneisses. The muscovite schist is overlain by the mid-Miocene Bear Canyon fanglomerate and interbedded dark basalt flows. These sands and gravels were deposited unconformably on the muscovite schist, as well as on the mineralized gneiss.

Tilting of these sands along spoon-shaped normal faults indicates that at least some of the deformation that put the muscovite schist on the gneisses is postdetachment-related extension in age. Because the Bear Canyon and overlying basalts were deposited after the mid-Tertiary extension, their deformation is probably related to gravitational motion into the Salton Trough. The scoop-shaped character of the faults and



Figure 4. Oblique aerial view of the Big Chief pit area in the Fall of 1985. Pit is enormously larger now, indicating the speed at which mining is taking place. Picacho Peak can be seen on the left skyline, with almost completely covered area in between the two deposits. Other deposits such as Mesquite and Picacho probably exist between the two, but are hidden. Lack of major outcrops in the area is a result of the highly shattered nature of the rock. Similar areas of low relief produced by the erosion of shattered crystalline rocks can be a major guide to finding other such deposits, in contrast to studying the unmineralized, but more highly resistant, rocks exposed in the range itself.

the abundant down-dip striae on the fault surfaces indicate that these faults are almost entirely normal faults, rather than strike-slip faults related to the San Andreas system itself. Abundant strike-slip striae and mullion structures are present on zeolitized surfaces within the Bear Canyon sands, but are mostly along faults striking NE-SW, perpendicular to the major normal faults. These near-vertical faults appear to have acted as tear faults accommodating differential motion of the landslidelike fault blocks.

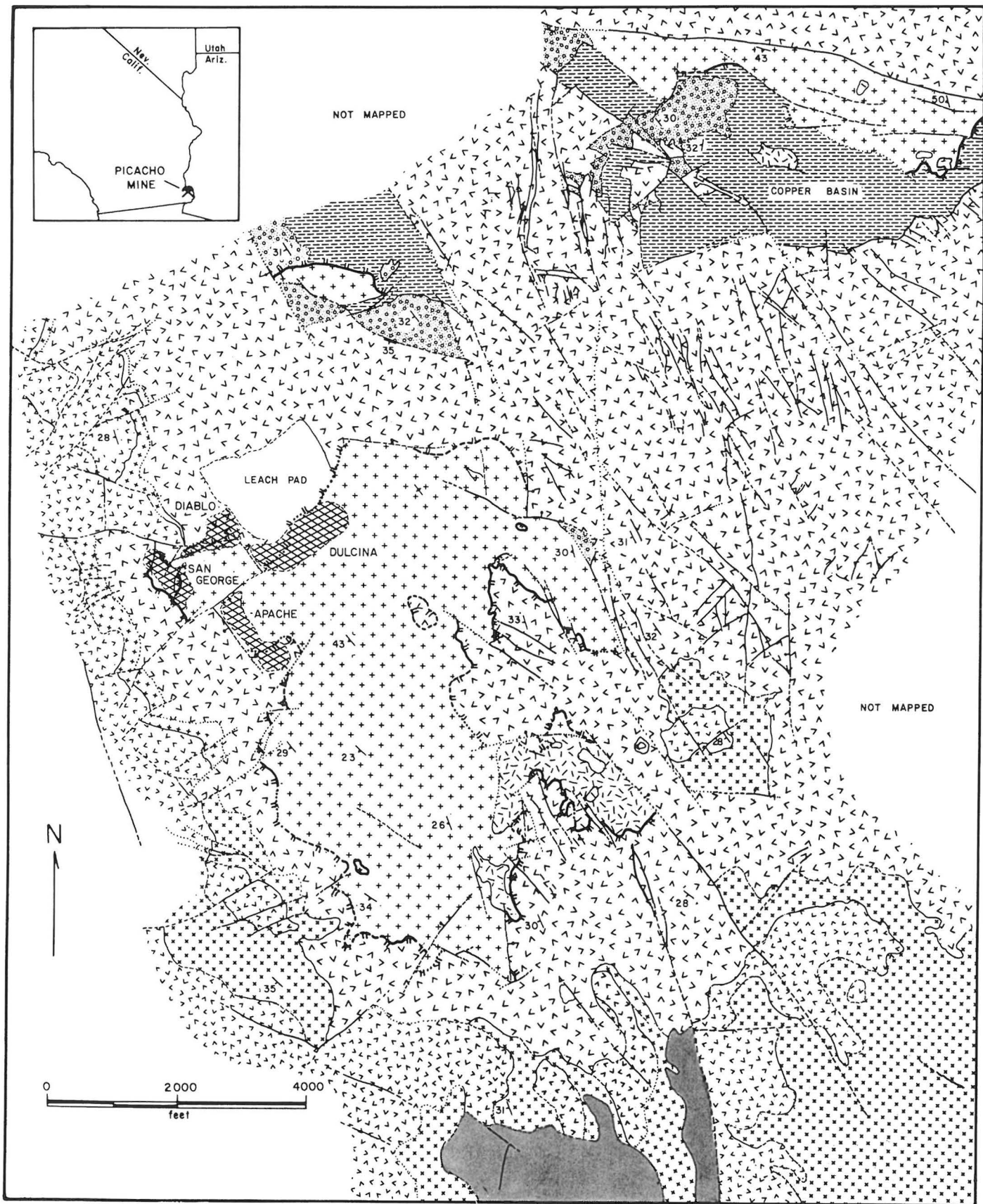
STOP 3: MINERALIZATION IN THE BIG CHIEF PIT

Drive to the ore faces on several benches for in-depth scrutiny of the general character of the mineralization within variations of biotite gneiss, hornblende-biotite gneiss, pegmatites, and leucogranite. The leucogranite, which contains garnet and tourmaline, appeared to be a fairly major body during the initial development stages of the pit, making it attractive as the cause for the formation of the deposit (S. Keith, pers. commun., 1986). Further mining has shown that the leucogranite is probably sill-like in form and is much less conspicuous in the pit as a major rock type. The unit has yielded a 38 Ma K-Ar age (Willis and Holm, 1987). However, a Cretaceous concordant U/Pb zircon age has been obtained on the unit (Frost, 1987), indicating a dis-

turbance in the K-Ar system.

Regional resetting of the K-Ar system within the metamorphic rocks of the southern Chocolate Mountains occurred at about 60 - 70 Ma (Frost and Martin, 1983a), an age similar to the 58 Ma K-Ar age on the muscovite schist (Manske and others, 1987). The 38 Ma age on mineralized rock suggests that mineralization occurred during the Tertiary and partially to completely reset the ages of formation and metamorphism of the various rocks to an unknown degree. Further geochronologic work is in progress to determine more completely the age and duration of mineralization.

Mineralization is "disseminated" in that the ore is along innumerable fractures, gouge zones, and breccia zones, as well as within apparently unbroken rock. Alteration varies from appearing intense, mostly because of a bleaching effect on the biotite gneiss, to appearing very subtle to absent. Detailed work on the mineralization by Manske and others (1987) has demonstrated that (1) the ore fluids were at temperatures of 210°- 230°C, (2) salinities were 1% NaCl equivalent, (3) boiling appears to have occurred during precipitation because of the presence of liquid and vapor-phase fluid inclusions, (4) gold is associated with pyrite and, to a much lesser degree, other sulphides, although most of the ore is highly oxidized, and (5) depths of formation are 300 m and less. These studies, together with the detailed pit mapping of



Gerry Willis (Willis and Holm, 1987) that shows the relationship between faulting and gold mineralization (Figure 3), very nicely define Mesquite as an epithermal deposit. Circulation of meteoric water through the structurally prepared rock appears to be a primary cause for localizing the deposit. Where the gold originated from and what the thermal regime driving the fluid system was are still major unknowns that are being actively investigated.

STOP 4: MINERALIZATION IN THE VISTA PIT AREA

Proceed across Highway 78 to the desert pavement just opposite the Big Chief pit (Figure 4), an area that is the proposed site for the Vista pit. This stop will emphasize the subtlety of the surface exposures of Mesquite-type deposits. Many of the low hills of gneiss in this area are ore or are underlain by ore. Most of the outcrops are pockmarked by old workings, indicating that the old-timers recognized the pervasiveness of the mineralization, but did not understand it. The bottoms of many of the small washes expose outcrops of the brittlely deformed gneisses and demonstrate the thinness of the alluvial veneer that has hidden these deposits from previous development. The low-relief character of the broken gneisses appears to be a definite characteristic of these deposits. If time allows, a short traverse through the various gneissic rocks and associated fault structures will be undertaken. Return to Yuma.

DAY TWO: PICACHO MINE AND DETACHMENT FAULT

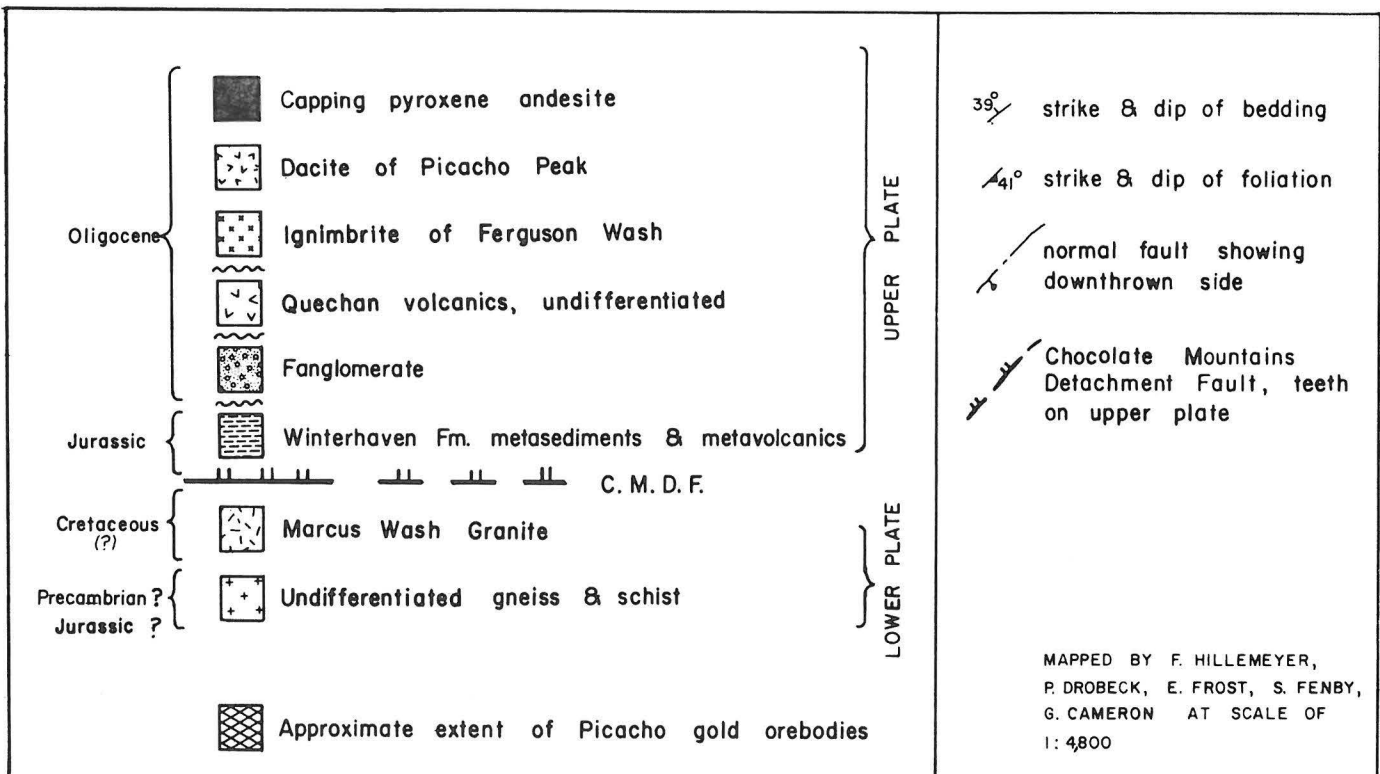
Leave Yuma going west toward Winterhaven, just

across the Colorado River. Turn right on County Road S24 and follow the signs toward Picacho State Recreation Area. Cross the All American canal and proceed on dirt road toward Picacho Peak and Picacho recreation area. Stop on low hill just over Picacho Pass (15.9 miles from Colorado River) for Picacho overview.

STOP 1: PICACHO BASIN OVERLOOK

From this vantage point, it is possible to see many of the tectonic elements of the southern Picacho region. In the volcanic cliffs that form the western margin of the Picacho basin, one can see a general stratigraphic section composed of dark, resistant flow units, interbedded white tuff, and other assorted volcanic units. The volcanic rocks in this region were mapped by Crowe (1978), who interpreted the high-angle faults that cut the volcanic section as recording the early development (Oligocene) of the Basin and Range Province. The multiple normal faults offset the volcanic section numerous times, repeating the relatively thin section over and over across the entire southern Chocolate and neighboring Trigo Mountains. The volcanic section is tilted about 20° or less, whereas the fanglomerates and other sedimentary and volcanic rocks that underlie the cliff-forming volcanic sequence are tilted significantly more, and are even overturned in places. Much of the extensional deformation, therefore, occurred prior to deposition of the widespread volcanic section, which is so prominent in the Picacho basin. Postdetachment deformation in the area has produced variable deformation along the volcanic-prevolcanic unconformity, making the relationship of the volcanic rocks to detachment

Figure 5. Geologic map and legend of the Picacho mine area from Drobeck and others (1986). Several pits that make up the Picacho mine are shown within the Jurassic(?) gneiss. Excellent exposures of the detachment fault are present in the structural window just north of the deposit. Other exposures have been and are being mined from within the Picacho pits. Mid-Tertiary volcanic units cover the deposit and the detachment fault and show little of the detachment-related deformation.



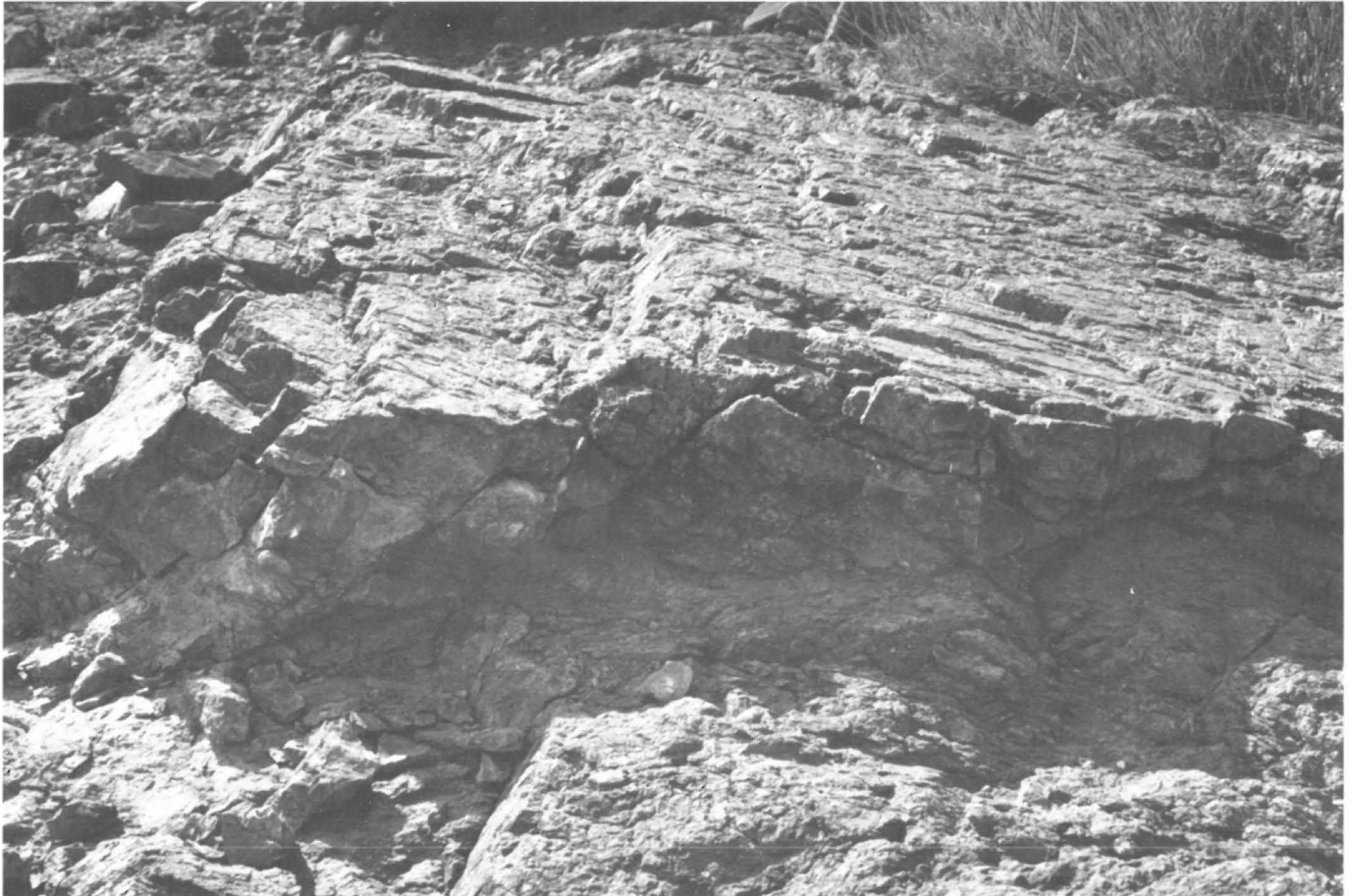


Figure 6. Small-scale view of a portion of the microbreccia ledge north of the Picacho mine. Area in the sunshine in the upper half of the photo is the fault surface. Small-scale normal faults have offset the detachment fault, progressively dropping it down to the south. Larger normal faults in the area follow the same geometry, dropping the detachment fault down from these exposures to those at the mine.

faulting more difficult to decipher. This is especially true where the volcanic rocks overlie the exhumed detachment fault or the shattered and eroded lower-plate rocks.

These volcanics uniformly contain almost no mineralization and serve to hide the underlying extensional deformation and associated ore deposits. The volcanics are involved in major postmineralization faulting that has segmented many of the known ore bodies, such as those exposed in the Picacho mine. Some of these postdetachment normal faults have offsets of several hundred meters, significantly disrupting the overall detachment-related deformation and mineralization. Most of the faults have offsets measured in meters to tens of meters, so that finding and mining offset pieces of exposed areas of mineralization is possible.

STOP 2: PICACHO MINE

Continue down the Picacho road and enter the Picacho mine; proceed to the top of the Dulcina pit (Figure 5) for an overview of the Picacho mine and its operations. Detailed descriptions of the history and mineralization at Picacho can be found in Van Nort and Harris (1984), Drobeck and others (1986), and Liebler (1986). Mineralization occurs in metaplutonic gneiss, which was once thought to be Precambrian, but which now appears to be Jurassic (Tosdal, 1986). These

gneisses occur above the Orocopia Schist, putting the structural setting of the mine well above the Chocolate Mountains thrust. Several small leucocratic intrusions occur within the gneiss and may be of various ages.

The original Picacho orebody was tabular in shape, but has now been segmented into at least five major pieces by postmineralization normal faulting (Figure 5). Ore grades occur in highly broken rock, making it possible to simply dump the blasted rock directly on the leach pads with no intervening crushing or agglomeration (Mike Fitzgerald, pers. commun., 1987). Most of the ore is highly oxidized, staining the Jurassic(?) gneiss a red or maroon color. At the base of the Dulcina pit (as of February 1987), the unoxidized gneiss is exposed beneath the oxidized ore across a major low-angle fault. Rocks on either side of the fault are highly deformed in a very brittle fashion. This fault is probably appropriately considered to be a detachment fault, although other subparallel detachment faults are also present in the area.

This low-angle deformation has been offset on the postdetachment and largely postmineralization normal faults (Figure 5). Offset on some of these high-angle faults was also clearly postextrusion of the Picacho volcanics because these volcanic units are variably disrupted throughout the region. Clasts of the mineralized gneiss and postdetachment volcanic rocks are

intermixed in several talus breccias that formed from spalling off these postdetachment normal faults. Some of the talus breccias compose significant bodies of ore and also made deciphering the mine geology rather perplexing during early studies of the ore deposit.

Mineralization at Picacho is distinctly epithermal in character, with the ore grades related to the degree of shattering more than any other single factor. Euhedral pyrite cubes in a breccia matrix of gneiss further indicate that the structural preparation of the rock controlled the localization of hydrothermal fluids. The more leucocratic units, such as the pegmatites and Marcus-Wash(?) type rocks, shatter more than the gneiss and form better host rocks. The leucocratic bodies appear to be related to mineralization by their ability to fracture rather than by their chemistry or original contribution of mineralizing fluids.

Fluid-inclusion studies of the Picacho ore by Liebler (Drobeck and others, 1986; Liebler, 1986) on quartz thought to be associated with mineralization indicate temperatures of 210°-230° C and very low salinities, much like those at Mesquite (Manske and others, 1987). Percolation of meteoric water through these rocks requires that fractures and cracks be open, suggesting a very shallow character of the mineralization. As such, mineralization like that at Picacho may characterize the upper portion of a detachment system, rather than deeper levels where more gold-barren systems are more characteristic.

Sucking of the fluids into the rock during earthquake motion on the normal-fault system in a fashion as suggested by Sibson (Sibson, 1986, 1987) forms a very attractive way of localizing ore fluids in the fault zones. According to Sibson's detailed studies of fluid-fault interaction in other parts of the world, earthquake rupture on the faults may be the driving mechanism for circulating fluids through extensional jogs within the overall deformational system. Continued work on the details of fault geometries and mineralizing systems may provide powerful insight into the genesis of these and other ore deposits.

STOP 3: PICACHO MINE DETACHMENT FAULT

Continue driving north on Picacho Road for 1 mile to the intersection of Little Picacho Wash with the road and park off the side of the road. Stop at the entrance to Little Picacho Wash and examine the Winterhaven Formation, which makes up both sides of the wash. The Winterhaven consists of metavolcanic, volcanoclastic, and metasedimentary rocks that are largely phyllitic in character. Elsewhere within the Picacho basin, the Winterhaven contains a clean quartzite that may be correlative with the Aztec Sandstone, making the unit Early Jurassic, or perhaps Late Triassic in age (Frost and Martin, 1983b).

A large normal fault drops the postmineralization volcanic rocks down against the Winterhaven at the entrance to the wash. The fault itself can be seen in the canyon wall just north of the entrance into Little Picacho Wash. Walking up the wash, one can see many other normal faults that are well exposed in the canyon wall. These normal faults offset and tilt the Winterhaven innumerable times, repeating distinctive metavolcanic and metaconglomeratic units over and over. The style of normal faulting visible here on a small scale seems characteristic of the style of normal faulting on a much wider scale within the entire detachment terrane. The detachment fault is only a few meters to tens of meters below the wash here, making this deformation typical of the lowermost portion of the upper plate. The intensity of faulting

increases as one progresses up the wash, i.e., as one moves down-structure. The intensity of alteration along the faults and fractures also increases, especially within a few meters of the detachment fault itself.

About 100 m up the wash from the main road, a small road crosses the wash where the canyon forks. Take the left fork to the Picacho mine detachment fault (Figures 6, 7), where upper-plate Winterhaven Formation is juxtaposed against lower-plate Jurassic(?) gneiss. The detachment fault forms a distinctive ledge in the middle of the wash, reflecting the sunlight in the afternoon light. This microbreccia ledge exposure is light brown and forms the top of the lower plate. Shattered gneiss that looks almost like a conglomerate underlies the microbreccia ledge. Highly deformed Winterhaven and Jurassic(?) gneiss sit above the microbreccia, which has anomalous gold and arsenic values in other exposures to the north (Drobeck and others, 1986). The degree of alteration and deformation seen here is characteristic of the detachment exposures elsewhere in the Picacho basin, providing a guide to similar structures that are buried by the thin alluvial cover or postdetachment volcanic rocks. The combination of yellow and green along the detachment zone is a color alteration that is extremely characteristic of the detachment-fault exposures in this whole region.

Offset of the microbreccia ledge by small-scale normal and strike-slip faults mimics the more regional deformation of the Picacho area (Figures 6, 7). Postdetachment faulting has segmented the detachment complex, making it more difficult to define and trace from point to point. The clear join of the detachment fault exposed here with the Picacho mine low-angle faults is difficult to discern because of these postdetachment normal faults. One such major fault is exposed just upstream from the detachment fault (Figure 5), where the maroon volcanic rocks are down-dropped against the detachment zone. From the top of the hill northwest of the detachment zone, this large normal fault can be traced across the foreground between the mine and the detachment fault. To the north, one can see the upper-plate rocks repeated along multiple normal faults that are truncated by the Picacho mine detachment fault.

This pattern of multiple normal faults that both feed into the detachment faults and cut them is typical of most of the areas of significant gold mineralization in the Picacho region. The complexity of the detachment-related deformation produced by these multiple generations of normal faults suggests that gold mineralization may be localized in the uppermost crustal levels of detachment systems, i.e., near their headwalls. Here the detachment faults would have been very near the surface and subjected to multiple periods of brittle overprinting by subsequent normal faults developed on progressively deeper detachment faults during continued extension. Such gold mineralization associated with shallow crustal levels probably forms one end of a continuum with the copper-iron mineralization that is so typical of many of the well developed and more coherent detachment systems, such as in the Buckskin and Whipple Mountains (Wilkins and Heidrick, 1982; Spencer and Welty, 1986; Lehman and others, 1987). These copper deposits seem to represent the mineralization along deeper levels of detachment systems and appear to lack economic quantities of gold.

Exploration for large-tonnage, low-grade gold deposits such as Picacho and Mesquite might thus be concentrated within exposures of the higher-level portions of regional detachment complexes, rather than near the detachment faults of some of the classical

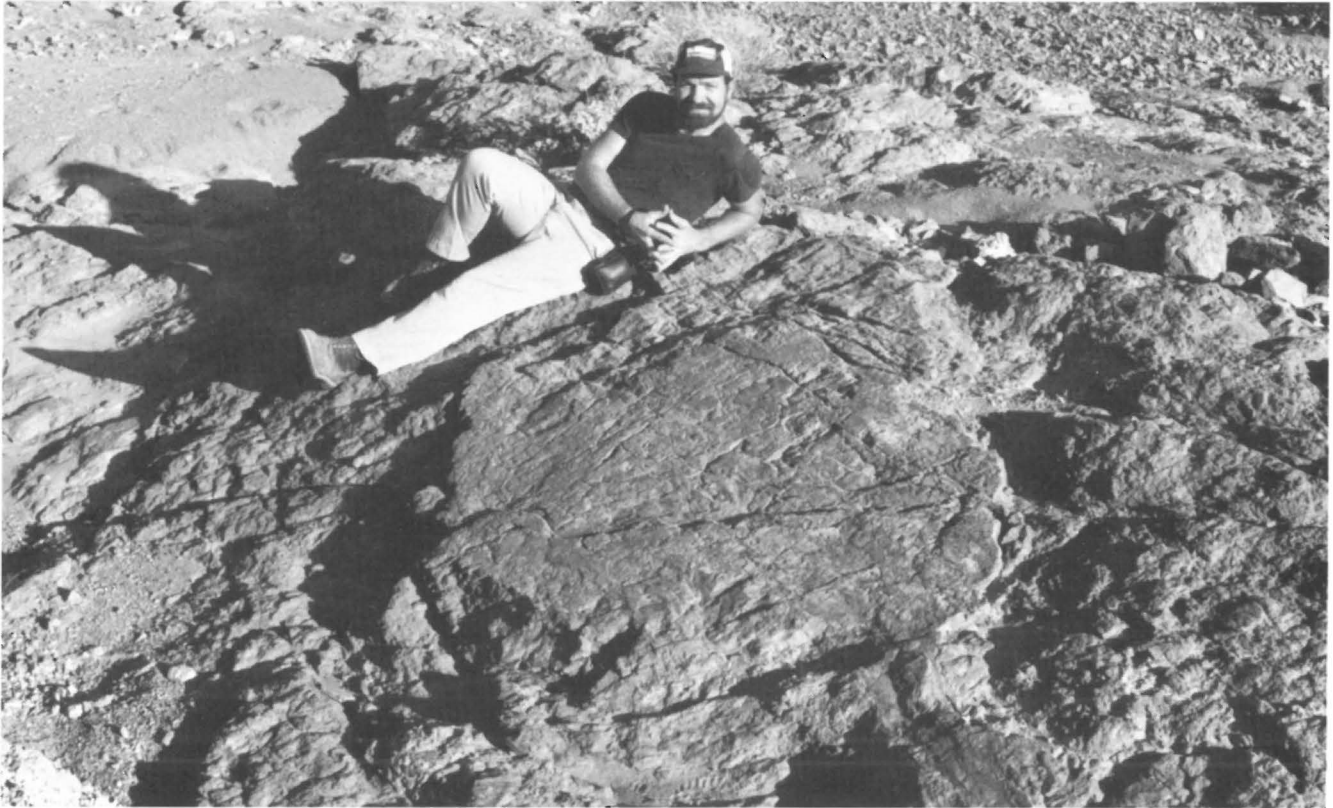


Figure 7. Picacho mine detachment fault with microbreccia ledge exposed about 250 m north of the Picacho mine. This is one of the uppermost of the multiple detachment faults exposed in the area and separates the Jurassic Winterhaven Formation from the underlying Jurassic(?) gneiss along this portion of its exposure. Up structure, this fault separates the Tertiary fanglomerate and volcanic units below the Quechan Volcanics from the lower-plate gneiss. Note the small-scale offset of the microbreccia by normal and strike-slip faults, which has effectively segmented this detachment fault and associated features into many individual slabs. The Picacho mine orebody has been similarly segmented from its original geometry of formation.

metamorphic core complexes. The spectacular fault exposures within the cores of many such detachment complexes are typically produced by the juxtaposition of middle-crustal rocks with upper-crustal rocks and do not represent the same structural or thermal regime that appears to have helped localize the gold mineralization at Picacho and Mesquite. Detachment faults in other ranges that have been called core complexes, such as the Black Mountains of Arizona, actually represent upper-crustal detachment faults that sit above deeper faults and would seem to represent attractive areas of exploration. Within individual complexes, such as the Whipple or the Chocolate Mountains, one side of the range is typically structurally higher than the other (SW side in both these ranges), making the higher structural level a more attractive target. In particular, exploration in the low-relief pediment regions around the margins of the upper-crustal portion of detachment complexes appears to hold the most promise for finding similar gold deposits.

Exploration for Mesquite- or Picacho-type orebodies should probably best begin with a geologic understanding of the diversity of detachment systems, the structural preparation produced by the multiple generations of faults, and the alteration and mineralization patterns that characterize such extensional fault complexes. Such an understanding can be most effectively gained by studying the Picacho and Mesquite regions within the context of the regional crustal extension and concomitant volcanism and plutonism that characterized this area in mid-Tertiary

time. The overprint of this extension on the Mesozoic deformational and magmatic features has produced a geologically complex terrane, but one that offers the possibility for the discovery of other major gold deposits. Return to Phoenix.

ACKNOWLEDGMENTS

We would like to thank George Davis, Jon Spencer, and Will Carr for helpful reviews. We especially thank Evelyn VandenDolder for her review, which provided numerous insights that substantially improved the clarity and presentation of this field guide.

REFERENCES

- Carter, J. N., Luyendyk, B. P., and Terres, R. R., 1987, Neogene clockwise tectonic rotation of the eastern Transverse Ranges, California, suggested by paleomagnetic vectors: *Geological Society of America Bulletin*, v. 98, p. 199-206.
- Crowe, B. M., 1978, Cenozoic volcanic geology and probable age of inception of basin-range faulting in the southeasternmost Chocolate Mountains, California: *Geological Society of America Bulletin*, v. 89, p. 251-264.
- Crowell, J. C., and Walker, J. W. R., 1962, Anorthosite and related rocks along the San Andreas fault, southern California: *University of California Publications in Geological Sciences*, p. 219-288.

- Dillon, J. T., 1975, Geology of the Chocolate and Cargo Muchacho Mountains, southeasternmost California (Ph.D. thesis): Santa Barbara, University of California, 575 p.
- Drobeck, P. A., Hillemeier, F. L., Frost, E. G., and Liebler, G. S., 1986, The Picacho mine; a gold mineralized detachment in southeastern California, *in* Beatty, B., and Wilkinson, P. A. K., eds., *Frontiers in geology and ore deposits of Arizona and the Southwest*: Arizona Geological Society Digest, v. 16, p. 187-221.
- Frost, D. M., 1987, Final report on U/Pb dating studies in the Mesquite pit and adjoining regions: Gold Fields Mining Corporation, unpublished report, 18 p.
- Frost, E. G., Drobeck, P., and Hillemeier, B., 1986, Geologic setting of gold and silver mineralization in southeastern California and southwestern Arizona: Geological Society of America, Cordilleran Section, 82nd Annual Meeting, Guidebook and Volume, Trips 5 and 6, p. 71-119.
- Frost, E. G., and Martin, D. L., 1983a, The Orocochia Schist and Chocolate Mountains thrust system of southeastern California and western Arizona; new insights from removing the overprint of Tertiary detachment faulting and folding: American Association of Petroleum Geologists, Pacific Section, Abstracts with Programs, p. 86-87.
- _____, 1983b, Overprint of Tertiary detachment deformation on the Mesozoic Orocochia Schist and Chocolate Mountains thrust: Geological Society of America Abstracts with Programs, v. 15, no. 8, p. 577.
- Haxel, G. B., and Dillon, J. T., 1978, The Pelona-Orocochia Schist and Vincent-Chocolate Mountains thrust system, southern California, *in* Howell, D. G., and McDougall, K. A., eds., *Mesozoic paleogeography of the western United States*, *in* Proceedings, Pacific Coast Paleogeographic Symposium, 2nd, Los Angeles: Society of Economic Paleontologists and Mineralogists, Pacific Section, p. 453-469.
- Haxel, G. B., and Tosdal, R. M., 1986, Significance of the Orocochia Schist and Chocolate Mountains thrust in the late Mesozoic tectonic evolution of the southeastern California-southwestern Arizona region--extended abstract, *in* Beatty, B., and Wilkinson, P. A. K., eds., *Frontiers in geology and ore deposits of Arizona and the Southwest*: Arizona Geological Society Digest, v. 16, p. 52-61.
- Haxel, G. B., Tosdal, R. M., and Dillon, J. T., 1985, Tectonic setting and lithology of the Winterhaven Formation, a new Mesozoic stratigraphic unit in southeasternmost California and southwestern Arizona: U.S. Geological Survey Bulletin 1599, 19 p.
- Keith, S. B., 1986, Petrochemical variations in Laramide magmatism and their relationship to Laramide tectonic and metallogenic evolution in Arizona and adjacent regions, *in* Beatty, B., and Wilkinson, P. A. K., eds., *Frontiers in geology and ore deposits of Arizona and the Southwest*: Arizona Geological Society Digest, v. 16, p. 89-101.
- Keith, S. B., and Wilt, J. C., 1986, Laramide orogeny in Arizona and adjacent regions; a stratotectonic synthesis, *in* Beatty, B., and Wilkinson, P. A. K., eds., *Frontiers in geology and ore deposits of Arizona and the Southwest*: Arizona Geological Society Digest, v. 16, p. 502-544.
- Lehman, N. E., Spencer, J. E., and Welty, J. W., 1987, Middle Tertiary mineralization related to metamorphic core complexes and detachment faults in Arizona and California: Society of Mining Engineers Preprint 87-21, 9 p.
- Liebler, G. S., 1986, Geology of gold mineralization at the Picacho mine, Imperial County, California (M.S. thesis): Tucson, University of Arizona, 57 p.
- Manske, S. L., Matlack, W. F., Springett, M. W., Strakele, A. E., Jr., Watowich, S. N., Yeomans, B., and Yeomans, E., 1987, Geology of the Mesquite deposit, Imperial County, California: Society of Mining Engineers Preprint 87-107, 9 p.
- Odens, P., 1973, Picacho--life and death of a great gold mining camp: 44 p.
- Sibson, R. H., 1986, Brecciation processes in fault zones--inferences from earthquake ruptures: PAGEOPH, v. 124, p. 159-175.
- _____, 1987, Earthquake rupturing as a mineralizing agent in hydrothermal systems: *Geology* (in press).
- Spencer, J. E., and Welty, J. W., 1986, Possible controls of base- and precious-metal mineralization associated with Tertiary detachment faults in the lower Colorado River trough, Arizona and California: *Geology*, v. 14, p. 195-198.
- Tosdal, R. M., 1986, Gneissic host rocks of gold mineralization at the Picacho mine, southeastern Chocolate Mountains, southeastern California: Geological Society of America, Cordilleran Section, 82nd Annual Meeting, Guidebook and Volume, Trips 5 and 6, p. 143-144.
- Van Nort, S. D., and Harris, M., 1984, Geology and mineralization of the Picacho gold prospect, Imperial County, California, *in* Wilkins, J., Jr., ed., *Gold and silver deposits of the Basin and Range Province, western U.S.A.*: Arizona Geological Society Digest, v. 15, p. 175-183.
- Wilkins, J., Jr., 1984, Editor's note--Picacho mine update, *in* Wilkins, J., Jr., ed., *Gold and silver deposits of the Basin and Range Province, western U.S.A.*: Arizona Geological Society Digest, v. 15, p. 182-183.
- Wilkins, J., Jr., and Heidrick, T. L., 1982, Base and precious metal mineralization related to low-angle tectonic features in the Whipple Mountains, California and Buckskin Mountains, Arizona, *in* Frost, E. G., and Martin, D. L., eds., *Mesozoic-Cenozoic Tectonic Evolution of the Colorado River region, California, Arizona, and Nevada*: San Diego, Cordilleran Publishers, p. 182-204.
- Willis, G. F., and Holm, V. T., 1987, Geology and mineralization of the Mesquite open-pit gold mine, *in* Proceedings, Conference on Bulk Mineable Precious Metals Deposits of the Western United States: Nevada Geological Society, 11 p.

Mesozoic Tectonics of Southeastern California

Warren Hamilton
U.S. Geological Survey
Denver, Colorado 80225

Richard M. Tosdal and Paul Stone
U.S. Geological Survey
Menlo Park, California 94025

Gordon B. Haxel
U.S. Geological Survey
Flagstaff, Arizona 86001

INTRODUCTION

Warren Hamilton

Southeastern California was part of the North American craton during Paleozoic time, and a platform Paleozoic section like that of the western Grand Canyon was deposited on a basement of Middle Proterozoic granites and gneisses. Platform conditions continued into the Early Jurassic, interrupted locally by Late Triassic granitic and volcanic magmatism and uplift, but during later Jurassic time granites and ignimbrites were emplaced widely through the region. The very thick Cretaceous fluvial McCoy Mountains Formation was deposited in a large basin. Severe deformation and metamorphism, accompanied by intrusion of leucogranites, affected the region during the late Late Cretaceous. At about the same time, the base of the continental plate was eroded tectonically against oceanic materials being subducted beneath it, and those materials are exposed, as Orocopia Schist, beneath the Chocolate Mountains thrust at the base of the plate. Severe extension, accompanied by more magmatism, affected the region during middle Tertiary time. Little of this complex geology has yet been described in detail in widely distributed publications, but much work has been done, particularly during the last decade, and there is an increasing body of information in guidebooks, reports, and maps of limited circulation.

Samples of the structural and lithologic products of most of the major events of Mesozoic time will be seen in superb desert exposures on this 3-day field trip in eastern Riverside and Imperial Counties. The trip begins in Blythe. The first day will be spent in the Big Maria Mountains, which display spectacular Late Cretaceous synmetamorphic deformation of cratonic Paleozoic and lower Mesozoic strata and of Proterozoic and Jurassic granites. The second morning we will go with Stone to the type area of the McCoy Mountains Formation. That afternoon we will see with Tosdal the Late Cretaceous Mule Mountains thrust zone at its type locality, where it can be argued that discrete faults are lacking and that we see only metamorphosed and transposed contacts. The third day we go with Haxel and Tosdal to Gavilan Wash to study the Chocolate Mountains thrust. Gavilan Wash is in a region of low-angle, middle Tertiary, top-to-the-northeast extensional faulting. An interpretation alternative to those suggested by Haxel and Tosdal, in the light of various features including the middle Tertiary K/Ar age of the fault rocks (Frost and others, 1982), is that the northeast-directed slip and mylonites that we will see record middle Tertiary extensional reactivation of a subduction overthrust that had the opposite sense of slip and a higher grade of syntectonic metamorphism.

The cratonic section of distinctive Paleozoic and lower Mesozoic formations that we will see in the Big Maria Mountains is known in many ranges from northwestern Sonora (south of the belt of exposures of Chocolate Mountains thrust and Orocopia Schist; Leveille and Frost, 1984) through southeastern California and western Arizona (Hamilton, 1982; Stone and others, 1983) to the western Grand Canyon and

southeastern Nevada. This continuity is among the features that disprove suggestions that southeastern California and southwestern Arizona are crossed either by a great Jurassic "Mojave-Sonora megashear" (Anderson and Silver, 1981) or by a Mesozoic suture between an allochthonous southwestern minicontinent and mainland North America (Harding and Coney, 1985).

DAY ONE: BIG MARIA MOUNTAINS

Warren Hamilton

The Big Maria Mountains have the most extensive exposures in the region of the metamorphosed cratonic section of Paleozoic, Triassic, and Lower Jurassic strata (Hamilton, 1982, 1984). The range is dominated by a northwest-trending synclinorium of these rocks, flanked by the granitic (ca. 1400 Ma, U/Pb: L. T. Silver, unpub.) and gneissic basement rocks on which they were deposited (Fig. 1). All of these rocks were intruded by Middle or Late Jurassic granodiorite and quartz monzonite (ca. 160 Ma, U/Pb: Silver, unpub.), now present on both sides of the synclinorium. Late Cretaceous (ca. 75 Ma, Ar/Ar: Hoisch and others, in press) regional metamorphism of upper greenschist to middle amphibolite facies was accompanied by extreme northeast-verging deformation and attenuation and by intrusion of voluminous postkinematic pegmatites.

The synclinorium perhaps formed between domiform Jurassic plutons, but whatever other structures and metamorphism accompanied Jurassic magmatism were overprinted so severely during Cretaceous time as to be unrecognizable. Minor structures show northeastward vergence throughout the range, regardless of position in the synclinorium and other large structures. Typical mid-size structures are recumbent folds that cascade northeastward over one another. Apparently the metasedimentary rocks dipped steeply when Late Cretaceous deformation began; vergence is shown by structural geometry, not by facing directions of strata within folds.

The section of metamorphosed cratonic strata in the Big Maria Mountains begins with the Cambrian Tapeats Quartzite, which is overlain by Bright Angel Schist, and that by calcitic Muav Marble. Thick dolomite marble comes next; Upper Cambrian, Ordovician, and Lower Devonian formations are present in unmetamorphosed sections but cannot be discriminated in the metadolomite. Next comes white calcite marble, which certainly includes the Mississippian and so is designated Redwall Marble, although Upper Devonian and Pennsylvanian rocks likely are present in it also. Next above are metamorphosed calcareous redbeds of the Upper Pennsylvanian and Lower Permian Supai Formation, and above that the Permian calc-silicate Hermit Schist, fine-grained eolian Coconino Quartzite, and chert-rich, mostly calcitic Kaibab and Toroweap Marbles (here lumped as Kaibab). The overlying Triassic metasedimentary rocks presumably include

equivalents of the Moenkopi, Shinarump, and Chinle Formations, but these or other Triassic units have yet to be discriminated systematically in the metamorphosed Big Maria section. Above the Triassic rocks is the eolian Lower Jurassic Aztec Quartzite, and above that a thick Lower(?) and Middle Jurassic metaignimbrite section, of which the lower part is more mafic than the upper.

The section from Tapeats through Aztec must have had a stratigraphic thickness near 3000 m. At Stop 1-6B, we will see it where it has been attenuated tectonically to 25 m, with all formations in proper order.

Middle Tertiary deformation is recorded by a major low-angle normal fault (detachment) in the northern part of the range, atop a mylonitic carapace formed early in the extensional episode; by subhorizontal shear zones at deeper levels; by a large moderate-dip normal fault through the range; and by a throughgoing strike-slip fault.

ROAD LOG

Mileage

- 00.0 HEAD N ON US 95 from Hobsonway, at E end of Blythe, on Holocene floodplain of Colorado River. Big Maria Mtns. come into view ahead. Dark hills directly ahead are of granitic rocks; layered rocks in left part of range are metamorphosed Paleozoic strata.
- 04.4 Pass transformer station. Rugged hills ahead and left are of Jurassic granitic rocks; lower hills and dissected pediment to right are of Proterozoic granite. Late Pleistocene fan surfaces are pediments on intercalated fanglomerates and river silts.
- 06.1 Cross large ditch and begin curving route along edge of floodplain. Wash cobbles for next 3 miles are mostly of Jurassic granites, with subordinate Proterozoic granites.
- 07.9 Roadcut in Proterozoic granite.
- 11.1 Restaurant on right. Dark Supai Fm at 10 and 11 o'clock; Kaibab and other Permian units at 10:30; lower Paleozoic at 9:30.
- 11.5-12.1 (Indian Reservation sign). Supai Fm on left: darkly varnished greenschist-facies calc-silicate and quartzitic rocks, derived from calcareous redbeds. At this grade (but not at amphibolite facies), the formation is typically covered by several m of jostled blocks solidly cemented by calcite.
- 12.4 Near hills at 10 o'clock are of recumbently interfolded dark Supai Fm, cream-colored Redwall Marble, and yellow dolomite marble. Tectonic attenuation here is to about 1/8 of initial stratigraphic thickness.
- 14.4 Highway rises from floodplain to fan; graded road to W.
- 16.2 TURN AROUND AND STOP (1-1) for view. Near hills at 280-290° (true bearing, 14.5° W of magnetic bearing) are on NE limb of synclinorium and mostly display dark Supai Fm, thin gray Redwall Marble, and tan metadolomite, repeated in tight recumbent folds. Cambrian strata and Proterozoic basement metagranite are present low in hills but are inconspicuous from here. A normal fault, near side down 1.5 km, intervenes between these hills and the distant ridge.

High peak at 265° is of Supai Fm with yellow Cambrian-Mississippian carbonates beneath and left, and dark metamorphosed Cambrian clastics and Proterozoic and Jurassic granites below those. Above and right of Supai are poorly exposed Hermit Schist and Coconino Quartzite, then cliffs of light Kaibab Marble, then dark Triassic rocks, Aztec Quartzite, and Jurassic meta-ignimbrite. Skyline at 276° is of inverted Paleozoic section, greatly attenuated tectonically but complete, which is connected to the thick section (265° etc.) by a syncline that is broadly upright although crossfolded by large recumbent folds.

Skyline peak at 301° displays a N-verging recumbent fold of a septum of Paleozoic metasedimentary rocks between metamorphosed plutons of Jurassic granitic

Figure 1. Geologic map of the Big Maria Mountains and south edge of the Riverside Mountains, showing Day 1 Stops, after Hamilton (1982, Fig. 2).

EXPLANATION

Cenozoic materials

- Q Quaternary sediments; locally includes Pliocene
 Tr Miocene or Oligocene intrusive rhyolite
 Tb Oligocene sedimentary breccias and clastic strata

Metamorphosed Middle Jurassic plutonic rocks

- Jg Granodiorite, quartz monzonite, and alaskite
 Jd Diorite
 Jgb Hornblende gabbro
 Jm Migmatitized Mesozoic and Proterozoic gneiss, much injected by unit Jg

Metamorphosed stratified rocks

- Mz Middle Jurassic metaignimbrite, Lower Jurassic Aztec Quartzite, and Triassic clastic metasedimentary rocks
 Pz Paleozoic cratonic metasedimentary rocks--Kaibab Marble through Tapeats Quartzite

Metamorphosed Proterozoic basement rocks

- Eg Megacrystic potassic granite
 Eu Fine-grained gneiss and granite of upper plate

Faults--dotted where concealed

-  Strike-slip, postdetachment
 Normal, postdetachment
 Detachment (low-angle normal fault)
 Type unspecified

Attitudes

-  Layering. In unit Tb, bedding dipping steeply to moderately; in unit Pz, showing generally upright or inverted sequence, dips mostly gentle
 Foliation. Mostly of very Late Cretaceous age

rocks. This is not part of the main synclinorium.

Skyline ridge at 310° is below the projection of a middle Tertiary detachment fault that dips down the far side. The light stripes, concordant to mylonitic-gneissic foliation, are boudinaged pegmatites of the latest Cretaceous swarm that are undeformed in most of the range and that here likely record mid-Tertiary extensional ductile deformation when this terrain was still at mid-crustal depths.

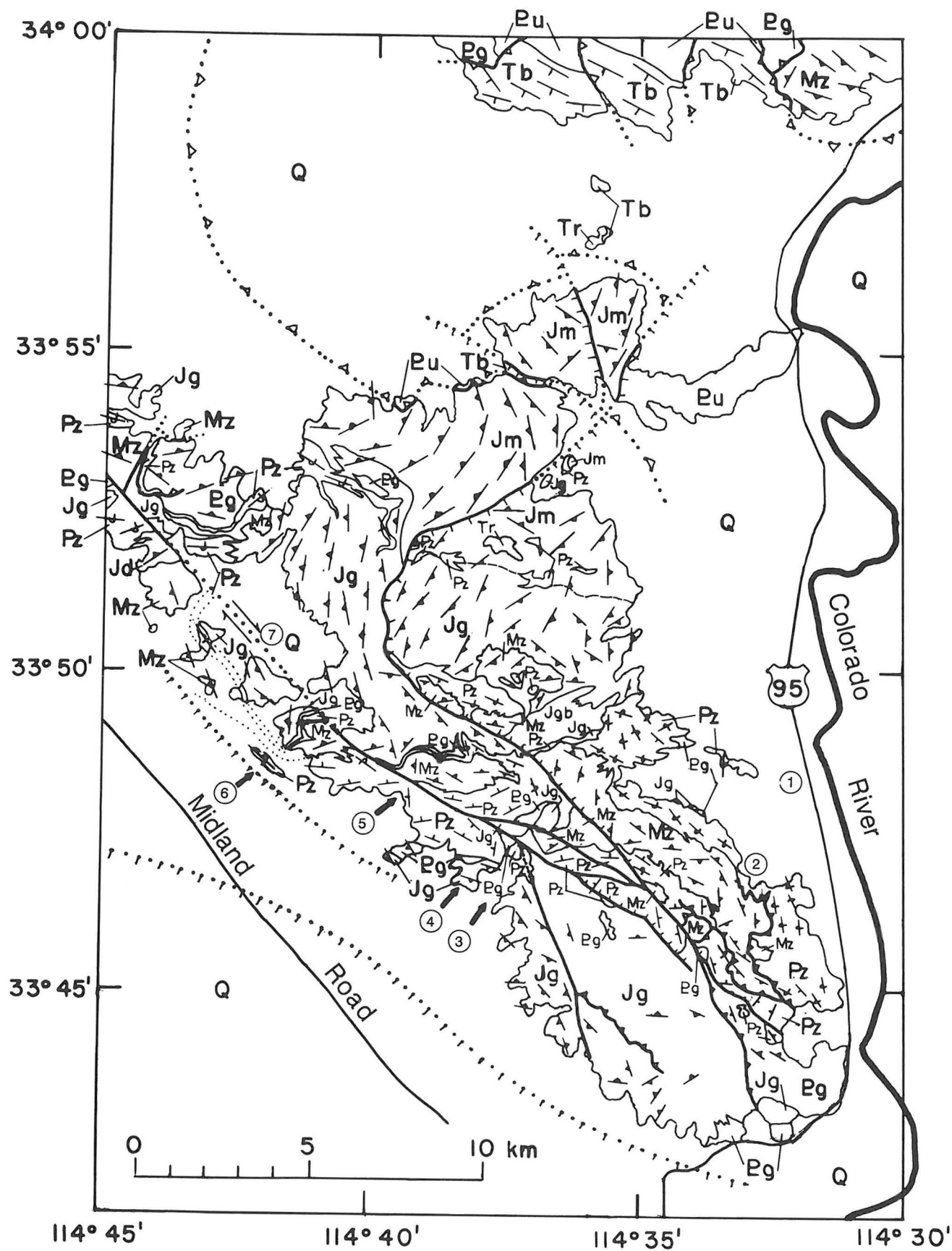
BACKTRACK S ON HIGHWAY.

18.0 (= 14.4 N-bound). TURN W on graded road.

18.45 Pass pile of schistose green Jurassic metaquartz monzonite, for dam riprap, from quarry at end of road.

19.35 STOP (1-2A) before iron posts for view. To NW is inverted upper Paleozoic and lower Mesozoic section in NE limb of synclinorium. Structurally highest in sight is dark Supai. Below it is striped Kaibab; between them are poorly exposed Hermit and Coconino. Below Kaibab are green Triassic rocks, and below those is reddish Aztec Quartzite, the tectonic thickness of which decreases greatly between peak at 295° and low knobs at 280°. Below Aztec is Jurassic metaignimbrite (green hills).

The discontinuous veneer of yellowish-gray travertine on the lower hills is the basal deposit of the marginally marine Bouse Fm of early or middle Pliocene age; the lower hills and canyons now being exhumed are of pre-Bouse age. The various alluvial-fan levels record late



Pleistocene exhumations and pedimentations in response to changing climates, not to local uplift.

19.5 Cross wash [walk from here if road washed out].

19.7 TURN AROUND AND STOP (1-2B) in wide area. Peak to SE has inverted upper Paleozoic section: Supai Fm at top, poorly exposed Hermit Schist beneath it, small cliffs of Coconino Quartzite next below, and cliffs of Kaibab marble and cherty marble near bottom; metamorphism, upper greenschist facies.

Near N end of exposures of Kaibab on W side of road are isoclinal folds refolded by recumbent folds showing overfolding NE down the dip. The Kaibab has plane-parallel external contacts so fold superpositions are due to combined simple and pure shear--laminar flow plus flattening--and not to superposed compressive deformations. Metamorphism was at upper greenschist facies.

WALK S on road, past small E-dipping normal fault that drops Triassic metaconglomerate (Shinarump?) against Kaibab, and TURN RIGHT into wash. Conglomerate on N has large boulders of Proterozoic granite and of all Paleozoic units, recording nearby uplift and trenching through the cratonic section. The Paleozoic section is preserved in ranges nearby to W, N, and E, so the eroded uplift likely was to S and may have been related to the emplacement of Late Triassic granites in the Mule Mountains (Stop 2-5B) although no clasts of those granites have been recognized here. Granite and quartzite boulders are flattened 1.5-2:1; limestone, now calcite marble, 50:1.

Cobbles in wash include abundant Jurassic granites, with proportion of felsic rocks increased over that in outcrop. Granodiorite and quartz monzonite are relatively rich in clotted mafic minerals, low in quartz, and characterized by equant lavender K-spar phenocrysts that often have white rims. Alaskitic granites form irregular masses within the other Jurassic granites. Subordinate cobbles of Proterozoic quartz-rich leucogranite consist mostly of megacrysts of K-spar. These rocks retain granitic fabrics despite upper-greenschist recrystallization. Farther NW in the range, amphibolite-facies metamorphism rendered all granites gneissic, but the contrasted Jurassic and Proterozoic types are easily distinguished even as extremely flattened augen gneisses.

WALK DOWNSTREAM across road through inverted Triassic conglomerate, epidotic Moenkopi(?) meta-sediments of lower part of Triassic section, and Kaibab. Kaibab and Triassic show mylonitic intershearing, perhaps by mid-Tertiary crustal extension. Farther down wash is Pliocene travertine, with cemented clastic strata that were foreset into standing water, barnacle coquinas, and small to very large algal heads.

RETURN TO HIGHWAY

21.4 (= 18.0 inbound). TURN S ON HIGHWAY.

29.7 (= 06.1 N-bound). Highway crosses ditch.

31.25 TURN W on paved Fourth Ave.

33.3 TURN N on paved Lovekin Blvd.= Midland Road.

34.3 Cross railroad tracks. [This is 5.5 miles N of Hobsonway in Blythe.]

37.0 TURN NE on dirt road at red pipeline marker 290.

41.6 Pass small rockpiles on left.

42.2 STOP (1-3) on high surface just short of outcrop hills. WALK E into main wash and then about 200 m N and NW up it, in rocks of lower (albite-epidote) amphibolite facies. First, moderately foliated Proterozoic meta-granite; then, basal Tapeats Quartzite, impure metasandstone dominant over quartzite, abundantly folded with NE vergence; then, higher Tapeats quartzite, cut by a mid-Tertiary dike. Wash boulders include metamorphosed Jurassic quartz monzonite.

CLIMB SW over ridges of dark, glossy muscovite-biotite Bright Angel Schist; dip mostly SW; calc-silicate ledge at top. Enter coarse, foliated calcite Muav Marble. Section continues upward (we will not) through

cliffs of brown metadolomite, white Redwall Marble, and dark Supai Fm; all units are internally isoclinal and externally recumbently folded, but structure looks simple because fold axes are subparallel to cliffs. A small normal fault high in the cliffs puts metadolomite against Supai and truncates a Tertiary dike. Wollastonitic Supai is prominent in talus; bulldozer tracks were made for gathering weathered blocks of it for decorative facing stone. Interfolded Coconino Quartzite and Kaibab Marble are visible on distant ridge to N.

RETURN to vehicles and BACKTRACK.

42.8 TURN RIGHT at rockpiles (= 41.6 inbound) and drive NW parallel to mountain front.

43.4 STOP (1-4) at S end of hill of Jurassic metagranodiorite (equant K-spars survive as augen) and meta-alaskite. Foliation dips W: this is in overturned limb of a recumbent fold relative to upright NE dips in mountain face. CLIMB HILL for view. Mountain face has Supai on Redwall on dolomite + Muav on (at lower right) dark Cambrian clastics, basement, and Jurassic granite. NE-verging Z fold at 342° involves Supai, Redwall, and dolomite. High Supai wollastonite layer weathers pink; green Hermit Schist shows locally at top.

44.7 Cross deep wash. [If impassable, backtrack to highway (= 37.0 inbound), drive NW 4.3 miles, turn right on road at phone pole 272620, and head for canyon through Supai ridge to rejoin roadlog at 47.3.]

44.9 TURN RIGHT on graded road.

46.1 Wooden posts by road. Hills of Jurassic metagranodiorite and alaskite on left, foliation dips SW; Supai-Redwall isocline in cliffs to right.

46.5 STAY LEFT on small road; main road swings up to marble prospect.

46.95 TURN LEFT into wash on rough track; STOP (1-5A). Hill at 350° has upright section of light Kaibab Marble, rubbly brown cliffs of Coconino Quartzite, recessive green Hermit calc-silicate schist, and dark Supai cliffs. At 312°, pink Supai wollastonite rolls down to right in asymmetric anticline. 325°, white Redwall exposed in anticline overturned to NE. 336°, large Z fold in Supai of near hill. 002°, top of Supai stepped down to right by isocline. CONTINUE across wash.

47.3 TURN RIGHT on road on terrace, and follow it back into wash and through Supai ridge.

47.7 STOP (1-5B). Supai shows extreme transposition in bluffs by road. Some isoclines are preserved; more commonly, section is shredded into lenses. Fold vergence NE. Tertiary dikes nearby to NE.

47.9 SWING SE, road permitting, into longitudinal valley.

48.5 TURN AROUND AND STOP (1-5C) at intersection of tracks. Longitudinal valley follows a Miocene strike-slip fault with 1.5 km of right slip. Near cliffs to N are of tightly folded Kaibab Marble. Upright section seen looking NE toward high ridge, in order downward: light Jurassic metavolcanics (Jv), dark Jv, red Aztec, Triassic clastics, Kaibab. All of these units go around a crossfolded synclorium (as seen from Stop 1-1) whose axis is here in light Jv. Above light Jv is the greatly attenuated N limb, inverted in a recumbent fold; in order going structurally upward: dark Jv, Aztec, Triassic; and, on the striped peak, the complete Paleozoic section. Above it is Proterozoic basement granite, and above that is Jurassic granodiorite and hornblende diorite. All rocks are metamorphosed at lower amphibolite facies, the granites to gneisses. The inverted section is attenuated to about 5% of stratigraphic thickness at the top of the hill, and is progressively more attenuated trending down the hill. Postkinematic pegmatites cut northern rocks.

FOLLOW ROAD BACK TO HIGHWAY; do not backtrack across wash (= 47.3 inbound).

53.0 TURN NW on highway at pole 272620.

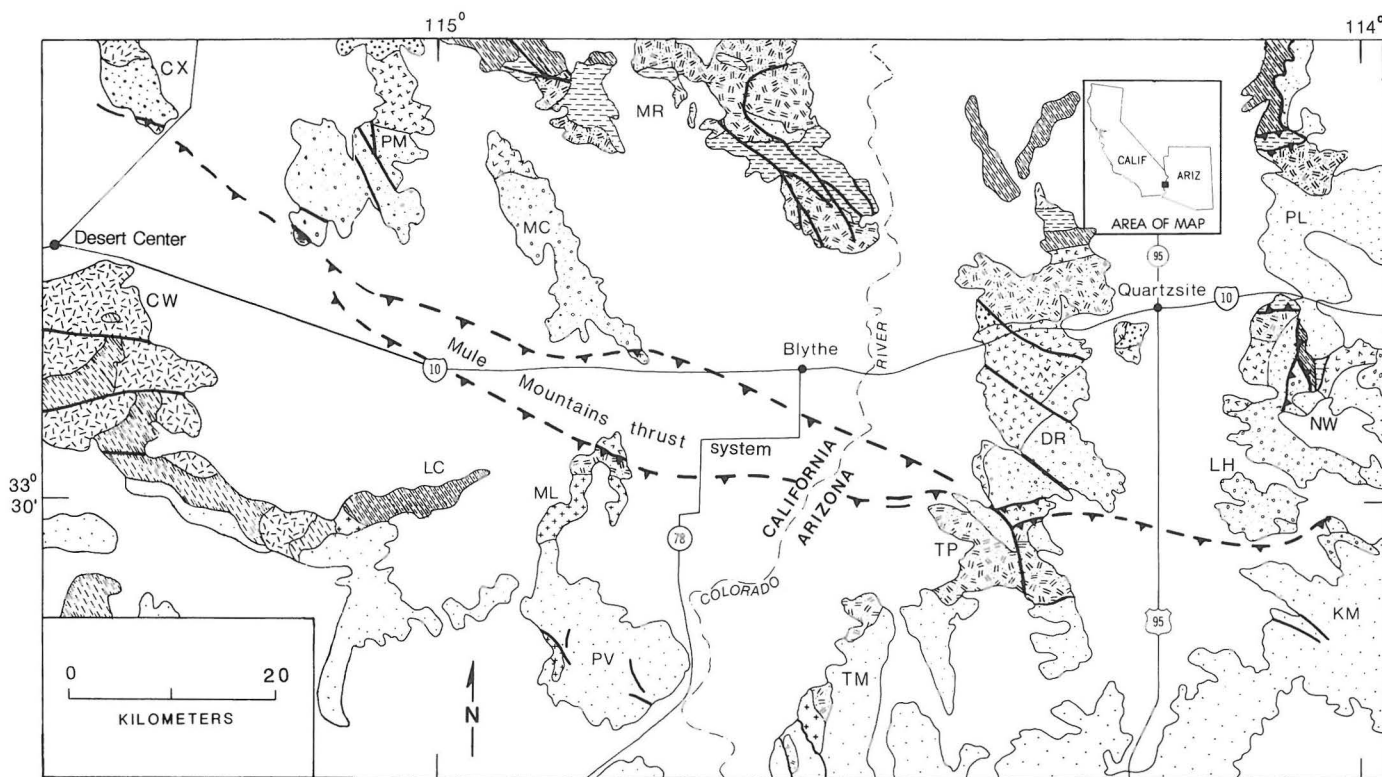
54.3 Double-pole power line crosses highway. In frontal ridge to right, units Kaibab/Coconino/ Hermit/Supai dip progressively to fan level going NW.

55.2 TURN NE on dirt road with small yellow BLM sign.
 57.1 Pass between hills of dark Supai; dip mostly SW because axis of recumbent fold lies between here and main ridge. STOP (I-6A) for view to SSE of thick S limb of syncline, and to ENE of very thin N limb.
 58.2 STOP (I-6B) below wollastonite prospect in N-dipping Kaibab. Peak to N has Mesozoic section. From top: inverted dark Jv; light Jv (contains isoclinal-syncline axis), rest of top half of hill; brown Aztec; and Triassic, in lower slopes; all cut by undeformed pegmatites.
 WALK NW through saddle, along E side of low hill of slightly micaceous Aztec, toward attenuated Paleozoic section low on small peak seen through saddle. Look E to isoclinal interfolding of Kaibab and Triassic on ridge.
 Continue NW through thick Jv to inverted Mesozoic and Paleozoic section, which dips 40° N and is metamorphosed at lower amphibolite facies. Section is complete despite tectonic attenuation to 1% of stratigraphic thickness. Outcrop appearance is not grossly different from that of sections much less attenuated: layering is controlled more by syntectonic recrystallization than by

initial bedding. Units in order going structurally upward and stratigraphically downward: dark Jv, 3 m; Aztec Quartzite, 2 m; green Triassic, 2 m; white and buff Kaibab Marble, 3 m; vitreous Coconino Quartzite, 0.5-2 m; gray Hermit Schist, 1 m; dark Supai cliff, 5 m; white Redwall Marble, tectonically intercalated with Supai, 1 m; yellow dolomite, 5 m; Muav Marble, 2 m; biotitic Bright Angel Schist, 1-2 m; brown Tapeats Quartzite, 2-3 m. Proterozoic metagranite lies above the Tapeats, and Jurassic metagranites lie higher. Numerous minor folds in Supai and Jv plunge WNW parallel to mineral lineation and show NNE vergence.

BACKTRACK TO HIGHWAY.

61.3 TURN NW on highway.
 63.9 TURN RIGHT on dirt road between last 2 power poles, opposite large rock and good road.
 66.6 STOP (I-7), past hill on right, for view. This is near the center of a great swarm of almost undeformed muscovite pegmatites that cut the extremely deformed metamorphic rocks. Dikes decrease upward in high ridge of augen gneiss (Jurassic metagranodiorite) to E. A large mass of



EXPLANATION

Alluvium (Quaternary)	McCoy Mountains Formation (Jurassic(?) and Cretaceous)	Gneissic and monzonitic rocks (Triassic? and Late Triassic)	Gneiss (Proterozoic)
Volcanic and sedimentary rocks (Tertiary)	Granitic rocks (Middle and Late Jurassic)	Clastic rocks (Triassic?)	Contact
Granitic rocks (Late Cretaceous)	Rhyolite and granite (Early and Middle Jurassic)	Sedimentary rocks (Paleozoic and Early Mesozoic)	Fault
			Thrust fault

Figure 2. Generalized geologic map of southeastern California and southwestern Arizona showing outcrops of McCoy Mountains Formation and Mule Mountains thrust system; by Tosdal. Names of ranges: CW, Chuckwalla Mtns.; CX, Coxcomb Mtns.; DR, Dome Rock Mtns.; KM, Kofa Mtns.; LC, Little Chuckwalla Mtns.; LH, Livingston Hills; MC, McCoy Mtns.; ML, Mule Mtns.; MR, Maria Mtns. (Little Maria Mtns. to W of symbol, Big Maria to right); NW, New Water Mtns.; PL, Plomosa Mtns.; PM, Palen Mtns.; PV, Palo Verde Mtns.; TM, Trigo Mtns.; TP, Trigo Peaks. Gavilan Wash (Day 3) lies 30 km south of the Palo Verde Mountains.

garnet-muscovite-biotite granite likely lies beneath us but is not exposed. The highest temperature metamorphism, of middle amphibolite facies, occurred in this area of voluminous pegmatites, so dikes and metamorphism likely reflect related sources of heat and volatiles.

High, dark ridge to N displays inverted N-dipping Paleozoic metasediments that intertongue to right into augen gneiss (Jurassic metagranodiorite) because of extreme Cretaceous transposition of a steep Jurassic intrusive contact. On the distant ridge to NE, a septum of Paleozoic metasedimentary rocks dips N between Jurassic augen gneisses. This is the upper limb of the recumbent fold seen at 301° from Stop 1-1.

RETURN TO BLYTHE (S on highway to Hobsonway, then E to central Blythe).

DAY 2, MORNING: MCCOY MOUNTAINS FORMATION, MCCOY MOUNTAINS

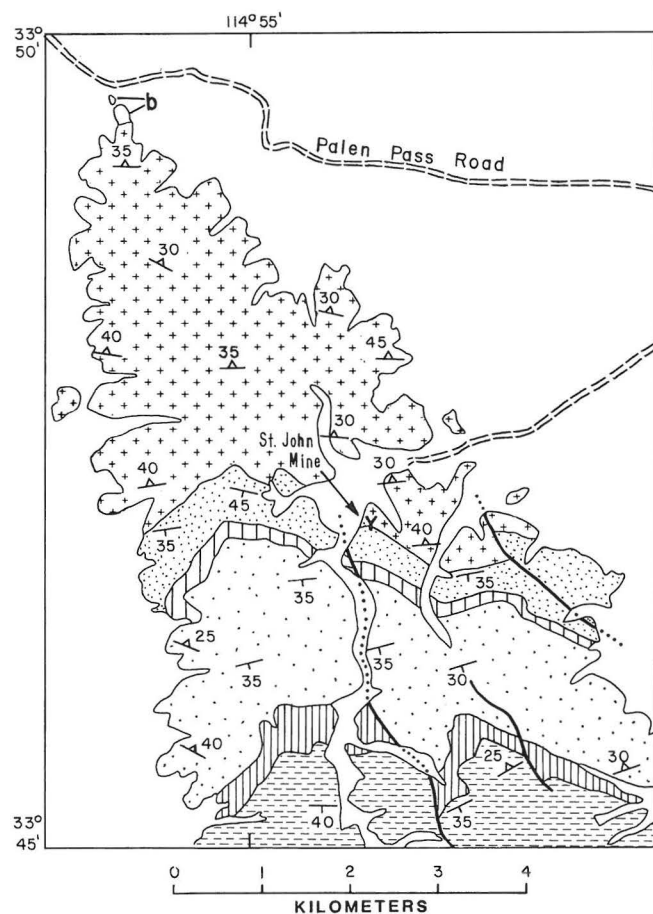
Paul Stone

A thick section of metamorphosed coarse clastic strata of Late Jurassic(?) and Cretaceous age overlies the Paleozoic to Middle Jurassic section, like that of the Big Maria Mountains, in this region. These upper Mesozoic strata are best known in an ESE-trending belt about 120 km long, where they are termed the McCoy Mountains Formation (Pelka, 1973; Harding and Coney, 1985). This formation records major syndepositional uplift and may be the youngest regionally metamorphosed supracrustal unit in the region.

The main belt of the McCoy Mountains Formation crops out in the Coxcomb, Palen, McCoy, Dome Rock, and Plomosa Mountains and the Livingston Hills (Fig. 2). The formation mostly dips southward and is underlain stratigraphically by Lower(?) and Middle Jurassic metaigneimbrites and(?) hypabyssal rocks, here referred to collectively as quartz porphyry. These igneous rocks are underlain in turn by festoon-bedded Lower Jurassic Aztec Quartzite, part of the regional cratonal section, so the McCoy Mountains Formation is tied to cratonal North America. The main belt of the formation is interpreted to be bounded at its top by the Mule Mountains thrust system, the upper plate of which consists of Jurassic and older crystalline rocks.

The McCoy Mountains Formation in its main outcrop belt is composed of metamorphosed sandstone, conglomerate, and subordinate siltstone and mudstone. Quartzose sandstones at the base of the formation are overlain by sandstone and conglomerate rich in volcanic detritus, and those by a thick sequence of arkose and granite conglomerate. An unconformity separates the arkosic rocks from lower strata of the formation in southwestern Arizona but not in southeastern California, where the sharpest lithologic break in the formation is between the basal quartzose rocks and the overlying rocks rich in volcanic detritus. The formation is broadly homoclinal in its main outcrop belt but is deformed locally by large, south-verging folds. It was metamorphosed at greenschist facies late in Cretaceous time, and it contains a penetrative axial-plane cleavage that mostly dips northward.

The age of the formation is constrained by the Middle Jurassic age of underlying quartz porphyry; by the latest Cretaceous isotopic age of granites that intrude the formation (Calzia and others, 1986); by fossil angiosperm wood, no older than late Early Cretaceous, in the arkosic part of the formation in the Palen and McCoy Mountains; and by intercalated metatuff, in the Dome Rock Mountains, that has a discordant U-Pb age of 77 ± 7.5 Ma (R. M. Tosdal, unpub.). Lower parts of the formation may be as old as Late Jurassic.



EXPLANATION

-  Alluvium (Quaternary)
-  Breccia (Tertiary?)
- McCoy Mountains Formation (Cretaceous and Jurassic?)**
 -  Light-gray shale and arkosic sandstone
 -  Dark maroon to greenish-gray siltstone
 -  Dark-gray volcanic-lithic sandstone and siltstone
 -  Maroon siltstone
 -  Tan quartzite and maroon siltstone
 -  Quartz porphyry (Jurassic)
-  Contact
-  Fault -- dotted where concealed
-  Strike and dip of bedding
-  Strike and dip of cleavage

Figure 3. Geologic map of northern McCoy Mountains, showing basal part of McCoy Mountains Formation. Stop 2-1 is in center of this area.

ROAD LOG

Mileage

- 00.0 HEAD N on Lovekin Blvd. from Hobsonway in W part of Blythe, curving NW at 05.5 miles to ascend fans. Gentle S dip of clastic strata of McCoy Mountains Formation (MMf) is obvious in McCoy Mtns. to left (W).
- 17.7 TURN LEFT (SW) on graded road (BLM P172).
- 19.3 Cross railroad tracks at Inca siding.
- 19.5 TURN LEFT (S) at fork, pass office of Superior Gypsum Co., and BEAR RIGHT (W) on graded road. To right, in S end of Little Maria Mtns., are metamorphosed Paleozoic sedimentary rocks and Jurassic granitic rocks like those of the Big Maria Mtns.
- 25.1 PROCEED STRAIGHT (W) on Palen Pass road (BLM P172) at fork, leaving main road, which bears right to gypsum pit in Little Maria Mtns. Drive only 50 m, then TURN LEFT (SW) on faint track toward McCoy Mtns.
- 25.8 Cross wash (may be difficult for 2WD vehicles).
- 27.8 Cross wash; if impassable, park and walk.
- 28.4 STOP (Z-1), at roadend at mouth of McCoy Wash, a major longitudinal canyon (Fig. 3). WALK about 1.2 km S in the canyon, passing first through the upper part of the quartz porphyry that underlies the MMf and then through the lower part of MMf. The quartz porphyry near the roadend and along E side of canyon contains abundant small phenocrysts of quartz and less conspicuous relics of feldspars. The strong N-dipping cleavage is parallel to that in overlying MMf. As we proceed S, the contact between drab, massive quartz porphyry to N and darker, well-bedded, S-dipping MMf to S comes into view in a saddle on the W skyline.

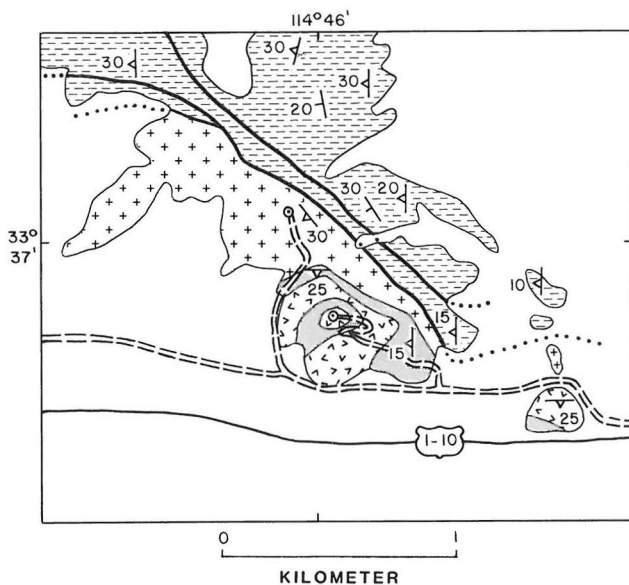
Examine base of MMf at St. John copper mine, 80 m above wash level on E side of canyon, 0.8 km from the roadend. The basal beds, exposed just above the mine entrance, are of laminated tan quartzite that contains pebbles and cobbles of quartzite as lenses and as isolated clasts. Between these beds and the underlying porphyry is a recessive interval, 30 m thick, in which the workings are located. The lower 5-10 m of this interval consist of quartz-porphyry conglomerate, and the rest consists of highly cleaved rock that may represent a fossil weathering zone at the top of the volcanic rocks.

Descend to the wash and continue S through 500 m of tan quartzite and quartzite-clast conglomerate interbedded with light-gray to maroon siltstone, and then through 50 m of maroon siltstone containing pods of tan carbonate. Abruptly overlying this siltstone is the thick middle part of the MMf--sandstone derived from volcanic rocks, with a thin basal conglomerate of volcanic clasts. About 1700 m of this volcanic sandstone is exposed in the canyon, and above that comes arkosic sandstone and polymictic conglomerate of the upper part of the MMf. The N-dipping cleavage that characterizes the main outcrop belt of the formation is interpreted to have developed on the upright limb of a large S-verging syncline, the overturned N limb of which may include the inverted Paleozoic to Jurassic strata exposed at the N end (Palen Pass) of the Palen Mtns. to the W.

BACKTRACK to Blythe.

- 56.8 (= 00.0 outbound) TURN RIGHT (W) from Lovekin Blvd. on Hobsonway.
- 63.9 CONTINUE W on gravel road past Union 76 station and I-10 freeway entrance. (The next stop may be omitted, in which case the trip will continue as at Mile 68.7.) Curve around dark hill after about 2 miles.
- 66.3 TURN RIGHT AND STOP (Z-2) at junction with road to tower at S end of the McCoy Mtns., where strongly foliated MMf metasandstone and metaconglomerate are overlain concordantly by equally metamorphosed igneous and sedimentary rocks along what is interpreted to be the floor thrust of the Mule Mtns. thrust system (Figs. 2, 4). Bedding dips gently W and S. WALK NW to the head of the ravine whose mouth is adjacent to the parking area. On the NE is MMf metaconglomerate containing

flattened clasts of quartzite, volcanic rocks, and granite. This conglomerate is the highest part of the formation known anywhere. On the SE are undated metaigneous rocks that contain small quartz phenocrysts and that resemble the Jurassic quartz porphyry that underlies MMf in the N (Stop 2-1). Above the metaigneous rocks here are intercalated phyllite, schist, greenstone, and minor quartzite. Some of these rocks resemble basal MMf rocks in the N McCoy Mtns. and some resemble basal MMf rocks in the Plomosa Mtns. 60 km to E, so these S McCoy rocks are inferred to be basal MMf rocks in upright stratigraphic position above quartz porphyry. The greenstone layers may correlate with



EXPLANATION

- Alluvium (Quaternary)
- McCoy Mountains Formation (Cretaceous and Jurassic?)--Strongly foliated, light-gray micaceous sandstone and conglomerate
- Metasedimentary rocks and greenstone (Cretaceous or Jurassic?)--May correlate with lower part of McCoy Mountains Formation
- Light-gray schist, phyllite, and minor quartzite
- Greenstone
- Quartz porphyry (Jurassic?)
- Contact
- Fault--Dotted where concealed
- Strike and dip of bedding
- Strike and dip of cleavage
- Radio tower

Figure 4. Geologic map of southern McCoy Mountains, showing structural relations at top of McCoy Mountains Formation. Stop 2-2 is at south tip of range.

greenstones in the basal MMf in the Plomosa Mtns., although no such rocks occur in the N McCoy Mtns.

If these correlations are valid, then the contact between metaigneous rocks and metaconglomerate must be a thrust fault (Fig. 2) with a stratigraphic separation equal to the 7-km thickness of the MMf. It is possible alternatively, in view of the unfaulted aspect of the contact and of the lack of structural evidence for N vergence, that this volcanic-and-sedimentary section lies in stratigraphic position atop MMf. Dating is needed.

BACKTRACK to I-10 freeway entrance.

DAY 2, AFTERNOON: MULE MOUNTAINS THRUST, MULE MOUNTAINS

Richard M. Tosdal

The Mule Mountains thrust system is a zone of ductile shear that crops out discontinuously for 120 km, between the Coxcomb Mountains in California and the Livingston Hills in Arizona (Fig. 2). The thrust system consists of imbricate slices between roof and floor thrusts. The lower plate of the floor thrust consists of the McCoy Mountains Formation and the rocks that underlie it; the upper plate of the roof thrust consists of Proterozoic, Late Triassic, and Middle and Late Jurassic plutonic and gneissic rocks, and a swarm of Late Jurassic dikes. The imbricate zone between roof and floor thrusts generally consists of Jurassic quartz porphyry and stratigraphically low parts of the McCoy Mountains Formation (as at Stop 2-2), but it includes in the Mule Mountains Jurassic granodiorite and dikes identical to those in the upper plate of the roof thrust in that range and in the southern Dome Rock Mountains.

Northeast-verging movement along the Mule Mountains thrust system occurred under greenschist facies conditions at midcrustal depths and represents both major discrete faults and pervasive ductile shear. The distribution of Mesozoic units across the thrust system is interpreted to indicate that slip along the gently dipping thrust system was between 9 and 18 km. K-Ar and U-Pb geochronology of rocks in both plates of the thrust system, of granites inferred to postdate thrusting, and of rocks within the thrust zone brackets the movement as Late Cretaceous, between about 70 and 85 Ma (Calzia and others, 1986; Tosdal, 1986 and unpublished data).

ROAD LOG

Mileage (Continued from morning log).

- 68.7 (= Mile 63.9 outbound). TURN S on paved road across freeway.
- 69.3 TURN RIGHT (W) on gravel road at T junction.
- 70.3 TURN LEFT (S). Follow road through two 90° turns.
- 73.2 VEER RIGHT (SW) on dirt road (not hard right on road along field).
- 73.6 VEER LEFT on faint road along W end of dark hill and drive W up old alluvium toward Mule Mtns.
- 74.9 STOP (2-3), park, and walk to range front on metamorphosed quartz porphyry that makes up most of the lower plate of the roof thrust of the Mule Mtns. thrust system (Fig. 5). Relict volcanic textures indicate that the original rock was mostly ignimbrite, with minor lithic tuff and ash. The layering in the rocks is due to ductile shear, not bedding. The upper plate of the roof thrust consists of metamorphosed porphyritic hornblende-biotite granodiorite (165 Ma, U/Pb: Tosdal, unpub.), which contains lavender phenocrysts of K-feldspar. The roof thrust is a ductile-shear zone that dips 40-45° S and is 50-300 m thick. The main structural break within the roof thrust is inferred to be at the contact between the porphyritic granodiorite and the quartz porphyry. The shear zone dips into the range and forms a recessive tabular horizon 200-300 m above the base of the range. Thinner ductile shear zones occur both above and below this main zone but are much less

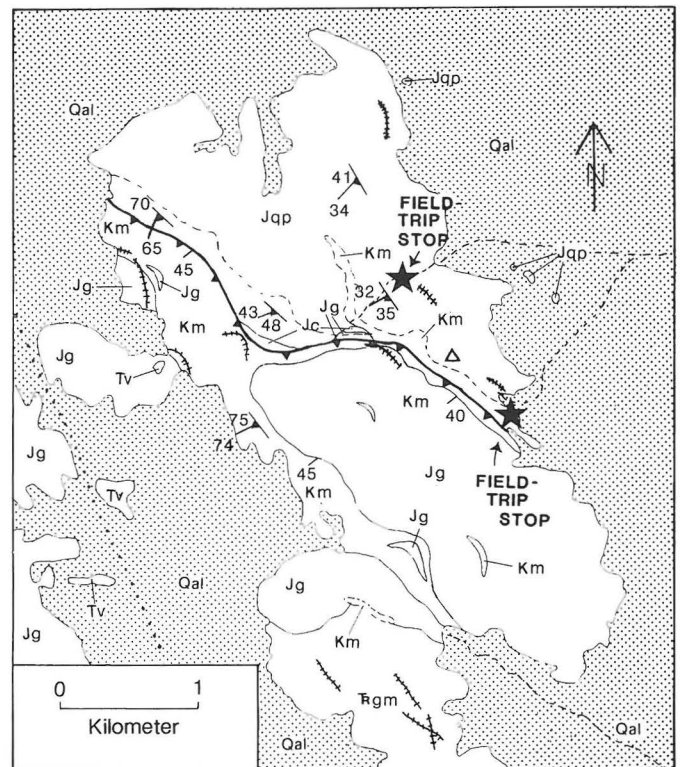
abundant in the metagranodiorite above it than in the metavolcanic rocks below it.

CLIMB SE into the ductile shear zone that marks the main structural break. The shear zone contains fault rocks representing different finite-strain states and including both coaxial and noncoaxial strains. Highly strained rocks characterize the central parts of the shear zone, and less strained ones the margins.

Exxon Mining Co. drilled a 200-m uranium-exploration hole at the end of the road to NW. The hole was collared in lower-plate quartz porphyry, of which abundant core pieces are scattered about the pad. Cores of porphyritic granodiorite identical to that of the upper plate also lie around the pad, so such rocks occur at shallow depths in the lower plate.

BACKTRACK to turnoff (mile 73.6 inbound).

- 76.2 TURN LEFT on main dirt road at W end of low dark hill and drive W toward mountains.
- 77.5 STOP (2-4) close to range front and WALK up washed-out road to where it starts switchbacking. The metaignimbrite-metagranodiorite break of the roof thrust strikes NW from Stop 2-3 to the notch in the ridge



EXPLANATION

Qal - Alluvium (Quaternary)	Jqp - Quartz porphyry (Early or Middle Jurassic)
Tv - Volcanic rocks (Tertiary)	Rgm - Gneissic and monzonitic rocks (Triassic? and Late Triassic)
Km - Mylonitic rocks (Late Cretaceous)	--- Contact
--- Monzodiorite (Late Jurassic) Fault (inferred)
Jg - Porphyritic granodiorite (Middle Jurassic)	▲ Main structural break
Jc - Clastic rocks (Early or Middle Jurassic)	△ Drill hole
	4/5 Foliation and lineation

Figure 5. Geologic map of northern Mule Mountains, showing structural relations across roof thrust of Mule Mountains thrust system. Stops 2-3 and 2-4 are marked by stars. Center of area is at about 33°31.6' N, 114°48.2' W.

spur E of this locality. The shear zone splits into lower and upper branches at the notch (Fig. 5). The lower branch trends down to the lowest switchback on the road and dies out 1 km to NW. The upper branch climbs structural section, strikes W from the saddle at the roadend, and continues across the back side of the high peak W of the saddle; it defines a lateral ramp. WALK directly uphill (S) from the lowest switchback to see the structural section between the branches of the shear zone. This section consists of, in order upward, quartz porphyry, micaceous quartzite, volcanoclastic phyllite and semischist, and metagranodiorite. The lower branch of the shear zone includes metasedimentary rocks and quartz porphyry; the upper branch is within granodiorite. The rocks between the two branches vary from penetratively foliated to undeformed. The main structural break again superposes granodiorite on quartz porphyry on the back side of the high peak to W.

The contact between the metagranodiorite and the metavolcanic and metasedimentary rocks is thus here only in part structural; where exposed near the road, the contact obviously is either intrusive or depositional. As porphyritic granodiorite of this type is known to intrude Jurassic quartz porphyry in other ranges in the region, the contact here is interpreted to be intrusive. The presence of the same porphyritic granodiorite, and of Late Jurassic mafic dikes in it, both above and below the upper branch of the shear zone shows that this roof thrust of the Mule Mountains thrust system is not a megathrust and that it cannot be a terrane boundary (as Harding and Coney, 1985, inferred it to be).

BACKTRACK to I-10.

- 83.5 TURN RIGHT (E) onto I-10 and go about 4 miles to Calif. Highway 78, then S on 78 about 70 miles to I-8, and E on I-8 about 15 miles to Yuma, where the group will spend the night.

[Late Triassic plutonic rocks will not be seen during the organized field trip but can be reached by driving W from Hwy. 78 on 30th St. (= Bradshaw Trail; about 10.5 road miles S of I-10) into the central Mule Mtns. Drive W on this road through a gap (STOP 2-5A) in a ridge of leucocratic Late Triassic biotite quartz monzonite that is intruded by both mafic and felsic Late Jurassic dikes and continue a few more miles to a pass (STOP 2-5B). To N are metamorphosed, modally layered hornblende diorite, hornblendite, and monzodiorite, darkly varnished in hillside outcrops but well exposed in washes. These mafic rocks are intruded by foliated leucocratic granitic rocks, exposed S of the pass. The distinctive hornblende monzodiorite and garnet-biotite quartz monzonite strikingly resemble phases of the Late Triassic Lowe Granodiorite of the San Gabriel Mountains north of Los Angeles (Tosdal, 1986), and presumably the two terranes were adjacent before late Neogene slip on faults of the San Andreas system.]

DAY 3: CHOCOLATE MOUNTAINS THRUST AND OROCOPIA SCHIST, GAVILAN WASH AREA

Gordon B. Haxel and Richard M. Tosdal

The late Mesozoic Orocopia Schist is the structurally lowest tectonostratigraphic unit exposed in southeastern California and southwestern Arizona. Metamorphosed oceanic sedimentary and volcanic rocks of the schist are overlain along the regional Chocolate Mountains thrust (CMt) by a slab or flake of continental crust (Crowell, 1981; Dillon and others, in review; Haxel and Dillon, 1978; Haxel and Tosdal, 1986; Jacobson and others, in press). The schist is dominated by quartzofeldspathic to semipelitic metasediments and includes minor metabasalt, ferromanganiferous metachert and marble, and rare ultramafic rocks. Thrusting and metamorphism evidently occurred between about 87 and 74 Ma (Haxel and Tosdal, 1986, and references therein), and

at least part of the protolith evidently is older than 163 Ma (Mukasa and others, 1984).

The Orocopia Schist and CMt are exposed in a series of uplifts that trend eastward from here into Arizona, and northward from here through the Chocolate and Orocopia Mountains. Schist and CMt are similar to the Pelona Schist and Vincent thrust of the central Transverse Ranges of southern California (Ehlig, 1981), and the two terranes were adjacent prior to Neogene displacement on faults of the San Andreas system.

Geochronologic evidence indicates that the Orocopia protolith is at least 75 m.y. older than the metamorphism of the schist; therefore, two separate tectonic models are required. We suggest that the Orocopia protolith basin linked the Mojave-Sonora megashear of northwest Mexico to Middle to Late Jurassic continental-margin basins of western California. The most straightforward model to account for the metamorphism of the schist is subduction of the protolith northeastward beneath southwestern North America (Crowell 1981); this model explains the high-P metamorphism of the schist but not the top-to-the-northeast movement along the CMt. An alternative model inferring that a microcontinent of southwestern North American origin overrode preexisting continental-margin strata before colliding with North America (Haxel and Tosdal, 1986) is consistent with northeastward overthrusting but not with the apparent absence of a suture northeast of the schist. Jacobson and others (in press) suggest that the northeast-directed "thrust" records latest Cretaceous, postsubduction uplift and tectonic unroofing. In this model, the original direction of overthrusting, related to subduction, was southwestward; but no direct evidence of such movement has been reported.

We will see the CMt in the Gavilan Wash area, about 30 km south of the Palo Verde Mountains shown on Fig. 2. A longer version of this field guide is available (Haxel and others, 1986).

FIELD LOG

Road Mileage

00.0. HEAD N on Ogilby Road (Imperial County road S34) from I-8 about 13 miles W of Yuma.

12.9 TURN RIGHT (NE) on graded Indian Pass road. From the N, this turnoff is 11.1 miles S on Ogilby Road from its junction with State Hwy. 78 between Blythe and Brawley.

21.7 Go through Indian Pass.

22.3 TURN RIGHT down Gavilan Wash.

23.6 TURN RIGHT on steep road up S side of wash just beyond low crops of purplish argillite. PARK on terrace.

STOP 3-0. The hills S of Gavilan Wash consist mostly of Orocopia Schist, which is separated from plutonic rocks (near slopes) by the N-dipping CMt (Figs. 6, 7). The Gatuna normal fault drops Mesozoic strata (low foreground) against crystalline rocks (hills).

Walking Traverse

WALK SE about 350 m over slightly metamorphosed purplish wackes and siltstones of argillitic siltstone member of Winterhaven Fm (Haxel and others, 1985; STOP 3-1). The formation is correlated on lithologic grounds with the lower part of the McCoy Mountains Formation (Haxel and others, 1985; Stop 2-1).

WALK ESE about 100 m to prominent Gatuna fault between Winterhaven Fm and plutonic rocks (STOP 3-2). This middle Tertiary fault, poorly exposed in several arroyos, is marked by 1 m or so of gouge and dips moderately N.

WALK E about 150 m to mouth of first prominent N-draining canyon, and S up this canyon to nearby crops of gneiss (STOP 3-3) in upper plate of CMt. These quartzofeldspathic and amphibolitic gneisses probably are derived from Jurassic or Triassic granitoids (Tosdal,

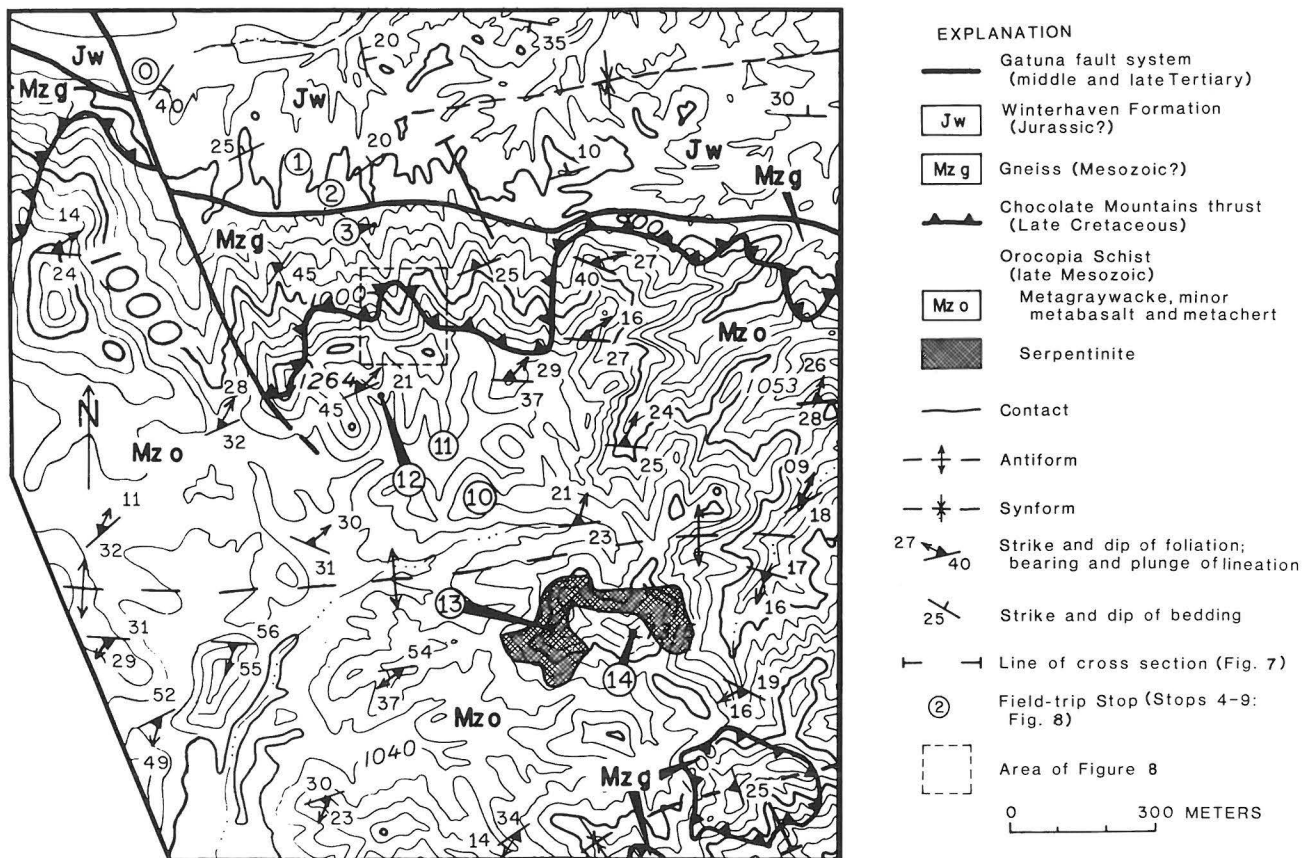


Figure 6. Geologic map of Gavilan Wash area, with locations of Stops 3-0 to 3-3 and 3-10 to 3-14. Area is at about $33^{\circ}01' N$, $114^{\circ} 45' W$. After Haxel and others (1986, Fig. 1).

1986). Gneissic layering predates the CMt and is overprinted by mylonitization and local folding within the CMt zone (Stops 3-4 to 3-8). Intensity of deformation increases downward through several tens of m to the base of the upper plate.

CONTINUE S up canyon about 250 m to where it splits into several tributaries and climb knob of Orocopia Schist in SE part of this confluence area for overview of CMt zone (Fig. 8; STOP 3-4). The sharp, planar CMt is within or at the base of the conspicuous resistant layer in the upper and middle part of E side of canyon, and dips about 40° NNW. The thrust lies within a zone, 10-100 m thick and comprising most of the rocks in view, of rocks that are texturally distinct from, but grade into, rocks farther above or below the thrust (Fig. 9). Within the thrust zone, upper-plate gneiss is mylonitic, and lower-plate schist is coarser than schist farther below the thrust. Metamorphic grade increases upward in the schist; albite gives way to more calcic plagioclase in basalt, and garnet appears in metasandstone. Lineations in mylonitic rocks at the base of the upper plate, in coarse schist beneath the thrust, and in the finer-grained schist below the thrust zone are all parallel. Thrusting and metamorphism were synchronous.

CLIMB ESE to CMt at base of highest part of small cliff high on the E side of canyon (STOP 3-5). Do not hammer on these outcrops: preserve them for other geologists to examine. The thrust surface is the sharp contact between moderately foliated mylonite above and strongly foliated coarse-grained Orocopia Schist below, in the lower 1 m or so of the cliff. Although easily distinguished in thin section, rocks on opposite sides of fault look similar in hand specimen because of their similar composition and metamorphic grade (Haxel and others, 1986). Mylonite just above the thrust surface

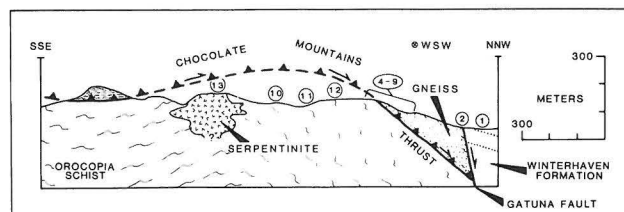


Figure 7. Cross section of Chocolate Mountains thrust and Orocopia Schist. Line of section is subparallel to field-trip traverse; stops are projected into the section. For ages of rock units and position of section, see Fig. 6.

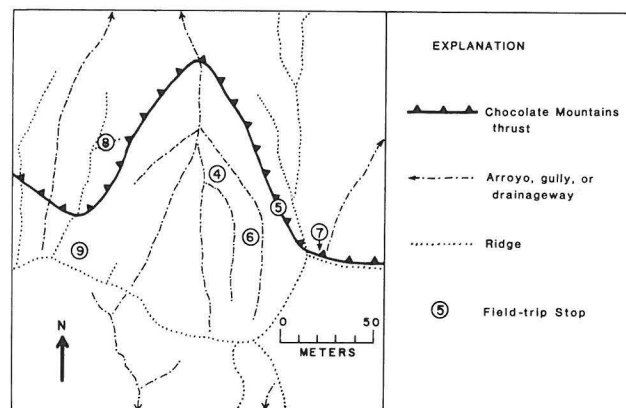


Figure 8. Sketch map of locations of Stops 3-4 to 3-9.

grades up, through several m, into protomylonite, which in turn grades up into gneiss streaked by protomylonite.

CONTOUR SW 10-15 m to large outcrop of coarse Orocopia Schist (STOP 3-6) with NNE lineation. This coarse schist that makes up the lower-plate part of the thrust zone is typically several tens of m thick and is characterized by flakes, several mm across, of muscovite and biotite. Coarse schist typically appears crystalloblastic in hand specimen, but some samples display in thin section a protomylonitic fabric superimposed on the crystalloblastic fabric.

CLIMB E to where the thin resistant layer along CMT passes through notch in ridge, then walk about 15 m E to knob of N-dipping mylonite (STOP 3-7), on the W side of which is a photogenic exposure of the thrust. (No hammering.) The fault trace runs E from here along the divide for a few hundred m and separates steep, brown, gneiss ridges to N from gentler hills of shiny Orocopia Schist to S.

WALK SW from notch, then W, along burro trails across dip slopes of schist at the head of the canyon, to broad divide on SW side of canyon; then walk NNW along burro trail, then N about 60 m along ridge to where it splits into several smaller ridges (Fig. 8). Search for outcrop-scale folds, which are most abundant low on ridge (STOP 3-8A). These thrust-zone folds deform slightly mylonitized prethrust gneissic layering and are variously monoclinial, open, tight, and isoclinal. This sequence of styles represents preservation of stages in progressive fold development. Many thrust-zone fold pairs are markedly asymmetric and define local senses of rotation. Although the asymmetry of folds at any one locality may not constrain movement direction along CMT, the collective asymmetry of 80 folds from 36 localities spread over 60 km uniquely indicates NE overthrusting (Dillon and others, in review). Simpson (1986) also recognized consistent NE vergence here. Paleomagnetic data suggest that part of the region of indicators of NE vergence rotated about 40° clockwise, relative to the continental interior, during Tertiary time (Costello, 1985), so the prerotation direction of overthrusting may have been N.

CLIMB for unobstructed view (STOP 3-8B) of thrust zone in bottom and E side of canyon. The thrust surface is within or at the base of the conspicuous resistant layer of mylonite that separates blocky upper-plate gneiss and derivative mylonite from less resistant, shiny, lower-plate Orocopia Schist. A discordance between two thrust-zone fabrics in the upper plate shows on E side of canyon. Mylonitic fabric below this interface dips moderately N within the resistant layer along the thrust. Above the interface, partially mylonitized gneissic fabric dips more gently. The marginal part of the shear zone appears to have been rotated toward parallelism with the more strongly mylonitic central part; the rotation implied is compatible with NE overthrusting.

BACKTRACK SSW about 60 m up ridge and find crop of coarse Orocopia Schist with shear bands (STOP 3-9). Several types of asymmetric microstructures within the thrust zone here, studied in outcrop, slab, and thin section, indicate NE overthrusting. Layers of high shear strain characterized by C' fabrics (shear bands) alternate with layers of low shear strain containing C-S fabrics. Other composite planar fabrics and directional indicators, chiefly asymmetric porphyroblasts and broken and displaced grains, can be seen in the thrust zone W of this locality in schist of moderate mica content.

BACKTRACK to Stop 3-7. WALK SE, THEN S, along gentle slope W of small arroyo that drains S from the divide running E from Stop 3-7. Cross arroyo just below where it turns WSW, and go S about 150 m to crops of flaggy schist on S side of small peak (STOP 3-10). Most of the Orocopia Schist is "grayschist"—quartzofeldspathic schist and minor interlayered semipelitic schist,

characterized by shear-transposed compositional layering and by gray to black porphyroblasts of graphitic albite (less common here than in much of the schist). Orocopia grayschist is composed essentially of albite, quartz, muscovite, biotite, microcline, and clinozoisite. Garnet is rare except in the zone of coarse schist beneath the thrust. Semipelitic schist is similar but more variable; chlorite is common, and garnet is more abundant than in metasediments; microcline is uncommon, and albite and clinozoisite are absent in some rocks; bright green fuchsite (chromian muscovitic mica) is sparse. Major-element composition of the grayschist is that of quartzose graywacke. Pb and Nd isotopic systematics, REE spectra, and other major- and trace-element data indicate a dominant continental provenance with a subordinate oceanic or continental magmatic-arc component (Haxel and Tosdal, 1986). Carbon (0.05-0.8%) correlates with $Al_2O_3/(Na_2O+K_2O)$, supporting the hypothesis that the graphite is derived from organic material concentrated in the pelitic fraction of turbidites. Foliation dips moderately N beneath CMT; lineation plunges NE or NNE.

WALK N AND DOWN, recross arroyo, and walk N or NW to outcrop of thin, resistant layers of dark-brown-weathering ferromanganiferous metachert within grayschist, STOP 3-11. The metachert contains about 85-90% SiO_2 , 1-2% Al_2O_3 , 7% total Fe as Fe_2O_3 , and 1.4% MnO, and consists essentially of quartz, spessartite, and porphyroblastic magnetite. The ferromanganiferous composition indicates the rocks to be cherts, not arenites. Chondrite- or shale-normalized REE spectra have pronounced negative Ce anomalies, indicating a marine origin. Trace-element and oxygen-isotope data indicate the cherts to be biogenic deposits with subordinate detrital and submarine hydrothermal components (Haxel and Tosdal, 1986). Some metachert layers grade into enclosing metagraywacke via micaceous metachert, so chert and sandstone were deposited together, not juxtaposed tectonically. Metachert is generally associated with metabasalt, presumably because chert accumulated on submarine volcanic highs not reached by most turbidites. A thin layer of metabasalt crops out between metachert and arroyo to S.

FOLLOW METACHERT W 100-150 m, crossing small S-draining arroyo. TURN N up second, larger arroyo and walk about 70 m to a fork, then about 40 m NNW up low ridge between the two branches. STOP (3-12) at crops of black hornblende schist (metabasalt) with thin layers of metachert. Orocopia metabasalts typically consist of hornblende, white nongraphitic albite (locally porphyroblastic), and epidote, with accessory chlorite,

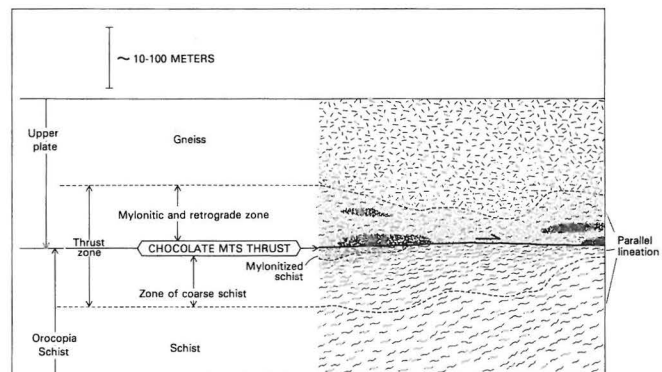


Figure 9. Schematic cross section of the Chocolate Mountains thrust zone, showing characteristic tectonic stratigraphy. Stippling represents mylonitic rocks; dashed contacts are gradational.

quartz, and garnet. Metabasalt within several hundred m of the CMt contains plagioclase, An₂₂₋₃₄, rather than albite. Some metabasalt contains minor prograde muscovite, suggesting affinity to high-P intermediate-T metamorphic facies.

Orocopia metabasalts plot within MORB fields or along MORB trends on such discrimination or variation diagrams as Th-Ta-Hf, Ti-Zr, Ti-V, Ti/Cr-Ni, and Ta-La. Absence of negative Nb-Ta anomalies on spidergrams suggests that the basalts are not arc-related. REE spectra are nearly flat at 10-30 times chondritic. In this and other aspects of their trace-element systematics, Orocopia basalts are transitional between normal and enriched MORB (Haxel and Tosdal, 1986; Jacobson and others, in press).

WALK SE about 0.5 km to prominent reddish-brown hill of serpentinite (STOP 3-13) within greyschist. The serpentinite is composed of antigorite with accessory magnetite and carbonate, grades into less common antigorite-carbonate rock, and is cut by thin veins of fibrous chrysotile. The irregular body of unfoliated serpentinite is semiconcordantly enclosed in greyschist but apparently intrudes it locally. Some of the serpentinite has a sill-like relation to foliation in the schist, but some of the contact is subvertical and the serpentinite appears pipelike, and serpentinite dikes intrude schist. A few small lenses of schist occur within the serpentinite. We infer solid-state emplacement of the serpentinite. The protolith presumably was oceanic mantle material, although its tectonic history is unclear.

CLIMB serpentinite hill (STOP 3-14). Top of hill (peak 1315) is underlain by greyschist and minor metabasalt in reentrant on S side of serpentinite. Large dark hill to SE and smaller one to S are capped by klippen of subhorizontal CMt. Dark, blocky upper-plate gneiss contrasts with lighter colored, shiny, less resistant lower-plate schist. These klippen are in the trough of a WSW-trending syncline that folds the CMt and the foliation of the schist. The crest of an E-W anticline passes near the N margin of the serpentinite. These small, open folds are third-order parts of the first-order Chocolate Mtns. anticlinorium, which itself consists of several second-order anticlinal segments. The Orocopia Schist of this area marks a culmination along the crest of one of these second-order anticlines. The area from here N to the middle Tertiary Gatuna fault, including Stops 3-3 to 3-12, is on the N limb of this second-order anticline.

RETURN TO VEHICLES. Walk W off serpentinite hill, then NW about 700 m to conspicuous pass in low hills. Note along the way the large quartz pods in schist. Follow burro trail N into Gavilan Wash from pass.

Roadlog. BACKTRACK to Ogilby Road. The organized trip will drive N to I-10, thence E to Phoenix.

REFERENCES CITED

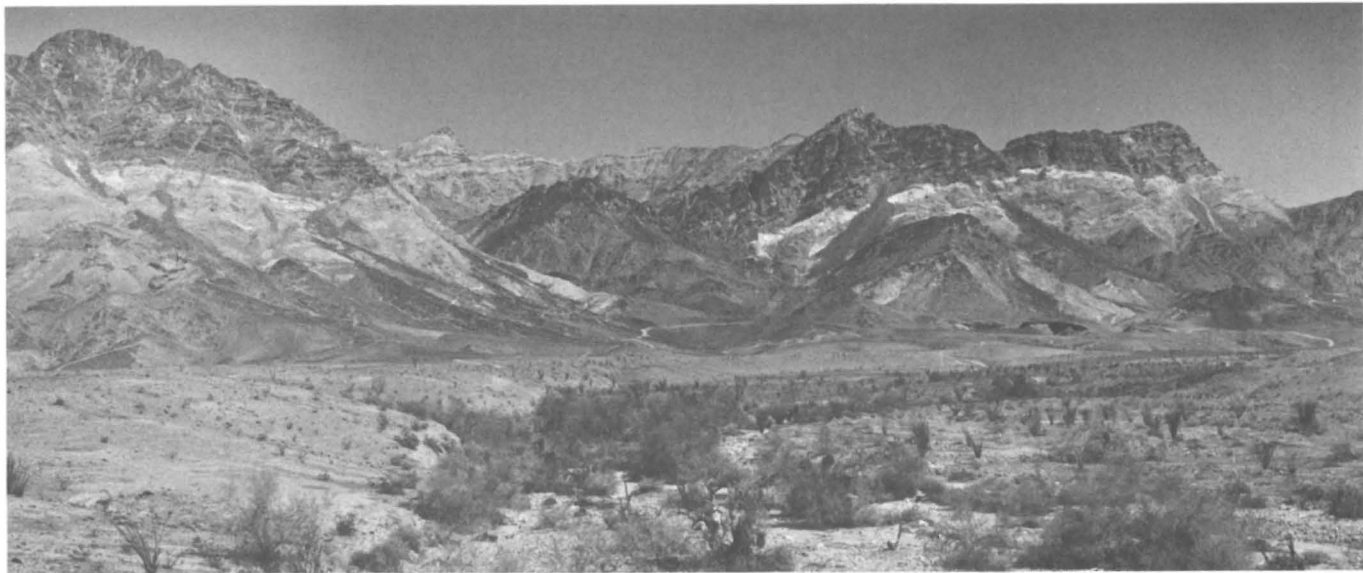
- Anderson, T.H., and Silver, L.T., 1981, An overview of Precambrian rocks in Sonora: Univ. Nat. Auton. Mexico, Inst. Geologia, Revista, v. 5, no. 2, p. 131-139.
- Calzia, J.P., DeWitt, E., and Nakata, J.K., 1986, U-Th-Pb age and initial strontium isotopic ratios of the Coxcomb granodiorite, and a K-Ar date of olivine basalt from the Coxcomb Mountains, southern California: *Isochron West*, no. 47, p. 3-8.
- Costello, S.C., 1985, A paleomagnetic investigation of mid-Tertiary volcanic rocks in the lower Colorado River area, Arizona and California: San Diego State Univ., M.Sc. thesis, 109 p.
- Crowell, J.C., 1981, An outline of the tectonic history of southeastern California, in Ernst, W. G., ed., *The geotectonic development of California*: Englewood Cliffs, N.J., Prentice-Hall, p. 583-600.
- Dillon, J.T., Haxel, G.B., and Tosdal, R.M., in review, Structural evidence for northeastward movement on the Chocolate Mountains thrust, southeasternmost California: submitted to *Jour. Structural Geol.*
- Ehlig, P.L., 1981, Origin and tectonic history of the basement terrane of the San Gabriel Mountains, central Transverse Ranges, in Ernst, W.G., ed., *The geotectonic development of California*: Englewood Cliffs, N.J., Prentice-Hall, p. 253-283.
- Frost, E.G., Martin, D.L., and Krummenacher, Daniel, 1982, Mid-Tertiary detachment faulting in southwestern Arizona and southeastern California and its overprint on the Vincent thrust system: *Geol. Soc. America Abstracts with Programs*, v. 14, p. 164.
- Hamilton, Warren, 1982, Structural evolution of the Big Maria Mountains, northeastern Riverside County, southeastern California, in Frost, E.G., and Martin, D.L., eds., *Mesozoic-Cenozoic evolution of the Colorado River region, California, Arizona, and Nevada*: San Diego, Cordilleran Publishers, p. 1-27.
- _____, 1984, Generalized geologic map of the Big Maria Mountains region, northeastern Riverside County, southeastern California: U.S. Geol. Survey Open-File Report 84-407, 7 p. + 1:48,000 map.
- Harding, L.E., and Coney, P.J., 1985, The geology of the McCoy Mountains Formation, southeastern California and southwestern Arizona: *Geol. Soc. America Bull.*, v. 96, p. 755-769.
- Haxel, G.B., and Dillon, J.T., 1978, The Pelona-Orocopia Schist and Vincent-Chocolate Mountains thrust system, southern California: *Pacific Sec. Soc. Economic Paleontologists and Mineralogists, Pacific Coast Paleogeography Symposium 2*, p. 453-469.
- Haxel, G.B., and Tosdal, R.M., 1986, Significance of the Orocopia Schist and Chocolate Mountains thrust in the late Mesozoic tectonic evolution of the southeastern California-southwestern Arizona region--extended abstract: *Arizona Geol. Soc. Digest*, v. 16, p. 52-61.
- Haxel, G.B., Tosdal, R.M., and Dillon, J.T., 1985, Tectonic setting and lithology of the Winterhaven Formation, a new Mesozoic stratigraphic unit in southeasternmost California and southwestern Arizona: *U.S. Geol. Survey Bull.* 1599, 19 p.
- _____, 1986, Field guide to the Chocolate Mountains thrust and Orocopia Schist, Gavilan Wash area, southeasternmost California: *Arizona Geol. Soc. Digest*, v. 16, p. 282-293.
- Hoisch, T.D., Miller, C.F., Heizler, M.T., Harrison, T.M., and Stoddard, E.F., in press, Late Cretaceous regional metamorphism in southeastern California, in Ernst, W.G., ed., *Metamorphism and crustal evolution of the western United States*: Englewood Cliffs, N.J., Prentice-Hall.
- Jacobson, C.E., Dawson, M.R., and Postlethwaite, C.E., in press, Structure, metamorphism, and tectonic significance of the Pelona, Orocopia, and Rand Schists, southern California, in Ernst, W.G., ed., *Metamorphism and crustal evolution of the western United States*: Englewood Cliffs, N.J., Prentice-Hall.
- Leveille, Gregory, and Frost, E.G., 1984, Deformed upper Paleozoic-lower Mesozoic cratonic strata, El Capitan, Sonora, Mexico: *Geol. Soc. America Abstracts with Programs*, v. 16, p. 575.
- Mukasa, S.B., Dillon, J.T., and Tosdal, R.M., 1984, A Late Jurassic minimum age for the Pelona-Orocopia Schist protolith, southern California: *Geol. Soc. America Abstracts with Programs*, v. 16, p. 323.
- Pelka, G.J., 1973, Geology of the McCoy and Palen Mountains, southeastern California: Univ. Calif. Santa Barbara, Ph.D. thesis, 160 p.
- Simpson, Carol, 1986, Microstructural evidence for northeastward movement on the Vincent-Orocopia-Chocolate Mountains thrust system: *Geol. Soc. America Abstracts with Programs*, v. 18, p. 185.

Stone, Paul, Howard, K.A., and Hamilton, Warren, 1983, Correlation of metamorphosed Paleozoic strata of the southeastern Mojave Desert region, California and Arizona: Geol. Soc. America Bull., v. 94, p. 1135-1147.

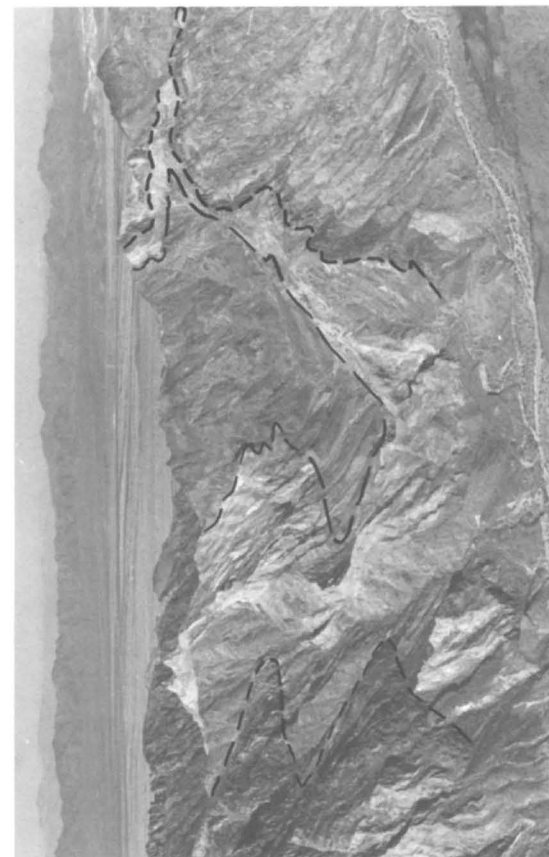
Tosdal, R.M., 1986, Mesozoic ductile deformation in the southern Dome Rock Mountains, northern Trigo Mountains, Trigo Peaks and Livingston Hills, southwestern Arizona, and Mule Mountains, southeastern California: Arizona Geol. Soc. Digest, v. 16, p. 62-71.



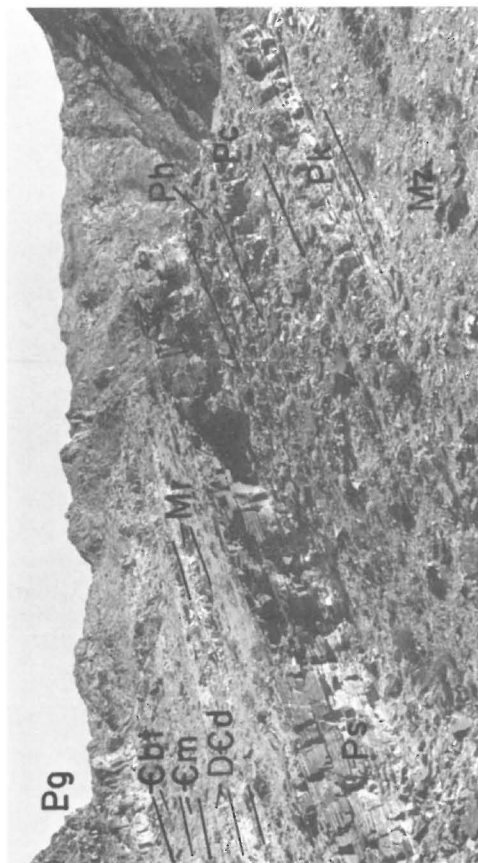
North along axes of isoclinal folds refolded by eastward-overturned recumbent folds, cherty Kaibab Marble, Stop 1-2B. The outer contacts of the formation are plane-parallel; this deformation records combined pure and simple shear, not superposed compressive refolding.



View northeast to metamorphosed Paleozoic strata of southwestern Big Maria Mountains. Stop 1-3 is in the center foothills. Kaibab Marble forms gray peak left of center distance, with Coconino Quartzite in slope beneath. The main, dark crest is of Supai Formation, above a thin band of white Redwall Marble; thick Devonian to Cambrian metadolomite forms the light-colored lower cliffs. The lower ridges and slopes are of various Cambrian formations, Proterozoic metagranite, and Jurassic metagranodiorite. Most rocks seen here dip gently northeastward, in overall upright order, but the simplicity is illusory as the rocks are, in fact, isoclinally folded on a large scale, as seen in two pictures on the next page.



Aerial view northwest along axis of major syncline in central part of range. Stratigraphic top of light Kaibab Marble is marked with long dashes, and top of dark Supai Formation with short dashes, to show recumbent crossfolds; units are greatly thinned tectonically going from left to right around the fold. This structure is seen from a distance from Stop 1-1.



Complete but severely attenuated inverted section of Paleozoic formations. Abbreviations: Eg, Proterozoic granite, now augen gneiss; Cbt, Bright Angel Schist and Tapeats Quartzite; Cm, Muay Marble; DCd, Devonian to Cambrian metadolomite; Mr, Redwall Marble; Ps, Supai Formation; Ph, Hermit Schist; Pc, Coconino Quartzite; Pk, Kaibab Marbles; Mz, Triassic rocks. This section is seen from a distance from Stop 1-5C.



View northwest at recumbently folded Supai Formation (between dashed lines). Arrows point to axes of isoclinal folds in metadolomite. The peak is the same as the one at the right end of the view on the preceding page.



Aerial view northwest along large, tight syncline of dark Supai Formation (left); the peak is the same as that at the left edge of the view on the preceding page). The valley along the center of the view follows a Miocene right-slip fault. Stop 1-3 is below the lower left corner of the picture, and 1-5C is in the medial valley.

Field-Trip Guide to Parts of the Harquahala, Granite Wash, Whipple, and Buckskin Mountains, West-Central Arizona and Southeastern California

Jon E. Spencer and Stephen J. Reynolds
Arizona Bureau of Geology and Mineral Technology
845 N. Park Ave., Tucson, Arizona 85719

J. Lawford Anderson and Gregory A. Davis
Department of Geological Sciences
University of Southern California
Los Angeles, California 90089-0714

Stephen E. Laubach
Bureau of Economic Geology
University of Texas
Austin, Texas 78713

Stephen M. Richard
Department of Geological Sciences
University of California
Santa Barbara, California 93106

Stephen Marshak
Department of Geology
University of Illinois
Urbana, Illinois 61801

INTRODUCTION

This three-day field-trip guide is intended to provide the reader with a guide to areas of the Harquahala, Granite Wash, Whipple, and Buckskin Mountains that are illustrative of regional geologic relationships and styles of mineralization. All field-trip stops are accessible by 2-wheel-drive vehicle with high clearance. Some of the field-trip stops are at patented or unpatented mining claims, and it is advisable to obtain permission to enter these areas.

The first day will be focused on the geology of Mesozoic thrust faults in the Harquahala, Little Harquahala, and Granite Wash Mountains. These ranges contain the most extensive exposures of stacked Mesozoic thrust faults known in Arizona (Spencer and others, 1985a; Laubach, 1986; Reynolds and others, 1986; Richard and others, in press). With minor exceptions, the thrusts are southwest, south, and southeast directed. The structurally lowest Hercules thrust, which is exposed in the western Harquahala, Little Harquahala, and Granite Wash Mountains, places Precambrian and Jurassic crystalline rocks over moderately to steeply dipping, southeast-facing sections of Paleozoic and Mesozoic sedimentary and volcanic rocks. All of the field-trip stops on the first day are at outcrops along the Hercules thrust or related subsidiary thrusts. Mineralization along the Hercules thrust zone is either pre- to synthrusting (Calcite mine) or is younger and was localized along the thrust zone (Yuma mine).

The second day will be focused on the Whipple Mountains detachment fault and structures and lithologies in the upper and lower plates. Upper-plate rocks consist of tilted Tertiary clastic and volcanic rocks that rest depositionally on primarily 1.4 to 1.7 Ga crystalline rocks. The lower plate consists of a variety of variably mylonitized crystalline rocks including granitic sills of Upper Cretaceous and middle Tertiary age. Brecciation and chloritic alteration have overprinted lower-plate rocks near the detachment fault (Davis and others, 1980, 1982; Wright and others, 1986).

The third day will be focused on the geology and mineralization of the Buckskin-Rawhide detachment fault in the Buckskin Mountains. The Buckskin-Rawhide detachment fault is thought to be correlative with the Whipple detachment fault in California and with the

Bullard detachment fault at the east end of the Harcuvar and Harquahala Mountains. Top-to-the-northeast displacement on this regional detachment fault has uncovered one of the largest Tertiary mylonite complexes in the North American Cordillera (Davis and others, 1980; Rehrig and Reynolds, 1980; Reynolds and Spencer, 1985; Spencer and Reynolds, 1986a). Mineralization along and near the detachment fault is better developed and more extensive than in any other Cordilleran metamorphic core complex (Wilkins and Heidrick, 1982; Spencer and Welty, 1985, 1986; Wilkins and others, 1986). Field-trip stops will be at areas of mineralization along and below the detachment fault, at exceptional exposures of the fault, and at areas in the upper and lower plates where characteristic structures and lithologies are well exposed.

DAY 1: HARQUAHALA AND GRANITE WASH MOUNTAINS (by S. J. Reynolds, J. E. Spencer, S. E. Laubach, and S. M. Richard)

Directions and Comments En Route to Stop A1

The trip starts at the Phoenix Civic Center. Proceed west on Van Buren Street, turn north (right) on 27th Avenue, and turn west (left) onto I-10 toward Los Angeles. The small mountain range on the south flank of Phoenix is the South Mountains, a geologically simple metamorphic core complex. The eastern half of the range consists of a middle Tertiary pluton and the western half is composed of Proterozoic gneiss. Both rock types are cut by a middle Tertiary mylonite zone formed by top-to-the-northeast ductile shear along a normal-displacement detachment zone that dips gently to the northeast and projects beneath tilted middle Tertiary sedimentary and volcanic rocks east of Phoenix (Reynolds, 1985; Reynolds and Lister, 1987). The breakaway of the detachment system is probably represented by the east margin of the Sierra Estrella, the large, rugged mountain range to the southwest of the South Mountains. The Sierra Estrella contain Proterozoic metamorphic and granitic rocks that lack Tertiary mylonitic fabric (Spencer and others, 1985b).

Northwest of Phoenix are the White Tank Mountains, another metamorphic core complex with mylonitic fabrics predominantly formed by top-to-the-northeast ductile shear along a northeast-dipping

detachment zone. The mylonitic fabrics have been overprinted on a basement of Proterozoic crystalline rocks, a peraluminous early Tertiary(?) granite, and middle Tertiary dikes.

West of the Hassayampa River and north of I-10 are the Big Horn and Belmont Mountains. The light-colored Belmont Mountains are underlain by a middle Tertiary fluorite-bearing granite, whereas the Big Horn Mountains to the west are composed of lower Miocene volcanic and sedimentary rocks that overlie Proterozoic crystalline rocks and Cretaceous granodiorite (Capps and others, 1985). The entire assemblage of rocks is cut by low- to high-angle normal faults that bound a series of north-northwest-trending tilted fault blocks.

Near Tonopah, I-10 passes north of the low-relief Palo Verde Hills (near Palo Verde Nuclear Generating Station) and more rugged Saddle Mountain, both of which are composed of middle Tertiary volcanic rocks. The larger range further south, the Gila Bend Mountains, is composed of Proterozoic crystalline rocks and Late Cretaceous(?) and middle Tertiary sedimentary and volcanic rocks.

Exit I-10 at mile post (MP) 69, proceed north (right) on maintained dirt road for 4 mi, and turn northwest (left) on the graded Salome-Buckeye Road. The topographically high Harquahala Mountains to the north are composed of Proterozoic, Paleozoic, and Mesozoic rocks that are metamorphosed and cut by major thrust faults (Figure 1). The top of the range consists of Proterozoic crystalline rocks that overlie Proterozoic granitoid rocks and tectonized Paleozoic and Mesozoic metasedimentary rocks along the south-vergent Harquahala thrust (Reynolds and others, 1986). The Paleozoic rocks, which contain large southeast-facing folds, extend along the ridge southwest of the high peak. These rocks have been intruded by a large Late Cretaceous granite and numerous pegmatitic and middle Tertiary dioritic dikes. Rocks in the Harquahala Mountains occur in the lower plate of the Bullard detachment fault, a regional low-angle normal fault with approximately 40 to 50 km of top-to-the-northeast displacement (Reynolds and Spencer, 1985). Rocks directly beneath the fault locally contain a Tertiary mylonitic fabric formed during top-to-the-northeast ductile shear along the detachment zone. The fault dips southeast under tilted fault blocks of Tertiary volcanic rocks in the Big Horn Mountains. Major topographic notches in the Harquahala Mountains were formed by preferential erosion along northwest-trending, high-angle faults that offset the Bullard detachment fault.

South of I-10 are the topographically impressive Eagle Tail Mountains, which are composed of southwest-dipping middle Tertiary volcanic rocks, middle Tertiary hypabyssal intrusions, and foliated granitic rocks.

The Salome-Buckeye Road passes between the Harquahala and Little Harquahala Mountains. Paleozoic rocks in the Little Harquahala Mountains form a northeast-trending, southeast-facing strike belt that projects to the northeast into similar rocks in the Harquahala Mountains. The Paleozoic rocks are successively overlain to the southeast by lower(?) Mesozoic sedimentary rocks, Jurassic(?) volcanic rocks, and Jurassic and/or Cretaceous clastic rocks of the McCoy Mountains Formation (Richard, 1982; Spencer and others, 1985a; Reynolds and others, 1986). To the north, the Paleozoic section is in depositional contact with Proterozoic granite. The entire southeast-facing Proterozoic to Mesozoic section is truncated at depth by two gently dipping thrust faults, the structurally higher Centennial thrust and the lower Hercules thrust. Beneath the Hercules thrust is a section of McCoy Mountains Formation that

is stratigraphically distinct from the section deposited on the Paleozoic rocks.

Two miles south of where the road crosses Centennial Wash, turn right (east) on the dirt road and park slightly in front of a small incised wash that is crossed by the road.

Stop A1: 'S' Mountain Window

At this stop we will proceed up the southern branch of this small wash to examine an excellent exposure of the Hercules thrust, which places mylonitic alaskite and quartz dioritic rocks over quartzite and stretched-pebble conglomerate of the basal part of the McCoy Mountains Formation. The quartzite rests depositionally on deformed and metamorphosed Jurassic volcanic, volcanoclastic, and hypabyssal rocks. Mylonitic lineation and stretched pebbles along the thrust trend north-south.

Directions and Comments En Route to Stop A2

En route to stop A2 we can see the Harquahala Mountains and the Harcuvar Mountains to the northeast. Each range is a northeast-trending culmination (antiform) of the Harcuvar metamorphic core complex (Rehrig and Reynolds, 1980) and is composed of metamorphic, mylonitic, and igneous rocks present beneath the Bullard detachment fault. The Harcuvar Mountains are composed of metamorphic and granitic rocks with a gently dipping, Tertiary mylonitic fabric that defines the broad northeast-trending Harcuvar Mountains antiform (which parallels and controls the overall topography of the range).

Return to the Salome-Buckeye Road, turn right toward Salome, and turn left onto U.S. Highway 60 in downtown Salome. Proceed west for approximately 2 blocks and turn right on Center Street, which is marked by a sign to the local VFW post. Begin cumulative mileage, which is listed within parentheses in following directions. Continue on the paved road as it turns to the left (0.3 mi) near a sign for "La Paz County Transfer Site." Continue straight where the pavement ends (0.8 mi). The western Harcuvar Mountains to the north contain dark-colored pendants of foliated crystalline rocks intruded by light-colored Late Cretaceous Tank Pass Granite. Turn left on the less-traveled dirt road where the main road turns north (right) and becomes Winchester Avenue (2.6 mi). Continue on the left forks of the road (2.7 mi and 3.3 mi) near a small knob of Late Cretaceous Granite Wash Granodiorite. At 4.1 mi the road crosses a stream along which we can view exposures of high-grade Proterozoic metamorphic rocks in the upper plate of the Hercules thrust. Continue on the main road to the right (4.5 mi) and park along the side of the road (4.6 mi).

Stop A2: Hercules Thrust Zone

At this stop we will traverse through the Hercules thrust zone, which regionally dips gently to the northeast but has been folded at this locality into a northwest-trending, near-vertical attitude. Lineation in the thrust zone plunges down the dip of the foliation. Starting several hundred meters north of the parking spot, we will walk southwest, down structural section, sequentially through the following structurally juxtaposed lithologies: (1) Proterozoic crystalline rocks that are most mylonitic down-section to the southwest; (2) mylonitic rocks along the Hercules thrust zone; (3) Mesozoic quartzofeldspathic schists situated directly beneath the thrust and derived from felsic volcanic rocks, intermediate-composition hypabyssal rocks, and sedimentary rocks,

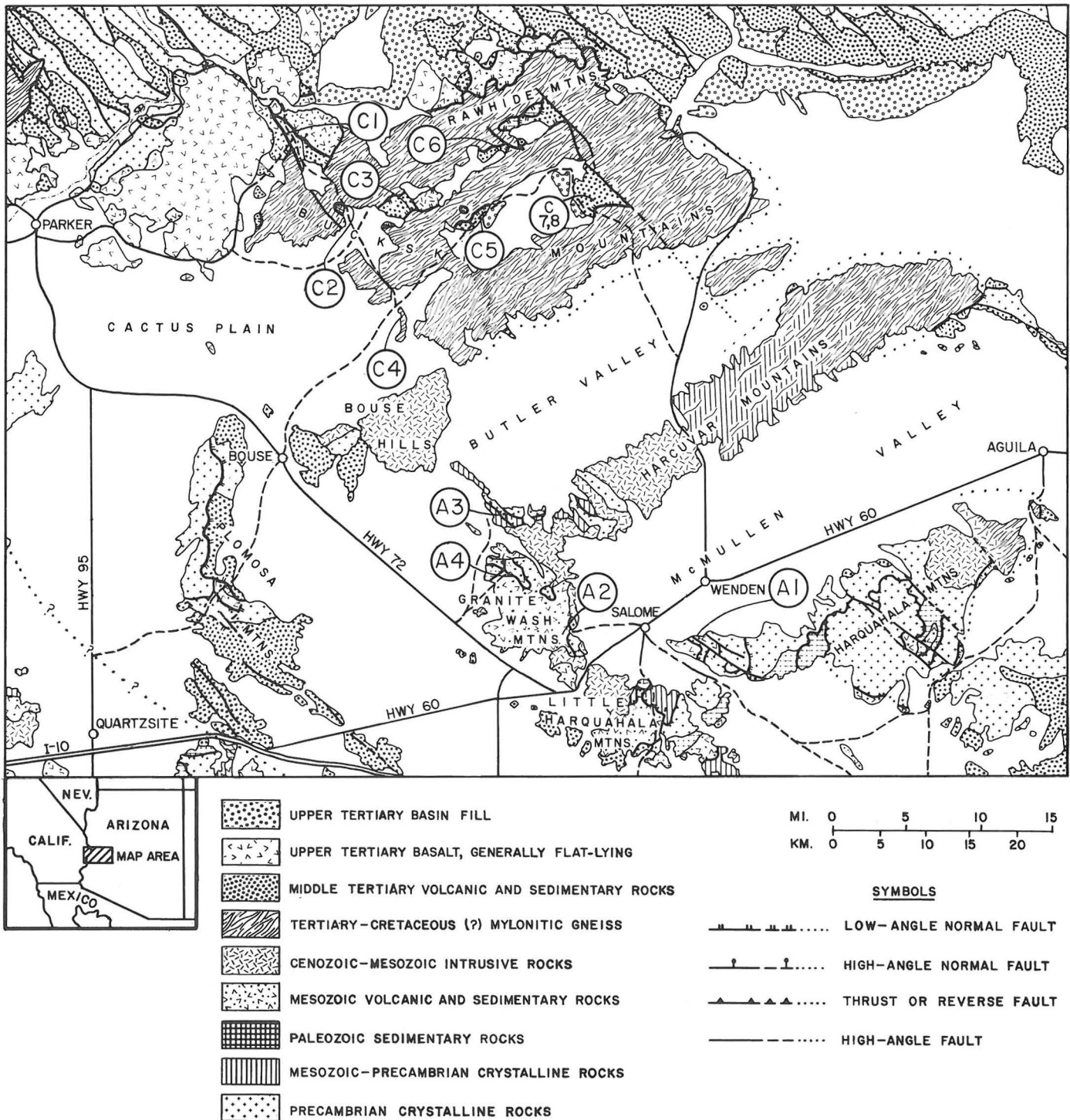


Figure 1. Simplified geologic map of west-central Arizona showing roads and locations of field-trip stops on days 1 and 3.

including ferruginous quartzite; and (4) locally calcareous metasedimentary rocks. The ferruginous quartzite and schists extend along strike into the Calcite mine area, where they are strongly pyritic and have been heavily prospected. These rocks are locally associated with andalusite-rich schists, which probably represent metamorphosed argillic-alteration zones within the volcanic sequence. The Calcite mine area

is interpreted as an occurrence of metamorphosed Mesozoic volcanogenic mineralization and alteration.

Directions and Comments En Route to Stop A3

Retrace your steps and return to Salome via the same route, making sure that you go straight and not left where the less-traveled Calcite mine road

intersects Winchester Avenue. At the main highway in Salome turn west (right) onto U.S. Highway 60 toward Quartzsite. Late Cretaceous Granite Wash Granodiorite is well exposed in Granite Wash Pass (MP 52) between the Little Harquahala Mountains to the south and the Granite Wash Mountains to the north. The Plomosa and New Water Mountains are the next mountain ranges to the west, across Ranegras Plain. At MP 49.5, turn northwest (right) toward Bouse and Parker and continue through Vicksburg (MP 46.5). Note Salome Peak, the highest point in the Granite Wash Mountains (to the east), which is composed of light-colored Late Cretaceous Tank Pass Granite. The dark-colored rocks in the foreground are mostly strongly cleaved Mesozoic volcanic and sedimentary rocks correlative with the regional Jurassic(?) volcanic suite and overlying McCoy Mountains Formation. The Mesozoic units define a large south-facing fold (not visible from this perspective) and are overlain along the Hercules thrust by Proterozoic crystalline rocks that form the top of the high, pyramidal hill in the middle distance, southwest of Salome Peak. At MP 42 note the ridge of light-colored Tank Pass Granite on the skyline to the right with mottled hills of steeply dipping Paleozoic strata along the front of the range.

Turn right at McVay Road (MP 40.4) and begin cumulative mileage (listed in parentheses below). Turn right (0.15 mi) and continue along the south side of the jojoba plantation. Continue straight (0.5 mi) across the Central Arizona Project Canal (1.6 mi), turn left at the fork (1.8 mi), bear right where the road crosses a wash (2.7 mi), and continue to the right (2.9 mi). At 3.4 mi note the light-colored patch of Paleozoic marble interleaved with crystalline rocks along the thrust zone on the ridge crest in the northern Granite Wash Mountains. Go slowly across the rough wash (4.4 mi).

The hills visible ahead at 4.5 mi contain a major steeply dipping shear zone that interleaves Proterozoic, Paleozoic, and Mesozoic rocks. These rocks are overlain along a low-angle thrust by vertical Paleozoic sedimentary rocks to the south. Take the left fork (5.0 mi); the right fork goes to tungsten occurrences near Three Musketeers mine. The small hill to the right (5.5 mi) has mylonitic Proterozoic crystalline rocks (out of view) thrust over Paleozoic dolomite and Mesozoic quartz porphyry. Tank Pass Granite is exposed to the right at 6.2 mi. Turn left (7.1 mi) and park along the road at 7.9 mi.

Stop A3: Northern Granite Wash Mountains

At this stop we will traverse up the high ridge to the east through a spectacular series of shear zones where thin lenses of Paleozoic and Mesozoic metasedimentary rocks are interleaved with Proterozoic and Jurassic crystalline rocks. Some shear zones in this traverse have top-to-the-southwest shear and are correlated with the Hercules thrust, whereas others have top-to-the-southeast shear and are correlated with an earlier, unrelated episode of Mesozoic thrusting (Reynolds and others, 1986).

Stop A4: Yuma Mine (Alternative Stop)

If the wash crossing at 4.4 mi is impassable, an excellent alternative stop is near the Yuma mine, which is reached by taking the right fork at 1.8 mi and then keeping left on the main road as long as it is passable. From this point, continue on foot up the road until it reaches the small shack and main adit of the Yuma mine. This adit has been driven into copper mineralization in a lens of Paleozoic carbonate rocks that overlie Mesozoic metasedimentary and metavolcanic

rocks. The Paleozoic rocks are overlain along the Yuma mine thrust, a subsidiary splay of the Hercules thrust, by Proterozoic crystalline rocks and Mesozoic alaskite, metavolcanic rocks, and metasedimentary rocks.

Directions and Comments En Route to Parker

Return to the intersection of the main highway and McVay Road and turn right toward Bouse and Parker. The dark-colored ridges in the northern Plomosa Mountains to the west are composed of southwest-dipping Tertiary volcanic rocks. Plomosa Pass is located north of this ridge and contains a southwest-dipping, structurally complex sequence of Proterozoic, Paleozoic, and Mesozoic rocks (Stoneman, 1985; Reynolds and others, 1986).

Near Bouse the road passes along the southwest side of the Bouse Hills, which are composed of middle Tertiary volcanic rocks in the foreground and crystalline rocks in the background. Continue through Bouse and toward Parker on Arizona Highway 72, which turns into Arizona Highway 95 at MP 131.8. The first day of the field trip ends at Parker.

DAY 2: WHIPPLE MOUNTAINS (by J. L. Anderson and G. A. Davis)

Leave Parker at 7:30 a.m. (Arizona time). The principal objective of the day's excursion is to study the Whipple detachment fault and its upper (non-mylonitic) and lower (mylonitic) plates in the spectacular canyon of Whipple Wash, eastern Whipple Mountains, California. This east-rooting detachment fault and subparallel related faults that compose the Whipple detachment system have had a cumulative displacement of greater than 40-45 km. The Whipple fault is possibly correlative with the Bullard fault of western Arizona. Today's guide is an abbreviated updated version of an older guide (Anderson and others, 1979).

Begin mileage at the intersection of Arizona Highways 95 and 72 (Chevron station on northeast corner) in Parker, Arizona. Drive northeast along Arizona Highway 95 toward Parker Dam and Lake Havasu City.

Stop B1: Areal Overview

Stop 2-3 mi from 0.0 for a visual overview and discussion of the geology of the western Buckskin Mountains (Arizona) and Whipple Mountains (California).

Geologic Highlights En Route to Stop B2

Leaving a terrace of Colorado River gravels, we drive down into Osborne Wash 3.4 mi and, after crossing the bridge, enter a section of subhorizontal Miocene and Pliocene strata deposited after detachment faulting in this region. The thin (1 m) bright-white layer visible to the northeast is a tuffaceous marl (ca. 5.5 Ma) at the base of the upper Miocene-Pliocene Bouse Formation, a marine to lacustrine unit deposited in an embayment of the Gulf of California (Metzger, 1968; Smith, 1970; Winterer, 1975). The marl rests on interbedded fanglomerates and alkali basalt flows of the Osborne Wash Formation; a 15.9±2.8 Ma K-Ar age has been reported for a basal flow in this formation (Davis and others, 1982).

The posttectonic Osborne Wash and Bouse section lies with angular unconformity across steep southwest-tilted Miocene strata (5.3 mi, east side of road). These older alluvial and lacustrine strata lie above

the Whipple detachment fault in rotated fault blocks. They rest unconformably on a crystalline basement composed largely of Proterozoic gneisses and plutonic rocks that is exposed along the road for several miles. Bright brick-red sandstones are visible in step-sided hills near the first major bend in the Colorado River at 9.6 mi. They lie in the hanging wall of the Copper fault, a major northwest-striking, northeast-dipping upper-plate normal fault that crosses the eastern Whipple Mountains. The coarse terrigenous sediments are folded into a syncline along the fault, but exhibit moderate southwest dips not far to the northeast. Although the Copper fault is not exposed here, we may stop briefly upstream near the aircraft-warning balls hung above the river to look at a well-exposed minor normal fault (at the south-facing base of the prominent cliff that overhangs the road). Leaving the sedimentary section, we enter its crystalline basement. A second major fault (Gene fault, 13.4 mi) separates basement rocks from another hanging-wall sequence of Tertiary strata. On the Arizona side of the river, tilted Tertiary strata and their basement rocks are overlain with pronounced angular unconformity by a thick sequence of mesa-forming Osborne Wash basalts.

At 15.4 mi from Parker, turn left to Parker Dam and leave Arizona Highway 95. The dam abutments (16.1 mi) are set into deformed Parker Dam granite, the subject of Stop B4. We are now in the area shown in Figure 2, which also shows the locations of all remaining stops. Reset mileage at the northwest end of the dam (California side). At 0.5 mi turn right onto the paved road that leads to the Metropolitan Water District headquarters and Black Meadow Landing. The nonconformity at the base of the steeply dipping Tertiary section is at 0.9 mi. Just after the second curve to the right (1.3 mi), park on the west side of the road at the first major turnout.

Stop B2: Mylonitic Clasts in Gene Canyon Formation

A debris flow exposed on the east side of the road contains fairly angular boulders of leucocratic monzogranite. Some of the clasts are mylonitic and contain a pronounced lineation. Samples from this locality have yielded rather concordant Late Cretaceous ages (sphene, fission track, 82.9±3 Ma, Dokka and Lingrey, 1979; biotite, K-Ar, 78.5±5.5 Ma, Davis and others, 1982). Contrary to earlier interpretations (Davis and others, 1980, 1982), these mylonitic gneisses are apparently unrelated to those in the Whipple lower plate, which formed during Oligo-Miocene crustal extension (see below).

Return to vehicles, continue to drive northwest. Park at the top of the hill (2.1 mi) where the highway bends left and a paved road (with sliding gate) leads off to the east. Walk around the gate and approximately 300 ft down the road past it.

Stop B3: Angular Unconformity Within Tilted Tertiary Strata

Looking to the north from this DWP service road, we see a prominent canyon leading down from the Gene Canyon Dam and reservoir (not seen here). Seepage from the reservoir has enabled lush native-palm growth. Low in the cliffs to the east of the stream valley is a prominent unconformity between the steeply dipping basal Tertiary unit in this area, the Gene Canyon Formation, and overlying, less steeply dipping strata of the Copper Basin Formation (Kemnitz, 1937). Two episodes of upper-plate normal faulting and rotation of strata can be inferred from these relationships. Attempts to apply this unconformity-defined stratigraphy to other rotated

fault blocks of the Whipple region have been frustrated by the absence of similar angular unconformities.

Geologic Highlights En Route to Stop B4

Return to the vehicles and continue driving northwest on the main road. East of the reservoir (3.0-3.5 mi) one can see redbeds of the Copper Basin Formation dipping moderately (25°-35°) southwestward, towards the crystalline rocks across which we are driving. The Gene fault, which lies hidden beneath the reservoir and alluvium at the base of the dip slope, truncates the Tertiary section and juxtaposes it against the footwall crystalline block. At 4.0 mi we begin to pass on the left a Cretaceous leucocratic biotite monzogranite intrusive in the Proterozoic complex of the Whipple upper plate. K-Ar dates from this pluton include 74±3 Ma (biotite) and 103±8 Ma (hornblende from crosscutting diabase). At 6.2 mi pull off into the open area on the left before heading down the steep grade.

Stop B4: Parker Dam Granite and View of Upper-Plate Crystalline Complex

The Parker Dam granite, dated at 1.40 Ga (U/Pb, zircon) by Jim Wright (in Anderson and others, 1987), is a major intrusion in the eastern and southeastern portions of the upper plate of the Whipple Mountains. The granite is distinctive in having abundant (>34 percent) K-feldspar phenocrysts aligned in a well-defined planar flow foliation. Described by Anderson (1987b), this granite and the Bowmans Wash quartz monzodiorite of similar age (dark hill 1 km to the north) are part of a transcontinental suite of Proterozoic anorogenic plutons (Anderson, 1983).

The view to the north displays a heterogeneous mosaic of colors representing the complex mixture of crystalline units that compose this upper-plate basement. The oldest rocks include paragneisses and migmatites (light-colored areas to the northwest), amphibolite (dark-grey areas), and foliated granites and augen gneisses (reddish area west of the road downhill). These rocks all possess a steep foliation that formed during high amphibolite-grade Proterozoic metamorphism. Orrell and Anderson (1987) have estimated peak metamorphic conditions (660°±40°C at 3.5±0.5 kb) and believe that this area is part of a regional high-amphibolite to granulite terrane that includes western Arizona and extends north to southern Nevada (Thomas and others, 1987).

Geologic Highlights En Route to Stop B5

Continue driving northwest and take the gravel road to the left (west) at the one Exxon sign (6.7 mi). We leave the Parker Dam granite and drive into older foliated granodiorite and a large area of gneiss and amphibolite. Swarms of Proterozoic ophitic diabase are notable, particularly on the right side after 7.7 mi. Turn left (8.9 mi) and continue on the dirt powerline road; the main road (to Havasu Palms Resort) turns right. Use of passenger vehicles past 8.9 mi is not recommended. At 10.0 mi pull off on the right shoulder for a view of both upper and lower plates.

Stop B5: View of Whipple Wash Area

Walk west across the road and follow the path 25 m to its end. From here we are afforded a spectacular view to the northwest into the low country of Whipple Wash. Rocks on the northern skyline are light-colored

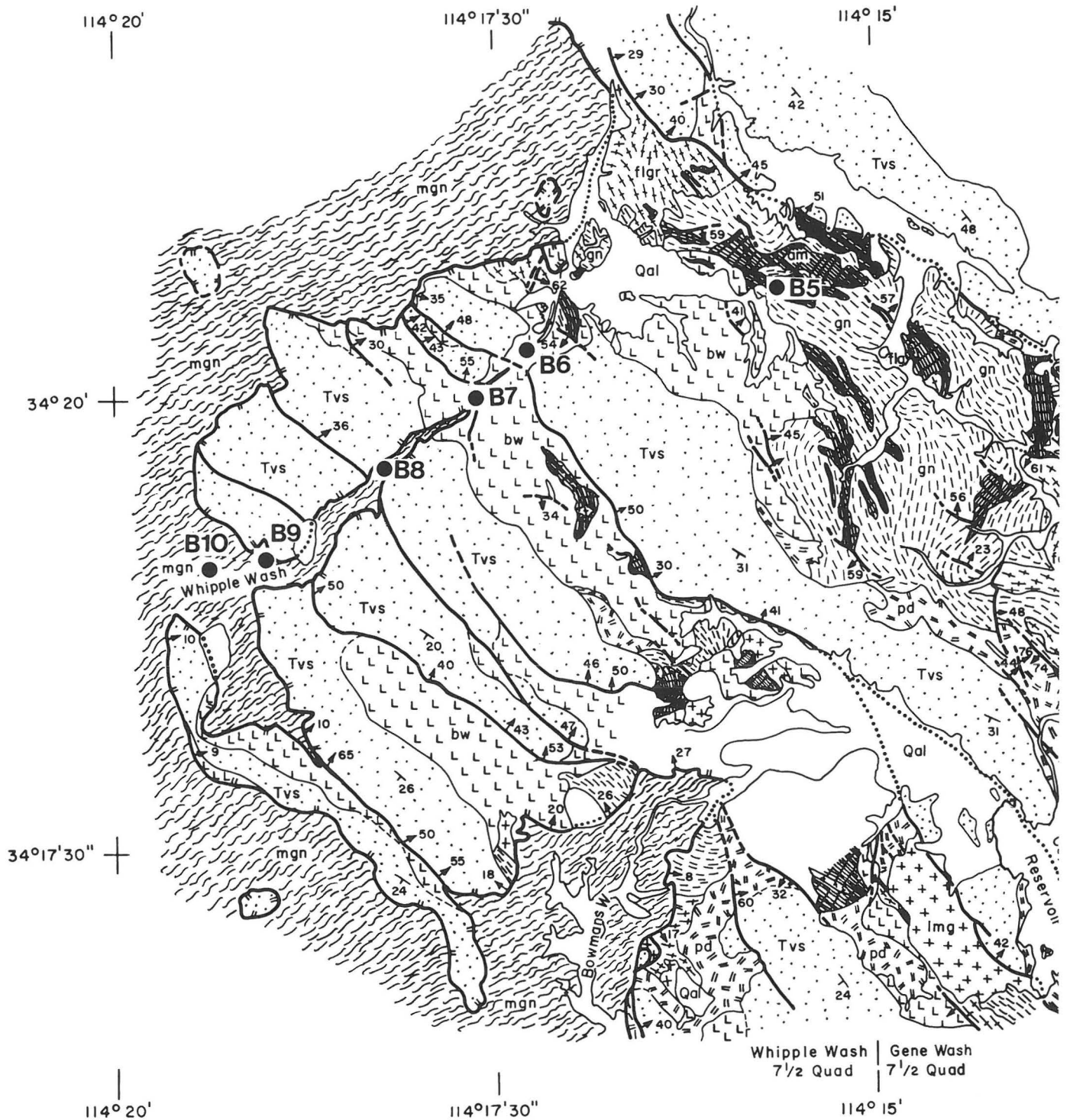


Figure 2. Simplified geologic map of the northeastern Whipple Mountains showing field-trip stops B2-B10.

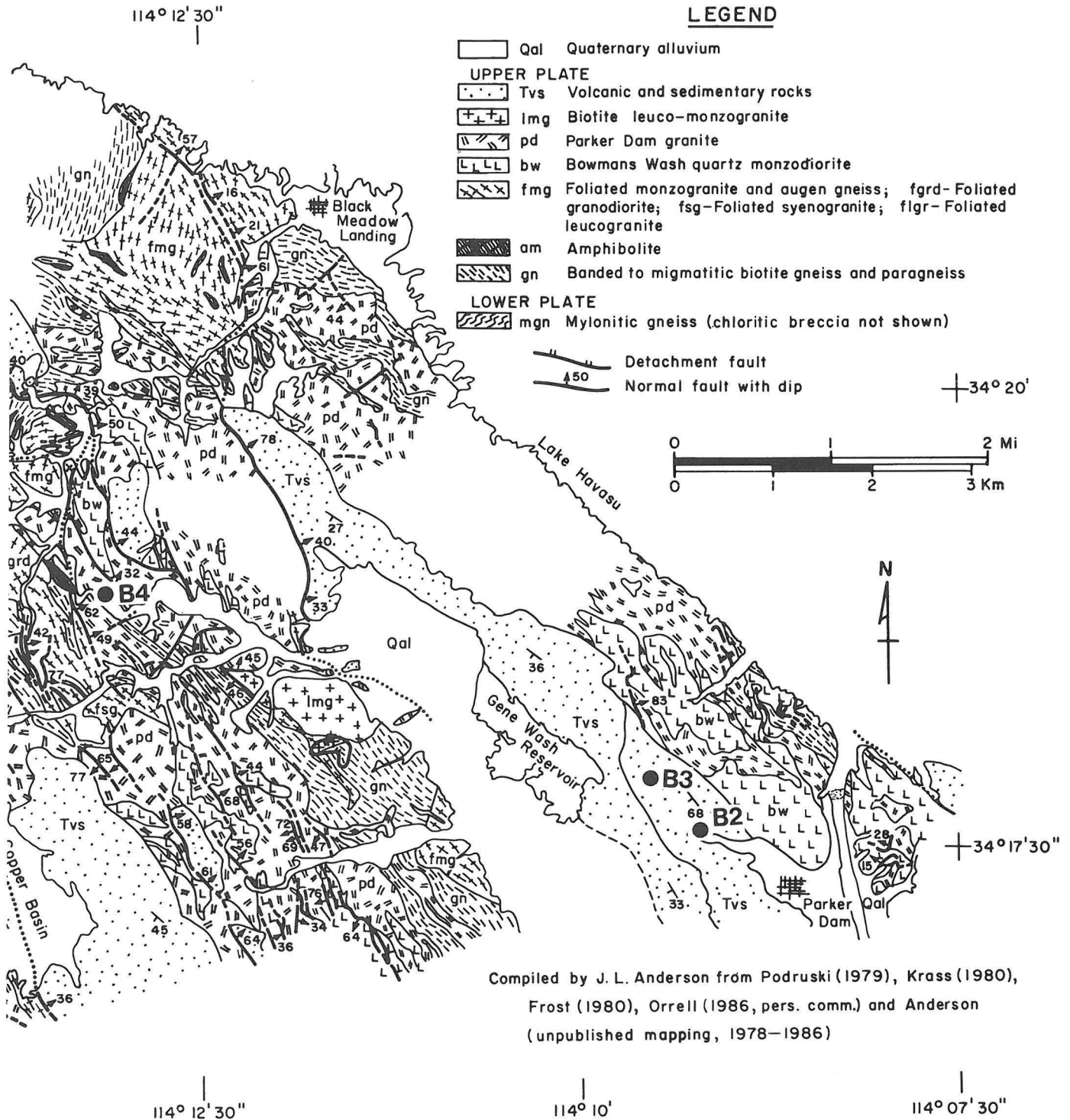
mylonitic gneisses of the Whipple lower plate. The Whipple detachment fault is the east-dipping planar surface beneath several dark-brown to reddish klippen containing Tertiary strata that dip steeply ($>50^\circ$) to the southwest into the truncating Whipple fault. The pale greenish tint of the lower-plate mylonitic gneisses is due largely to the development of chlorite in lower-plate rocks that have undergone retrograde metamorphism, including chloritic breccias directly

below the fault.

The contrast in appearance between the upper and lower plates is strikingly evident from this vantage point. We are standing on amphibolite; other upper-plate units nearby include quartzofeldspathic gneisses, the Bowmans Wash quartz monzodiorite, diabase, and a few Tertiary basalt dikes. Overlying this basement to the west are cliff-forming Tertiary volcanic and sedimentary rocks.

LEGEND

- Qal Quaternary alluvium
- UPPER PLATE**
- Tvs Volcanic and sedimentary rocks
- + + + + + lmg Biotite leuco-monzogranite
- ||| pd Parker Dam granite
- L L L L L bw Bowmans Wash quartz monzodiorite
- x x x x x fmg Foliated monzogranite and augen gneiss; fgrd-Foliated granodiorite; fsg-Foliated syenogranite; flgr-Foliated leucogranite
- ▨ am Amphibolite
- ▧ gn Banded to migmatitic biotite gneiss and paragneiss
- LOWER PLATE**
- ▨ mgn Mylonitic gneiss (chloritic breccia not shown)
- / — Detachment fault
- / 450 — Normal fault with dip



Compiled by J. L. Anderson from Podruski (1979), Krass (1980), Frost (1980), Orrell (1986, pers. comm.) and Anderson (unpublished mapping, 1978-1986)

Geologic Highlights En Route to Stop B6

Continue driving northwest and descend into Whipple Wash. At 10.4 mi, enter the wash and turn left. Drive up the alluvium in the wash as far as possible (usually about a mile). At 11.4 mi, park and gather field gear, water, and lunch for a 7- to 8-mi round-trip hike. All stops are in the canyon bottom, an area within the 7 1/2-minute Whipple Wash

quadrangle. The rest of this guide is written for foot travelers and mileages starting from 0.0 at the parking area are estimated. All map distance measurements are in feet or miles.

Stop B6: Bowmans Wash Quartz Monzodiorite (0.6 Mi)

The Bowmans Wash quartz monzodiorite, dated at 1.41 Ga (U/Pb, zircon) by Jim Wright (in Anderson and

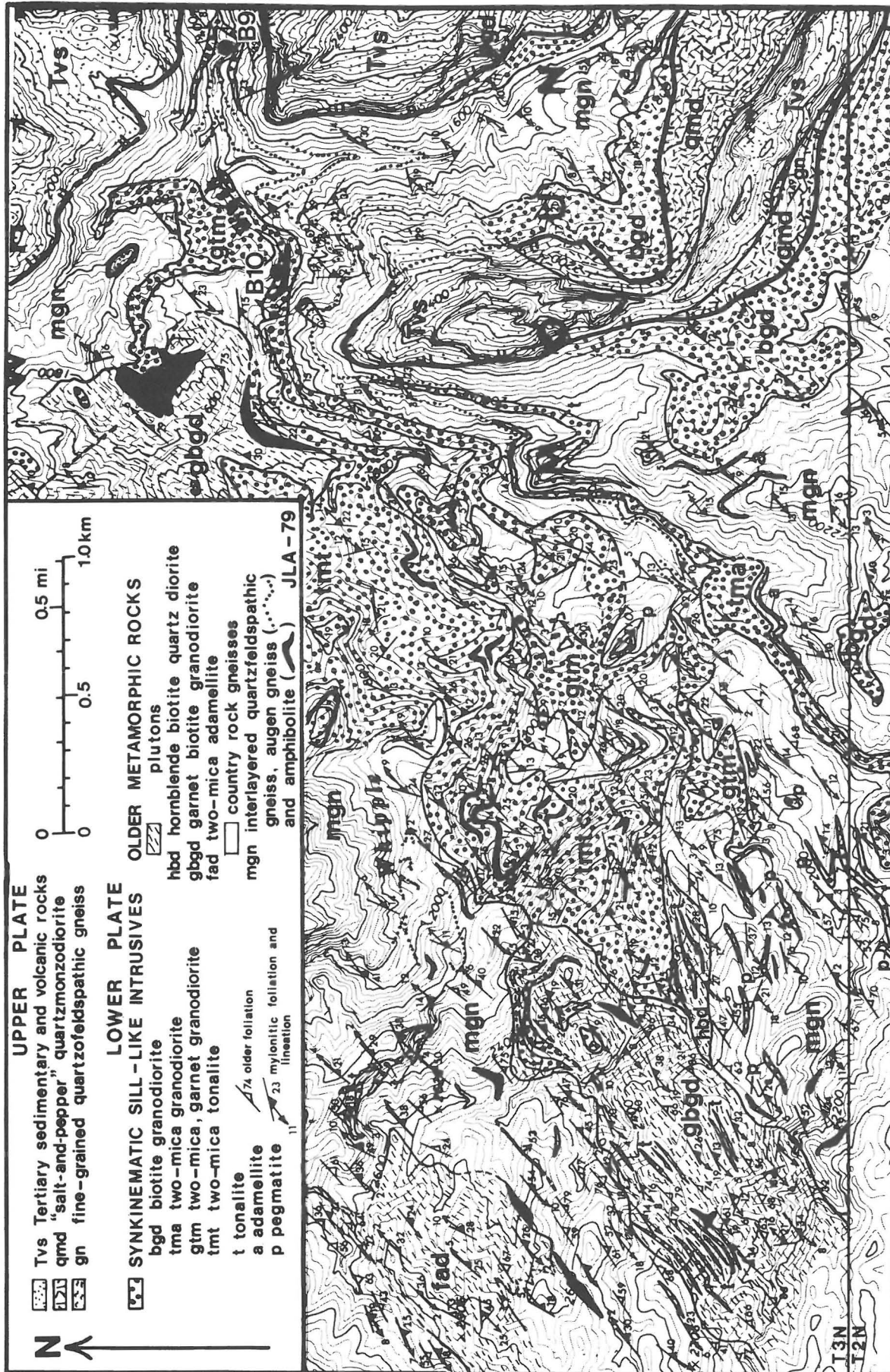


Figure 3. Geologic map of the upper Whipple Wash area.

others, 1987), is the dominant Proterozoic unit of the northeastern Whipple Mountains. The "salt-and-pepper" texture visible in this dark outcrop is typical of most of the pluton. The pluton ranges in composition from quartz diorite to quartz monzonite and is one of the more mafic 1.4 Ga intrusions of the region, with SiO₂ ranging from 60.7 to 63.8 wt. percent. It is commonly foliated near contacts with the younger Parker Dam granite.

Continue walking upstream. At 0.9 mi, up on the left bank, is a small upper-plate fault marked by a spring nourishing one of the few native palm trees in this part of the eastern Whipple Mountains. The sheared unconformity at the base of the Tertiary volcanic section is about a third of the way up the canyon wall. Many faults in the Tertiary section will be visible on this trek, but none are believed to cut the detachment fault that lies beneath us (Gross and Hillemeier, 1982). At 1.3 mi is a greenish exposure of the exhumed Whipple detachment-fault surface.

Stop B7: Whipple Detachment Fault

The Whipple detachment fault is the tectonic boundary between the contrasting upper and lower plates. The fault, as seen here in a small prospect pit, is underlain by a 1- to 3-m-thick ledge of dark brown cataclasite or microbreccia, which passes downward into altered lower-plate rocks of the "chloritic breccia zone." This zone, up to 300 m thick in the range, is so pervasively fractured, sheared, and layered by chloritization and epidotization that the foliation and lineation of its protolith mylonitic gneisses are generally not discernible. The low-grade copper mineralization of the fault and the retrogression of lower-plate rocks below it are regional phenomena.

The first 200 m of our trek upstream is within the chloritic-breccia zone. The detachment fault is intermittently exposed on the canyon walls below the cliff-forming Tertiary section. Its gentle dip is evident as it gradually climbs in elevation westward above us. Gradually, the mylonitic foliation of lower-plate rocks becomes evident within the chloritized gneisses with dips of 20°-44° SW and a lineation plunging at low angles to the southwest (S 45°-53° W). These mylonitic gneisses, last deformed during the Miocene, are Proterozoic quartzofeldspathic gneiss, augen gneiss, and amphibolite. At 1.9 mi is a ledge of mylonitic gneiss, our next stop.

Stop B8: Juxtaposition of Older Gneissic and Younger Mylonitic Foliations

Giving the outcrop a crossbedlike appearance, gneiss layers with a steeper, older (Mesozoic?) foliation are preserved within the mylonitic gneisses. This older foliation (N 87° E, 41° SE) is also present locally in Cretaceous plutons to be seen at Stop B10. The attitude of the mylonitic foliation is N 64° W, 31° SW with a lineation plunging 29°, S 52° W. A gray-colored mylonitic tonalite sheet, contained in the mylonitic gneisses, is considered equivalent to one dated at 26 Ma (U/Pb, zircon) by Wright and others (1986). As seen here, the transition from nonmylonitic to mylonitic fabrics involves a gradual rotation to lower dips, with mylonitic fabric becoming discernible as the dip lessens.

Toward Stop B9, the mylonitic foliation begins to dip to the SE (9°-25°), which is the norm for this area of the range (Figure 3). Some folds in the gneisses will be evident. At 2.4 mi a landslide of Tertiary rocks covers the detachment surface, now far above us, on the north side of the wash. At 3.1 mi, we gather for the next stop.

Stop B9: Lower-Plate Low-Angle Fault and Mylonitized Augen Gneiss

A gentle ramp of augen gneiss is exposed approximately 150 m past the landslide below an east-dipping low-angle fault. Rocks above the fault are more altered. The augen gneiss is a distinctive lithology that occurs in the lower-plate gneisses as 2-10-m-thick layers exposed continuously for distances up to 2 km. Ranging from monzogranite to syenogranite in composition, the augen gneiss is a metaigneous rock containing large (to 5 cm) augen of K-feldspar set in a biotitic mylonitized matrix. Where it is not mylonitized, the gneiss contains the Mesozoic(?) fabric seen earlier. Recently, Sam Bowring has dated the intrusive at 1.41 Ga (U/Pb, zircon, pers. comm., 1987). Although not correlative with plutons of similar age in the upper plate, the rock is similarly potassic (4.5 to 5.5 wt. percent K₂O over 62.9 to 72.7 wt. percent SiO₂) and iron-rich.

Continue walking upstream past a spring and inviting pools in the augen gneiss. At 3.3 mi a major valley appears from the left. At 3.6 mi is a broad, stream-washed exposure of a garnetiferous two-mica granodiorite, our final stop of the day.

Stop B10: Cretaceous Garnet, Two-Mica Granodiorite and Miocene Synkinematic Tonalite

At this outcrop old Proterozoic gneisses and amphibolite are intruded by a garnetiferous two-mica granodiorite and crosscutting, shallow-dipping, low-angle dikes of gray biotite, tonalite, and white trondhjemitic aplite. From samples collected at this locality, the granodiorite and tonalite have been dated by U/Pb (zircon) at 89±2 Ma and 26±5 Ma, respectively (Wright and others, 1986). All of the lithologies are mylonitized, demonstrating a Tertiary age for this deformation. The mylonitic foliation in the granodiorite and surrounding gneisses strikes N 18° E, dipping 19° SE with a lineation plunging 8° N 44° E. The younger tonalite and aplite dikes cut this mylonitic fabric by as much as 25° and have mylonitic foliations parallel to their walls. Mylonitic lineations are closely parallel in all rock units. These relations require the tonalite and aplite to have been intruded synkinematically during a protracted period of mylonitization. The older, steeper nonmylonitic foliation viewed earlier at Stop B8 is locally present in the granodiorite, indicating a maximum Cretaceous age for that deformation. The older foliation at this locality strikes N 53° E, dips 44° SE, and does not contain a lineation.

The mylonitized granodiorite is a major intrusive in this area of the core (Figure 2) and forms a shallow-dipping body with a maximum thickness of 70 m. The rock is light gray and medium grained and contains porphyroclasts of garnet, feldspar, and two-micas set in a fine-grained mylonitic matrix. Anderson and Rowley (1981) have described the compositional features of this and the other intrusions of the lower plate. Data given by Anderson and others (1979) and Anderson and Rowley (1981) show that the mineral phases in this and other mylonitic gneisses have a wide range of composition, including porphyroclasts of apparent igneous chemistry and matrix grains reequilibrated during mylonitization conditions of upper greenschist to lower amphibolite grade.

The plutonic conditions of this and other Cretaceous intrusions of the Whipple metamorphic core complex require depths of emplacement within the middle crust of greater than 28 km. This is not only indicated by the calcic nature of the garnets in this granodiorite (the mole fraction grossular ranges up to

0.24), but also by the aluminous nature of hornblende in a quartz diorite (exposed elsewhere) dated by Wright and others (1986) at 783±3 Ma. Barometric estimates for mylonitization (16±4 km) and postkinematic Tertiary plutons (4-8 km) indicated successively shallower crustal depths demonstrating dramatic decompression of the complex (Anderson, 1985; Anderson, 1987a; Anderson and others, 1987).

Return to the vehicles and return to Parker.

DAY 3: BUCKSKIN MOUNTAINS
(by J. E. Spencer, S. J. Reynolds,
and S. Marshak)

Directions and Comments En Route to Stop C1

Drive northeast from downtown Parker on Arizona Highway 95 toward Lake Havasu City, as was done yesterday. The Central Arizona Project pump station is visible to the right at 17.8 mi from Parker. This station serves as the intake for water for the CAP system. The levy visible in Lake Havasu to the left is intended to prevent sediment from the Bill Williams River from clogging the intake. The northeast-dipping Havasu Springs normal fault, which places Miocene sandstone against Proterozoic crystalline rocks, is exposed in the large cuts on both sides of the pump station.

At 18.4 mi from Parker (0.6 mi from the CAP pump station), turn right on the dirt road. If you cross the Bill Williams River you have gone too far. Drive 7 mi up the Bill Williams River and note the tilted Tertiary sandstone and fanglomerate beneath flat-lying 10 Ma mesa-forming basalt. The tilted sedimentary rocks are the youngest tilted rocks in the Tertiary section and become less steeply tilted to horizontal up-section. Turn right up Mineral Wash. The sign "COUNTY MAINTENANCE ENDS" marks the turnoff. Drive 2 mi up the wash through tilted Mesozoic and Tertiary rocks (Spencer and others, 1986), then turn right to go to Mineral Hill mine.

Stop C1: Mineral Hill Mine

Park at the flat area above the white "sulfuric acid" tanks. You are at the Mineral Hill mine, which is one of the largest mines in the Buckskin Mountains. From where the vehicles are parked, we will walk west and northwest, beginning a 0.5- to 1.0-mi-long, clockwise loop through the mine workings and adjacent areas. We will observe styles of mineralization, the detachment fault, carbonate replacements, and the Mineral Wash fault that displaces the orebody and underlying detachment fault. Please note that the Mineral Hill mine is a patented claim; permission to enter should be obtained from the owner.

Host rocks for mineralization are variably calcareous lower Mesozoic quartzites and sandy phyllites that form the lowest stratigraphic member of the Triassic(?) Buckskin formation. This lowest member is overlain in ascending order by the phyllite member, quartzite member, and upper sedimentary member. These four members compose the informally named Buckskin formation. The Buckskin formation is overlain with low-angle angular unconformity by the informally named Vampire formation, a light-colored quartzite with a local conglomeratic base, which is overlain by the massive quartz porphyry of the informally named Planet volcanics. This tripartite stratigraphic sequence was first recognized by Norm Lehman during detailed mapping for AMAX Inc. The Buckskin formation is tentatively correlated with the

Triassic Moenkopi Formation, the Vampire formation is tentatively correlated with the Lower Jurassic Aztec-Navajo Sandstone, and the Planet volcanics are almost certainly correlative with Jurassic quartz porphyries that are widespread in southern Arizona. Middle Tertiary sandstone, conglomerate, megabreccia, and volcanic rocks overlie the Mesozoic section. All of these rocks are tilted and unconformably overlain by flat-lying, upper Miocene mesa-forming basalt (Spencer and others, 1986).

Mesozoic and Tertiary rocks are cut by numerous normal faults and are tilted to moderate or steep attitudes. The normal faults are truncated by, or flatten with depth and merge into, the basal Buckskin-Rawhide detachment fault (see cross section of Mineral Hill-Planet area in Wilkins and Heidrick, 1982).

The Mineral Hill mine is located in rocks that are within about 50 m of the Buckskin-Rawhide detachment fault, which is exposed at several locations in the mine area. Hydrothermal circulation within brecciated rocks along and above the detachment fault caused the mineralization. The high-angle, northeast-side-down, Mineral Wash fault offsets the detachment fault and the Mineral Hill orebody and passes approximately through the flat area where the vehicles are parked. The location of the offset continuation of the orebody is unknown.

Mineralization at the Mineral Hill mine is typical of upper-plate, detachment-fault-related deposits in the Whipple-Buckskin-Rawhide Mountains area (Wilkins and Heidrick, 1982; Spencer and Welty, 1986). Hematite and specular hematite form pervasive fracture fillings, disseminations, and replacements throughout the mine area, and mineralized rocks are typically dark red or black in color as a consequence. Sparse fracture-filling specular hematite is characteristic of the margins of the mineralized area. Chrysocolla and malachite fill thin fractures in the hematite-mineralized rocks. Quartz and calcite are locally present on fracture surfaces. Minor hematite and chrysocolla are present in lower-plate, chloritically altered mylonitic gneisses (Spencer and Welty, 1985).

Massive brown carbonate overlies the basal detachment fault at the northern edge of the mine workings. Carbonate lenses and sheets such as this one are locally present throughout the Buckskin-Rawhide Mountains, especially in areas of mineralization, and are interpreted as replacements of upper-plate rocks along the detachment fault (Wicklein, 1979; Spencer and others, 1986).

Directions and Comments En Route to Stop C2

Leaving Mineral Hill mine, drive approximately 1/2 mi up Mineral Wash. Mineral Wash fault is clearly visible on the right side of the wash, where it places Tertiary breccia of Planet volcanics to the southwest over postdetachment basin-fill fanglomerate to the northeast. The fault dips to the southwest and thus has apparent reverse offset. The fault dip is highly variable, and the fault has horizontal striations on slickenside surfaces.

Continue driving up Mineral Wash. Follow the road to the left as it leaves Mineral Wash approximately 1 mi from the Mineral Hill mine and drive another 5 mi to the pass over the northernmost of three foliation arches that form the lower plate of the central and eastern Buckskin Mountains. To the south of the pass is Squaw Peak, a klippe composed primarily of Paleozoic carbonates. Drive another 1.3 mi and turn left onto the straight road that becomes an old landing strip. Drive 3/10 mi and turn right to go by four white claim posts.

Stop C2: BCC Mines

Stop and walk east or southeast to the open cuts and mine dump. This is an excellent example of lower-plate mineralization consisting of specular hematite-chlorite-quartz with local chrysocolla along fractures and shear zones in lower-plate gneiss. Specular hematite here is unusually coarse grained and hard. This is part of the Squaw Peak subdistrict of the Swansea mineral district (Keith and others, 1983; Spencer and Welty, 1985).

Directions and Comments En Route to Stop C3

Return to the vehicles, drive back to the main road, and turn left at the stop sign. Drive 1.4 mi to the stop sign at the four-way intersection. Turn left and drive approximately 5.5 mi to a pass. Stop at the pass and walk up the ridge to the left (north).

Stop C3: Swansea Overlook

Lower-plate crystalline rocks are well exposed in road cuts near the pass. Walk up the ridge on the north side of the pass to the detachment fault and upper-plate carbonates. The carbonates probably were originally Paleozoic carbonates but have been so modified by Tertiary hydrothermal activity that their protolith is uncertain. Walk further up the carbonate ridge if you want a better view. From here, looking east and northeast, you can see upper-plate rocks in the Swansea synform, and the Clara Peak klippe on the Clara arch, which forms the south flank of the Swansea synform. Beyond the Bill Williams River, which crosses the Swansea synform approximately 10 mi to the east-northeast, are the Rawhide Mountains. Dark upper-plate Paleozoic, Mesozoic, and Cenozoic rocks in detachment-fault contact with light-gray, lower-plate mylonitic crystalline rocks are clearly visible in the Rawhide Mountains (Shackelford, 1980). Approximately 12 mi to the east-northeast, the northwest-trending, northeast-side-up Lincoln Ranch reverse fault offsets the detachment fault and forms an abrupt termination of exposures of upper-plate rocks in the Swansea synform.

One-and-a-half miles to the east along the south side of the Swansea synform is the Swansea mine. A 1-mi-long sliver of dominantly Paleozoic carbonates is bounded by the detachment fault to the southeast and upper-plate crystalline rocks to the northwest. The carbonate sliver dips northeast beneath the crystalline rocks (see cross section in Wilkins and Heidrick, 1982). Mineralization at surface exposures consists of massive specular hematite replacing carbonates, with fracture-filling chrysocolla. Nineteenth-century underground mining was focused on chalcopyrite veins up to 1-2 m thick within specular hematite (J. Challinor, pers. comm., 1984).

Directions and Comments En Route to Stop C4

Drive 5.5 mi back to the four-way intersection and turn left at the intersection. Drive 5.8 mi over the Clara arch to the intersection with the Bouse-Lincoln Ranch Road. Turn left, then immediately turn right onto the powerline road. Drive approximately 1/2 mi and park near the base of the hill to the south.

Stop C4: Starting Point Knob

Walk up the ridge to the south through tectonized lower-plate metasedimentary rocks and locally interleaved crystalline rocks. The southwest end of the Ives Peak arch, the southern of three lower-plate arches that form much of the Buckskin and Rawhide

Mountains, is clearly visible to the east. Tectonized metasedimentary rocks form a southwest-dipping carapace over the southwest end of the arch and are underlain by crystalline rocks. The metasedimentary rocks contain at least six map units (Marshak and Vander Muelen, 1987), which were probably derived from lower Mesozoic and possibly Paleozoic sedimentary protoliths. The contact between the metasedimentary cover sequence and underlying basement crystalline rocks is everywhere parallel to mylonitic foliation and local lithologic layer in cover rocks, but is discordant to more steeply dipping, premylonitization, crystalloblastic foliation in basement rocks. Mylonitic shear zones in basement rocks overprint and transpose older foliation and gneissic layering. Slip-line calculations based on tight inclined to recumbent folds in cover rocks indicate top-to-the-northeast shear parallel to the direction of mylonitic lineation (Marshak and Vander Muelen, 1987).

Directions and Comments En Route to Stop C5

Return to the vehicles, turn around, drive back (1/2 mi) to Bouse-Lincoln Ranch Road, and turn right. Drive 8.5 to 9 mi northeast along the axis of the Lincoln Ranch synform to the second of two adjacent roads joining the main road from the left. Turn left on the second road and drive up the canyon for several hundred yards to an area that is suitable for parking and for turning around and that is next to a mine.

Stop C5: Clara Mineral District

The detachment fault in the Clara mineral district places Miocene sandstone and conglomerate above mylonitic crystalline rocks. Most of the mineralization in the Clara district is represented by fracture-filling chrysocolla and iron oxides in microbreccia below and adjacent to the detachment fault. The mine at the area where the vehicles should be parked contains typical detachment-related mineralization. Note that mineralization ends abruptly upward at the detachment surface, indicating that mineralization at this mine ended before faulting ended.

Directions and Comments En Route to Stop C6

Drive back to the main road, turn left, and continue down the Lincoln Ranch synform. After 2 to 2.5 mi, the main road will fork. Take the left fork to Johnson Ranch, not the right fork, to Lincoln Ranch. At 2.5 to 3 mi past the fork, the road will merge with a gasoline road as the road you are on turns left. Continue north-northwest for 3.5 mi along the gasoline road until you are at the Bill Williams River crossing. Do not cross the river! Go left up the wash that enters the river at the crossing. Approximately 1/4 mi up the wash is a wide concave-eastward bend. Stop here.

Stop C6: Upper-Plate Normal Fault

Along the outside bend in the wash is a gently dipping normal fault that places steeply tilted, massive to very poorly bedded, Miocene conglomerate on top of gently tilted Miocene sandstone. The conglomerate unit is the stratigraphically highest tilted Tertiary unit in the central Buckskin Mountains and depositionally overlies the sandstone unit. The major difference in bedding attitudes above and below this gently northeast-dipping normal fault is interpreted as a product of rotation of the upper unit above a listric normal fault. Mylonitic clasts derived from completely denuded lower-plate rocks

during detachment faulting are present in the conglomerate unit.

Stop C8: Manganese Mine

Directions and Comments En Route to Stop C7

Drive the vehicles 1/3 mi up the wash and note the detachment fault descending into the wash from the left side. If we have time, we will stop here and examine the fault and upper-plate, mylonite-clast-bearing conglomerate.

Continue up the wash for perhaps 100 to 200 yd and turn left on the road that ascends out of the wash and returns to the gasline road. Turn right on the gasline road and drive 3 to 3.5 mi to the fork in the road. Take the left fork, which will keep you on the gasline road. Drive another mile until you reach the point where the gasline road crosses the Lincoln Ranch Road. Turn left onto the Lincoln Ranch Road and drive 2 mi until you approach the gate to Lincoln Ranch. At approximately 150 yd before the gate to Lincoln Ranch, note the mileage, turn right onto an old road, and follow the road around the base of the cliffs of upper Tertiary basin fill. The road eventually leads to the south, up and out of the Lincoln Ranch area. After you have driven 3.6 mi from the intersection with the Lincoln Ranch Road, you will be at the top of a hill in light-colored, older Quaternary alluvium. Turn left on the old road and drive down the ridge crest to the flat area.

Stop C7: "A-Bomb Canyon"

Stop at the flat cleared area that looks like an old drill pad. Walk approximately 50-100 yd farther down the road and look for the burro trail descending into the canyon to the east. Follow the trail down to the wash. A detachment fault is beautifully exposed in the canyon bottom. Chloritic breccia and microbreccia below the fault contain "floating" clasts of protolith mylonitic granitic and gneissic rocks. The fault contact is sharp, with shattered granite forming the upper plate. A broken lens of dark-brown carbonate is exposed at the base of the upper-plate granite.

Walk down the canyon through shattered, upper-plate granite to a high-angle normal fault in the upper plate that places red Miocene sandstone down against the shattered granite. Note the high-angle discordance between the bedding and fault plane.

Return to the exposure of the detachment fault and, if there is time, walk up the canyon. Various upper-plate rock types, consisting primarily of mid-Tertiary volcanic and sedimentary rocks, are crushed, brecciated, and cut by a reverse fault. Upper-plate conglomerate and sandstone locally contain manganese oxides that occur at the same stratigraphic level throughout the Lincoln Ranch basin (Spencer and Reynolds, 1986b). The deposits are stratabound sedimentary deposits similar to those in the Artillery Mountains to the east (Lasky and Webber, 1949).

Directions and Comments En Route to Stop C8

Return to the vehicles, drive back to the gasline road, and turn left. At about 1 mi from the intersection with the gasline road, you will see a klippe of mid-Tertiary volcanic and sedimentary rocks that forms a dark-brown hill to the left. Drive another 1/4 mi past the klippe to a point where the road crosses a wash. Turn left down the wash, drive for approximately 1/2 mi, and ascend to the right on a road leading out of the wash. Drive another 1/4 mi and stop at the manganese mine.

A sandstone and conglomerate unit forms a small fault block bounded below by the detachment fault and bounded above by several intersecting upper-plate faults. Manganese mineralization occurs within this stratigraphic unit elsewhere in the Lincoln Ranch basin, but not in other units. Mineralization is interpreted to be sedimentary, as are deposits to the northeast in the Artillery Mountains (Lasky and Webber, 1949). At this locality, aqueous fluids are interpreted to have mobilized the manganese slightly after sedimentary deposition, resulting in manganese coatings along some well-exposed fault surfaces. Manganese mineralization ends abruptly downward at the detachment fault, indicating that detachment faulting ended after mineralization.

Directions and Comments En Route to Phoenix

Return to the gasline road (3/4 mi), turn left, and proceed over Ives Peak arch to Butler Valley. The Little Buckskin Mountains form the small range to the east in Butler Valley. The Harcuvar Mountains form the large range-flanking Butler Valley to the south. These two ranges are composed of lower-plate, variably mylonitic crystalline rocks, and each represents an east-northeast-trending foliation arch like the three in the Buckskin and Rawhide Mountains (Rehrig and Reynolds, 1980). Approximately 15 mi from the last stop, the gasline road will intersect a paved road. Turn right, drive over Cunningham Pass, and turn left when you reach the town of Wenden. The highway continues up McMullen Valley, which is interpreted to be a synform in the Bullard detachment fault between the antiformal crests of the Harquahala Mountains to the south and Harcuvar Mountains to the north.

At MP 74, the bench slightly below and to the north of Harquahala Peak, the highest point in the Harquahala Mountains, contains the Harquahala thrust, a major thrust that here places Proterozoic crystalline rocks over a deformed Proterozoic porphyritic granite and slices of Paleozoic metasedimentary rocks (Reynolds and others, 1986). Lower-plate granite and thrust-zone mylonites are cut by numerous light-colored pegmatites and northwest- to west-trending dioritic dikes that readily weather to form small topographic notches.

The small dark-colored hills along the southeastern flank of the Harcuvar Mountains are Tertiary volcanic and sedimentary rocks in the upper plate of the Bullard detachment fault, which dips southeast off the flanks of the range. Bullard Peak, the low, dark peak at the base of the range, is composed of moderately dipping to vertical Miocene andesite flows that strike east-west, directly into the underlying detachment fault. Aguila Ridge, the long ridge north of Aguila, is composed of southwest-dipping, upper-plate middle Tertiary volcanic and sedimentary rocks that depositionally overlie Proterozoic crystalline rocks (Reynolds and Spencer, 1985).

Eagle Eye Peak, the dark reddish-brown peak on the northeast end of the Harquahala Mountains (south of Aguila), is composed of southwest-dipping, middle Tertiary volcanic and sedimentary rocks that are underlain by the northeast-dipping Bullard detachment fault. South of Eagle Eye Peak are the Big Horn Mountains.

Closer to Wickenburg, the highway passes north of the Vulture Mountains. This range contains a series of tilted fault blocks of moderately northeast-dipping middle Tertiary volcanic and sedimentary rocks, underlying Proterozoic crystalline rocks, and Late Cretaceous granodiorite (Rehrig and others, 1980). A

low-angle normal fault that places tilted volcanics over Proterozoic crystalline rocks is exposed at MP 102.1. Gently dipping 13.5-m.y.-old basalt that unconformably overlies the tilted Vulture volcanics is present near MP 103.

From Wickenburg proceed to Phoenix via U.S. Highway 60 to either (1) the Carefree Highway past Lake Pleasant and south on I-17, or (2) Litchfield Park Road south past Luke Air Force Base and east on I-10. Do not take U.S. Highway 60 all the way to Phoenix; it is a very slow route because of numerous six-way stop lights.

REFERENCES CITED

- Anderson, J. L., 1983, Proterozoic anorogenic granite plutonism of North America, *in* Medaris, L. G., Jr., and others, eds., Proterozoic geology; selected papers from an international Proterozoic symposium: Geological Society of America Memoir 161, p. 133-154.
- _____ 1985, Contrasting depths of "core complex" mylonitization, barometric evidence: Geological Society of America Abstracts with Programs, v. 17, p. 337.
- _____ 1987a, Core complexes of the Mojave-Sonoran Desert; conditions of plutonism, mylonitization, and decompression, *in* Ernst, W. G., ed., Metamorphism and crustal evolution of the western conterminous U.S.: Englewood Cliffs, Prentice-Hall (in press).
- _____ 1987b, Proterozoic anorogenic granites of the southwestern U.S., *in* Jenney, J. P., and Reynolds, S. J., eds., Geologic evolution of Arizona and the Southwest: Arizona Geological Society Digest, v. 17 (in press).
- Anderson, J. L., Barth, A. P., and Young, E. D., 1987, Mid-crustal roots and tectonic decompression of metamorphic core complexes: Geological Society of America Abstracts with Programs, v. 18 (in press).
- Anderson, J. L., Davis, G. A., and Frost, E. G., 1979, Field guide to regional Miocene detachment faulting and early Tertiary(?) mylonitic terranes in the Colorado River Trough, southeastern California and western Arizona, *in* Abbott, P. L., ed., Geological excursions in the southern California area: San Diego, San Diego State University, p. 109-133.
- Anderson, J. L., and Rowley, M. C., 1981, Synkinematic intrusion of two-mica and associated metaluminous granitoids, Whipple Mountains, California: Canadian Mineralogist, v. 19, p. 83-101.
- Capps, R. C., Reynolds, S. J., Kortemeier, C. P., Stimac, J. A., Scott, E. A., and Allen, G. B., 1985, Preliminary geologic maps of the eastern Bighorn and Belmont Mountains, west-central Arizona: Arizona Bureau of Geology and Mineral Technology Open-File Report 85-14, 25 p.
- Davis, G. A., Anderson, J. L., Frost, E. G., and Shackelford, T. J., 1980, Mylonitization and detachment faulting in the Whipple-Buckskin-Rawhide Mountains terrane, southeastern California and western Arizona, *in* Crittenden, M. D., Jr., and others, eds., Cordilleran metamorphic core complexes: Geological Society of America Memoir 153, p. 79-129.
- Davis, G. A., Anderson, J. L., Martin, D. L., Krummenacher, Daniel, Frost, E. G., and Armstrong, R. L., 1982, Geologic and geochronologic relations in the lower plate of the Whipple detachment fault, Whipple Mountains, southeastern California; a progress report, *in* Frost, E. G., and Martin, D. L., eds., Mesozoic-Cenozoic tectonic evolution of the Colorado River region, California, Arizona, and Nevada: San Diego, Cordilleran Publishers, p. 408-432.
- Dokka, R. K., and Lingrey, S. H., 1979, Fission-track evidence for a Miocene cooling event, Whipple Mountains, southeastern California, *in* Armentrout, J. M., and others, eds.: Cenozoic paleogeography of the western United States: Society of Economic Paleontologists and Mineralogists, Pacific Section, Pacific Coast Paleogeography Symposium #3, p. 141-146.
- Frost, E. G., 1980, Whipple Wash Pump Storage Project, California; appraisal design data, structural geology and water-holding capability of rocks in the Whipple Wash area, San Bernardino County, California: U.S. Water and Power Resources Service, Boulder City, Nevada, unpublished report, 88 p.
- Gross, W. W., and Hillemeier, F. L., 1982, Geometric analysis of upper-plate fault patterns in the Whipple-Buckskin detachment terrane, *in* Frost, E. G., and Martin, D. L., eds., Mesozoic-Cenozoic tectonic evolution of the Colorado River region, California, Arizona, and Nevada: San Diego, Cordilleran Publishers, p. 256-266.
- Keith, S. B., Gest, D. E., and DeWitt, Ed, 1983, Metallic mineral districts of Arizona: Arizona Bureau of Geology and Mineral Technology Map 18, scale 1:1,000,000.
- Kemnitzer, L. E., 1937, Structural studies in the Whipple Mountains, southeastern California [Ph.D. thesis]: Pasadena, California Institute of Technology, 150 p.
- Krass, V. A., 1980, Petrology of upper-plate and lower-plate crystalline terranes, Bowman's Wash area of the Whipple Mountains, southeastern California [M.S. thesis]: Los Angeles, University of Southern California, 252 p.
- Lasky, S. G., and Webber, B. N., 1949, Manganese resources of the Artillery Mountains region, Mohave County, Arizona: U.S. Geological Survey Bulletin 961, 86 p.
- Laubach, S. E., 1986, Polyphase deformation, thrust-induced strain and metamorphism, and Mesozoic stratigraphy of the Granite Wash Mountains, west-central Arizona [Ph.D. thesis]: Urbana-Champaign, University of Illinois, 180 p.
- Marshak, Stephen, and Vander Muelen, Marc, 1987, Geology of the Battleship Peak area, southern Buckskin Mountains; structural style below the Buckskin detachment fault, *in* Spencer, J. E., and Reynolds, S. J., eds., Geology and mineral resources of the Buckskin and Rawhide Mountains: Arizona Bureau of Geology and Mineral Technology Bulletin 198 (in press).
- Metzger, D. G., 1968, The Bouse Formation (Pliocene of the Parker-Blythe-Cibola area), Arizona and California: U.S. Geological Survey Professional Paper 600-D, p. 126-136.
- Orrell, S. E., and Anderson, J. L., 1987, Proterozoic metamorphism in the Whipple Mountains, southeastern California: Geological Society of America Abstracts with Programs, v. 18 (in press).
- Podruski, J. A., 1979, Petrology of the upper plate crystalline complex in the eastern Whipple Mountains, San Bernardino County, California [M.S. thesis]: Los Angeles, University of Southern California, 192 p.
- Rehrig, W. A., and Reynolds, S. J., 1980, Geologic and geochronologic reconnaissance of a northwest-trending zone of metamorphic core complexes in southern and western Arizona, *in* Crittenden, M.

- D., Jr., and others, eds., Cordilleran metamorphic core complexes: Geological Society of America Memoir 153, p. 131-157.
- Rehrig, W. A., Shafiqullah, M., and Damon, P. E., 1980, Geochronology, geology, and listric normal faulting of the Vulture Mountains, Maricopa County, Arizona, in Jenney, J. P., and Stone, Claudia, eds., Studies in western Arizona: Arizona Geological Society Digest, v. 12, p. 89-110.
- Reynolds, S. J., 1985, Geology of the South Mountains, central Arizona: Arizona Bureau of Geology and Mineral Technology Bulletin 195, 61 p.
- Reynolds, S. J., and Lister, Gordon, 1987, Field guide to lower- and upper-plate rocks of the South Mountains detachment zone, Arizona: Arizona Bureau of Geology and Mineral Technology Special Paper 6 [this volume].
- Reynolds, S. J., and Spencer, J. E., 1985, Evidence for large-scale transport on the Bullard detachment fault, west-central Arizona: *Geology*, v. 13, p. 353-356.
- Reynolds, S. J., Spencer, J. E., Richard, S. M., and Laubach, S. E., 1986, Mesozoic structures in west-central Arizona, in Beatty, Barbara, and Wilkinson, P. A. K., eds., *Frontiers in geology and ore deposits of Arizona and the Southwest*: Arizona Geological Society Digest, v. 16, p. 35-51.
- Richard, S. M., 1982, Preliminary report on the structure and stratigraphy of the southern Harquahala Mountains, Yuma County, Arizona, in Frost, E. G., and Martin, D. L., eds., *Mesozoic-Cenozoic tectonic evolution of the Colorado River region, California, Arizona, and Nevada*: San Diego, Cordilleran Publishers, p. 235-242.
- Richard, S. M., Reynolds, S. J., and Spencer, J. E., 1987, Mesozoic structure and stratigraphy of the Little Harquahala Mountains, west-central Arizona: *Geological Society of America Bulletin* (in press).
- Shackelford, T. J., 1980, Tertiary tectonic denudation of a Mesozoic-early Tertiary(?) gneiss complex, Rawhide Mountains, western Arizona: *Geology*, v. 8, p. 190-194.
- Smith, P. B., 1970, New evidence for Pliocene marine embayment along the lower Colorado River area, California and Arizona: *Geological Society of America Bulletin*, v. 81, p. 1411-1420.
- Spencer, J. E., and Reynolds, S. J., 1986a, Some aspects of the middle Tertiary tectonics of Arizona and southeastern California, in Beatty, Barbara, and Wilkinson, P. A. K., eds., *Frontiers in the geology and ore deposits of Arizona and the Southwest*: Arizona Geological Society Digest, v. 16, p. 102-107.
- _____ 1986b, Geologic map of the Lincoln Ranch Basin, eastern Buckskin Mountains, western Arizona: Arizona Bureau of Geology and Mineral Technology Open-File Report 86-2, 6 p., scale 1:24,000.
- Spencer, J. E., Reynolds, S. J., Anderson, Phillip, and Anderson, J. L., 1985, Reconnaissance geology of the crest of the Sierra Estrella, central Arizona: Arizona Bureau of Geology and Mineral Technology Open-File Report 85-11, 20 p.
- Spencer, J. E., Reynolds, S. J., and Lehman, N. E., 1986, Geologic map of the Planet-Mineral Hill area, northwestern Buckskin Mountains, west-central Arizona: Arizona Bureau of Geology and Mineral Technology Open-File Report 86-9, 13 p., scale 1:24,000.
- Spencer, J. E., Richard, S. M., and Reynolds, S. J., 1985, Geologic map of the Little Harquahala Mountains: Arizona Bureau of Geology and Mineral Technology Open-File Report 85-9, scale 1:24,000.
- Spencer, J. E., and Welty, J. W., 1985, Reconnaissance geology of mines and prospects in parts of the Buckskin, Rawhide, McCracken, and northeastern Harcuvar Mountains: Arizona Bureau of Geology and Mineral Technology Open-File Report 85-6, 31 p.
- _____ 1986, Possible controls of base and precious-metal mineralization associated with Tertiary detachment faults in the lower Colorado River trough, Arizona and California: *Geology*, v. 14, p. 195-198.
- Stoneman, D. A., 1985, Structural geology of the Plomosa Pass area, northern Plomosa Mountains, La Paz County, Arizona [M.S. thesis]: Tucson, University of Arizona, 99 p.
- Thomas, W. M., Clarke, H. S., Young, E. D., Orrell, S. E., and Anderson, J. L., 1986, Precambrian granulite facies metamorphism in the Colorado River region, Nevada, Arizona, and California, in Ernst, W. G., ed., *Metamorphism and crustal evolution, western conterminous U.S.*: Englewood Cliffs, Prentice-Hall (in press).
- Wicklein, P. C., 1979, Geologic map of the Bill Williams district, Yuma County, Arizona: Arizona Bureau of Geology and Mineral Technology Open-File Report 80-2, scale 1:24,000.
- Wilkins, Joe, Jr., Beane, R. E., and Heidrick, T. L., 1986, Mineralization related to detachment faults; a model, in Beatty, Barbara, and Wilkinson, P. A. K., eds., *Frontiers in geology and ore deposits of Arizona and the Southwest*: Arizona Geological Society Digest, v. 16, p. 108-117.
- Wilkins, Joe, Jr., and Heidrick, T. L., 1982, Base and precious metal mineralization related to low-angle tectonic features in the Whipple Mountains, California and Buckskin Mountains, Arizona, in Frost, E. G., and Martin, D. L., eds., *Mesozoic-Cenozoic tectonic evolution of the Colorado River region, California, Arizona, and Nevada*: San Diego, Cordilleran Publishers, p. 182-203.
- Winterer, J. I., 1975, Biostratigraphy of Bouse Formation, a Pliocene Gulf of California deposit in California, Arizona, and Nevada [M.S. thesis]: Long Beach, California State University.
- Wright, J. E., Anderson, J. L., and Davis, G. A., 1986, Timing of plutonism, mylonitization, and decompression in a metamorphic core complex, Whipple Mountains, CA: *Geological Society of America Abstracts with Programs*, v. 18, p. 201.

Metamorphic Core Complexes, Mesozoic Ductile Thrusts, and Cenozoic Detachments: Old Woman Mountains-Chemehuevi Mountains Transect, California and Arizona

Keith A. Howard
U.S. Geological Survey
Menlo Park, California 94025

Barbara E. John
Department of Earth Sciences
University of Cambridge
Cambridge, CB2 3EQ England

Calvin F. Miller
Department of Geology
Vanderbilt University
Nashville, Tennessee 37235

INTRODUCTION

The Phanerozoic Cordilleran orogen mostly follows a continental margin formed in Late Proterozoic time, except in the southwestern United States, where the orogen involves the older North American craton. Consequently Proterozoic crystalline basement rocks there (Figure 1) were reworked by Phanerozoic magmatic and tectonic events. Cenozoic extensional detachments and midcrustal roots of Mesozoic magmatic arcs and thrusts are well displayed there. This field guide is designed to introduce these features through a west-to-east transect across a series of desert mountain ranges in southeastern California and western Arizona (Figures 2, 3). The report is a contribution of the U.S. Geological Survey's Pacific to Arizona Crustal Experiment (PACE) and of the combined Old Woman-Piute interdisciplinary effort (COWPIE)—two multidisciplinary team efforts that are addressing the nature and evolution of the crust in the region.

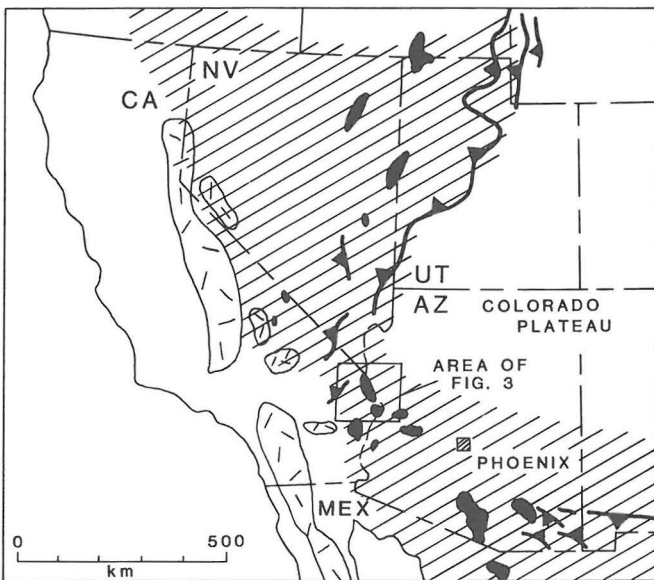


Figure 1. Tertiary extension (shaded) overprints an area previously affected by Mesozoic compression in the North American Cordillera. The Colorado River extensional corridor lies between the central Mojave Desert in California and the unbroken Colorado Plateau. The corridor encompasses metamorphic core complexes (black) and lies on the inboard (E) side of the Mesozoic batholith belt (randomly oriented dashes).

GEOLOGIC FRAMEWORK

Continental crust in SW North America has a long and diverse tectonic history (Figure 4). The formation of early Proterozoic crust and its incorporation into the North American continent and craton were followed much later by intense Mesozoic and Cenozoic modification involving both compressional and extensional tectonism and multiple magmatic episodes.

Neodymium- and lead-isotope studies suggest that SE California is part of a N-trending block of crust with model ages of 2.0–2.3 Ga; in contrast, model ages in Arizona are less than 2.0 Ga (Bennett and De Paolo, 1984; Wooden and others, 1986b). Early Proterozoic metaplutonic rocks (STOPS 1 and 19) and supracrustal rocks (STOP 3) of high metamorphic grade are widely exposed. Where dated, most have yielded ages of 1.6–1.8 Ga, although zircons with ages of about 2.0 Ga are locally present (Wooden and others, 1986a).

Rock units, foliations, and the traces of large upright isoclines (e.g., Howard and others, 1982a) commonly trend northeast and dip steeply where not reworked by Phanerozoic events. Regional aeromagnetic lineaments (U.S. Geological Survey, 1981) and some Mesozoic plutons (Howard and others, 1987) parallel them. "Anorogenic" 1.4 Ga granites (Anderson, 1983; STOP 7) and probable 1.1–1.2 Ga diabase dikes (Burchfiel and Davis, 1981; Hammond, 1986) (STOPS 1 and 7) are also present in the region. A striking feature of most of these dikes is their subhorizontal original orientation where Tertiary tilting can be restored (STOP 7). This orientation is unusual for dikes, and suggests emplacement during a neutral or compressive stress regime, in contrast with extensional conditions inferred for Proterozoic aulacogens in Death Valley and Arizona and extensional features such as the

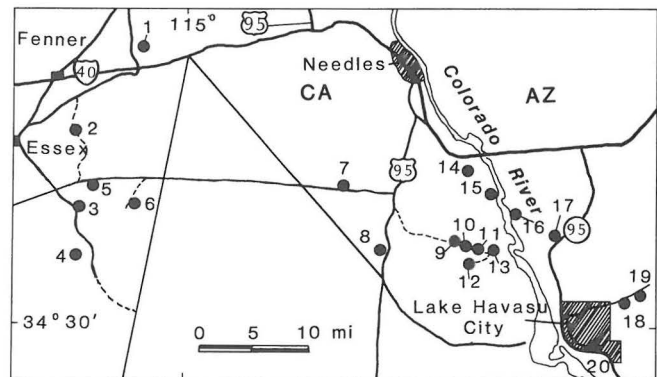


Figure 2. Road map showing numbered stops.

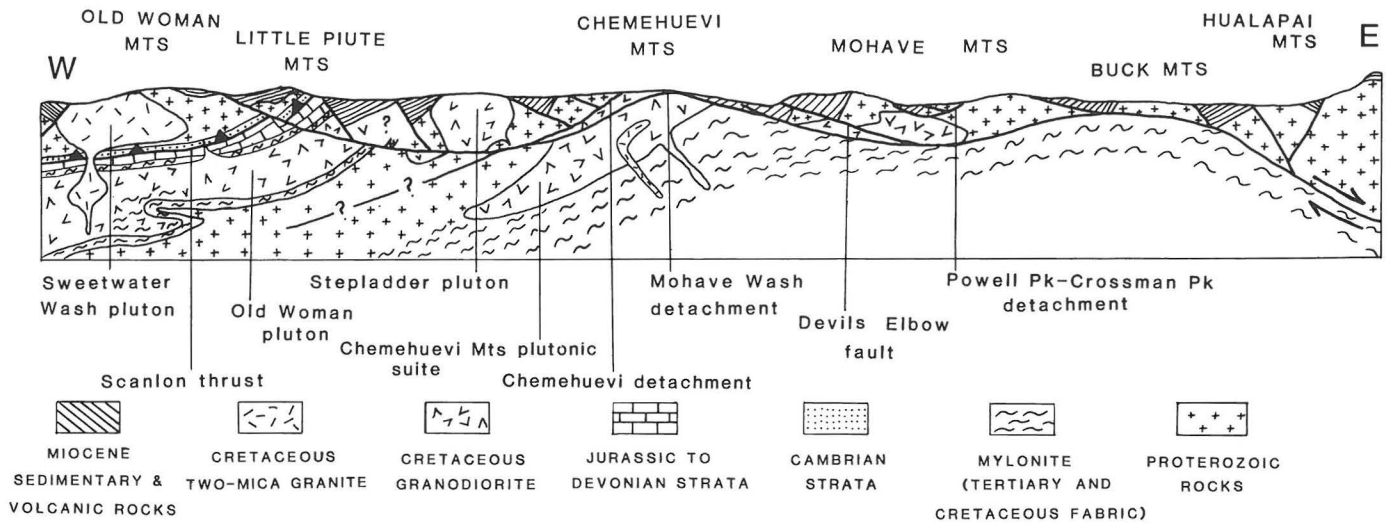
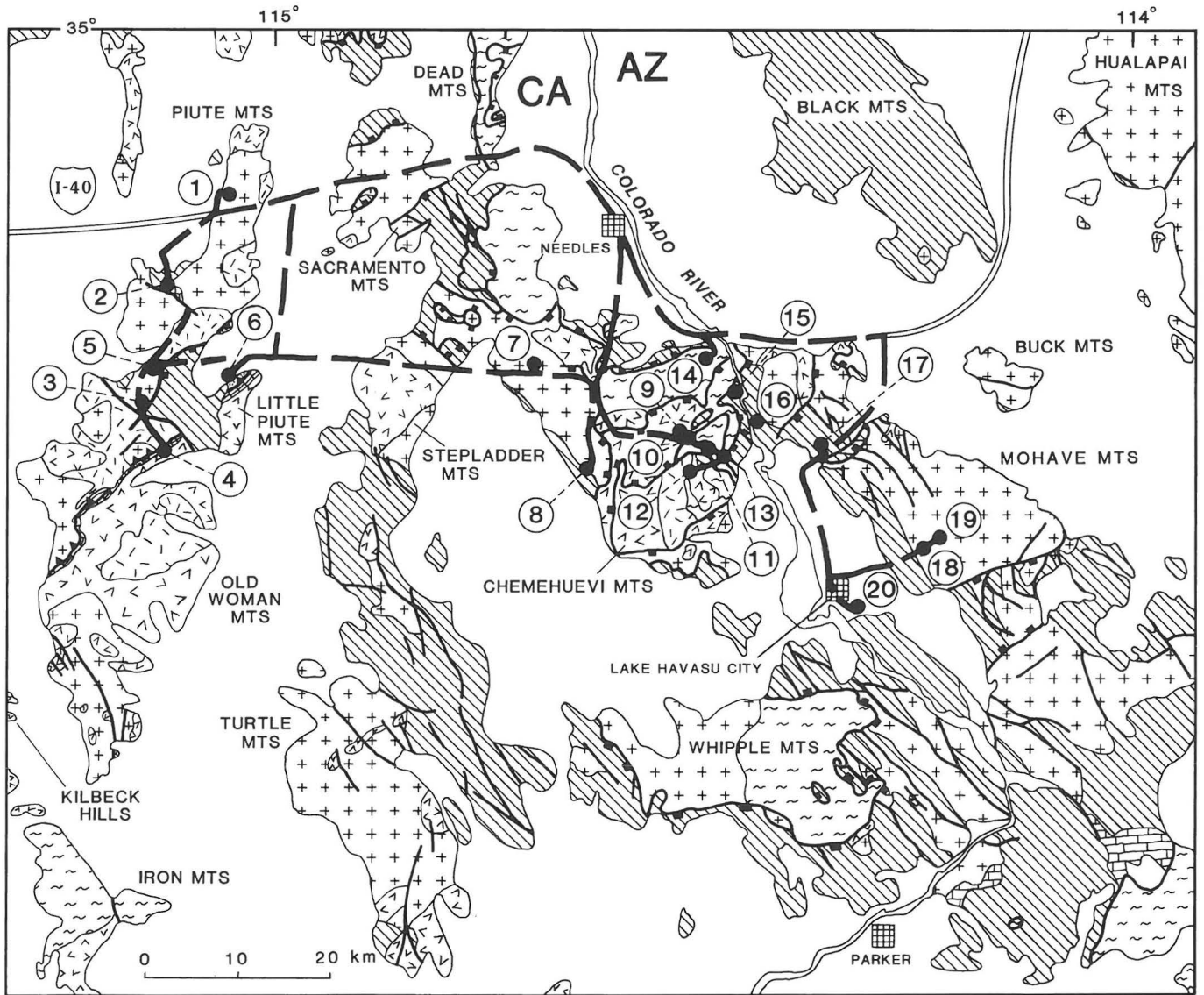


Figure 3. Geologic map and schematic east-west section across the Colorado River extensional corridor, showing field-trip route and numbered stops. Mesozoic thrust shown with barbed teeth on upper plate. Cenozoic detachments shown with square teeth on upper plate. Quaternary deposits not patterned. Vertical scale is inexact and exaggerated $\sim 2\times$. The base of the Chemehuevi Mountains plutonic suite (an informal unit) dips SE about 15° .

midcontinent gravity high associated with magmas of similar age and composition in the midcontinent (Fitzgibbon and Howard, 1987).

Cambrian through Triassic marine strata (Figure 5) are transitional from cratonal to miogeoclinal, and they record general crustal stability (Stone and others, 1983). Igneous rocks of Paleozoic age are unknown.

Reactivation of the craton during Mesozoic time was characterized by magmatism, intense deformation, and associated regional and contact metamorphism. Thrusting occurred in several episodes from Triassic through Late Cretaceous time (Burchfiel and Davis, 1981). Structures that may be components of the east-directed Cordilleran thrust belt in the eastern Mojave Desert show more ductile deformation than do counterparts to the north in Nevada and Utah (Burchfiel and Davis, 1981). Great nappes involving basement and highly attenuated Paleozoic strata are present (Howard and others, 1980; Hamilton, 1982).

Mesozoic plutonic rocks range in age from Late Triassic or Jurassic through Late Cretaceous and correspond approximately to magmatic arcs that extend into the Sierra Nevada, Nevada, and Arizona (Burchfiel and Davis, 1981). Jurassic intrusions are common in the central Mojave Desert. Cretaceous granitoids, common in the eastern Mojave Desert, include strongly peraluminous, muscovite-bearing granitoids derived from ancient crust; they form part of an inland belt of such granites that extends along the Cordillera (Miller and Bradfish, 1980; John, 1981). Irregular shifts through time in the eastern limit of Mesozoic magmatic activity is thought to have affected the locus and style of deformation (Burchfiel and Davis, 1981).

Evidence of sporadic Mesozoic continental sedimentation and volcanism (Burchfiel and Davis, 1981) is preserved locally, and ages of many sequences are poorly known (Harding and Coney, 1985). Regional Mesozoic metamorphism has been documented in several areas and is associated with basement-involved ductile thrusts and mylonitization (Miller and others, 1981, 1982; Hamilton, 1982; John, 1987, 1986; Hoisch and others, 1987).

Extensional tectonism began in the late Oligocene and continued until middle Miocene (about 14 Ma) time (Davis and others, 1980; 1982; Spencer, 1985). This episode is marked by low-angle extensional (detachment) faults and local basins filled chiefly with coarse clastic debris and volcanic rocks. The Colorado River extensional corridor crossed by the field trip includes the Chemehuevi-Whipple Mountains system of detachment faults (Figure 3).

The field trip transects a variety of Mesozoic and Cenozoic tectonic and magmatic features, outlined below.

Mesozoic Plutonic Rocks

Pre-Cretaceous plutonic rocks are scarce within the area of Figure 3, although the axis of a Jurassic southeast-trending plutonic and volcanic arc lies about 100 km to the west. Small sheets of ductilely deformed granitoids in the Old Woman Mountains (STOP 3) probably correlate with Jurassic granitoids west of the Old Woman Mountains. The Whale Mountain sequence of intermediate-composition rocks in the Chemehuevi Mountains may be of Jurassic or Cretaceous age. Mid-Cretaceous granodiorite plutons are present in the Turtle Mountains (Howard and others, 1982b; Allen, 1986).

Late Cretaceous plutons are voluminous in the western part of the transect region, but decrease in relative volume to the east. Four plutons in the Old Woman-Piute range (STOPS 4 and 5), some dikes and plutons in the Sacramento Mountains, and felsic differentiates associated with a large plutonic suite in the Chemehuevi Mountains are strongly peraluminous granite. Other Cretaceous intrusive rocks are weakly peraluminous to metaluminous granite and granodiorite, including the Old Woman granodiorite pluton (STOPS 4 and 6) and a large mass of porphyritic granodiorite in the plutonic suite of Chemehuevi Mountains (John, 1982;

hereafter referred to for the sake of brevity as the Chemehuevi Mountains plutonic suite; STOP 12). The Late Cretaceous rocks have Sr, Nd, and Pb isotopic values indicative of crustal derivation (Miller and others, 1982, 1984; John, 1986). Peraluminous granite and hornblende granodiorite plutons in the Old Woman Mountains have been dated at about 72 Ma by U-Pb (Miller and others, 1984); further U-Pb dating by J. E. Wright of Stanford University and K-Ar dating by R. F. Marvin and by J. K. Nakata of the U.S. Geological Survey, all in progress, confirm that many plutons in the region have a similar age.

Structure of Cretaceous Plutons

The Cretaceous plutons were emplaced in the upper to middle crust, their shapes reflecting intrusive behavior at different depths. The highest level plutonic rocks are represented by dikes of quartz-phyric rhyolite porphyry present in the Sacramento, Chemehuevi, and Turtle Mountains. A deeper level is represented by a granite pluton in the southern Sacramento Mountains, from which some of these porphyry dikes emanate; the pluton exhibits chilled porphyry textures against its exposed wall or roof. The North Piute pluton of two-mica granite, visible en route to STOP 1, discordantly dikes its roof. At apparently deeper structural levels of emplacement the plutons tend to be more concordant with their wall rocks. The Sweetwater Wash pluton of two-mica granite in the Old Woman Mountains has a mostly concordant floor against Paleozoic strata (Figure 6;

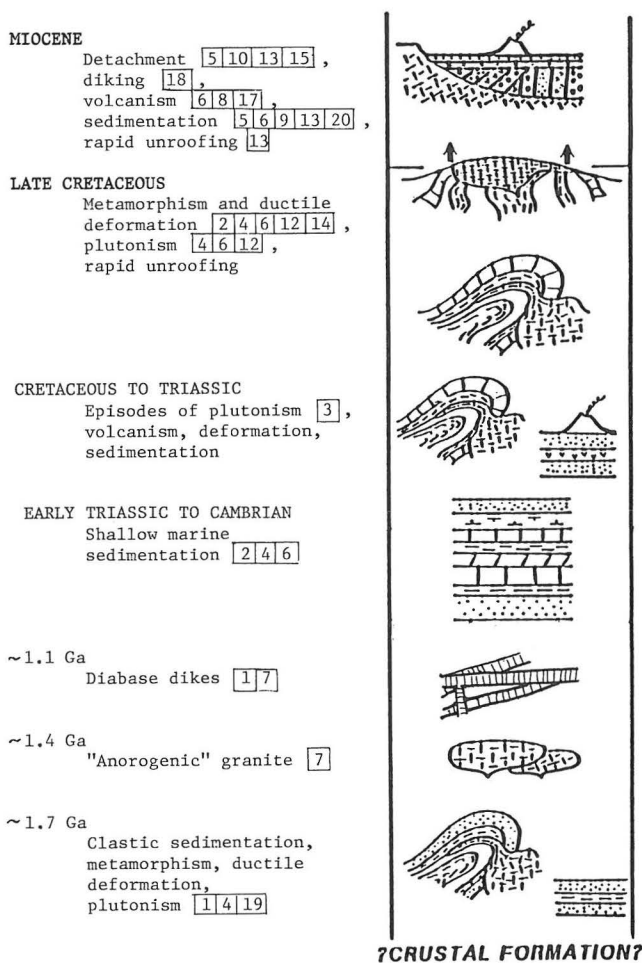


Figure 4. Schematic crustal history of SE California-W Arizona showing numbered field-trip stops (boxes).

STOP 4). The deeper Painted Rock pluton of two-mica granite, however, discordantly intrudes the slightly older granodiorite of the Old Woman pluton (Figure 6). The two structurally deepest plutonic bodies, the Old Woman pluton and the Chemehuevi Mountains plutonic suite, as described below, are the most concordant. Both show unusually well defined plutonic floors, as in the model of floored batholiths visualized by Hamilton and Myers (1967). The field trip will visit the Old Woman pluton on the **FIRST** and **SECOND DAYS** and the Chemehuevi pluton on the **THIRD DAY**.

The Old Woman granodiorite pluton (Figures 3, 6) extends 50 km and is several kilometers thick between concordant roof and floor. Surrounding the pluton at both top and base is a layer of older, highly foliated heterogeneous dark gneiss and schist about 10 to 100 m thick. The gneiss forms a concordant envelope that roofs the pluton against Paleozoic marble above (Figure 7; **STOPS 4B and 6**); and floors the pluton against migmatitic, ultrametamorphosed granodiorite gneiss derived from Proterozoic augen gneiss (Miller and others, 1982), below. The dark gneiss sheaths the pluton even around parts of a tongue or infold of the normally subjacent migmatite. These relations suggest a model in which the enveloping gneiss was carried as a distending skin on the pluton as the pluton was emplaced in nappe-like lobes.

The Chemehuevi Mountains plutonic suite farther east forms a compositionally zoned sill- or laccolith-like body, shown in cross-sectional view in Figure 8. The magma chamber evidently grew laterally in stages, with each pulse more fractionated than the preceding one. Pegmatite and aplite dikes are concentrated along the tops of both bodies of porphyritic granodiorite, and along the top of a younger body of two-mica granite. The reconstructed shape shows a flat floor for the lower part of the suite, which was intruded by at least three feeder dikes that provided magma to the chamber. This floor is characterized by lit-par-lit intrusions. The unexposed roof possibly is represented by discordant contacts of the granitic rocks against Proterozoic rocks in the Sacramento Mountains and in the Mohave Mountains.

The initial geometry of the Chemehuevi Mountains plutonic suite is thus interpreted to have been grossly tabular. Mylonitic foliation and SW-trending lineation in the country rocks and in the oldest (hornblende-biotite granodiorite) phase of the suite are cut by younger phases of the suite, and indicate that the earliest part of the plutonic suite was emplaced while the rocks of the concordant floor and northern wall were undergoing ductile shear. The plutonic suite is viewed as magma that ponded at and inflated the contact between undeformed Proterozoic basement above and subhorizontally foliated mylonitic basement below.

Cretaceous Folding, Thrusting, Metamorphism, and Uplift

Late Cretaceous structures and metamorphism record deformation at midcrustal levels in close association with plutonism. Structures to be visited include the Scanlon fold-thrust nappe in the Old Woman and Little Piute Mountains (**STOPS 4 and 6**), possibly related polyphase folds in the Piute Mountains (**STOP 2**), and thick shear zones of steep and gently dipping mylonitized rocks in the Chemehuevi Mountains (**STOPS 12 and 14**).

The nappe and perhaps the mylonites represent crustal shortening near the inboard side of the orogen, and may tie the foreland fold-thrust belt of Utah and Nevada (Burchfiel and Davis, 1981) to belts of thrusts in Arizona and to the SE (Figure 1). Along most of the foreland belt the thrusts ramp as brittle faults through the hinge of a thick miogeoclinal sedimentary wedge, but ductile thrusts in southern California and Arizona involve mostly basement and appear to have been controlled in position by ductility contrasts due to crustal heating, softening, and plutonism (Burchfiel and Davis, 1981; Miller and others, 1982; Haxel and others, 1984).

The Scanlon thrust at the base of the basement-cored Scanlon nappe lies within a narrow NW-dipping belt of

metamorphosed Paleozoic and Triassic strata, above the dark gneiss skin that roofs the Old Woman pluton. The belt of strata (and the base of the nappe) traces from the Little Piute Mountains 45 km SW through the Old Woman Mountains to the Kilbeck Hills. (We previously referred to the nappe as the Old Woman nappe, and we erroneously portrayed it in cross section as cut by Jurassic granite--Miller and others, 1982.) Inverted Cambrian rocks and Proterozoic basement are thrust over highly folded, but mostly upright, upper Paleozoic and Triassic rocks. Thrust horses due to imbrication are present in both the hanging wall and the footwall. At **STOP 4** in the Old Woman Mountains the thrust zone is sillimanite-grade and is partly obliterated by younger Cretaceous granite and granodiorite. At **STOP 6** in staurolite-grade rocks in the Little Piute Mountains the main thrust juxtaposes mylonitized Proterozoic gneiss over upper Paleozoic marble, and it floors imbricate slices composed of inverted Proterozoic and Cambrian rocks (Figure 7).

Timing of the thrusting and its associated metamorphic fabric is constrained to be about the same age as the concordant Old Woman and Sweetwater Wash plutons that locally intrude it, based on argon 40/39 studies reported by Hoisch and others (1987). Argon 40/39 and fission-track studies further show that the rocks in the Old Woman Mountains were very rapidly denuded from midcrustal depths and quenched to less than about 100°C within a few million years after metamorphism, thrusting, and plutonism (Knoll and others, 1985). This thermal history contrasts sharply with that in adjacent ranges to the west and the east. Unmetamorphosed Cambrian rocks in the Ship and Marble Mountains a few kilometers to the W stand in remarkable contrast to the sillimanite-grade equivalents in the Old Woman Mountains.

The lack of stratigraphic relief along the exposed length of the Scanlon thrust system suggests a thrust flat. Thick basement in the hanging wall, on the other hand, requires that the thrust ramped through some thickness of crust at a deeper level. As one possible model, thrusting up a steep ramp could have emplaced a thick upper plate above the thrust flat, burying it to metamorphic depths of 10-15 km, and ultimately causing gravity-driven denudation.

In the Chemehuevi Mountains, mylonitization affected rocks beneath the Chemehuevi Mountains plutonic suite and

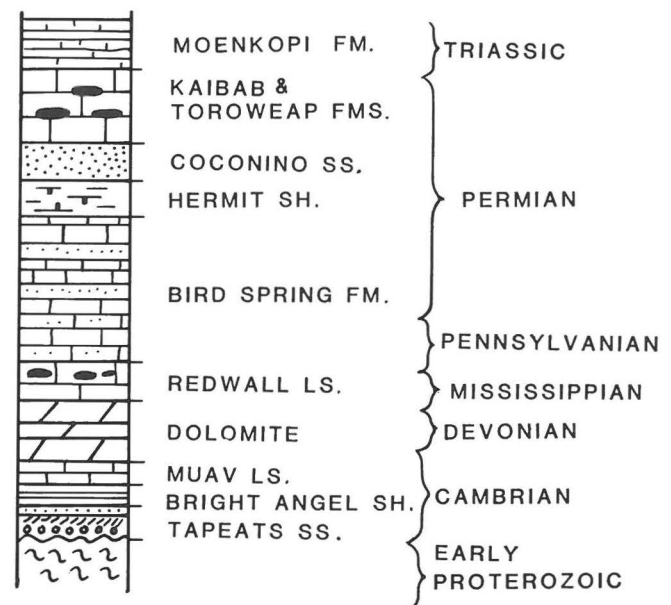


Figure 5. Stratigraphic section of metamorphosed Paleozoic and Triassic strata, naming the equivalent unmetamorphosed formations. Total initial thickness is estimated at about 2 km (**STOPS 2, 4, and 6**).

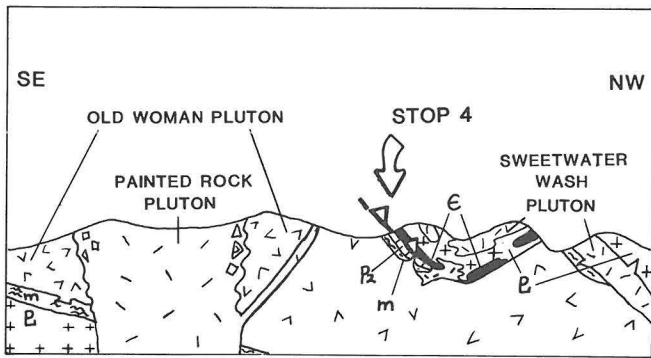


Figure 6. Diagrammatic section about 20 km long across the northern Old Woman Mountains, showing the setting of **STOP 4** along the Scanlon thrust. The thrust places Proterozoic (Pz) and Cambrian (C) over upper Paleozoic (Pz) rocks. Late Cretaceous two-mica granite (dashes) and granodiorite (V's) intrude the thrust zone and mylonitic gneiss (m) that envelops the Old Woman pluton.

beside its steep NW wall (Figure 8). Mylonitic fabrics are present through structural thicknesses of 5 km in the steep rocks (Whale Mtn.) and greater than 1.5 km in the floor rocks. Stretching lineations are coaxial to the gently SW-plunging common axis of mylonitic foliation (the down-structure direction in Figure 8). Shear-sense indicators in the floor mylonites are mainly top-to-NE, and in the steep NE-striking mylonites are left-lateral. The mylonitic rocks are viewed as two parts of a NE-directed Mesozoic shear zone, perhaps a thrust- and tear-fault system (John, 1986).

The subhorizontal mylonite zone has very similar W-dipping counterparts along strike to the S in the Whipple Mountains and en echelon to the NW in the Sacramento Mountains (Figure 2 -- Davis and others, 1980, 1982; McClelland, 1982). The three subhorizontal mylonite zones are therefore viewed as aligned except for a 15-km left-lateral dog leg on the steep mylonite zone in the northern Chemehuevi Mountains. Even though the Whipple Mountains mylonites are known to be in part Tertiary in age (Wright and others, 1986), this regional alignment suggests the possibility that they were originally part of a regional Mesozoic shear zone and were later reworked during Tertiary deformation (John, 1986).

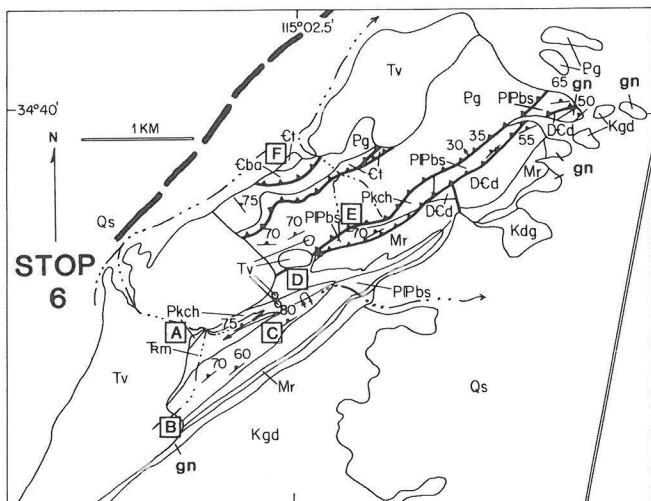


Figure 7. Geologic map of the Little Piute Mountains showing stops 6A to 6F (boxes; map is slightly modified from Stone and others, 1983).

Thrusting enhanced by melt (Hollister and Crawford, 1986) may explain the close association in space and time of Cretaceous plutons with mylonitic shear zones in the Chemehuevi Mountains and Old Woman Mountains. Hollister and Crawford (1986) propose that melt lubrication allows tectonic surges, which result in rapid uplift and decompression from peak metamorphic conditions; the Old Woman Mountains show such an uplift history. Correspondence of mylonitic zones with plutons also in the Whipple Mountains (Davis and others, 1980, 1982) and Iron Mountains (Miller and others, 1981; see Figure 3) suggest that shearing enhanced by melt played a dominant role regionally in Late Cretaceous deformation.

Cenozoic Rocks

Cenozoic rocks comprise volcanic and sedimentary rocks deposited during middle Cenozoic tectonic extension, dike swarms emplaced during extension, and postextensional deposits. The synextensional deposits (Figure 10) consist of a lower sequence (**STOPS 6 and 8**) of 21-18 Ma volcanic and clastic sedimentary rocks, the Peach Springs Tuff overlying them, and a higher 18-12 Ma sequence of coarse-grained clastic rocks and interspersed olivine basalt flows. The Peach Springs Tuff (**STOPS 6 and 17**) is a 19-18 Ma ignimbrite that stretches nearly 400 km westward from the Colorado Plateau to Barstow, California, and serves as an exceptional marker of Neogene deformation (Glazner and others, 1986; Wells and Hillhouse, 1986; Gusa and others, 1987). Undeformed basalts and fanglomerates that cap the deformed rocks and mark the end of the extension have yielded ages of 14.6-11.4 Ma (Spencer, 1985; John, 1986).

The Miocene rocks accumulated in evolving continental basins during normal and detachment faulting, uplift, and denudation of rising metamorphic core complexes (Knoll and others, 1985; Leach, 1986; Miller and John, 1986; Nielson and Glazner, 1986). Studies of clast sequences in fanglomerates and sedimentary landslide breccias indicate progressive unroofing of the metamorphic core complexes (**STOPS 9, 13, 20**), with locally continued movement on detachments even after the lower plates were breached (John, 1986, 1987; Miller and John, 1986).

Swarms of dacitic to mafic dikes were emplaced during the extension (**STOPS 8, 10, 18**) (Spencer, 1985; John, 1982, 1986; Nakata, 1982). NW-trending sheeted dikes that yield K-Ar biotite ages of 21-18 Ma in the Mohave Mountains (**STOP 18**), for example, account for a combined thickness of about 2.5 km in the NE direction of distension (Nakata, 1982; Light and others, 1983).

EXPLANATION

Qs	Surficial deposits (Quaternary)
Tv	Volcanic and sedimentary rocks (Tertiary-Miocene)—Welded tuff, basalt, sandstone, and conglomerate
Kgd	Granodiorite (Cretaceous)
sc	Schist and gneiss, possibly metaplutonic (Pre-Cretaceous)
Rm	Metamorphosed Moenkopi(?) Formation (Triassic?)—Laminated calcareous schist
Pkch	Metamorphosed Kaibab, Coconino, and Hermit Formations (Permian)—Cherty calcitic marble, platy fine-grained quartzite, and calc-schist and phyllite
PPbs	Metamorphosed Bird Spring Formation (Permian and Pennsylvanian)—Calcitic marble, quartzitic marble, and quartzite
Mr	Metamorphosed Redwall Limestone (Mississippian)—Massive white calcitic marble
DCd	Dolomitic marble (Devonian and/or Cambrian)
Cba	Metamorphosed Bright Angel Shale (Cambrian)—Pelitic schist
Ct	Metamorphosed Tapeats Sandstone (Cambrian)—Quartzite, in part cross-bedded, and metaconglomerate
Pg	Gneiss, schist, and amphibolite (Proterozoic)
—	CONTACT
—	THRUST FAULT—Teeth on upper plate
37	STRIKE AND DIP OF FOLIATION OR BEDDING
U	OVERTURNED SYNCLINE—Showing direction of plunge

Cenozoic Tectonic Extension

The Colorado River extensional corridor is 50-100 km wide and is characterized by SW-tilted fault blocks above regional low-angle detachment faults. Shingled upper-plate blocks are progressively more steeply tilted, farther from a breakaway (**STOP 5**) where the detachments shoal on the west side of the corridor. Seismic-reflection data (Frost and Okaya, 1986) support the concept that the breakaway fault in the Old Woman Mountains dips east under the Turtle and Stepladder Mountains and to the east is domed to the surface as the Chemehuevi detachment fault (Howard and others, 1982b; Figure 3). Deep reflection data also suggest the possibility that part of the detachment system may split to a deeper level under the Old Woman Mountains, isolating them as an extensional lens (Frost and Okaya, 1986). Howard and John (1987) conclude that the exposed detachments started as an east-dipping shear zone, along which the middle crust of California moved up and to the W by at least 50 km relative to upper crust in Arizona. Extreme thinning of the upper plate is inferred to have led to updoming and breaching of the footwall in metamorphic core complexes. The core complexes were at midcrustal levels when extension began, based on the 8-15-km paleothickness of allochthonous blocks that tilted and slid off them (Howard and others, 1982a; Howard and John, 1987; John, 1987).

The Chemehuevi detachment fault (**STOPS 8, 10, 13**) formed apparently with a gentle dip at midcrustal depths (John, 1987). It shows tens of kilometers of top-to-NE offset. It is a brittle fault; however, ductile equivalents from deeper levels may be represented by Tertiary mylonites in the Whipple Mountains, described by Wright and others (1986) and Davis and Lister (1987). Cataclases and local thin mylonites that formed in association with the Chemehuevi fault are overprinted by breccia and gouge representing movement at shallower depths as extension progressed (John, 1987). The deeper Mohave Wash detachment fault (**STOP 11**) offsets plutonic contacts 2 km NE and predates final motion on the Chemehuevi fault. Both faults show large corrugations along the NE slip direction (John, 1987). These faults project under successively higher low-angle faults: the Devils Elbow fault (**STOP 15**), and the Powell Peak-Crossman Peak fault system (**STOP 17**) in the Mohave Mountains.

Each of these stacked faults shows relative upper-plate motion to the NE, toward where the fault system is rooted under the untilted Hualapai Mountains and nearby ranges that merge with undeformed rocks of the Colorado Plateau (Lucchitta and Suneson, 1981; Howard and John, 1987). This uniform shear sense at all exposed crustal levels seems to require a crustal-scale simple-shear system (Wernicke, 1981, 1985; Davis and others, 1986; Davis and Lister, 1987; Howard and John, 1987).

FIELD-TRIP ROAD LOG

FIRST DAY

The first day is devoted to the Piute and Old Woman Mountains on the west side of the transect. Products of Proterozoic and Mesozoic metamorphism and Mesozoic plutonism, the Scanlon thrust, and a Miocene extensional breakaway fault can be examined.

Highlights En Route to Stop 1

Enter I-40 westbound (N) from "J" Street in Needles and travel 27.7 mi. After 23 mi (near Water Road exit), the Piute Mountains ahead expose a sharp contact at the roof of the light-colored North Piute pluton of two-mica granite, against the dark Proterozoic Fenner Gneiss of Hazzard and Dosch (1937). The granite is similar to other Cretaceous plutons to the south, but their adjacent country rocks are more pervasively injected and metamorphosed. Light-colored rock on the N side of the pluton, indistinguishable from the pluton at this distance, is intensely lineated, mylonitized,

Proterozoic two-mica-garnet granite, which also intrudes the Fenner.

Nearby E-W ribs in the Piute Mountains and to the east in the Sacramento Mountains are dikes that are part of a middle Tertiary dike swarm (Spencer, 1985). Dikes range from basaltic to rhyolitic in composition and, where fresh, show magma mingling and mixing textures. A diverse suite of lower crustal garnet granulite xenoliths is present in some dikes (Staudé and Miller, 1987).

At 27.7 mi beyond Needles, exit at Mountain Springs Road. Turn right (N) 2.1 mi, right 0.4 mi on a dirt road, and left 0.5 mi to **STOP 1** in the Piute Mountains (30.7 mi beyond Needles).

Stop 1

Park near sharp right bend in the road; walk 1/4 mi NW to diabase dikes that cut the Fenner Gneiss. The gneiss is a distinctive Proterozoic (about 1.7 Ga) metaplutonic rock of batholithic extent (Bender and Miller, 1987). It underlies much of the Piute Mountains and parts of several surrounding ranges (Howard and John, 1983). It is granodiorite to granite in composition, with 55-70 wt% SiO₂, 3-6 wt% K₂O, and high REE content (to 350 x chondrite LREE). Most of the Fenner is highly porphyritic, typically with 10-20% coarse-grained K-feldspar phenocrysts larger than 2 cm. The grain size of the matrix is commonly reduced by low-grade metamorphism and ductile shearing, so that a highly distinctive rock results with large, in some cases stretched and aligned, megacrysts of K-feldspar and smaller ones of plagioclase set in a dark, fine-grained matrix with obvious stringers of polycrystalline quartz.

Vicki Bennett (UCLA) determined initial E(Nd) of -1 (t approx. 1.7 Ga), indicating that continental crust existed here for an appreciable period of time prior to emplacement of the Fenner Gneiss (Miller and others, 1984). This is consistent with Ed Bender's observation (personal commun., 1986) that the Fenner intrudes higher grade rocks at its margins.

The large diabase dikes that cut the Fenner are part of the probable 1.1-1.2 Ga suite. The dike rock contains fresh plagioclase and delicately preserved ophitic texture though pyroxene has been replaced by actinolitic amphibole. The dikes appear to cut the intense foliation in the Fenner here, indicating a middle or early Proterozoic fabric age.

Goffs Butte to the NW is capped by flows of quartz-xenocryst-bearing, hornblende-two-pyroxene andesite, which overlies basement-clast conglomerate deposited on the Fenner Gneiss.

Highlights Between Stops 1 and 2

Retrace route 3.0 mi to S, cross I-40, and continue SW 6.1 mi. Turn left (S) on dirt road. After 1.6 mi, keep right across the tip of a low ridge of the Peach Springs Tuff; angle right (S) up a shallow valley on the E side of a hogback of the tuff dipping NW.

Hills to the left (E) are underlain by metamorphosed Paleozoic strata above Proterozoic gneiss. A series of north-trending high-angle faults to the E place the Peach Springs and underlying Miocene conglomerates against Proterozoic and Paleozoic rocks.

In another 0.8 mi (42.4 mi beyond Needles), cross a saddle by a Miocene paleohill held up by resistant quartzite of the metamorphosed Tapeats Sandstone (which again forms a hill today, to the left), which was topped by the Peach Springs Tuff. Valleys ahead and behind are also paleovalleys, filled by weak pre-Peach Springs conglomerate and tuff. Continue S 2.0 mi, across the paleovalley, then over Proterozoic basement, then through the valley in Paleozoic carbonate rocks; turn left 0.8 mi on road up valley to E (43.0 mi beyond Needles).

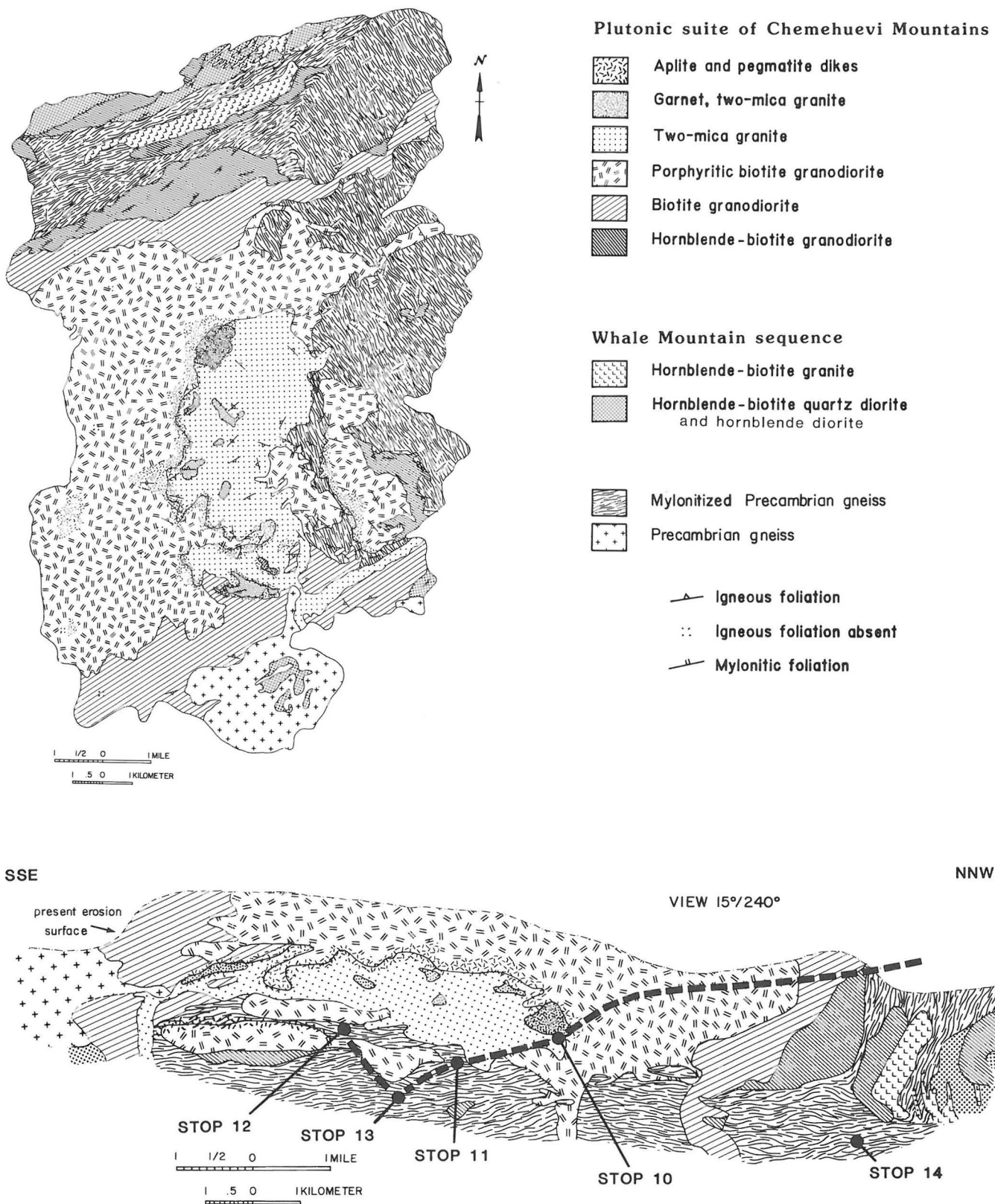


Figure 8. Reconstructed geologic map and down-plunge section of the Chemehuevi Mountains plutonic suite and the Whale Mountain sequence (both are informal units), based on restoration of 2-km ENE slip on the Mohave Wash fault (Figure 9; John, 1986). The projection direction for the section plunges 15° at 240° trend (SW), parallel to the common axis of foliations (and lineations) in the plutonic wall and floor; the axis is inferred to have been more nearly horizontal prior to Tertiary tilting. Approximate positions of the field-trip route and stops are projected onto the section.

Stop 2

Park in broad valley where road curves sharply to the right. Walk to the left (E) side of the valley, up a small, narrow canyon, and explore the multiply deformed, metamorphosed Paleozoic strata.

This area includes the hinge and inverted NE limb of a syncline. The geometry and development of the structures is complex (Stone and others, 1983, 1984; Brown, 1984).

It is clear that the Cambrian section (Figure 5)--the Tapeats Sandstone (here quartzite), Bright Angel Shale (here pelitic schist with minor marble and calc-silicate), and Muav Limestone (gray, banded marble at its base)--underwent syn-metamorphic multiple deformation. Limbs of F1 overturned fold-and-thrust nappes display a strong NE-SW-trending stretching lineation, which defines the direction of tectonic transport. A NW-trending, large-scale, downward-facing, F2 antiform has highly attenuated limbs of Proterozoic and lower Paleozoic rocks. Marbles here may form a stratigraphically intact Cambrian and Devonian sequence (Stone and others, 1983, 1984) or they may include a thrust sheet of the Mississippian Redwall Limestone (Brown, 1984). Staurolite + garnet + andalusite schists within the Bright Angel define the amphibolite-facies metamorphism here. Metamorphic grade decreases to the NW and increases to the SE, reaching a maximum (sillimanite-muscovite) adjacent to the Late Cretaceous Lazy Daisy pluton 1.5 km to the S. The Bright Angel displays an early metamorphic foliation which parallels compositional layering and a later axial-plane foliation, parallel to which a second generation of biotite and a first generation of staurolite have grown. Andalusite appears to postdate both foliations near the contact with the Lazy Daisy pluton to the south. Hoisch and others (1987) believe that the earlier mineral growth reflects syntectonic regional metamorphism, and the latest growth was induced by heating during emplacement of Lazy Daisy pluton (probably shortly after the peak of the regional event).

Highlights Between Stops 2 and 3

Retrace route 0.8 mi back to "main" road. Turn left and go 1.7 mi SE to a contact of the Lazy Daisy pluton with Proterozoic gneiss and schist. This pluton is one of four nearly identical, and probably related, two-mica granite plutons in the Old Woman and Piute Mountains. Here it injects numerous dikes and sills of aplitic garnet-bearing granite into its country rock. The next 2 mi of the route is through the pluton. A Tertiary(?) fault offsets the contact of the pluton across the valley in which the road lies.

In another 0.8 mi (46.3 mi beyond Needles), turn right (W) and go 1.2 mi to the western contact of the Lazy Daisy pluton. The hill ahead to the left is capped by quartzite of the Tapeats, with schist of the Bright Angel on the S side.

In another 0.2 mi is the Lazy Daisy Ranch. Please close the gate and let the owners know that geologists (not hunters) are crossing their land. Turn left (S) at 1.5 mi beyond the ranch, go 1.2 mi, and turn right on second pipeline road (this road has a powerline along it).

In 2.3 mi (52.7 mi beyond Needles) turn left on Sunflower Spring Road. After 0.7 mi take left fork of "Y," go 0.5 mi, and turn left up wash 0.1 mi to **STOP 3** (54.0 mi beyond Needles).

Stop 3

Walk left (E) out of the wash to a large exposure on the far side of a second wash 0.1 mi away. The rock here is primarily Proterozoic schist, much of it bearing large, well-formed staurolite. A dike of K-feldspar-phyric porphyry intrudes the schist.

The garnet-staurolite (+ andalusite) schist is a widespread, distinctive unit in the SW Piute Mountains and NE Old Woman Mountains. The schist is associated in this region with Proterozoic migmatites. The staurolite and

sparse andalusite appear to be late, postdating most of the fabric development and growth of large, now deformed garnets. Limited exposures of contacts suggest that the migmatite/schist package was metamorphosed and deformed prior to intrusion of the Fenner batholith (Bender, personal commun., 1986). Growth of staurolite and local andalusite may represent Mesozoic retrograde metamorphism; occurrences of staurolite and andalusite in Proterozoic pelites is spatially consistent with distribution of the same minerals in Bright Angel Shale pelites.

The moderately foliated dike is similar to dikes and an internal facies of a potassic pluton in the SE Piute Mountains. The pluton is largely undeformed, preserving chilled margins and cross-cutting relationships with country rocks. Near its S margin it has a strong deformational fabric. The dike is also similar to middle Mesozoic dikes in the southern Old Woman Mountains and Kilbeck Hills with typically rounded phenocrysts. Dikes like this are extremely common in the NE Old Woman and SW Piute Mountains.

Highlights Between Stops 3 and 4

Retrace route 0.1 mi to road; turn left (S). At 1.3 mi is the approximate location of the Tertiary high-angle Carson Wash fault. It strikes about N60°W and is expressed by thick gouge zones and local brecciation. It truncates Tertiary volcanic rocks and a major Tertiary normal fault (see **STOP 5**) N of it, and the Cretaceous Sweetwater Wash pluton S of it. Precise movement is uncertain, but the S side (Old Woman Mountains) appears to be uplifted considerably.

Beyond this point the road crosses the Late Cretaceous Sweetwater Wash pluton, a two-mica granite (Miller and Stoddard, 1981; Mittlefehldt and Miller, 1983). High $^{87}\text{Sr}/^{86}\text{Sr}$ and low $E(\text{Nd})$ indicate that this granite was derived from Proterozoic crust (Miller and others, 1984). After 4 mi we pass through highly injected Proterozoic and Paleozoic rocks that form the floor of the pluton; continue 0.1 mi (59.5 mi beyond Needles) and turn right (W) into Paramount Wash (use 4WD).

Stop 4

Paramount Wash trends subparallel to structure, crossing it obliquely from the top of the Old Woman pluton up through the Proterozoic and Paleozoic rocks that form its roof (and the floor of the Sweetwater Wash pluton), and then back down structure into the Old Woman pluton again (Figure 6).

STOP 4A -- The Old Woman pluton is a hornblende-biotite-sphene granodiorite. Its isotope chemistry indicates that it also has a major Proterozoic crustal component (Miller and others, 1984).

In 0.1 mi, take right-hand sandy wash; continue 0.9 mi up through Paleozoic rocks heavily injected by granite of the Sweetwater Wash pluton.

STOP 4B -- Park where walls of wash are low, before reaching the gray hills on the left (S). On the right side of the wash the Bright Angel Shale has been metamorphosed to sillimanite-grade schist. The Bright Angel here includes the attenuated but readily recognizable Chambless Limestone. A short distance farther N, Tapeats Sandstone quartzite is exposed, and beyond that are Proterozoic rocks including the Fenner Gneiss. On the left side of the wash amphibolites mark slices of Proterozoic rock thrust in with the Cambrian rocks.

An approximately 0.7 mi walking loop around the gray hill to the SW allows examination of part of a zone of NW-dipping structures that characterize the zone above the Old Woman pluton, from the Little Piute Mountains NE of us 45 km to the Kilbeck Hills to the SW (Howard and others, 1980; Miller and others, 1982). The NW-dipping structures (Figure 6) include a zone of gneisses ("enveloping gneiss")--probably including both Proterozoic and Mesozoic protoliths--structurally overlain by generally upright, locally isoclinally

folded upper Paleozoic rocks, overlain in turn by inverted Cambrian strata unconformably against structurally higher Proterozoic rocks. Proterozoic sheets and other complexities are present locally within this sequence and there are some apparently unique differences in the structure in the Kilbeck Hills (Horringa, 1986), but the most impressive aspect of this structural sequence is its consistency and lateral continuity, even where it is heavily injected by granite.

The gray hill is capped by marble of the lower part of the Muav, structurally under the stratigraphically lower Cambrian rocks where we parked. On the far side of the hill is the major Scanlon thrust which separates Cambrian from upper Paleozoic strata. This fault is injected by undeformed

granite of the Sweetwater Wash pluton. Beyond are complexly folded upper Paleozoic marbles, calc-silicate rocks with a variety of mineral assemblages (including wollastonite, diopside, grossular, idocrase) and minor amounts of quartzite.

Return to vehicles and drive 2.3 mi up the wash, first through Cambrian strata, then into the overlying Proterozoic rocks. The Sweetwater Wash pluton injects and locally brecciates these rocks, but has disturbed the structure remarkably little. The Proterozoic rocks include the Fenner Gneiss, schists and paragneisses, and lineated two-mica + garnet granite leucogneisses.

STOP 4C -- Stop where the trail gets bad and walk up the wash, which turns southward and starts traversing back

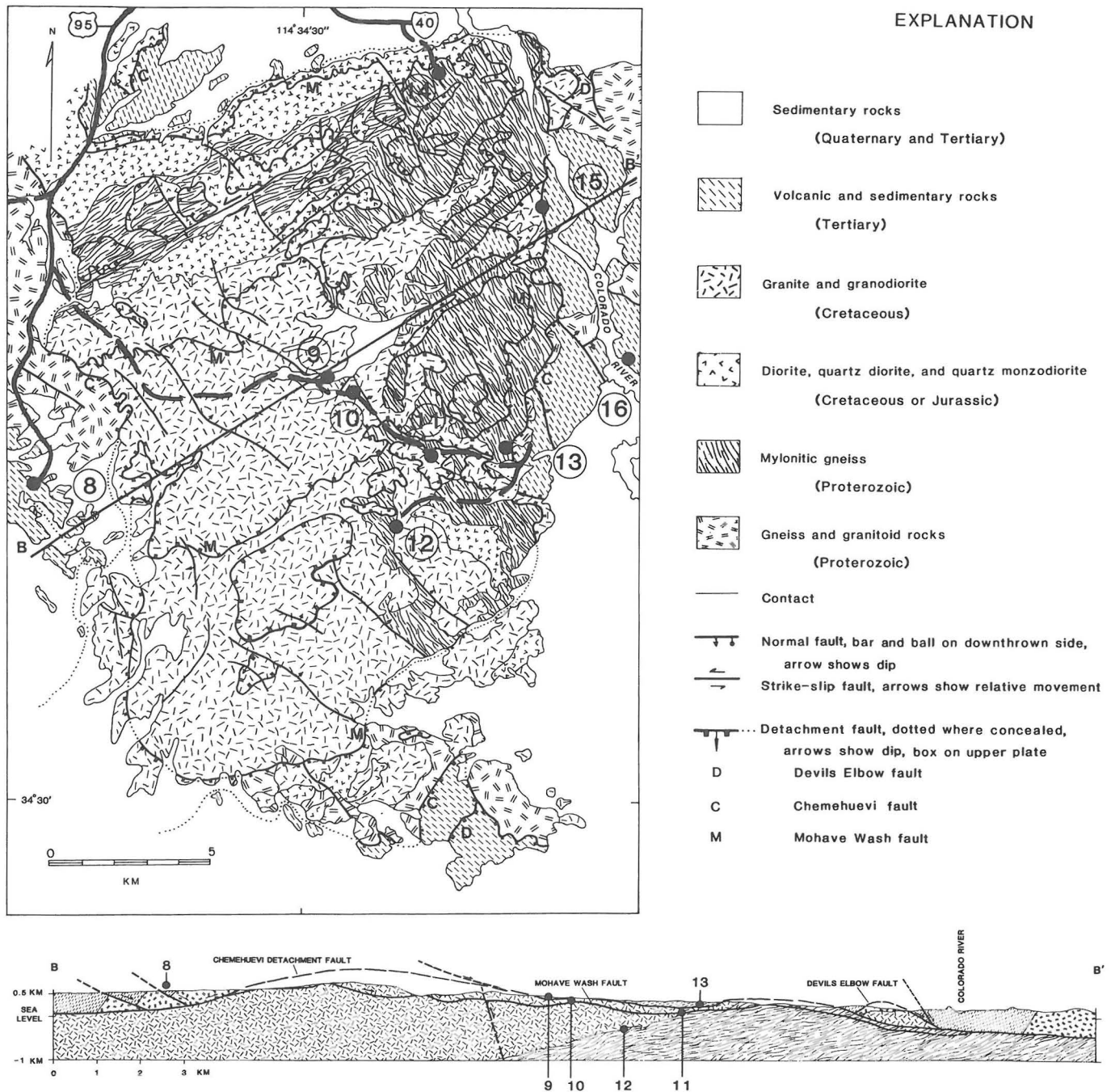


Figure 9. Generalized geologic map and cross section of the Chemehuevi Mountains (John, 1986, 1987) showing field-trip stops (stops on the cross section are projected).

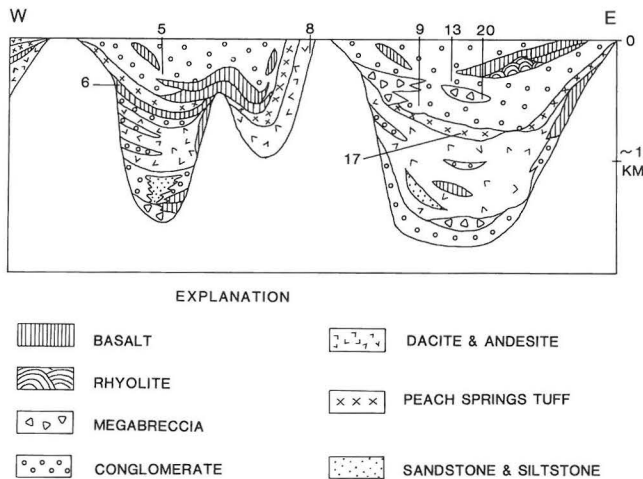


Figure 10. Generalized stratigraphic section of Miocene strata across the area of Figure 3, showing relative position of numbered field-trip stops.

downsection. Proterozoic leucogranite gneisses are cut by similar but undeformed Cretaceous granite of the Sweetwater Wash pluton. In 0.1 mi is a well displayed fold on the left (SE) side of the wash in lit-par-lit schist and leucogranite gneiss. This fold is cut by undeformed dikes.

If time permits, continue up the wash (down the structure) for a mile to the Old Woman pluton. On the way, pass through more granites injecting gneisses, cross a highly attenuated part of the Paleozoic band (at the Lady Jeanne prospect just S of here and W of the wash, the upper Paleozoic is less than 20 m thick), and traverse the lowest gneissic unit to the contact between the Old Woman and Sweetwater Wash plutons. The two-mica granite intrudes the granodiorite here and elsewhere, but relations in this area suggest mingling, consistent with Jim Wright's zircon dating, which indicates that the ages are very similar (Miller and others, 1984).

To drive to **STOP 5**, retrace the route 10.8 mi to the pipeline road, turn right (E), and go 3.0 mi (76.4 mi beyond Needles).

Stop 5

From the pipeline road, walk 1 mi S slightly above the W base of the unconsolidated boulder-capped hill to see a Miocene low-angle normal fault proposed as a breakaway. The fault places Miocene arkose above basement of the Lazy Daisy pluton and Proterozoic gneiss, and dips 35-40°E. Howard and others (1982b) and Howard and John (1987) have interpreted this fault to be the headwall breakaway of the Whipple-Chemehuevi detachment fault system, which lies to the E. All rocks from here to the transition zone adjacent to the Colorado Plateau that are older than 14-15 Ma are tilted to the west. Hileman and others (1987) have studied middle extensional Tertiary structures in this area.

This fault can be traced for 10 km to the NE before it is lost under alluvium, and for 6 km to the S, where it truncates against the Carson Wash fault. Much, quite likely all, movement along the fault here postdates the Peach Springs Tuff. Dips of Tertiary strata as far E as the Little Piute Mountains are approximately 15° NW except near faults. This is oblique to W to SW dips that characterize the majority of the Colorado River extensional corridor (Whipple detachment terrane).

Effects of faulting here include alteration and brecciation of underlying crystalline rocks and rotation of overlying sandstones, many of which have steep north dips. Dips may be related to a change in strike of the fault just to the north, as well as to drag. The section immediately above the fault

includes sandstone, conglomerate, tuff, and small amounts of siltstone and carbonate rock. The conglomerate contains abundant Peach Springs Tuff clasts, in contrast to post-Peach Springs conglomerates adjacent to the Little Piute Mountains, which lack such clasts. The sequence here is capped unconformably by unconsolidated conglomerate at the top of the hill. Attitudes are difficult to measure in this upper unit, but it appears to dip slightly to the northwest, perhaps indicating late movement on the fault.

For the return to Needles, continue E 7.2 mi along the PG&E gasoline road, with a view of our route for tomorrow and a panorama of the Little Piute, Stepladder, Sacramento, Chemehuevi, Turtle, Whipple, Mohave, and Hualapai Mountains. Turn left (N) and follow the good powerline road 11.2 mi to I-40. Turn right (E) on I-40, 23 mi back to Needles (Figures 2, 3).

SECOND DAY

This day is chiefly dedicated to examination of Cretaceous folds and thrusts of the Scanlon thrust system, and Cenozoic cover rocks, in the Little Piute Mountains. From there, a traverse eastward across the Stepladder and Sacramento Mountains introduces Miocene tilt blocks on the west flank of the metamorphic core complex exposed in the Chemehuevi Mountains.

Highlights En Route to Stop 6

Enter I-40 westbound (N) again at "J" Street in Needles. Several features related to Tertiary detachment faulting that can be viewed from the freeway are here described.

The domal Sacramento Mountains on the W (left) form a metamorphic core complex ringed by Tertiary detachment faults. The freeway passes W between this dome and the Dead Mountains on the north, on the E flank of which a red klippe of Tertiary rocks can be seen, resting in fault contact on lower-plate gneiss (look 3 o'clock at 7 mi beyond Needles, where the freeway turns W). A lower detachment lies within the gneiss. Low rubbly greenish-brown outcrops of chloritized and brecciated gneiss at the S end of the Dead Mountains are on the right, 0.5 mi E of the U.S. 95 (Searchlight) exit. Red upper-plate Miocene conglomerates are visible on the S side of I-40 0.5 mi W of that exit.

Beyond Needles 12 mi, view Flattop Mtn., ahead at 10 o'clock in the Sacramento Mountains. The flat top is basalt that dated at 14.6 Ma, an age that dates the cessation of detachment faulting because the basalt unconformably overlies a tilted, allochthonous section including a basalt also dated at 14.6 Ma (Spencer, 1985).

Most of the mountains in this area formed of domal lower plates to detachments. As the pass over the Sacramento Mountains is approached, note lowland roadside outcrops of brecciated gneiss on the west flank, near a detachment. Roadcuts in the pass (14.4 mi beyond Needles) are in lower-plate gneiss cut by steep Tertiary dikes, part of the swarm studied by Spencer (1985).

On the west side of the pass, 18 mi beyond Needles, the swale occupied by the Sacramento Mountains Cholla Reserve is underlain by upper-plate Tertiary strata and Proterozoic granitoids above a detachment. Roadcuts expose the footwall gneiss, cut by Cretaceous(?) muscovite granite and by the dense swarm of Tertiary dikes. The Piute Mountains ahead expose counterparts of the lower-plate Cretaceous(?) and Tertiary intrusions, but not of the upper-plate granitoids. Their absence in the Piute Mountains is surprising in view of the inferred E movement of the upper plate.

Exit the freeway 22.3 mi beyond Needles at Water Road. Go 0.8 mi, left over the freeway, turn right, and turn S along the powerline road, along the W side of Ward Valley. Dark Proterozoic gneiss crops out along both sides of the valley. The light-colored Cretaceous East Piute pluton, ahead 3 mi in the Piute Mountains on the right, intrudes the

dark Fenner Gneiss. The pluton consists of porphyritic two-mica granodiorite (Sparkes, 1981) and has a tectonite fabric (steep mylonitic foliation, subhorizontal lineation) cut by late-plutonic pegmatite dikes.

Beyond I-40 12.2 mi, turn right (W) on the PG&E gasline road (which is preceded by two other crossroads within a mile). The Little Piute Mountains ahead on the left expose cliff-forming light-colored outcrops of Paleozoic marble. After 1.5 mi, turn left (SW) on 4WD jeep trail and proceed 2.7 mi (38.7 mi beyond Needles).

Stop 6

Park near low outcrops (Peach Springs Tuff) for a 5-mi hike (bring water). The purpose of this hike is to examine the Scanlon thrust, folded rocks in the footwall, imbricated rocks in the hanging wall, and gneiss that envelopes the subjacent Old Woman pluton.

Proceed into the Little Piute Mountains (Figure 7) up "footprint gully," through the Peach Springs Tuff (look for flame structure, blue sanidine, honey-colored sphene) and underlying mafic flows. The volcanic rocks dip 10-15° NW, showing the Miocene tilt toward the breakaway fault of STOP 5. The Little Piute Mountains block is displaced less than 1-2 km relative to the Old Woman Mountains, based on the position of the Scanlon thrust system in both.

STOP 6A -- Beneath the volcanic rocks is a basal Miocene unit of red sandstone and tuffaceous sandstone, which has yielded numerous vertebrate bones and footprints (Knoll, 1985). Knoll documented 800 m of stratigraphic relief on the irregular sub-Miocene unconformity, with a varied section of sedimentary and volcanic (see J. S. Miller and others, 1987) units beneath the Peach Springs filling deep paleovalleys. A basal conglomerate (seen in float near STOP 6B) contains boulders of the Tapeats Sandstone.

The traverse to STOP 6B crosses a steeply NW-dipping, NW-plunging isoclinal syncline in an uninterrupted section of Devonian to Triassic strata. From youngest to oldest (Figure 5), the strata traversed are Triassic laminated calc-silicate rocks, Kaibab Limestone (cherty marble), Coconino Sandstone (pink laminated quartzite), Hermit Shale (metamorphosed calcareous mudstone), Bird Spring Formation (metamorphosed sandy limestone containing dark quartzitic marker beds; cross-beds are locally preserved), and Redwall Limestone (white, coarsely crystalline marble). Lineations and parasitic folds plunge steeply W down the dip; to the NE this W plunge shallows.

STOP 6B -- The deformed middle Paleozoic strata are structurally underlain by foliated dark gneiss--the enveloping gneiss on the top of the Old Woman pluton. Mylonitic foliation and lineation in the gneiss, now recrystallized and intruded by dikes from the pluton, parallel the fabric in the adjacent strata. Gouge and brecciation provide evidence of local brittle faulting at the gneiss-marble contact. The ductile origin and kinematic significance of the contact remain puzzling.

Traverse toward STOP 6C in the synclinal keel of the Kaibab Limestone and note that the plunge of parasitic folds in the Paleozoic strata shallows to about 30°W, yet the axial-plane foliation remains constant in orientation. This is one clue that the syncline may be a huge sheath fold formed during movement on the overlying Scanlon thrust.

STOP 6D is on a high ridge of brecciated quartzitic marker bed in the Bird Spring Formation on the inverted limb of the syncline. The ridge offers a good overview of this range and ranges eastward to the Chemehuevi Mountains.

STOP 6E marks the Scanlon thrust contact of mylonitic Proterozoic gneiss over upper Paleozoic marble. The mylonitic fabric in the gneiss appears in thin section to be annealed. Coaxial fabrics in the gneiss and the marbles suggest that folding in the Paleozoic units relates to movement on the thrust.

Traverse down the wash toward STOP 6F through varied Proterozoic gneisses. Their foliations dip parallel to the

underlying thrust and evidently were reoriented during thrusting. Cross several imbricate slices of inverted Cambrian strata (metamorphosed Tapeats, Bright Angel, and Muav Formations). Staurolite is an index metamorphic mineral in both Proterozoic and Cambrian pelites here (Miller and others, 1982; Hoisch and others, 1987).

At STOP 6F, examine inverted cross-bedding in the Tapeats Sandstone in one of the imbricate thrust slices.

Highlights Between Stops 6 and 7

Backtrack by car 2.7 mi to the PG&E gasline road. Turn right and proceed E toward the Stepladder Mountains. In 6.2 mi (47.6 mi beyond Needles), an isolated hill exposes olivine basalt (K-Ar whole-rock age 18.2 Ma) that dips gently W over Proterozoic gneiss. To the S, the basalt forms a series of W-dipping mesas, representing extensional fault blocks. The basalt unconformably overlies more steeply W-tilted 19-21 Ma volcanic rocks in the Stepladder and Turtle Mountains, showing a growth-fault relationship (Howard and others, 1982b; Nielson and Turner, 1986).

Seismic-reflection profiles a few miles to the S show that the block-bounding faults terminate downward against a low-dipping reflector, interpreted as a detachment, at about 3-5-km depth (1.5-2 sec two-way travel time), that appears to connect the Old Woman Mountains breakaway fault with the Chemehuevi detachment fault to the E (Frost and Okaya, 1986). The synformal character of the detachment (Figure 3, section) was predicted from the surface geology (Howard and others, 1982b; Spencer, 1985).

Ahead the road crosses a wide pediment exposing light-colored porphyritic granodiorite of the Cretaceous Stepladder pluton (72 Ma by K-Ar biotite; Armstrong and Suppe, 1973). The pluton and capping Miocene volcanic rocks are tilted and faulted. Allochthonous Miocene conglomerates in the central Sacramento Mountains 10 km to the NE (McClelland, 1982; Leach, 1986) contain clasts of the distinctive rock from this pluton, as well as clasts of the Fenner Gneiss.

Dark Proterozoic rocks in the floor or wall of the Stepladder pluton are exposed on the east side of the Stepladder Mountains pediment dome. Seven miles beyond STOP 6 (55.7 mi beyond Needles), at the junction with a powerline road, a concealed large Miocene normal fault juxtaposes steeply W-dipping Tertiary rocks ahead against the Stepladder block to the west. To the S (right) the Turtle Mountains expose a series of W-tilted fault blocks bounded by E-dipping Miocene faults. To the east, stratal tilts on fault blocks steepen and fault dips decrease (Figure 3).

In another 4 mi, pointed hills S of the road expose 65° SW-dipping Miocene andesite, which nonconformably overlies 1.4 Ga megacrystic granite in a large tilt block above the Chemehuevi detachment fault. Continue another 1.3 mi (61.0 mi beyond Needles).

Stop 7

Park at slight left bend in the otherwise straight road to examine middle Proterozoic rocks in the upper plate of the Chemehuevi detachment fault. Megacrystic granite here is part of the 1.4 Ga suite studied by Anderson (1983). A diabase dike 40 m thick that cuts the granite here is part of an extensive swarm believed to be 1.1-1.2 Ga. The diabase characteristically is ophitic and contains accessory biotite and ilmenite. The dip of this dike is 65° SW, parallel to Tertiary strata in the same structural block. This indicates an originally subhorizontal dike orientation, a relation found consistently for the Middle Proterozoic diabase throughout nearby ranges and much of Arizona (Howard and others, 1982a; Fitzgibbon and Howard, 1987).

Highlights Between Stops 7 and 8

Continue ahead 2.6 mi through upper-plate crystalline rocks toward the underlying Miocene Chemehuevi detachment

fault. Green- and orange-weathering rocks encountered 0.1 mi before the highway mark alteration along the Chemehuevi fault. At the stop sign, turn right (S) on U.S. 95 and go 5.9 mi to **STOP 8**.

Stop 8

Pull off U.S. 95 on the N side of the highway at Snaggletooth, rock pinnacles that consist of upper-plate SW-dipping Tertiary andesite and dacite. The Peach Springs Tuff is at the top of the sequence here. The Tertiary section nonconformably overlies Proterozoic gneisses, granites, and ophitic diabase dikes, like those at **STOP 7**. Toward the east, the dark Proterozoic rocks are in fault contact over light-colored Cretaceous granitic rocks, along the west-dipping Chemehuevi detachment fault that encircles the range (Figure 7). The fault domes over its light-colored footwall, and it also crops out in the eastern Chemehuevi Mountains. The dark dikes that cut the footwall are part of a voluminous dike swarm, thought to include two generations: the first related to late-stage Cretaceous magmatism and the second related to Tertiary extension.

For the return to Needles, head 17.7 mi N along U.S. 95. Turn N on I-40 (toward Barstow) and go 1.2 mi to the "J" Street exit.

THIRD DAY

Day 3 is devoted to the metamorphic core complex exposed in the Chemehuevi Mountains (Figure 9), and the road log addresses Mesozoic mylonitization and plutonism, and the evolution of Tertiary detachment faulting expressed by fault surfaces, brecciation, and syntectonic sediments.

Highlights En Route to Stop 9

Go eastbound (S) on I-40 1.2 mi from "J" Street and exit right on U.S. 95 toward Parker. The domal Sacramento Mountains (at 3 o'clock) and Chemehuevi Mountains (ahead left) are windows of lower-plate crystalline rocks, and are surrounded by lowlands of upper-plate rocks. Upper-plate Miocene sandstone and chloritically altered crystalline rocks are exposed in roadcuts en route to Lobecks Pass between the two ranges. In 12.9 mi (14.1 mi beyond Needles), turn left onto an unimproved jeep trail 5 m N of the first white reflector on the left side of the highway (at the right-hand curve in U.S. 95). The first mile of the jeep trail cuts through broken and altered granitic and gneissic rocks in plates above both the regionally developed Chemehuevi and structurally deeper Mohave Wash detachment faults. The local green color of the rocks is a result of extensive chlorite and epidote alteration that occurred during the middle Tertiary extensional faulting. At 1.0 mi beyond the highway are exposures of equigranular biotite granodiorite, a border phase of the Chemehuevi Mountains plutonic suite, the Late Cretaceous light-colored rocks that the route traverses until **STOP 9**. Two miles farther SE the jeep trail crosses a steep narrow 4WD pass. Beyond the pass, dark dikes ahead can be seen cutting the Chemehuevi Mountains plutonic suite.

Nine-tenths of a mile SE of the pass (18.0 mi beyond Needles), keep left at the fork and continue down the wash. To this point the traverse has been across the northern wall and margin of the laccolith-shaped plutonic suite. Continuing on this route will begin a traverse down section across the plutonic suite as shown diagrammatically in Figure 8. The majority of the route is in the porphyritic biotite granodiorite phase of the suite.

Continue down the wash, keeping left in another 0.8 mi. Note the regular, wide spaced jointing in the porphyritic granodiorite. The joint spacing decreases and relative intensity of fractures in these rocks increases ahead across klippen above the Mohave Wash fault, and toward the structurally higher Chemehuevi detachment fault (Figure 9). A broad, E-draining valley 1.8 mi ahead provides a view of

the central Chemehuevi Mountains. The valley follows a synformal corrugation in the Chemehuevi detachment fault. To the E (11 o'clock) in the distance are the Mohave Mountains, a large allochthonous block of crystalline rocks that lies structurally above this detachment fault.

After 0.7 mi, a low red-brown hill on the left is basalt dated at 11.45 ± 0.26 Ma (K-Ar, whole-rock). Compositionally identical basalt about 1 km S intrudes and locally fuses altered cataclasites associated with the Chemehuevi detachment fault. This relationship suggests that detachment faulting in the central Chemehuevi Mountains was over by roughly 12 Ma. In 0.4 mi veer left at the fork before reaching red rocks; continue 0.1 mi from the junction to **STOP 9** at the low red hill on your right.

Stop 9

This stop in the central Chemehuevi Mountains serves to introduce the central part of the extensional corridor (John, 1987). The stop is in Miocene alluvial-fan deposits that dip $55-60^\circ$ in a klippe above the Chemehuevi detachment fault (Figure 9). These deposits include clasts of the 1.4 Ga anorogenic granite and associated rocks, and rare clasts of the Peach Springs Tuff. Outcrops along the western margin of this exposure are fan deposits made up predominantly of leucocratic granitic clasts from the Chemehuevi Mountains plutonic suite. Older fan sediments are made up predominantly of Tertiary mafic to silicic volcanic flows similar to those exposed at **STOP 8**. The alluvial-fan deposits exposed in the central and eastern Chemehuevi Mountains apparently represent an unroofing sequence—the oldest fan sediments are made up of volcanic clasts, and interfinger with younger deposits composed mainly of clasts of Proterozoic gneissic and granitic material. The youngest deposits are monomictic breccias composed of granitic clasts and dike rocks typical of the rocks that the route to here has traversed. The sediments are preserved here in the trough of a major synformal corrugation of the Chemehuevi detachment fault.

Retrace the route 0.1 mi back to the major junction, go left, and continue 0.6 mi SE down Trampas Wash to a large pinnacle (tor) on the left.

Stop 10

The tor outcrop is brecciated leucocratic two-mica granite cut by mafic dikes. It is a few meters below the Chemehuevi detachment fault. Large tors of brecciated and weakly silicified granitic rocks like these are characteristic of the footwalls along the lateral walls or strike-slip segments of the corrugations of the Chemehuevi and Mohave Wash detachment faults. Originally steep NE- and NW-trending mafic dikes have been rotated into rough parallelism by cataclasis. The dikes at this exposure dip gently N, roughly parallel to the Chemehuevi detachment fault.

Highlights Between Stops 10 and 11

Keep left and continue down the main wash, which follows just below the level of the Mohave Wash fault (Figure 11). The ridge tops are granitic rocks in the hanging wall to that fault. The roadside exposures are granites and their gneissic country rocks in the footwall of the fault, and represent the floor zone of the plutonic body. **STOP 11** is 2.0 mi beyond **STOP 10** (24.3 mi beyond Needles).

Stop 11

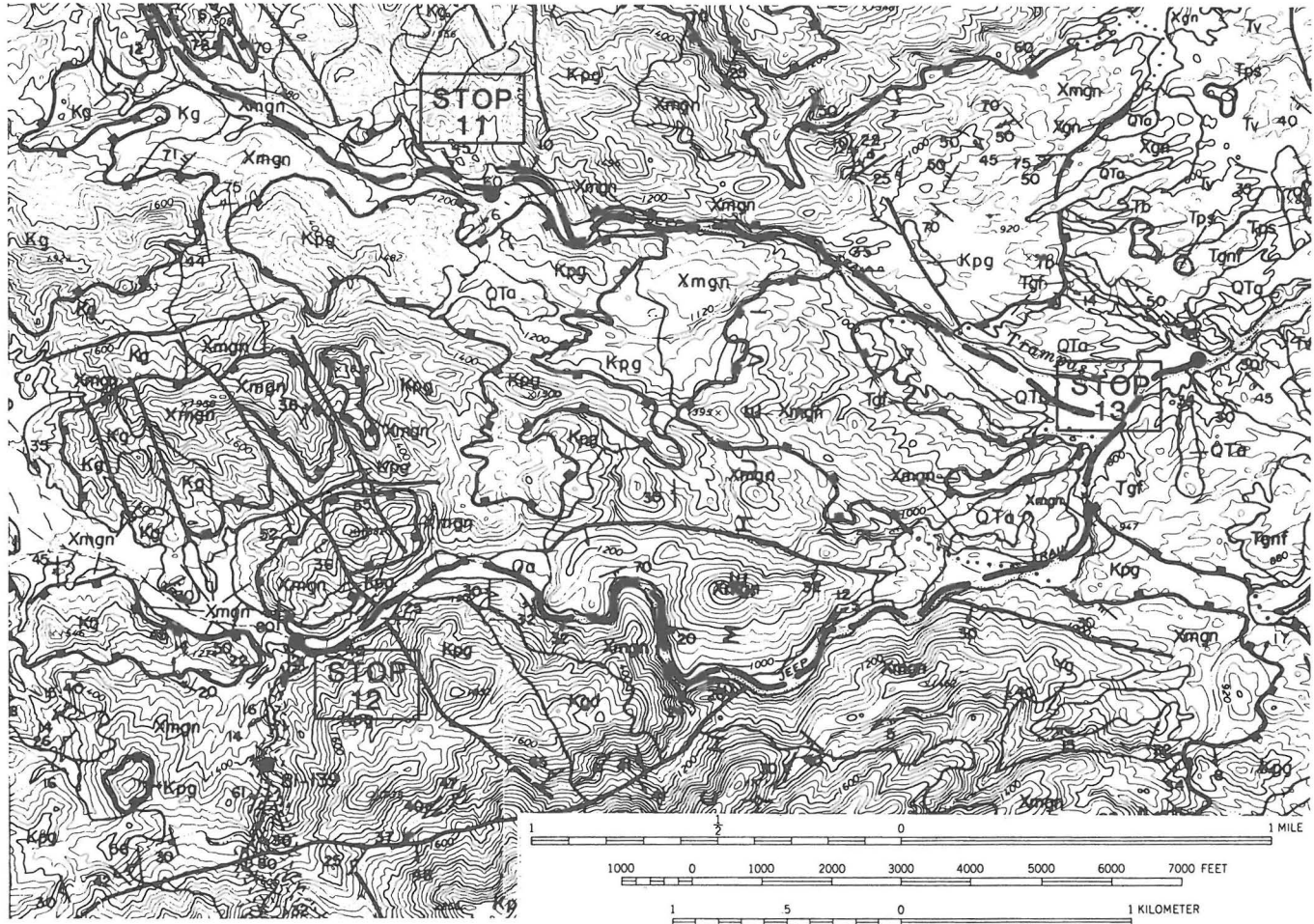
This stop (Figure 11) is to see the Mohave Wash fault, the structurally deeper low-angle normal fault that crops out beneath the Chemehuevi detachment fault throughout the Chemehuevi Mountains (Figure 9). The stop is a short climb up the low, dark exposures on the south side of the wash. The denuded fault surface is a domical window; upper-plate rocks

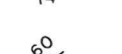
include porphyritic biotite granodiorite cut by dark dikes; the lower-plate rocks are gently SW-dipping Proterozoic gneisses within the structural floor of the plutonic suite. The low-angle foliation in the footwall rocks is a product of reorientation during late Mesozoic metamorphism and deformation, and is overprinted by brittle effects of the Tertiary extensional deformation. Where slip can be determined by slickensides and offset plutonic contacts, the hanging wall is offset 2 km to the NE. The fault surface has

a characteristic deep red-brown patina and well-developed slickenside striae. Weak azurite, malachite, and chrysocolla mineralization is concentrated in the associated fault rocks.

Highlights Between Stops 11 and 12

Continue down the wash past Proterozoic gneiss and migmatite, which floor the Chemehuevi Mountains plutonic suite (Figure 8). On the left (NE) side of the route 0.6 mi



-  AREA OF APLITE AND PEGMATITE DIKES
-  FAULT -- Showing dip. Teeth on upper plate of detachment. Dotted where concealed
-  STRIKE AND DIP OF BEDDING
-  STRIKE AND DIP OF FOLIATION
Primary igneous
-  Mylonitic -- Showing trend and plunge of mylonitic lineation

- Qa ALLUVIUM (HOLOCENE)
- QTa OLDER ALLUVIUM (PLEISTOCENE AND PLIOCENE)
- Tb BASALT (MIOCENE)
- Tgf GRANITE-CLAST FANGLOMERATE (MIOCENE)
- Tgnf GNEISS-CLAST FANGLOMERATE (MIOCENE)
- Tps PEACH SPRINGS TUFF (MIOCENE)
- Tv VOLCANIC ROCKS (MIOCENE AND OLIGOCENE?)
- Kg TWO-MICA GRANITE (CRETACEOUS)
- Kpg PORPHYRITIC GRANODIORITE (CRETACEOUS)
- Kgd BIOTITE-HORNBLLENDE GRANODIORITE (CRETACEOUS)
- Yg GRANITE (PROTEROZOIC Y)
- Xmgm MYLONITIZED GNEISS (PROTEROZOIC X)
- Xgn GNEISS (PROTEROZOIC X)

Figure 11. Geologic map showing field-trip route in lower Trampas Wash, Chemehuevi Mountains (Chemehuevi Peak and Castle Rock 7-1/2' quads) (from John, 1986; plate 1).

beyond **STOP 11** are hanging-wall granites above the Mohave Wash fault; on the right are footwall gneisses. Where Trampas Wash broadens, the rocks on the NE are undeformed capping Quaternary gravels.

Beyond **STOP 11** 1.4 mi turn right at road intersection, and proceed upstream (Figure 11). In 1.1 mi, the fault on the left (S) is a steep segment of the Mohave Wash fault that juxtaposes light-colored granitic rocks in the hanging wall against footwall Proterozoic gneisses. The route is in these gneisses for 2.6 mi to **STOP 12**. This heterogeneous package of rocks includes augen gneiss, layered gneiss, leucocratic migmatite, hornblendite, biotitite, and pods of amphibolite. As you approach the Chemehuevi Mountains plutonic suite (continuing upstream), notice the increase in volume of undeformed leucocratic aplite and pegmatite material.

After 1.7 mi, the light-brown outcrops on the right are porphyritic biotite granodiorite above the Mohave Wash fault, along the floor of the Chemehuevi Mountains plutonic suite.

Stop 12

Park at the mouth of the small wash on your left for a foot traverse S up the wash. The traverse takes 2-1/2 hours and requires a few-hundred-foot climb (take water). The purpose of this stop is to walk through the roof and floor of the lower and upper sill-like intrusions of the Chemehuevi Mountains plutonic suite (Figure 11) and to look at the relationships between the deformed country-rock gneisses, the plutonic suite, and the Tertiary detachment faults. The first half of the traverse is progressively upsection through parts of the two gently tilted concordant intrusions and intervening Proterozoic gneisses (Figure 8).

The traverse begins in undeformed, light-gray porphyritic biotite granodiorite, cut by numerous pegmatite dikes. The first 0.6 mi is along the upper part or roof of the lower concordant intrusion. Proceed up the wash and cross the contact into moderate- to shallow-dipping heterogeneous Proterozoic gneisses. Locally these rocks bear a mylonitic foliation and ENE-trending stretching lineation. The majority of these rocks have undergone relatively low-strain deformation in the Mesozoic. The Proterozoic layering and fabric is still preserved, but was reoriented to its present shallow dip during Mesozoic deformation and was subsequently intruded by the plutonic suite. The porphyritic granodiorite is cut by thin (up to 1 m) high-strain ductile shear zones, which represent the extent of ductile deformation related to Tertiary extension exposed in the range.

Continue up the wash through the narrow water-worn exposures. Note that the igneous foliation, defined by biotite-rich selvages, segregations of mafic and felsic minerals, and the alignment of K-feldspar megacrysts, roughly parallels the gneissic foliation. The whole sequence is cut by late aplite and pegmatite dikes. The concentration of the aplite and pegmatite dikes and the coarse grain size of the megacrysts (up to 3-5 cm) suggest that the magma in this lower sill was quite rich in volatiles near its roof.

At the head (NW) of the waterwashed exposures, pass back into moderately to gently WSW-dipping Proterozoic gneisses. They form a large septum or screen between the two intrusive bodies (Figure 8). The lower sill apparently intruded into the reoriented gneisses. The upper one intruded at the margin and spread out laterally along the interface between subhorizontally and subvertically foliated gneisses. The gneisses project as a floor under the main upper intrusion of the Chemehuevi Mountains plutonic suite (Figure 8).

Continue up the wash about 0.1 mi to good exposures of the Proterozoic gneisses (SW-dipping). As the wash begins to narrow, turn up a small stream on the right and follow it N to the ridge top, passing through Proterozoic gneisses and thin intrusions of subequigranular biotite granodiorite. From the saddle, the leucocratic phases of the concentrically zoned Chemehuevi Mountains plutonic suite can be seen to the N. The dark red-brown slope-covering material at 10 o'clock is

11-12 Ma basalt that intrudes and fuses cataclasites associated with the Chemehuevi detachment fault.

Descend the hill to the wash below, walking through biotite granodiorite and mafic (dark) and dacite and rhyolite (light) dikes. Exposures in the stream bed show examples of the numerous, brittle mineralized microfaults associated with extensional deformation. Keep left and contour around the side of the small hill cut by two dark-weathering dikes, to exposures of the upper porphyritic biotite granodiorite and good examples of Indian petroglyphs. Continue downstream. The granitic rocks are cut by numerous subhorizontal and subvertical ductile shear zones--evidence of the limited Tertiary ductile deformation.

Downstream beyond the abrupt turn (90°) NE, continue 0.2 to 0.3 mi. Exposures of the Mohave Wash fault can be reached by climbing up along the low ridge on the north side of the wash. There the fault dips gently N and is characterized by altered and brecciated two-mica granite against Proterozoic gneiss.

The parking place is down the main wash and 0.1 mi to the E on the jeep trail.

To reach **STOP 13**, retrace the jeep trail 3.4 mi to the road intersection in Trampas Wash, and continue straight 0.2 mi to the E, toward the red rocks.

Stop 13

This stop is to examine Tertiary deposits and the Chemehuevi detachment fault on which they rest, and requires a half-mile walk to the NW. Walk up the major gully to the left (N), keeping left. The traverse is through Miocene alluvial-fan deposits dipping 55°-60° to the SW above the Chemehuevi detachment fault (Figure 9). The deposits are high in the deformed Miocene section (Figure 10) and are made up predominantly of granitic clasts derived from the Chemehuevi Mountains plutonic suite. Uncommon clasts of chloritically altered breccia show that the source area exposed faults of the detachment system, denuded from moderate crustal levels. Sedimentation, faulting, and tilting evidently continued even as other faults were denuded.

Continue up the gully to irregular deep red-brown exposures of the Chemehuevi detachment fault. Footwall rocks are hydrothermally altered Proterozoic gneisses. The fan deposits in the hanging wall are cut by numerous steep faults. To the SW are light-gray undeformed Quaternary gravels, capping the tilted Miocene section. This is one of the easternmost exposures of the Chemehuevi detachment fault. The fault at this stop dips 10° SE and projects under the massive Mohave Mountains allochthon off toward the SE. The fault describes an eroded antiform between here and **STOP 10** on the west side of the Chemehuevi Mountains.

Highlights Between Stop 13 and Needles

Turn right up the N fork of Trampas Wash and retrace the jeep trail route back past **STOPS 11, 10, and 9** (Figure 9). At 11.8 mi beyond **STOP 13** (0.9 mi before reaching U.S. 95) is a distant view ahead of a light-colored Cretaceous(?) plutonic mass intruding dark porphyritic anorogenic granite (1.4 Ga) in the southern Sacramento Mountains. The Cretaceous(?) body resembles rocks of the Chemehuevi Mountains plutonic suite but has hypabyssal textures at the contact. It may be a translated cupola. In another 0.9 mi turn right onto U.S. 95 and return 14.6 mi to Needles.

FOURTH DAY

This day describes mylonites and detachments on the east side of the Chemehuevi Mountains, including features that can be reached by boat on the Colorado River in scenic Topock Gorge. A traverse eastward to the Mohave Mountains allows examination of a tilt block that exposes a thick section of Proterozoic crust and sheeted Miocene dikes.

Leave Needles on I-40 eastbound (S) toward Kingman. Roadcuts 10 mi S are through fine-grained clastics of the Pliocene Bouse Formation, deposited in an estuary at about the time the Gulf of California formed.

Beyond Needles (10.9 mi) take the Park Moabi exit. At the stop sign, turn right and follow the graded gravel road. At the junction 0.3 mi ahead, keep left. Continue straight (toward the mountains) another 0.5 mi ahead. The high ridge at 10 o'clock is Whale Mountain, underlain by steeply foliated mylonitic rocks that bear a NE-trending subhorizontal stretching lineation. Beyond I-40 1.2 mi, keep right on the main road, and enter the Bureau of Reclamation "Bat Cave Wash" riprap quarry. In another 0.5 mi, cross the gently N-dipping Mohave Wash fault. An outcrop on the right exposes cataclasites associated with this lower detachment fault. Hanging-wall rocks are mylonitic, porphyritic quartz-poor biotite-hornblende granite of the Whale Mountain sequence. The footwall is composed of subhorizontally foliated Proterozoic gneiss. Keep right, out of the main quarry area, to the mouth of the wash (12.7 mi beyond Needles).

Stop 14

The purpose of this stop is to walk through gneisses strongly mylonitized during late Mesozoic deformation (Figure 8). The deformation reoriented, if not largely obliterated, preexisting fabrics. Rocks with the low-angle mylonitic foliation and NE-trending stretching lineation are intruded by the Chemehuevi Mountains plutonic suite. Walk 0.3 mi up the wash through outcrops of very heterogeneous, foliated and lineated Proterozoic gneiss, and thin (up to 1 to 2 m) metaluminous to peraluminous sheetlike intrusions.

Route Between Stops 14 and 15

Boat trips can be arranged to reach **STOPS 15** and **16**. To reach boats at the Park Moabi Marina, retrace route back to Park Moabi overpass (1.9 mi), cross over I-40, and continue 0.7 mi, straight through roadcuts of the Bouse Formation and keeping right to the marina. **STOP 15** is 4 mi by boat downstream of the I-40 bridge along the Colorado River in Topock Gorge.

Stop 15

The purpose of this stop is to view an exposure of the Devils Elbow fault, which lies structurally above the Chemehuevi and Mohave Wash detachments. From the west river bank, walk up the main wash toward the W and SW 0.5 mi. At the stream fork keep left and follow the burro trail 0.3 mi over the low saddle through Colorado River gravels that unconformably overlie altered and fractured granitic rocks in the hanging wall to the Chemehuevi detachment fault. Red rocks on the E are altered Tertiary volcanic rocks and interstratified alluvial fan deposits above the Devils Elbow fault. The Devils Elbow fault at this exposure dips roughly 35°, with slickenside striae plunging 33° down-dip.

Stop 16

STOP 16 is Picture Rock on the east side of the Colorado River downstream by boat another 4.8 mi through Topock Gorge. The gorge is cut through steeply SW-dipping Tertiary volcanic and sedimentary rocks, cut by numerous high-angle and low-angle faults. The Tertiary section lies nonconformably above thick sections of light-colored Proterozoic crystalline rocks, all structurally above the Chemehuevi and Devils Elbow faults. The Peach Springs Tuff forms prominent hogbacks along both sides of the river. Return to the Park Moabi Marina.

Drive back to I-40 from Park Moabi and turn E onto I-40. Cross the Colorado River and enter Arizona (Mountain Time zone); on the right at 3 o'clock are dark-red SW-dipping Miocene alluvial-fan deposits above the Chemehuevi detachment fault. The footwall is composed of hydrothermally altered and brecciated mylonitized gneisses like those in Bat Cave Wash. The Chemehuevi detachment fault makes a major bend in its orientation, from N-dipping along the northern range front to E-dipping along the Colorado River. This bend defines the nose to a NE-plunging antiformal corrugation of the Chemehuevi fault, unroofed as an erosional surface and nicely expressed by the slope west of the river.

Ahead on the right, the Needles Mountains, after which the town of Needles was named, are made of tilted rocks above the Chemehuevi and Devils Elbow faults. Straight ahead are the distant Hualapai Mountains, a large untilted block of Proterozoic rocks beyond the eastern margin of the extensional corridor. Toward the left (N) in the Black Mountains, basalts cap a sequence of tilted lower Miocene rocks including the Peach Springs Tuff. The conical peak on the left is Boundary Cone, a Miocene rhyolite neck. Just beyond it is the historic town of Oatman and the Oatman gold-silver-mining district.

In Arizona 9.6 mi beyond the Colorado River, take exit 9 and turn right (S) on Arizona 95 toward Lake Havasu City. Ahead to the S the high Mohave Mountains expose a giant tilt block. To the E (left), distant low hills are the Buck Mountains, another large tilt block of Proterozoic gneiss capped by steeply dipping Tertiary strata. The gneisses there describe a large fold cut by Middle Proterozoic diabase sheets (Howard and others, 1982a).

South of I-40 4.1 mi, volcanic rocks 1/2 mi to the W (right) of the road dip steeply SW. The most prominent unit is olivine basalt from which M. A. Pernokas obtained an age (K-Ar, whole-rock) of 14.1 Ma (Nielson, 1986), one of the younger dates on highly tilted rocks in the region.

The distant light-colored peak to the W (right) is Powell Peak, made of allochthonous biotite granodiorite believed to be transported from part of the Chemehuevi Mountains plutonic suite. Powell Peak lies above the projected Chemehuevi and Devils Elbow faults and below the Powell Peak detachment fault. Roadcuts of broken Proterozoic gneiss are along the highway, and hogbacks of Tertiary volcanic rocks are on either side, in blocks upper-plate to the Powell Peak detachment fault. The Powell Peak fault is believed to project over the high Mohave Mountains to the SE and correlate with the Crossman Peak detachment fault, which projects over the same mountains on their S side.

Nine miles south of I-40 are prominent pinnacles on the E side of Arizona 95, remnants of a rhyolite dike dated by M. A. Pernokas (Nielson, 1986) at 16.2 Ma (K-Ar, plagioclase). West of the road are tilted blocks of Tertiary rocks nonconformably on Proterozoic rocks. The dipping cap rock is the Peach Springs Tuff. **STOP 17** is 11.0 mi beyond I-40, where cars may be parked on a spur road that leads W toward a radio tower.

Stop 17

The hill surmounted by the radio tower 0.3 mi W is in the Peach Springs Tuff and provides views of the detachment terrane in the Mohave, Chemehuevi, and Whipple Mountains. The Peach Springs here has large pumice blocks and prominent blue sanidine.

The hill is in one of a series of tilt blocks that occupy a synformal trough in the upper plate of the Powell Peak detachment. That fault dips 35° W toward us at Powell Peak, to the N. The NE-trending trough is 4 km wide between Powell Peak and the high Mohave Mountains block, to the SE. The upper-plate tilt blocks in this trough face SW and are shingled on NE-dipping faults. Several of the tilt blocks are asymmetric synclines (Nielson, 1986) with short SW limbs

attributed to fault drag and long NE limbs reflecting "reverse drag" (block tilt). Sub-Tertiary basement rocks above and below the Powell Peak detachment are unmylonitized Proterozoic rocks cut by Cretaceous granite and granodiorite.

The high Mohave Mountains to the SE represent a large upended tilt block (Howard and others, 1982a) of Proterozoic gneiss overlain by Tertiary strata and volcanic rocks (now subvertical) and cut by Tertiary dikes (now NE-dipping). Gently dipping siliceous volcanic rocks in the foreground (N of Lake Havasu City) unconformably overlie steeply tilted rocks in this block, and have yielded K-Ar dates of 18 and 19.8 Ma (Nielson, 1986).

Highlights Between Stops 17 and 18

Proceed S 6.9 mi on U.S. 95 to Lake Havasu City. Turn left (E) onto Kiowa Blvd. (17.9 mi S of I-40), go 4.2 mi, and turn left (E) onto Bison Blvd., continuing past the end of pavement. Red hills on the left (N) are made of Miocene rhyolite dipping steeply SW. East beyond Kiowa 1.6 mi, Tertiary andesite exposed in the gully on the left (N), and Proterozoic gneiss in the red hill ahead on the left, mark the approximate position of the nonconformity, which here is totally obscured by Miocene silicic intrusions. Elsewhere along this contact basal Tertiary tuffs and locally derived arkose are vertical.

One mile ahead to the E in the Mohave Mountains can be seen a mass of light-colored hills formed by wall-to-wall Tertiary dikes. Individual dikes are visible in the high ridge of the Mohave Mountains beyond, cutting Proterozoic gneiss.

Beyond Kiowa 2.0 mi veer left (NE) down into Fall Springs Wash and follow the main road up it 0.9 mi to **STOP 18**. Light-colored dacite dikes and darker mafic dikes exposed along the wash intrude gray Early Proterozoic granodiorite augen gneiss.

Stop 18

This stop is in the sheeted Miocene dikes. Mullion structures on a dike surface beside the road are likely primary flow structures; they plunge gently now, but would restore to a steep plunge if the Mohave Mountains block were rotated to its pre-Miocene orientation. Mineral K-Ar ages on dacite dikes in this range are 18-21 Ma (Light and others, 1983; Nielson, 1986). Nakata (1982) measured 15-20 volume percent of dikes across the whole Mohave Mountains block, and found that most dikes dip moderately NE. This orientation and intrusive relations into the tilted Tertiary section suggest that most of the dike swarm may be less rotated than the vertical Tertiary strata (and the gneisses) and that intrusion may have occurred while the block was undergoing its rotation.

Continue 2.3 mi up Fall Springs Wash, keeping left, past dikes and intervening screens of Proterozoic amphibolite and leucocratic gneiss.

Stop 19

The purpose of this stop is to examine Proterozoic gneiss in the tilt block and to discuss implications of the tilt block for the Tertiary detachment geology and for the nature of the pre-Tertiary crust.

Proterozoic spotted leucocratic gneiss with granulitic texture and pseudomorphs of retrograded garnet is one of the most distinctive rocks of the Mohave Mountains. Gneiss and amphibolite commonly strike NE and dip steeply. Amphibolite bodies define the limbs and nose of a SW-plunging antiformal isocline that stretches across much of the width of the Mohave Mountains block. The fold restores to a NE plunge before block tilting (Howard and others, 1982a) and conforms to Proterozoic trends elsewhere in the SW that are typically NE-SW.

Return a total of 9.3 mi back along Fall Springs Wash, Bison Blvd., and right on Kiowa Blvd. to stop sign at Lake

Havasu Blvd. (one block east of Arizona 95). Turn S (left) 4 mi.

Stop 20

Parking may be found on the right where the road veers E oblique from the highway in the SE part of Lake Havasu City. The purpose of this stop is to examine megabreccia interpreted as a Miocene gravity glide or landslide. It forms a mass of broken crystalline rocks several kilometers long, and is exposed also along Arizona 95. A NE direction of gliding for the megabreccia, over post-Peach Springs Tuff Miocene sandstone, is indicated in the Aubrey Hills S of here by basal striae and nearby subadjacent drag folds. The megabreccia ranges in structure from chaotic to intact. Pre-brecciation intrusive igneous relations are commonly preserved, even where fracturing is intense. Mylonitic two-mica granite gneiss in the megabreccia suggests an unroofed lower-plate source below the Whipple Mountains detachment fault in the western Whipple Mountains.

Backtrack N to the nearest left turn onto Arizona 95, turn left, and return to Phoenix.

REFERENCES CITED

- Allen, C.M., 1986, Rb-Sr pseudochron; the result of mixing in a reversely zoned, calc-alkaline pluton, Turtle Mountains, SE California: Geological Society of America Abstracts with Programs, v. 18, p. 81.
- Anderson, J.L., 1983, Proterozoic anorogenic granite plutonism of North America, in Medaris, L.G., Jr., and others, eds., Proterozoic geology; selected papers from an international Proterozoic symposium: Geological Society of America Memoir 161, p. 133-154.
- Armstrong, R.L., and Suppe, J., 1973, Potassium-argon geochronology of Mesozoic igneous rocks in Nevada, Utah, and southern California: Geological Society of America Bulletin, v. 84, p. 1375-1391.
- Bender, E.E., and Miller, C.F., 1987, Petrology of the Fenner gneiss, a major Proterozoic metaplutonic unit in the eastern Mojave Desert, California: Geological Society of America Abstracts with Programs, v. 19, p. 358.
- Bennett, V., and DePaolo, D.J., 1984, The distribution of 2.0-2.3 b.y. neodymium model-age rocks in the western United States: Geological Society of America Abstracts with Programs, v. 16, p. 442.
- Brown, H.J., 1984, Correlation of metamorphosed Paleozoic strata of the southeastern Mojave Desert region, California and Arizona; discussion: Geological Society of America Bulletin, v. 95, p. 1482-1485.
- Burchfiel, B.C., and Davis, G.A., 1981, Mojave Desert and environs, in Ernst, W.G., ed., The geotectonic development of California, Rubey volume 1: Englewood Cliffs, N.J., Prentice-Hall Inc., p. 217-252.
- Davis, G.A., Anderson, J.L., Frost, E.G., and Shackelford, T.J., 1980, Mylonitization and detachment faulting in the Whipple-Buckskin-Rawhide Mountains terrane, southeastern California and western Arizona, in Crittenden, M.D., Jr., and others, eds., Cordilleran metamorphic core complexes: Geological Society of America Memoir 153, p. 79-129.
- Davis, G.A., Anderson, J.L., Martin, D.L., Krummenacher, D., Frost, E.G., and Armstrong, R.L., 1982, Geologic and geochronologic relations in the lower plate of the Whipple detachment fault, Whipple Mountains, southeastern California; a progress report, in Frost, E.G., and Martin, D.L., eds., Mesozoic-Cenozoic tectonic evolution of the Colorado River region, California, Arizona, and Nevada: San Diego, Cordilleran Publishers, p. 408-432.
- Davis, G.A., and Lister, G.S., 1987, Detachment faulting in continental extension; perspectives from the southwestern U.S. Cordillera: John Rodgers symposium volume, Geological Society of America Memoir (in press).

- Davis, G.A., Lister, G.S., and Reynolds, S.J., 1986, Structural evolution of the Whipple and South Mountain shear zones, southwestern United States: *Geology*, v. 14, p. 7-10.
- Fitzgibbon, T.T., and Howard, K.A., 1987, Tectonic significance of Middle Proterozoic diabase sheets in southeastern California and Arizona: *Geological Society of America Abstracts with Programs*, v. 19, n. 6, p. 377.
- Frost, E.G., and Okaya, D.A., 1986, Application of seismic reflection profiles to tectonic analysis in mineral exploration, in Beatty, B., and Wilkinson, P.A.K., eds., *Frontiers in geology and ore deposits of Arizona and the Southwest: Arizona Geological Society Digest*, v. 16, p. 137-152.
- Glazner, A.F., Nielson, J.E., Howard, K.A., and Miller, D.M., 1986, Correlation of the Peach Springs Tuff, a large-volume Miocene ignimbrite sheet in California and Arizona: *Geology*, v. 14, p. 840-843.
- Gusa, Sharon, Nielson, J.E., and Howard, K.A., 1987, Heavy mineral suites confirm wide distribution of the Peach Springs Tuff, California and Arizona, USA: *Journal of Volcanology and Geothermal Resources* (in press).
- Hamilton, W.B., 1982, Structural evolution of the Big Maria Mountains, southeastern Riverside County, southeastern California, in Frost, E.G., and Martin, D.L., eds., *Mesozoic-Cenozoic tectonic evolution of the Colorado River region, California, Arizona, and Nevada*: San Diego, Cordilleran Publishers, p. 1-27.
- Hamilton, W., and Myers, W.B., 1967, The nature of batholiths: U.S. Geological Survey Professional Paper 554-C, 30 p.
- Hammond, J.G., 1986, Geochemistry and petrogenesis of Proterozoic diabase in the southern Death Valley region of California: *Contributions to Mineralogy and Petrology*, v. 93, p. 312-321.
- Harding, L.E., and Coney, P.J., 1985, The geology of the McCoy Mountains Formation, southeastern California and southwestern Arizona: *Geological Society of America Bulletin*, v. 96, p. 755-769.
- Haxel, G.B., Tosdal, R.M., May, D.J., and Wright, J.E., 1984, Latest Cretaceous and early Tertiary orogenesis in south-central Arizona; thrust faulting, regional metamorphism, and granitic plutonism: *Geological Society of America Bulletin*, v. 95, p. 631-653.
- Hazzard, J.C., and Dosch, E.F., 1937, Archean rocks in the Old Woman and Piute Mountains, San Bernardino County, California: *Geological Society of America Proceedings* 1936, p. 308-309.
- Hileman, G.E., Miller, C.F., and Knoll, M.A., 1987, Middle Tertiary structure of the Old Woman Mountains region, southeastern California: *Geological Society of America Abstracts with Programs*, v. 19 (in press).
- Hoisch, T.D., Miller, C.F., Heizler, M.T., Harrison, T.M., and Stoddard, E.F., 1987, Late Cretaceous regional metamorphism in southeastern California, in Ernst, W.G., ed., *Metamorphism and crustal evolution in the western Cordillera, conterminous United States*, Rubey volume 7: Englewood Cliffs, New Jersey, Prentice-Hall Inc. (in press).
- Horringa, E.D., 1986, Mesozoic tectonism in the northern Kilbeck Hills, southeastern California: *Geological Society of America Abstracts with Programs*, v. 18, p. 118.
- Howard, K.A., Goodge, J.W., and John, B.E., 1982a, Detached crystalline rocks of the Mohave, Buck and Bill Williams Mountains, western Arizona, in Frost, E.G., and Martin, D.L., eds., *Mesozoic-Cenozoic tectonic evolution of the Colorado River region, California, Arizona, and Nevada*: San Diego, Cordilleran Publishers, p. 377-390.
- Howard, K.A., and John, B.E., 1983, Geologic map of the Sheep Hole-Cadiz Wilderness Study Area (CDCA-305), San Bernardino County, California: U.S. Geological Survey Misc. Field Studies Map MF-1615-A, scale 1:62,500.
- _____ 1987, Crustal extension along a rooted system of low-angle normal faults; Colorado River extensional corridor, California and Arizona, in Coward, M.D., and others, eds., *Continental extensional tectonics: Geological Society of London Special Publication*, p. 299-311 (in press).
- Howard, K.A., Miller, C.F., and Stone, P., 1980, Mesozoic thrusting in the eastern Mojave Desert, California: *Geological Society of America Abstracts with Programs*, v. 12, p. 112.
- Howard, K.A., Nielson-Pike, J.E., Simpson, R.W., Hazlett, R.W., Alminas, H.V., Nakata, J.K., and McDonnell, J.R., Jr., 1987, Mineral resources of the Turtle Mountains Wilderness Study Area, San Bernardino County, California: U.S. Geological Survey Bulletin (in press).
- Howard, K.A., Stone, P., Pernokas, M.A., and Marvin, R.F., 1982b, Geologic and geochronologic reconnaissance of the Turtle Mountains area, California; west border of the Whipple detachment terrane, in Frost, E.G., and Martin, D.L., eds., *Mesozoic-Cenozoic tectonic evolution of the Colorado River region, California, Arizona, and Nevada*: San Diego, Cordilleran Publishers, p. 341-354.
- John, B.E., 1981, Reconnaissance study of Mesozoic plutonic rocks in the Mojave Desert region, in Howard, K.A., and others, eds., *Tectonic framework of the Mojave and Sonoran Deserts, California and Arizona*: U.S. Geological Survey Open-File Report 81-503, p. 48-50.
- _____ 1982, Geologic framework of the Chemehuevi Mountains, southeastern California, in Frost, E.G. and Martin, D.L., eds., *Mesozoic-Cenozoic tectonic evolution of the Colorado River region, California, Arizona, and Nevada*: San Diego, Cordilleran Publishers, p. 317-325.
- _____ 1986, Structural and intrusive history of the Chemehuevi Mountains area, southeastern California and western Arizona [Ph.D. thesis]: Santa Barbara, University of California, 295 p.
- _____ 1987, Geometry and evolution of a midcrustal extensional fault system; Chemehuevi Mountains, southeastern California, in Coward, M.D., and others, eds., *Continental extensional tectonics: Geological Society of London Special Publication*, p. 313-335 (in press).
- Knoll, M.A., 1985, The early Miocene geologic history of the Old Woman Mountains area, eastern Mojave Desert, California [M.S. thesis]: Nashville, Vanderbilt University, 186 p.
- Knoll, M.A., Harrison, T.M., Miller, C.F., Howard, K.A., Duddy, I.R., and Miller, D.S., 1985, Pre-Peach Springs Tuff (18 m.y.) unroofing of the Old Woman Mountains crystalline complex, southeastern California; implications for Tertiary extensional tectonics: *Geological Society of America Abstracts with Programs*, v. 17, p. 365.
- Leach, B.R., 1986, Petrology and depositional history of Miocene nonmarine sedimentary rocks, central Sacramento Mountains, San Bernardino County, California: *Geological Society of America Abstracts with Programs*, v. 18, p. 126.
- Light, T.D., Pike, J.E., Howard, K.A., McDonnell, J.R., Sompson, R.W., Raines, G.L., Knox, R.D., Wilshire, H.G., and Pernokas, M.A., 1983, Mineral resource potential map of the Crossman Peak Wilderness Study Area (5-7B), Mohave County, Arizona: U.S. Geological Survey Miscellaneous Field Studies Map MF-1602-A, scale 1:48,000.
- Lucchitta, I., and Suneson, N., 1981, Comment and reply on 'Tertiary tectonic denudation of a Mesozoic-early Tertiary(?) gneiss complex, Rawhide Mountains, western Arizona': *Geology*, v. 9, p. 50-52.
- McClelland, W.C., 1982, Structural geology of the central Sacramento Mountains, San Bernardino County, California, in Frost, E.G., and Martin, D.L., eds., *Mesozoic-Cenozoic tectonic evolution of the Colorado River region, California, Arizona, and Nevada*: San Diego, Cordilleran Publishers, p. 401-406.
- Miller, C.F., Bennett, V., Wooden, J.L., Soloman, G.C., Wright, J.E., and Hurst, R.E., 1984, Origin of the composite metaluminous/peraluminous Old Woman-Piute batholith, SE California; isotopic constraints: *Geological*

- Society of America Abstracts with Programs, v. 16, p. 596.
- Miller, C.F., and Bradfish, L.J., 1980, An inner Cordilleran belt of muscovite-bearing plutons: *Geology*, v. 8, p. 412-416.
- Miller, C.F., Howard, K.A., and Hoisch, T.D., 1982, Mesozoic thrusting, metamorphism, and plutonism, Old Woman-Piute Range, southeastern California: in Frost, E.G., and Martin, D.L., eds., *Mesozoic-Cenozoic tectonic evolution of the Colorado River region, California, Arizona, and Nevada*: San Diego, Cordilleran Publishers, p. 561-581.
- Miller, C.F., and Stoddard, E.F., 1981, The role of manganese in the paragenesis of magmatic garnet; an example from the Old Woman-Piute Range, California: *Journal of Geology*, v. 89, p. 233-246.
- Miller, D.M., Howard, K.A., and Anderson, J.L., 1981, Mylonitic gneiss related to emplacement of a Cretaceous batholith, Iron Mountains, southern California, in Howard, K.A., and others, eds., *Tectonic framework of the Mojave and Sonoran Deserts*: U.S. Geological Survey Open-File Report 81-503, p. 73-75.
- Miller, J.M.G., and John, B.E., 1986, Sedimentology and tectonic significance of Miocene sedimentary rocks, Chemehuevi Mountains, E. California: *Geological Society of America Abstracts with Programs*, v. 18, p. 158.
- Miller, J.S., Hazlett, R.W., Knoll, M.A., and Miller, C.F., 1987, Petrology and geochemistry of Tertiary volcanics in the Old Woman Mountains region, southeastern Mojave Desert, California: *Geological Society of America Abstracts with Programs*, v. 19, p. 433.
- Mittlefehldt, D.W., and Miller, C.F., 1983, Geochemistry of Sweetwater Wash pluton, California: Implications for "anomalous" trace element behavior during differentiation of felsic magmas: *Geochimica et Cosmochimica Acta*, v. 47, p. 109-124.
- Nakata, J.K., 1982, Preliminary report on diking events in the Mohave Mountains, Arizona, in Frost, E.G., and Martin, D.L., eds., *Mesozoic-Cenozoic tectonic evolution of the Colorado River region, California, Arizona, and Nevada*: San Diego, Cordilleran Publishers, p. 85-90.
- Nielson, J.E., 1986, Miocene stratigraphy of the Mohave Mountains, Arizona, and correlation with adjacent ranges, in *Cenozoic stratigraphy, structure, and mineralization in the Mojave Desert*: Geological Society of America Cordilleran Section, 82nd Annual Meeting, Guidebook and Volume, Trips 5 and 6, p. 15-24.
- Nielson, J.E., and Glazner, A.F., 1986, Introduction and road log, in *Cenozoic stratigraphy, structure, and mineralization in the Mojave Desert*: Geological Society of America Cordilleran Section, 82nd Annual Meeting, Guidebook and Volume, Trips 5 and 6, p. 1-8.
- Nielson, J.E., and Turner, R.D., 1986, Miocene rocks of the northern Turtle Mountains, San Bernardino County, California, in *Cenozoic stratigraphy, structure, and mineralization in the Mojave Desert*: Geological Society of America Cordilleran Section, 82nd Annual Meeting, Guidebook and Volume, Trips 5 and 6, p. 25-32.
- Sparkes, A.K., 1981, Petrology of the East Piute pluton [M.S. thesis]: Nashville, Vanderbilt University, 119 p.
- Spencer, J.E., 1985, Miocene low-angle normal faulting and dike emplacement, Homer Mountains and surrounding areas, southeastern California and southernmost Nevada: *Geological Society of America Bulletin*, v. 96, p. 1140-1155.
- Staudé, J.-M.G., and Miller, C.F., 1987, Lower crustal xenoliths from a Tertiary composite dike, Piute Mountains, SE California: *Geological Society of America Abstracts with Programs*, v. 19, p. 454.
- Stone, P., Howard, K.A., and Hamilton, W., 1983, Correlation of metamorphosed Paleozoic strata of the southeastern Mojave Desert region, California and Arizona: *Geological Society of America Bulletin*, v. 94, p. 1135-1147.
- _____, 1984, Reply to Discussion on 'Correlation of metamorphosed Paleozoic strata of the southeastern Mojave Desert region, California and Arizona' by H.J. Brown: *Geological Society of America Bulletin*, v. 95, p. 1485-1486.
- U.S. Geological Survey, 1981, Aeromagnetic map of the Needles 1° x 2° quadrangle, California and Arizona: U.S. Geological Survey Open-File Report 81-85, scale 1:250,000.
- Wells, R.E., and Hillhouse, J.W., 1986, Paleomagnetism of the Peach Springs Tuff and correlative outcrops from Barstow, California, to the Colorado Plateau: *Geological Society of America Abstracts with Programs*, v. 18, p. 421.
- Wernicke, B., 1981, Low-angle normal faults in the Basin and Range province; nappe tectonics in an extending orogen: *Nature*, v. 291, p. 645-646.
- _____, 1985, Uniform-sense simple shear of the continental lithosphere: *Canadian Journal of Earth Science*, v. 22, p. 108-125.
- Wooden, J., Miller, D., and Elliott, G., 1986a, Early Proterozoic geology of the northern New York Mountains, southeastern California: *Geological Society of America Abstracts with Programs*, v. 18, p. 424.
- Wooden, J., Stacey, J., Howard, K., and Miller, D., 1986b, Crustal evolution in southeastern California: *Geological Society of America Abstracts with Programs*, v. 18, p. 200.
- Wright, J.E., Anderson, J.L., and Davis, G.A., 1986, Timing of plutonism, mylonitization, and decompression in a metamorphic core complex, Whipple Mountains, California: *Geological Society of America Abstracts with Programs*, v. 18, p. 201.

Miocene Extension, Volcanism, and Sedimentation in the Eastern Basin and Range Province, Southern Nevada

Eugene I. Smith
Department of Geoscience
University of Nevada
Las Vegas, Nevada 89154

R. Ernest Anderson
U.S. Geological Survey
Denver Federal Center
Denver, Colorado 80225

Robert G. Bohannon
Branch of Pacific Marine Geology
U.S. Geological Survey
Menlo Park, California 94025

Gary Axen
Department of Geology
Northern Arizona University
Flagstaff, Arizona 86011

The Basin and Range Province in southern Nevada provides the opportunity to observe a diverse array of structures that formed during regional extension, as well as the products of coeval volcanism and sedimentation. This trip will emphasize the structural evolution of the eastern margin of the Basin and Range Province, the volcanic history, geochemistry and petrology of mid-Tertiary volcanic rocks, and the nature of the boundary between the Basin and Range and the Colorado Plateau. The first day of the trip is devoted to mid-Miocene detachment structures and the relationship of these structures to late Mesozoic thrust faults in the Beaver Dam Mountains, Tule Springs Hills, and East Mormon Mountains. During the second day, strike-slip faults, detachment structures, and the stratigraphy of coeval mid-Miocene sedimentary rocks will be observed in the Muddy and northern Black Mountains. The last day the trip will concentrate on the stratigraphy of volcanic centers in the River Mountains and at Hoover Dam, and on a mid-Miocene detachment fault on Saddle Island in the eastern River Mountains.

INTRODUCTION

Day 1-Tule Springs Hills and Beaver Dam Mountains
(R.E. Anderson and Gary Axen)

The Beaver Dam Mountains are east of the eastern limit of thrusting of the Sevier thrust belt. They are separated from the Colorado Plateau by a 45-km-wide, slightly faulted and mildly extended to unextended structural block situated between the northerly projection of the Grand Wash fault and the

Hurricane fault (Figure 1). The Beaver Dams are part of a major uplift that forms the footwall breakaway zone of a large, late Tertiary detachment-fault system whose upper plate moved to the southwest and west. The uplift is marked by topographic highs of exposed Precambrian rocks that swing southwestward from the Beaver Dams through the Virgin and South Virgin Mountains. We interpret the uplift as a rebound response to late Cenozoic tectonic unloading by detachment faulting. An alternative interpretation of the uplift as an anticline that formed during late Mesozoic compressional deformation was advanced by Hintze (1986). Phanerozoic rocks throughout the South Virgins are structurally attenuated. Whether or not this extension reflects late Cenozoic southwestward and westward withdrawal of the structurally elevated rocks from beneath the unextended terrane to the east is not known.

The detachment fault is corrugated parallel to a southwest-trending kinematic axis at three scales: (1) Broad warps with 15-30-km wavelengths, (2) sharp undulations with 1-2-km wavelengths superimposed on the broad warps [stop 4], and (3) outcrop-scale corrugations [stop 5]. The kinematic axis is inferred from the down-plunge trend of the corrugations and from a study of the geometry of faults and fault slip along the detachment [stop 3]. This axis is consistent with paleostress axes computed from fault-slip data gathered from basin-fill sediments of Pliocene(?) age to the west [stop 1] and from Mesozoic rocks on the northeast flank of the uplifted Beaver Dam Mountains block.

The detachment fault system is buried beneath sediments of the Virgin River basin where parts of it

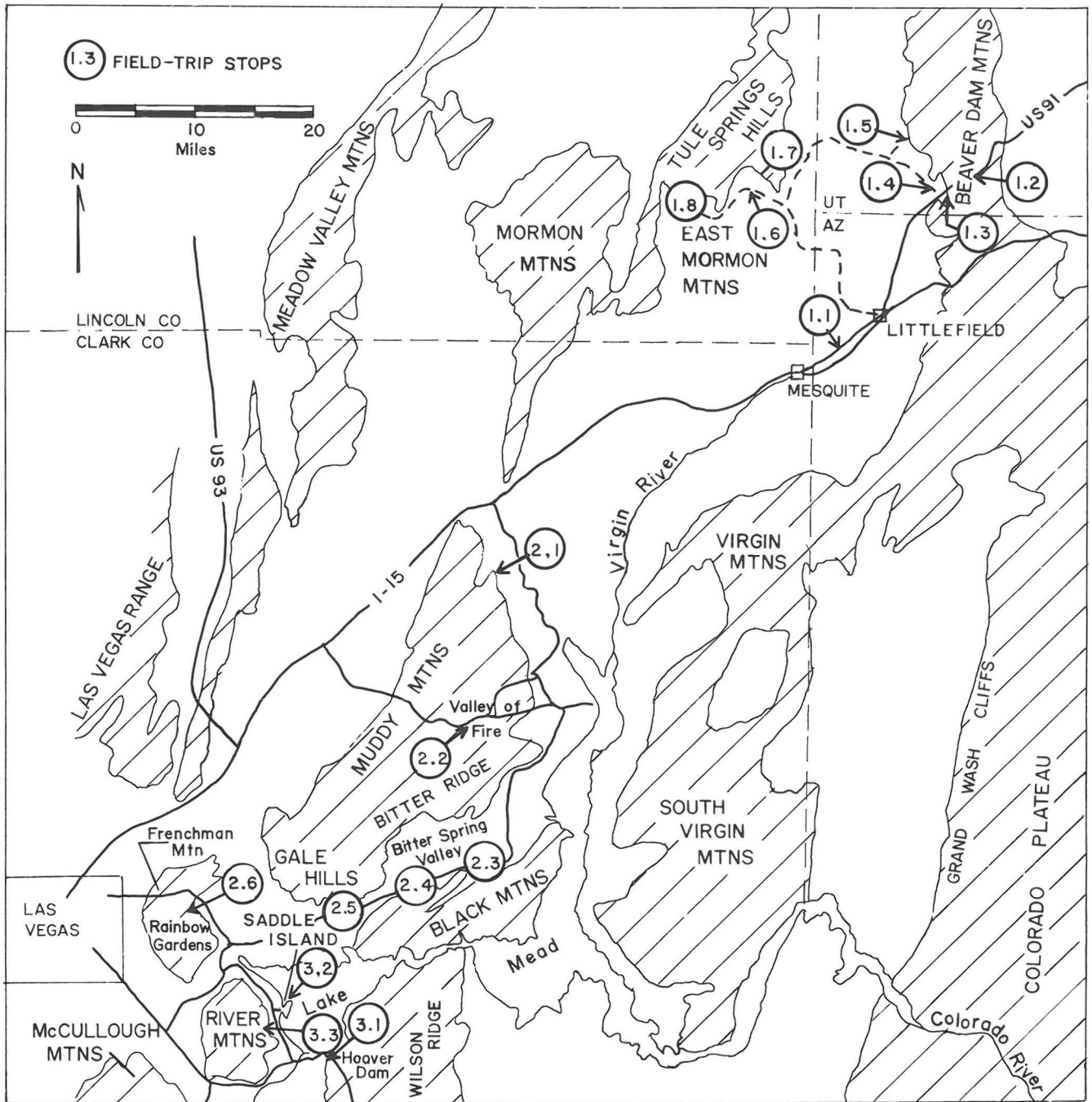


Figure 1. Index map of southern Nevada and adjacent areas showing the field-trip route and location of stops.

have been imaged on reflection seismic profiles. Fortunately, major components of the system are exposed north of the basin in the Tule Springs Hills and Mormon Mountains where extensive studies reveal many details of the geometry and mechanics of extensional deformation.

The Tule Springs Hills are a broad series of northerly trending low ridges situated between the East Mormon and Beaver Dam Mountains (Figure 1). They contain the easternmost exposures at that latitude of a major thrust of the Sevier thrust belt (the Tule Springs thrust). The Tule Springs thrust carried a

sequence of Middle Cambrian to Pennsylvanian carbonate rocks of transitional miogeoclinal facies eastward above a Colorado Plateau (cratonic) sequence ranging in age from Permian to Jurassic (Figures 2 and 3). Parautochthonous thrust slivers of Permian redbeds, Kaibab/Toroweap Limestone, and Moenkopi Formation are common along the thrust.

In the western Tule Springs Hills, there is a zone of thrust imbrications of units 3 and 4 of the Banded Mountain Member of the Bonanza King Formation (Figure 3). Because a similar imbricate thrust zone

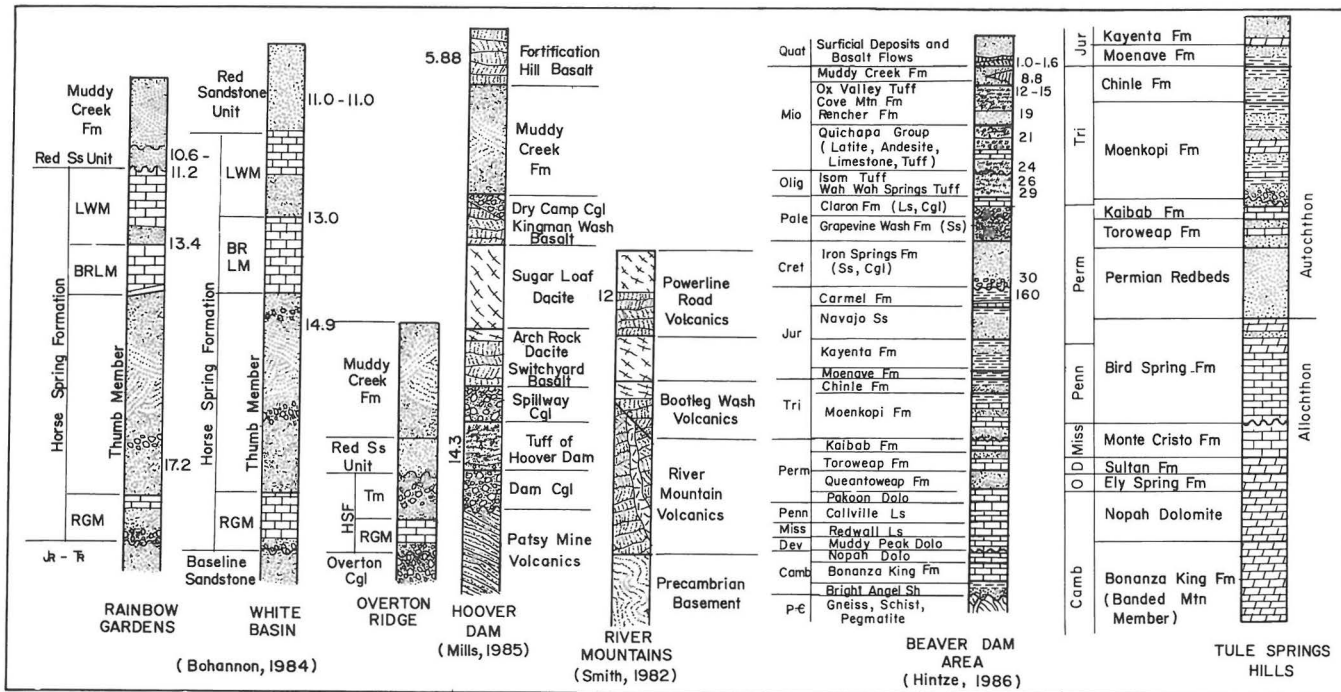


Figure 2. Stratigraphic nomenclature and lithology.

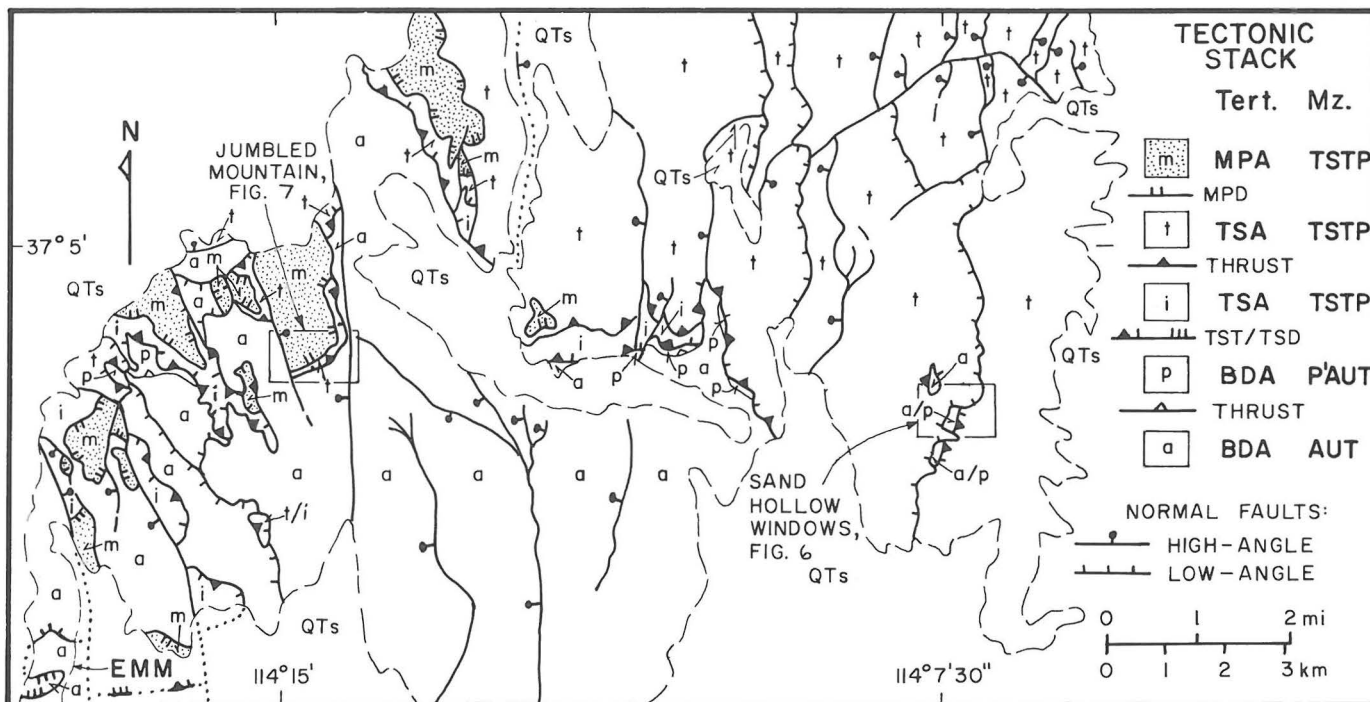


Figure 3. Tectonic map of the Tule Springs Hills and northeasternmost East Mormon Mountains (EMM). Units are based primarily on the stacking order at the end of the Sevier Orogeny: a = autochthon (AUT) to Tule Springs thrust (TST), p = parautochthonous (P'AUT) thrust slivers (Permian-Triassic), i = imbricate thrusts in the upper plate of the TST (Cambrian), t = Cambrian to Pennsylvanian strata of the Tule Springs thrust plate (TSTP), m = Mormon Peak allochthon (MPA). MPD = Mormon Peak detachment, TSD = Tule Springs detachment, TSA = Tule Springs allochthon, BDA = Beaver Dam allochthon, QTs = Quaternary and Tertiary sediments.

is present above the Mormon thrust in the northeastern Mormon Mountains (Wernicke, oral commun., 1985) above Permian redbeds, the Tule Springs thrust is correlated with the Mormon thrust.

The geology of the Tule Springs Hills is shown on the geologic map of Lincoln County (Tschanz and Pampeyan, 1970) at a scale of 1:250,000. The westernmost part was mapped by Olmore (1971) at 1:24,000 scale, but he did not differentiate Cambrian to Devonian rocks in the hanging wall of the thrust. Reconnaissance mapping by Wernicke suggested that the Tule Springs thrust was reactivated as a low-angle normal fault (Wernicke and others, 1984). For this reason, detailed geologic mapping (1:12,000 scale) was begun to determine the relation between thrusting and extension in the Tule Springs Hills. An east-west transect was mapped across the southern Tule Springs Hills and northern East Mormon Mountains (Figure 3). Initial conclusions from that mapping are presented here.

Extensional Faults of the Tule Springs Hills

Using crosscutting relations, at least three extensional episodes can be documented in the southern Tule Springs Hills transect (Figure 3). The Mormon Peak detachment (Wernicke and others, 1985) is the oldest major extensional structure. The second episode is represented by reactivation of the Tule Springs thrust as a low-angle normal fault. The youngest normal faults are steep and north trending and cut all earlier structures.

In the southwestern Tule Springs Hills are numerous klippen above the Mormon Peak detachment that places Mississippian and Devonian strata above Cambrian rocks, omitting the Ordovician and all or part of the Upper Cambrian Nopah Formation and lower Sultan Formation (Devonian). The upper-plate rocks are highly extended by listric, domino-style, and low-angle normal faults.

The Mormon Peak detachment and Mormon thrust are cut by down-to-the-west normal faults in the eastern Mormon Mountains ("eastern imbricate normal fault zone" of Wernicke and others, 1985). In the southeast Mormons, the Mormon thrust is tilted east by these faults and climbs stratigraphic section in the footwall from the Mississippian to the Bird Spring Formation. The Mormon Peak detachment is cut by similar normal faults in the southwestern Tule Springs Hills. There, however, the more easterly faults sole into the Tule Springs thrust, indicating that it was reactivated after most, if not all, of the movement on the Mormon Peak detachment had occurred. The more westerly faults cut the Tule Springs thrust also.

These relations are interpreted to indicate that the subhorizontal part of the Tule Springs thrust was reactivated as a low-angle normal fault, but the thrust ramp was not. Rather, the Tertiary detachment ramped down to the west in a position east of the older thrust ramp. West of the detachment ramp, both the Mormon Peak detachment and thrust are exposed in normal-fault-bounded blocks (of the "eastern imbricate normal fault zone") in the upper plate of the detachment. East of the detachment ramp, the detachment and Tule Springs thrust coincide. In the East Mormon Mountains, the Tule Springs detachment is the low-angle fault mapped by Olmore (1971), which places rocks as young as Pennsylvanian on crystalline basement.

Farther east in the southern Tule Springs Hills, north-trending normal faults sole into the Tule Springs thrust [Stop 7]. These faults carry a complete, albeit highly extended, stratigraphic section

from Cambrian to Pennsylvanian in their hanging walls. Locally, Tertiary volcanic rocks are involved. Because the Mormon Peak detachment omits Ordovician strata, its breakaway zone is located in the central Tule Springs Hills, west of these complete sections.

The youngest faults in the Tule Springs Hills are high-angle, north-trending normal faults with moderate displacements [Stop 8]. This set includes the steep faults that bound the East Mormon Mountains (Olmore, 1971). All faults in the area are overlapped by calichified pediment gravels. These are continuous with those of Mormon Mesa where the ancient soil is developed on beds of the Muddy Creek Formation. The gravels are incised by streams that are graded to the Virgin River, indicating that faulting in the Tule Springs Hills ended prior to formation of the Colorado River drainage network (about 4-5 Ma; Lucchitta, 1979).

Conclusions

1. Late Tertiary deformation produced several kilometers of vertical structural relief near the margin of the Colorado Plateau in areas that were little disturbed during previous episodes of compressional deformation.
2. The uplifts are probably a rebound response to tectonic stripping and westward transport of broad terranes on systems of low-angle normal faults.
3. Deformational kinematics associated with the youngest stage of the tectonic stripping are consistent with those recorded in the sediments deposited in adjacent deep basins to the west.
4. Although the Tule Springs thrust was locally reactivated as a low-angle normal fault, the reactivation was concentrated on the flat portion and the ramp was not reactivated.
5. Other low-angle normal faults or detachments did not reactivate previous thrust structures, and this is probably the most common case.
6. The order of formation of the three major detachments in the area (Mormon Peak detachment, Tule Springs thrust/detachment, and Castle Cliff detachment) was from west to east, each younger allochthon carrying the older allochthons "piggyback."

Day 2-Muddy Mountains and Rainbow Gardens (Robert G. Bohannon)

The six stops on Day 2 serve as an introduction to the stratigraphy and general tectonic significance of the region between Mesquite and Las Vegas. For a more detailed discussion of the stratigraphy and structure of this area, refer to articles by Anderson (1973) and Bohannon (1979, 1983a and b, 1984).

Muddy Mountains

The Muddy Mountains, south of the Valley of Fire (Figure 1), are formed by Paleozoic carbonate rocks in the upper plate of the Muddy Mountain thrust. This thrust is exposed in the western part of the Muddy Mountains where it places Cambrian Bonanza King Formation over Jurassic Aztec Sandstone. The large east-trending fault south of the Valley of Fire is continuous with the thrust in the western Muddy Mountains, but there is evidence of Tertiary movement on this part of the fault. Abundant high-angle normal faults that offset Tertiary beds in White Basin flatten and merge with the thrust south of the Valley of Fire. They do not cut rocks in the lower plate.

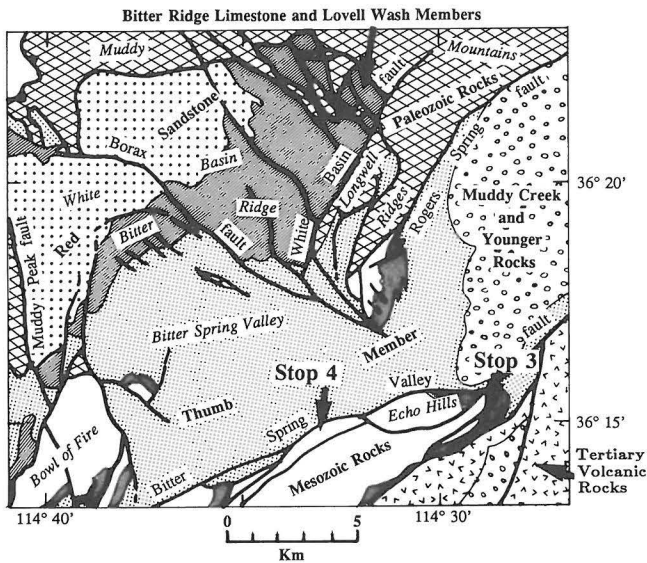


Figure 4. Simplified geologic map of the southern Muddy Mountains [stops 3 and 4]. Bitter Spring Valley fault is part of the Lake Mead fault system, which has 65 km of left slip. Contact between the allochthon and autochthon of the Muddy Mountain thrust follows the Rogers Spring fault and is exposed in the northern part of the Bowl of Fire.

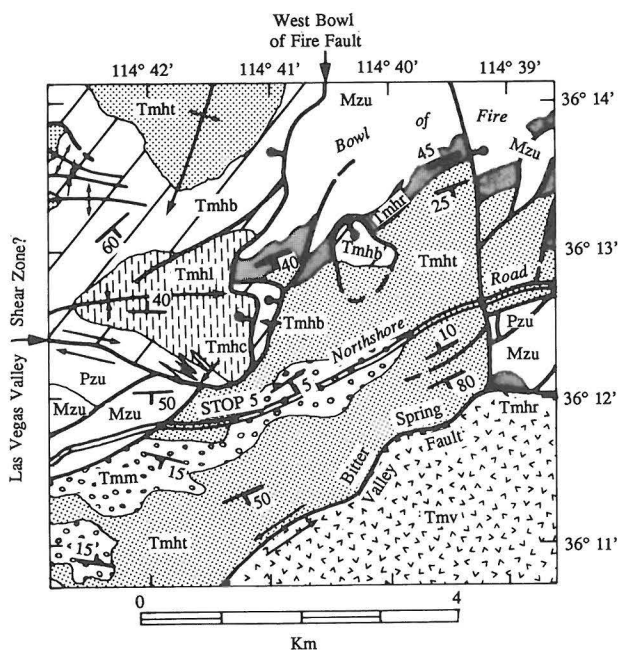


Figure 5. Simplified geologic map of the Lovell Wash area (stop 5-Day 2). Undifferentiated rocks, Pzu = Paleozoic, Mzu = Mesozoic. Horse Spring Formation: Tmhr = Rainbow Gardens Member, Tmht = Thumb Member, Tmhb = Bitter Ridge Limestone Member, Tmhl = Lovell Wash Member. Tmv = volcanic rocks. Tmm = Muddy Creek Formation.

Thus, this part of the thrust was reactivated during the Tertiary as a detachment fault with a gentle west dip.

The Rogers Spring fault forms the southeastern front of the Muddy Mountains (Figure 4). It has a steep east dip and cuts Tertiary beds that are exposed in the downthrown block to its east. Allochthonous rocks above the Muddy Mountain thrust form the Muddy Mountains west of the fault and autochthonous Mesozoic beds underlie the Tertiary strata to its east. The apparent up-to-the-east displacement of the Muddy Mountains thrust is at odds with the normal offset indicated by the Tertiary beds, so the important allochthon-autochthon relations along the fault are not explained by a simple Tertiary normal-fault solution. Tertiary strike-slip solutions are not feasible because the Rogers Spring fault ends abruptly south of East Longwell Ridge where beds of the middle Miocene Thumb Member of the Horse Spring Formation cross the fault trace unbroken (Figure 4). The Rogers Spring fault probably had a complex history, involving an early stage of tear faulting during thrusting followed by a stage of late Tertiary normal faulting.

Southwest of the Rogers Spring fault, the autochthon-allochthon contact trends west through the Bitter Spring Valley where it is buried beneath the Tertiary rocks (Figure 4). This contact is regionally significant, although it is inconspicuous here. The allochthonous rocks north of the contact are about 60 to 70 km east of any other allochthonous rocks to the south (those in the Spring Mountains). Also, a wide variety of allochthonous rock units are juxtaposed to the autochthon along the contact. Thus, it is not simply the buried trace of the Muddy Mountains thrust, which ordinarily juxtaposes Cambrian Bonanza King Formation above the thrust to Aztec Sandstone below it. There is no evidence for Tertiary displacement along the contact, so a Tertiary right-slip solution (Las Vegas Valley shear zone) will not explain the apparent east displacement of the allochthonous rocks. Royse (1983) suggested that at least part of the offset of the Sevier thrust plates might be explained by right-slip tear faulting during the late Mesozoic to Paleogene (?) thrust event. His tear-fault model explains many of the problems associated with this allochthon-autochthon contact. Las Vegas Valley Shear Zone and Lake Mead Fault System

The two principal strike-slip fault systems of southern Nevada, the left-slip Lake Mead system and the right-slip Las Vegas Valley shear zone, are possibly present in the Lovell Wash and Bowl of Fire areas (Figure 5). The Lake Mead system, south of Lovell Wash [Stop 5], continues to the southwest towards Lake Mead. The Las Vegas Valley shear zone may be represented north of Lovell Wash by a prominent fault that trends west-northwest towards Las Vegas Valley. Although the sense of displacement on this fault is poorly known, its trend is consistent with a Las Vegas Valley shear zone interpretation. The two fault systems do not actually join because the latter fault bends sharply north to become the West Bowl of Fire fault, which is a normal fault with an intermediate to shallow northwest dip (Figure 5). The west-northwest-striking fault (Las Vegas Valley shear zone?) separates Paleozoic and Mesozoic autochthonous strata on its south side from a variety of Tertiary rocks to its north near Lovell Wash. Six km west of Lovell Wash, this fault becomes a complex zone that is marked by faulted ridges of resistant Permian limestone that are sandwiched between Tertiary rocks on the north and south. This

geometry suggests strike-slip displacement.

The limestone and tuffaceous sandstone of the Bitter Ridge Limestone and Lovell Wash Members of the Horse Spring Formation undergo an abrupt facies change into conglomerate in the wash north of Lovell Wash and the Northshore Road (Figure 5). The facies change is adjacent to the Las Vegas Valley shear zone(?) near where it bends into the West Bowl of Fire fault. The oldest beds of the Muddy Creek Formation are cut and folded by the same fault, but younger Muddy Creek beds overlap it, so the shear zone was active 13 to about 9 Ma locally.

All of the Tertiary beds between the Bowl of Fire to the east and the Gale Hills to the west are folded into open, upright folds with various trends (Figure 5). These folds are localized north of the join between the two strike-slip systems. They record crustal shortening that apparently was associated with the interaction of the right- and left-slip fault systems.

Day 3-River Mountains and Hoover Dam Area (Eugene I. Smith)

The River, McCullough, and Eldorado ranges in the Lake Mead-Eldorado Valley area (LMEV) of southern Nevada (Figure 1) form part of an extensive mid-Tertiary volcanic terrane that extends into the Mojave Desert area of California and western Arizona. The LMEV area is characterized by andesite-dacite stratovolcanoes lying directly on Precambrian basement. Basalt forms shields and extensive flows but is a subordinate rock type. Rhyolite domes and flows are locally common in the McCullough and Eldorado ranges (Anderson, 1971; Smith and others, 1986). The LMEV area is unique in many respects. It is one of the few areas of the Great Basin where volcanic rocks are associated with exposed cogenetic plutons (Boulder City and Wilson Ridge). It is also unique in its lack of extensive locally derived ash-flow sheets. Only the Tuff of Hoover Dam and the McCullough Pass Tuff originated from sources in the LMEV area (Mills, 1985; Schmidt, in preparation). The Tuff of Bridge Spring, exposed in the Eldorado and McCullough ranges, probably originated in the Mojave Desert of southern California. An unnamed tuff at the base of the volcanic section in the McCullough Range may be equivalent to the Peach Springs Tuff, an ash-flow tuff that is exposed over a wide area of southern California and western Arizona (source unknown) (Young and Brennan, 1974; Glazner and others, 1986). Volcanic rocks in the LMEV area vary continuously in SiO_2 content from 50 to 70%. Basalts ($\text{SiO}_2 < 50\%$) and rhyolites ($\text{SiO}_2 > 70\%$) erupted during the waning stages of extension (post 12 Ma). Petrochemical modelling studies suggest that basalt was derived by partial melting of garnet-bearing peridotite and the more felsic rocks were formed by partial melting of a granulite or amphibolite in the lower crust.

Structurally, the LMEV area is part of a zone of major mid-Tertiary detachment faulting that extends from the Lake Mead area southward to the Whipple, Buckskin, and Rawhide Mountains (Anderson, 1971; Frost and others, 1982; Spencer, 1985). Studies of the Eldorado, River, and McCullough Mountains demonstrated that extension was important in the structural development of each range (Anderson, 1971; Bell and Smith, 1980; Smith, 1982 and 1984; Weber and Smith, 1986), and that each range was subjected to varying amounts of extension. Normal- and strike-slip faulting occurred contemporaneously in the LMEV area. Normal faulting related to the main phase of extension occurred after 13.4 Ma in the River

Mountains and after about 14.5 Ma in the Eldorado and McCullough Ranges. Strike-slip faults of the Lake Mead Fault Zone and Las Vegas Valley Shear Zone were active between 14 and 10 Ma (Anderson, 1982; Bohannon, 1984).

River Mountains and Hoover Dam

In the River Mountains a 13.5 Ma (Anderson and others, 1972) andesite-stratovolcano complex is partially surrounded by a field of dacite domes and flows. Flows of alkali-basalt dated at 12 Ma (Anderson and others, 1972) erupted from a shield volcano in the northern part of the range (Smith, 1982). Volcanic activity occurred in four pulses. Each pulse is characterized by a range of compositions from andesite to dacite. Commonly, eruptions began with the eruption of andesite flows and terminated with the eruption of dacite domes and flows; during the last pulse simultaneous eruption of andesite, dacite, and basalt occurred. Each pulse is characterized by decreasing rare-earth element (REE) content with increasing SiO_2 . This trend suggests that biotite-plagioclase-dominated fractional crystallization was important during each episode of eruption.

Units within the range are tilted to the east or southeast by west-dipping, predominately northwest-striking, high-angle normal faults. An earlier set of east-west-striking faults and dikes is truncated by northwest-striking faults. In the eastern part of the range, east-west structures are cut by west-dipping, low-angle normal faults that are in turn truncated by the northwest-trending high-angle faults. Along the steep eastern face of the range several of the northwest trending faults are down to the east. These faults dip steeply, and only locally are volcanic units tilted to the west within fault blocks. A detachment structure on Saddle Island, just to the east of the River Mountains, dips to the northwest and juxtaposes two lithologically different Precambrian terranes (Choukroune and Smith, 1985). The least principle stress axis (σ_3), based on fault-slip data, was oriented $\text{N } 80^\circ\text{E}$ during detachment, but apparently rotated to $\text{N } 40^\circ\text{E}$ during the formation of the high-angle normal faults (Choukroune and Smith, 1985).

Volcanic rocks at Hoover Dam vary in composition from andesite to dacite and display decreasing REE content with increasing SiO_2 . Geochemistry and field relationships suggest that they are more closely related to the volcanic section in the River Mountains and to the plutonic rocks of Wilson Ridge than to the Eldorado-McCullough and Boulder City sections. The Tuff of Hoover Dam (14.3 Ma) is unusual in that it displays reverse chemical and mineralogical zonation. The Tuff of Hoover Dam probably erupted from a sag-graben caldera located just to the northwest of Hoover Dam (Mills, 1985).

At Hoover Dam (Figure 1) the main phase of extension occurred after the eruption of the Tuff of Hoover Dam (Smith, 1984) at 14.3 Ma, however, faulting began earlier during Patsy Mine time (15 to 21 Ma) (Mills, 1985). Early northeast-southwest-directed extension was followed by west-northwest-east-southeast extension (Angelier and others, 1985).

Conclusions

Based on recent field work in the Lake Mead area (Smith and others, 1986; Weber and Smith, 1986) and a synthesis of previous field mapping, Weber and Smith (1987) proposed a model that suggests the following:

- 1) The River, Eldorado, and McCullough Mountains lie

- in the upper plate of a west-dipping detachment zone.
- 2) West-dipping detachment faults and the strike-slip faults of the Lake Mead Fault Zone are part of the same fault system and formed contemporaneously.
 - 3) The strike-slip faults of the Lake Mead Fault Zone represent zones of adjustment in the upper plate of a regional detachment structure that separate zones of variable extension.
 - 4) Strike-slip faults of the Lake Mead Fault Zone turn to the south in the Lake Mead area to become normal faults.
 - 5) Prior to the major phase of mid-Tertiary extensional faulting, the LMEV area was characterized by three stratovolcano complexes (River-Hoover Dam, McCullough-Eldorado, and Hamblin Cleopatra) aligned in a northeast direction above their respective subjacent plutons.

GUIDE TO STOPS--DAY 1
(R.E. Anderson and Gary Axen)

Mileage=[between stops cumulative]

[0.0 0.0] Depart toward I-15 (north) from the Post Office, Mesquite, Nevada.

[0.4 0.4] Turn right on old highway 91 (about 1/4 mile before I-15).

[5.1 5.5] Coon Creek Wash, turn left onto dirt road.

[0.7 6.2] STOP 1.

Culvert under I-15. Park, walk through culvert and about 1/4 mile up the wash to stop 1. Numerous small-displacement normal faults cut basin-fill sediments of the Muddy Creek Formation in wash cutbanks. Many fault surfaces contain slickenlines, and the displacement on some faults decreases upward. Systematic study of faulted sediments throughout the Virgin Basin area reveals early displacements that are consistent with a NE-SW minimum compressional paleostress (σ_3) and late displacements consistent with more easterly trending σ_3 . The purpose of stop 1 is to show the kinds of data that are sampled in regional fault-slip studies of weakly deformed sediments, and to discuss their significance. Turn around, return to old highway 91.

[0.5 6.7] Old highway 91, turn left.

[5.1 11.6] Stop sign, continue NW under I-15.

[1.0 12.6] Littlefield, Arizona.

[11.8 24.4] Enter Beaver Dam Mountains.

[1.2 25.6] STOP 2.

Turn around at corral and park on the west side of the highway. Stop 2 is an overview of the evidence for stratigraphic attenuation of Paleozoic rocks by brittle failure in the chaos zone of the late Cenozoic Castle Cliff detachment. Stop 2 will also serve as an orientation for stop 3. Retrace route along US 91.

[0.9 26.5] STOP 3.

Park on right. Walk up the slope south of the

highway to observe exposures of brecciated Precambrian crystalline rocks overlain by a highly attenuated sequence of fractured to brecciated Paleozoic clastic and carbonate rocks. Some key stratigraphic intervals are identifiable in the Cambrian Bonanza King and Nopah Formations allowing for thickness estimates of structurally thinned or missing parts of the sequence. The massive to thick-bedded cliff-forming rock capping the slope is the Mississippian Redwall Limestone, which generally dips eastward and is cut and repeated by several curved and planar west-dipping normal faults. These faults generally terminate downward at a major low-angle fault strand of the Castle Cliff detachment zone. The amount of stratigraphic attenuation between the Precambrian crystalline rocks and this fault strand is approximately 1.4 km. Some of the normal faults that cut the Redwall contain slickenlines that are suggestive of structural transport of hanging-wall rocks to the southwest. Return to vehicles and proceed south on US 91.

[0.4 26.9] Turn right onto graded dirt road along range front.

[2.6 29.5] STOP 4.

Overview of landslide blocks of Mississippian rocks intercalated with basin-fill sediments that probably correlate with the Muddy Creek Formation. The slide blocks and the enclosing clastic sedimentary strata (which lack clasts of Precambrian rocks) dip gently to moderately to the northeast, probably reflecting back tilting into the Castle Cliffs detachment. Road cuts and a few natural exposures reveal small-displacement striated faults that cut the basin-fill strata and may be cogenetic with tilting. The striations are generally consistent with northeast-southwest extension. Continue northwest on the dirt road.

[2.2 31.7] Turn right on road to Crazy Spring.

[1.4 33.1] Bear right at fork.

[0.3 33.4] Turn right on ungraded road up wash.

[1.2 34.6] STOP 5.

The purpose of stop 5 is to observe anomalously well-exposed Precambrian rocks in the Castle Cliffs detachment zone. Northeast of the road, a band of exposures of silicified breccia that apparently formed from Precambrian protoliths reveals some details of fault-zone fabric as well as some corrugations and striations that provide information about the late-phase motion direction on this part of the Castle Cliff detachment. These corrugations and striations are the smallest scale features suggestive of fault motions. Larger scale features and their possible kinematic significance will be discussed. Southwest of the road, a prospect pit reveals part of a thick zone of brecciated and altered Precambrian rock. On the basis of sparse exposures along the range front, these rocks are typical of those in the Castle Cliff detachment zone. They may be the unsilicified equivalent of those northeast of the road. They form the footwall block of a major strand of the Castle Cliff Detachment, which here underlies masses of Mississippian limestone. In this part of the range, the Castle Cliff detachment dips west to southwest 25 to 30 degrees, which is consistent with an interpretation of gravity data (Baer, 1986). Turn around and return to the main graded road via Crazy Spring Road.

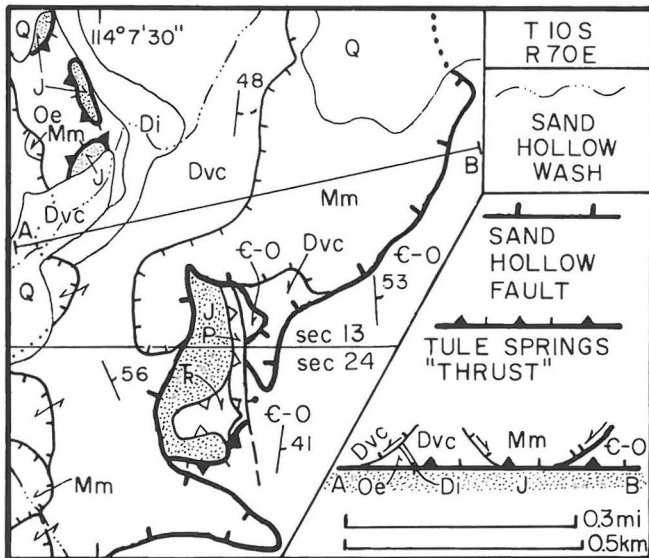


Figure 6. Geologic map of Sand Hollow windows (stop 7-Day 1). Q = Quaternary alluvium, J = Kayenta and Moenave, T = Moenkopi, P = Kaibab/Toroweap, Mm = Monte Cristo, Dvc, Di = Valentine and Crystal Pass and Iron Side Members, respectively, of the Sultan, Oe = Ely Springs, C-O = Bonanza King, Nopah and Pogonip.

- [3.3 37.9] Turn right (NW) on main dirt road.
- [3.8 41.7] Bear right at fork.
- [7.0 43.5] Bear left at fork to cross Beaver Dam Wash.
- [1.1 44.6] Turn left onto one-lane dirt road at top of hill.
- [1.9 46.5] Snow Spring Wash. Turn left and follow road across the wash.
- [5.4 51.9] Turn right onto powerline road.
- [2.9 54.8] Veer south away from powerline.
- [1.1 55.9] Sand Hollow Wash.
- [0.5 56.4] Turn right (west) at "T" onto two-lane graded road.
- [1.1 57.5] Turn right (northeast) onto powerline road.
- [0.6 58.1] Turn left onto the inconspicuous dirt track.
- [0.3 58.4] STOP 6.

The purpose of stop 6 is to present an overview of the geology of the Tule Springs Hills. Continue on the inconspicuous track.

- [1.1 59.5] STOP 7.

Stop 7 is located in Sand Hollow windows, an approximately 5-mile round-trip hike to the north across relatively smooth terrane. Reactivation of the Tule Springs thrust as a normal fault is best demonstrated in two adjacent windows in the upper Sand Hollow Wash area (Figure 6). In the eastern window, the listric, down-to-the-west Sand Hollow

normal fault merges with the thrust plane. On the east side of the window, parautochthonous slivers of the Virgin Limestone Member of the Moenkopi Formation and the Kaibab/Toroweap limestone overlie the Kayenta (?) Formation and are in turn overlain by uppermost Bonanza King Formation (Middle Cambrian). This is a fairly typical exposure of the Tule Springs thrust structural sequence. The Sand Hollow fault intersects the window on the north and south and juxtaposes highly extended Mississippian and Devonian strata above Cambrian rocks on the northeast and southeast and above the Kayenta Formation on the west. In the western window, stratigraphically lower rocks of the hanging wall of the Sand Hollow fault, lower Sultan Formation (Devonian), and Ordovician Ely Springs Dolomite overlie Kayenta Formation. Turn around and return to powerline road via the inconspicuous track.

- [0.4 60.9] Powerline road, turn right.
- [0.6 61.5] Two-lane main dirt road, turn right.

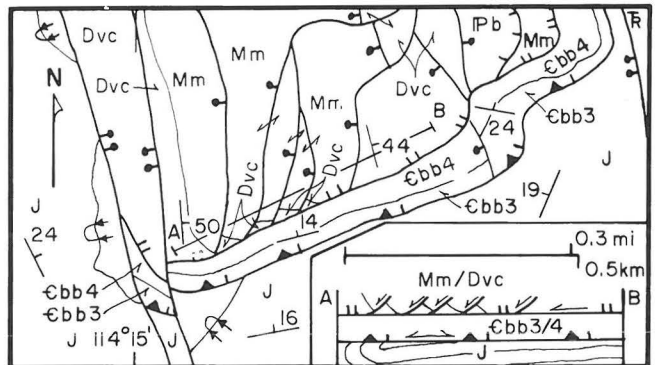


Figure 7. Geologic map of Jumbled Mountain (stop 8-Day 1). Faults and other units defined in Figures 3 and 6, except: Pb = Bird Spring, Cbb3, Cbb4 = units 3 and 4 of the Banded Mountain Member of the Bonanza King Formation.

- [10.5 72.0] STOP 8-Jumbled Mountain.

The Tule Springs thrust and Mormon Peak detachment are spectacularly exposed in section view (Figure 7) on the south-facing cliffs of Jumbled Mountain. Olmore (1971) originally mapped the relations here. At the base are redbeds of the lower Kayenta Formation, which are folded into an east-vergent overturned syncline on the west. Overlying the Kayenta Formation are flat-lying, brecciated beds of units 3 and 4 of the Banded Mountain Member of the Bonanza King Formation above the Tule Springs thrust. These Middle Cambrian beds were first transported eastward on the Tule Springs thrust system in Mesozoic time, then moved westward when the Tule Springs thrust was reactivated by faults like the Sand Hollow fault. In the flat fault contact (the Mormon Peak detachment) above the Cambrian rocks are strata of the uppermost Sultan Formation and the Mississippian Monte Cristo Limestone. These rocks are cut by many small, west-dipping normal faults, and the strata dip moderately to steeply eastward. Here, the Mormon Peak detachment omits all the Upper Cambrian and Ordovician strata, most of the Devonian on the west, and most of the Mississippian strata on the east. At the extreme west are steep east- and west-dipping normal faults, which cut both the Tule Springs thrust and Mormon Peak detachment. These faults are members of the youngest set, as is the fault that uplifted the Kaibab/Toroweap/Moenkopi ridges to the east. Turn around and return to US 91

via this well-graded dirt road.

[29.6 101.6] Turn right at intersection with old US 91.

[0.1 101.7] Turn right at ramp to I-15 south and return to Mesquite.

[8.9 110.6] Exit 122, Mesquite, return to Peppermill Motel.

GUIDE TO STOPS--DAY 2
(Robert G. Bohannon)

Geologic Highlights--Mesquite to Stop 1

Most of the bedrock in the Virgin River Valley is Muddy Creek Formation of late Miocene age. Interstate 15 crosses Mormon Mesa, where it is capped by a widespread calcrust that developed on the Muddy Creek. Calcrust once formed the entire valley floor prior to regional dissection by the Colorado River and its tributaries. Two kilometers south of the intersection on the interstate and State Highway 12, the resistant, light-colored outcrops are nonmarine limestone of the Miocene Rainbow Gardens Member of the Horse Spring Formation. Conglomerate of the Upper Cretaceous Overton Fonglomerate Member of the Baseline Sandstone underlies the resistant limestone.

Virgin Peak and Black Ridge are visible from Mormon Mesa and form the skyline south of the Virgin River. The main branch of the Lake Mead fault system is interpreted to be buried beneath Muddy Creek strata at the base of Virgin Peak and Black Ridge.

STOP 1--Abandoned Magnesite Mines at Overton Ridge

Rainbow Gardens Member (16 to 19 Ma) consists of 50 m of basal conglomerate overlain successively by 30 m of pink dolomite and 60 m of white magnesite at Overton Ridge. There is an angular unconformity between the Rainbow Gardens Member and the underlying Baseline Sandstone of Albian and Cenomanian(?) age (Fleck, 1970; Ash and Read, 1976), but the slight discordance is only evident because the Rainbow Gardens laps onto older Baseline to the south. Most of the deformation on the eastern side of the North Muddy Mountains is younger than 16 to 19 Ma.

The unconformity beneath the Rainbow Gardens Member is a regional feature that I used to reconstruct the pre-Miocene geology (Bohannon, 1984, plate 1). Stop 1 is located north of a large pre-Miocene arch. Proterozoic crystalline rocks in the core of the arch are exposed in western Arizona and in Nevada south of Lake Mead.

Proprietary drilling data from Mobil Oil and petroleum-industry seismic-reflection surveys in the Virgin River Valley east of stop 1 indicate that a thick section of Horse Spring Formation is preserved beneath the Muddy Creek Formation. These data also suggest that the Horse Spring Formation is cut by several large listric and low-angle normal faults that dip southwest and project beneath the North Muddy Mountains.

Geologic Highlights Between Stops 1 and 2

The Muddy Creek Formation is exposed in the hills south of Overton. The resistant brown outcrops at the low summit on the south end of Overton Ridge are the basal conglomerate of the Rainbow Gardens Member. Overton Mesa, west of the road, is capped by calcrust similar to that exposed on Mormon Mesa. The calcrust is formed on a thin unit of conglomerate, which is a

facies of the Muddy Creek Formation that overlies the Jurassic and Triassic Aztec Sandstone. Valley of Fire follows the axis of a large Sevier-age anticline that plunges east. The anticline is in rocks of the autochthon of the Muddy Mountains thrust of Late Cretaceous to early Tertiary(?) age (Longwell, 1949).

STOP 2-- Detachment Fault(?), Western Valley of Fire

Remnants of a regionally continuous detachment fault are exposed in the southern part of the North Muddy Mountains (Figure 8). The detachment is evident at several localities where a conglomeratic facies of the middle and late Miocene red sandstone unit dips steeply to the east above a flat contact. The contact between conglomerate and Aztec Sandstone exposed in the hill 2 km north of stop 2 may be part of this detachment fault. This contact, which has a gentle east dip, was mapped as depositional (Longwell, 1949; Bohannon, 1983b), but bedding in the conglomerate dips steeply east and conglomerate beds are truncated downward at the contact.

Large coherent blocks of Devonian and Mississippian limestone are also involved in the detachment fault terrane. One block that dips steeply east tectonically overlies the conglomerate a few kilometers to the northwest of stop 2 (Figure 8). The blocks compose all that remains of the upper plate of the Muddy Mountains thrust which once covered the Mesozoic rocks of the North Muddy Mountains. They were probably emplaced as landslides and their presence suggests high local topographic relief.

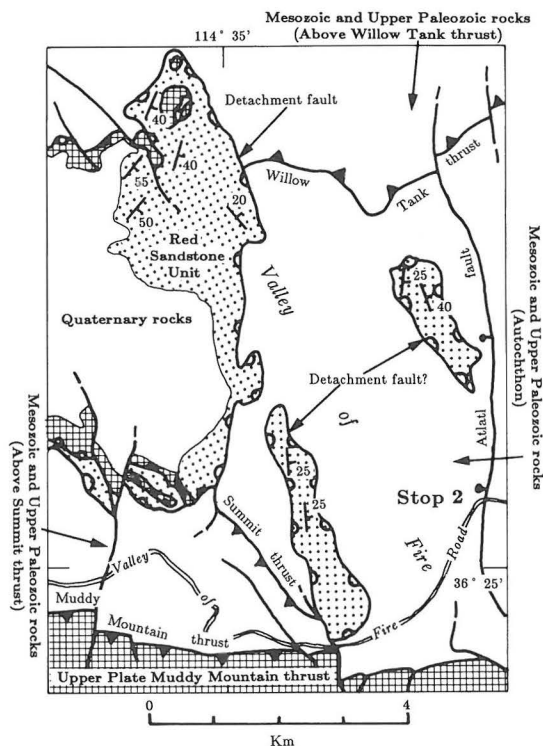


Figure 8. Simplified geologic map of the detachment fault in the southwestern Valley of Fire (modified from Bohannon, 1983a). Upper plate consists of Red Sandstone unit which dips steeply into gently dipping fault. Several blocks of Paleozoic carbonate rocks of the Muddy Mountain thrust allochthon are also involved in detachment faulting. In some places they tectonically overlie steep-dipping red sandstone.

Other remnants of the red sandstone unit are preserved in the Muddy Mountains between stop 2 and its type section in White Basin, so the unit evidently once covered most of the Muddy Mountains and a large part of the North Muddy Mountains. The Muddy and North Muddy Mountains were the site of sedimentation and extensional tectonism during middle to late Miocene time, so the present ranges must be younger features.

Geologic Highlights Between Stops 2 and 3

The Muddy Mountains to the north of the road are formed by Paleozoic carbonate rocks in the upper plate of the Muddy Mountain thrust. The Northshore Road passes just to the east of several springs that are associated with the Rogers Spring fault, a northeast-trending fault that forms the eastern front of the Muddy Mountains in this area.

STOP 3- Echo Hills Area

The Rainbow Gardens Member, south of the highway at stop 3, consists of 30 m of basal conglomerate overlain successively by 60 m of interbedded calcareous sandstone and limestone and 50 m of resistant, white, thick-bedded limestone. This section, which lies between branches of the Lake Mead fault system (LMFS), is similar to the type section of the member in Rainbow Gardens to the northwest of the LMFS system and to another in the southern Virgin Mountains to the southeast of the LMFS. The similarity of these widely separated sections, in an otherwise variable unit, supports the inferred 65-km left slip on faults of the LMFS (Anderson, 1973; Bohannon, 1979). Another exposure of the Rainbow Gardens Member, nearby in the northern Echo Hills, is distinctly different and consists of thin basal conglomerate overlain by conglomeratic sandstone and thin limestone beds in gypsum. The Bitter Spring Valley fault of the LMFS occurs between the Echo Hills and stop 3 (Figure 4).

The high, dark-colored hills southeast of stop 3 are andesite flows and flow breccias of the eastern part of the Hamblin-Cleopatra volcano (Anderson, 1973). The flows dip radially outward from a center 2.5 km east of this stop. A swarm of vertical dikes fans radially out from the same center. These features define the east-southeast half of a stratocone that is cut by the northeast-trending Hamblin Bay fault (Figure 4). The other half of the cone is about 14 km to the southwest across the fault at Hamblin Mountain (Anderson, 1973). The fault is also the contact between sedimentary and volcanic rocks 1.5 km southeast of stop 3.

Geologic Highlights between Stops 3 and 4

Most of the rocks in the Echo Hills, north of the road, are complexly faulted Kaibab, Toroweap, and Moenkopi Formations. Numerous faults, including the Bitter Spring Valley fault, cut these strata (Figure 4). Pinto Valley, southwest of the road, is floored by Triassic and Jurassic clastic rocks and Kaibab and Toroweap Formations are exposed on the ridge northwest of the valley. The trace of the Bitter Spring Valley fault is at the contact between light-colored Rainbow Gardens Member and darker volcanic and intrusive rocks (Figure 4).

STOP 4- Southern Bitter Spring Valley

The view to the north of this stop includes Bitter Spring Valley in the foreground, Bitter Ridge (light-colored ridge in the middle ground), White Basin behind Bitter Ridge, and the Muddy Mountains on the skyline (Figure 4). Bitter Spring Valley is

underlain by possibly a kilometer of well-bedded sandstone, siltstone, green tuff, conglomerate, and gypsum of the Thumb Member (14 to 16 Ma) of the Horse Spring Formation. Bitter Ridge is the type section of the Bitter Ridge Limestone Member (about 13 to 14 Ma). The Thumb in the southern part of Bitter Spring Valley is folded in several broad, open, and upright folds, but it and the Bitter Ridge Limestone dip uniformly north at Bitter Ridge.

White Basin is underlain by the Lovell Wash Member (12 to 13 Ma) of the Horse Spring Formation and by the red sandstone unit (10.6 to 11.9 Ma). The Muddy Peak and White Basin faults, two large north-trending normal faults with minimal amounts of oblique slip, bound the valley on the west and east, respectively (Figure 4), and were active 10.6 to 13 Ma.

Stop 4 is located near the trace of the left-slip Bitter Spring Valley fault of the Lake Mead fault system. This fault is marked by the northern termination of several prominent ridges of late Paleozoic to Tertiary rocks. This branch of the Lake Mead system incurred 40 km of left slip and was deformed during movement on the younger Hamblin Bay fault to the south.

Geologic Highlights Between Stops 4 and 5

The Northshore Road follows the trace of the Bitter Spring Valley fault between stops 4 and 5. The fault zone is well exposed in a small canyon southeast of the road about halfway between the stops. The nonresistant strata with vertical to overturned dips on the south side of the fault are Thumb Member and resistant Permian beds are south of the fault. The western half of the Hamblin Cleopatra volcano (Anderson, 1973) forms the ridge of dark-colored rocks on the skyline about 2 km south of the road.

STOP 5- Lovell Wash Area

The purpose of stop 5 is to discuss the relationship between the left-slip Lake Mead fault zone and the right-slip Las Vegas Valley shear zone. Both faults are probably present in the Lovell Wash and Bowl of Fire areas.

The Anniversary Mine in Lovell Wash was operated by the West End Chemical Company from 1922 to 1928 and produced 200,000 tons of crude colemanite, a hydrous, calcium borate (Longwell and others, 1965). The borate is associated with algal limestone in the Lovell Wash Member.

Geologic Highlights Between Stops 5 and 6

The basalt flows that cap Callville Mesa, south of the road, were dated at 11.3 Ma and those on Fortification Hill, across the Lake, at 10.6 Ma (Anderson and others, 1972). However, Damon and others (1978) redated the Fortification Hill flows and report an age of 5.88 Ma. The Callville Mesa flows have not been redated, but are probably equivalent to those on Fortification Hill. An age of 13.2 Ma was determined for a tilted lahar beneath the Callville Mesa flows (Anderson and others, 1972).

The low, resistant ridge of dark-gray rocks, 3 to 4 km north of the road, marks the trace of the Las Vegas Valley shear zone(?). The Lake Mead fault system takes an uncertain course to the southwest beneath the lake waters, but Weber and Smith (1987) discuss a possible geometry for it there. The nonresistant rocks along the road, chiefly Muddy Creek Formation and young volcanic and intrusive

rocks, fill the large triangular space between the two major fault systems.

STOP 6- Rainbow Gardens Area

The Rainbow Gardens Member, which is about 250 m thick here, is similar to the section at stop 3. It consists of a basal conglomerate beneath interbedded sandstone and limestone, all underlying a thick, resistant, bedded limestone unit. The member unconformably overlies successively older Mesozoic strata from north to south. At stop 6 the Rainbow Gardens Member overlies the Triassic Moenave Formation. Seven km south of the stop at Las Vegas Wash, it overlies Middle Triassic(?) Virgin Limestone Member of the Moenkopi. Bedded sandstone, siltstone, and tuff of the Thumb Member, dated at 14.8 to 16.2 Ma, conformably overlie it and include large, unsorted lenses of rapakivi granite.

The Rainbow Gardens Member dips the same as the older units at Frenchman Mountain. The tilt was generated by displacement on several normal faults that have U-shaped surface traces (open to the southeast) and outward dips. The faults form dome-shaped surfaces that plunge west-northwest. Bedding tilt decreases systematically in younger units so fault activity appears to have spanned Horse Spring to early Muddy Creek time (about 9 to 18 Ma).

GUIDE TO STOPS--DAY 3 (Eugene I. Smith)

Gold Strike Inn to Hoover Dam

Leave the Gold Strike Inn. Turn left on U.S. 93 toward Hoover Dam. For the next mile, the road follows a strike-slip fault zone that places intrusive rocks of the Boulder City Pluton against Patsy Mine aged volcanic flows and volcanoclastic units. Note the numerous fault surfaces and evidence of alteration in exposures on the north side of the highway.

A northwest-striking, east-dipping normal fault at the turn off to Lakeview Point marks the western boundary of exposures of the Tuff of Hoover Dam. This tuff is dated at 14.3 Ma and erupted from a sag-graben-caldera at Hoover Dam.

Cross Hoover Dam. Turn into parking lot No. 9. Park and walk back to the dam.

STOP 1-Hoover Dam

The purpose of stop 1 is to view the spectacular exposures of mid-Tertiary volcanic and volcanoclastic rock in Black Canyon just below Hoover Dam, and to discuss the complex volcanic and structural history of the Hoover Dam area.

Geology of Black Canyon

Three stratigraphic units are exposed on the west wall of Black Canyon (Nevada side) (Figure 2). The lowermost unit is the Dam breccia, a fanglomerate containing volcanic and plutonic clasts. Above the Dam breccia is the Tuff of Hoover Dam, and lying above the Tuff are flows of dacite (the Sugarloaf Dacite). This section is tilted approximately 30 degrees to the northeast and is cut by basalt dikes.

In the immediate vicinity of Hoover Dam the Tuff of Hoover Dam is 600 feet thick. It thins rapidly in all directions and is not exposed more than 7 km from the Dam. The Tuff is gray-brown to white in outcrop and contains phenocrysts of plagioclase, biotite, and hornblende. It displays both chemical and mineralogical zonation and is reversely zoned. It

varies from 66% SiO₂ at the top to 59% SiO₂ at its base. The total rare-earth element content decreases in a steplike fashion as SiO₂ increases. Biotite and hornblende increase in abundance upward, and clinopyroxene and plagioclase increase downward. The Sugarloaf dacite continues these trends and probably represents residual magma erupted after ash-flow eruption and caldera collapse. The Tuff commonly displays eutaxitic texture and ramplike folds. There are at least two cooling units, but flow surges followed each other quickly. Chemical data do not suggest any re-equilibration of the magma in the chamber at the time of the cooling break.

The Tuff probably erupted from a sag-graben-caldera just to the northwest of Hoover Dam. Within the sag graben, the Tuff is nearly 700 feet thick and is characterized by large xenoliths of dacite. Northwest-striking faults were active at the time of eruption of the Tuff. As a result, its eruption was controlled by normal faults bounding a northwest-trending graben or half graben. The eruption probably caused the collapse of the floor of the graben, producing a sag-graben caldera (Mills, 1985).

Volcanic units in the vicinity of the dam are rotated to the northeast by a series of northwest-striking faults down to the southwest. Stratigraphic throw is usually less than 100 m. Volcanic units dip from 20 to 65 degrees to the northeast. Old units are displaced more and dip more than younger units. The synchronous tectonic and volcanic activity is also evidenced by numerous unconformities, and by numerous beds of coarse-clastic sedimentary units that are interbedded with the volcanic section (Angelier and others, 1985; Mills, 1985).

Angelier and others (1985) described a two-stage late Cenozoic tectonic history for the Hoover Dam area. These stages are (1) strike-slip and dip-slip faulting associated with stratal tilting, and (2) post-tilt strike-slip, oblique-slip, and dip-slip faulting. During the second stage, dip-slip and strike-slip faulting may have alternated in time. These changes in fault style may be related to the switching of the stress directions (sigma 1, 2, and 3); the least principal stress axis probably rotated from N 50° E to N 75° W from stage 1 to stage 2.

Hoover Dam to Saddle Island

Cross Hoover Dam and reenter Nevada. Continue driving on U.S. 93 for 4.2 miles past the Gold Strike Inn to the Allen Bible Visitors Center (Lake Mead National Recreation Area).

The mountains to the south of the visitors center are formed by the Boulder City Pluton. The pluton appears to have two geomorphic expressions. The uppermost exposures are composed of smooth rolling hills; the lower part is composed of rugged cliffs. The contact between these terranes is nearly horizontal. Longwell and others (1965) originally interpreted this surface as the contact of altered volcanic rock (below) and a laccolith of the Boulder City quartz monzonite (above). Anderson (1969), however, suggested that the difference in appearance of the rock is due to the presence of an old paleohydrologic surface (water table). Rocks below the surface are highly altered and rocks above are relatively fresh. This surface forms a "bathtub ring" on both sides of Hemenway Wash.

Turn right on Lake Shore Drive (Highway 166).

To the left is the eroded central crater area of the River Mountains stratocone. Light-colored rocks form the River Mountains quartz monzonite stock that occupies the vent area of the volcano. The pluton is composite and is formed by fine-grained to medium-grained plagioclase-orthoclase quartz monzonite and

biotite-granite. The pluton contains many xenoliths of basalt and dolomite. Dikes of porphyritic dacite radiate from the plug. The pluton is chemically equivalent to rocks of the Wilson Ridge Pluton and may represent the detached apex of one of the Wilson Ridge Intrusions. Reddish rocks above the intrusion are altered and mineralized andesite and plutonic rock cut by numerous dacite dikes that emanate from the River Mountains stock. Alteration is primarily argillic and ferric; mineralization is characterized by barite, specular hematite, and manganese oxide. The dark rocks at the summit are andesite and dacite flows that formed on the flanks of the stratocone. This view of the River Mountains provides an excellent geologic section through the core of a mid-Tertiary volcano.

Continue driving north on Lake Shore Drive. In 4.3 miles (from the visitors center) turn left onto paved road to Southern Nevada Water System Treatment and Pumping Plant. Saddle Island lies directly ahead.

Drive 0.6 mile to the gate at the entrance to the Saddle Island causeway.

STOP 2A-Saddle Island Detachment Structure: Lower Plate Geology

After crossing the causeway, follow the gravel road to the south. Pass the Pumping Plant and stop at the first exposure on the left side (east side) of the road.

The purpose of this stop is to study the complex structural history of the lower plate of the Saddle Island detachment.

Rocks at this exposure were affected by three tectonic events. These are: (1) Subhorizontal mylonitic foliation with an east-west lineation is superimposed on Precambrian amphibolites and pegmatites of the lower plate. The foliation is gently undulating; fold axes trend east-northeast. Locally the original fabric of the rock is well preserved and the amphibolite-grade mineral assemblage (hornblende and plagioclase) is still present, but in other localities the rock is intensely deformed and mylonitic textures are dominant. In transitional rocks the mineral assemblage chlorite-epidote-sericite-plagioclase is the result of retrograde metamorphism of an amphibolite-grade protolith to the greenschist grade. Choukroune and Smith (1985), using pressure shadows and the vergence direction of overturned folds, suggested that the direction of tectonic transport of the mylonites was to the east and that they were formed during the Late Cretaceous or early Tertiary. Recent work using S-C directional criteria suggests that the direction of tectonic transport was in fact to the west. This new work reopens the possibility that the mylonites are mid-Miocene in age. (2) Mylonitic foliation is cut by subhorizontal east-west-trending fault zones that dip either to the north or south. The fault zones vary in width from an inch to 5 feet and are characterized by brittlely deformed amphibolite that is converted into a chlorite "schist." These faults break the lower plate into small lenses (3.5 to 35 m in size) that either trend parallel to the mylonitic foliation or truncate it near lens terminations. In this exposure, faults are coplanar with the mylonitic fabric. This event is Tertiary in age and is related to the formation of the detachment fault. (3) The near-horizontal fault zones are themselves cut by high-angle normal faults that are related to a second brittle deformational event (Choukroune and Smith, 1985).

STOP 2B-Saddle Island Detachment Structure: The Saddle

The purpose of this stop is to view the zone of intense shearing and the microbreccia just below the detachment fault. Hike to the saddle from the east end of the causeway.

The hike begins in weakly foliated Precambrian amphibolite cut by scattered dikes of muscovite-bearing pegmatite. In some areas the Precambrian amphibolite is weakly foliated and contains hornblende, plagioclase, and chlorite as dominant minerals. In other areas, amphibolite displays a strong near-horizontal mylonitic foliation.

Thin zones of brittle shearing are superimposed on the mylonitic fabric. In these zones, the rock develops a schistose fabric and earlier textures are rarely preserved.

The reddish rocks on the north side of the saddle are brecciated Tertiary-aged dacites that form the lowermost part of the upper plate on Saddle Island. The detachment fault is located about half way up the ridge at the color change (green rock=lower plate, red rock=upper plate). On the south side of the saddle, amphibolite displays a weak mylonitic foliation, but little evidence of brittle shearing is present. About 50 feet below the fault, amphibolite begins to show the effects of brittle shearing. As the fault is approached, the lower-plate rock progressively becomes more intensely sheared and is converted into a chlorite schist. The attitude of the brittle foliation is N 30° E (coplanar with the detachment). Notice the small-scale lenslike pattern of foliation and the boudin of quartz-feldspar rock (intensely sheared pegmatite dikes?).

Just below the fault, a black, fine-grained microbreccia is exposed. This rock displays strong ferric alteration (hematite). The microbreccia marks the uppermost part of the lower plate and represents the most intense shearing along the detachment fault. The fault itself is not exposed in the saddle. There is an excellent exposure, however, on the east side of island, just below the saddle.

STOP 2C-Saddle Island Detachment Structure: The Upper Plate

Four lithologically distinct terranes are recognized in the upper plate (Sewall, in preparation). These are: (1) Precambrian amphibolite, schist, gneiss, and granite; (2) Precambrian basement intruded by dikes and small plugs of quartz monzonite and hypabyssal dacite and diorite; (3) a Lower Cambrian section consisting of the Tapeats Sandstone, Bright Angel Shale, and Bonanza King Dolomite. These sedimentary rocks strike to the northwest and are vertical or overturned; (4) conglomerate and megabreccia of Tertiary (?) age (possibly correlative with the Rainbow Gardens Member of Horse Spring Formation) containing clasts of Paleozoic carbonate and Precambrian basement. Clasts in the megabreccia reach 10 m in size. The conglomerate is intruded by hornblende-quartz monzonite and basalt.

These terranes are apparently fault slices that are bound above and below by low-angle faults and display a reverse stratigraphic order. Precambrian rocks form the structurally highest terrane and Tertiary conglomerate forms the lowest. Geochemical data demonstrate that the intrusive rocks of Tertiary age on Saddle Island are correlative with the Wilson Ridge Pluton (to the east of Lake Mead in Arizona). Both this correlation and the structural data discussed earlier suggest that the upper plate of Saddle Island is composed of structurally bound plates formed by the unroofing of the Wilson Ridge

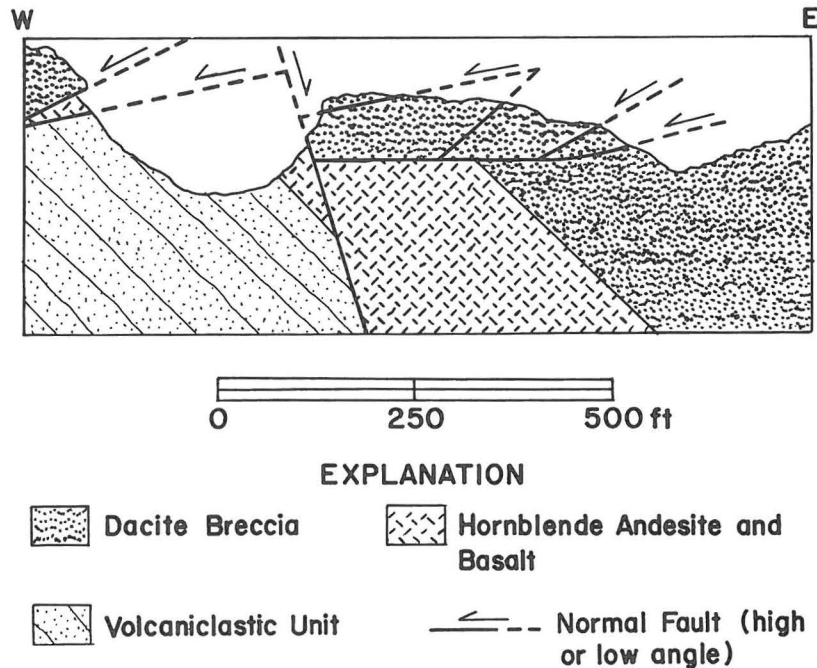


Figure 9. Geologic section across the Fault Basin, River Mountains.

Pluton. Most of these plates can be observed by walking the spine of the island to Moon Cove at the northern tip of Saddle Island.

Drive back to Lakeshore Road. Turn left on Lakeshore Road.

Saddle Island to Fault Basin

Drive 0.6 mile south on Lake Shore Drive. At the base of the incline is the turnoff to the fault basin [Stop 3].

Turn right on the gravel road to fault basin and stop 3. Drive 0.2 miles to end of road (keep left). Stop vehicles at "no motor vehicles" sign. Continue on foot up the wash into the fault basin.

STOP 3-Fault Basin

The purpose of stop 3 is to study the geology and structure of the eastern part of the River Mountains in the upper plate of the Saddle Island detachment. Along the wash that drains the fault basin a telescoped section of the Powerline Road volcanics is exposed (Figure 9). Dacite breccia derived by the explosive disruption and erosion of nearby dacite domes, bedded-volcaniclastic units, hornblende andesite, and pyroxene basalt are the important rock types.

In the fault basin, three episodes of faulting are clearly observed: (1) east-west-striking, high-angle normal faults are the oldest structures, (2) low-angle normal faults cut the high-angle structures and are in turn cut by (3) northwest-striking, high-angle normal faults. The direction of displacement of the low-angle structures can be unequivocally determined by observing S-C relationships in thin cataclasite zones beneath the fault surfaces.

The traverse begins in a wash deeply cut into pediment and fan deposits of the River Mountains. In 0.1 mile, the wash narrows and on its north side

there is a west-dipping basalt flow interbedded with dacite breccia. These units are part of the upper Powerline Road section.

Continue walking through the narrows to the first dry waterfall. At this locality, monolithological dacite breccias are exposed. The unit probably represents block-avalanche and debris-flow deposits from nearby dacite domes. Clast size varies from less than one inch to over 5 feet.

Farther up the wash are exposures of hornblende andesite of the middle Powerline Road volcanics. Hornblende orientation and weak flow banding indicate that the unit dips to the east.

Walk 50 yards to the west, then turn south (left) and climb to the small rock knob that overlooks the wash. This vantage point provides a panorama of most of the fault basin (Figure 9). Especially notice the low-angle fault on the hill to the south. Higher angle faults in the upper plate are truncated by this structure. The upper plate is composed of upper Powerline Road dacite breccia; the lower plate is formed by east-dipping upper Powerline Road dacite breccia (east side) underlain by hornblende andesite. S-C relationships (axial-plane cleavage, overturned folds) in a microbreccia just below the low-angle fault indicate that the upper plate moved to the west. The low-angle structure is cut by an east-dipping, northwest-striking, high-angle normal fault. The low-angle structure reappears approximately halfway up the escarpment that bounds the fault basin on its west side. Notice the prominent overhang produced by differential erosion along the fault. There is a thin slice of basalt between the green volcaniclastic unit and the Upper Powerline Road dacite breccia (Figure 9). The style of faulting, so nicely displayed here, reflects the structural style of the eastern River Mountains. The lower Powerline Road section is composed of light-green bedded volcaniclastic deposits having a compound origin.

Some units are debris flows, others are waterlain, and still others may be primary air-fall deposits. At the fault exposure note the S-C relationships in the microbreccia zone below the fault surface that indicate movement of the upper plate to the west.

From this vantage point above the basin, note that the green volcanoclastic unit does not crop out to the north of this location. It is faulted against basalt by an east-west-striking, north-dipping fault. This fault is entirely a lower-plate structure. A key exposure lies 5 m to the north of the adit. There, an east-west-striking, north-dipping fault is clearly cut by the low-angle structure. Striations on the high-angle fault parallel those on the low-angle structure, suggesting that it was reactivated by motion along the low-angle fault.

Return to Lake Shore Drive (Nevada Highway 166). Turn left and drive to Henderson and Las Vegas.

REFERENCES CITED

- Anderson, R.E., 1969, Notes on the geology and paleohydrogeology of the Boulder City Pluton, southern Nevada, *in* Geological Survey Research 1969: U.S. Geological Survey Professional Paper 650B, p. B35-B40.
- _____ 1971, Thin skin distension in Tertiary rocks of southeastern Nevada: Geological Society of America Bulletin, v. 82, p. 42-58.
- _____ 1973, Large-magnitude late Tertiary strike-slip faulting north of Lake Mead, Nevada: U.S. Geological Survey Professional Paper 794, 18 p.
- _____ 1982, Miocene structural history south of Lake Mead, Nevada-Arizona: Geological Society of America Abstracts with Programs, v. 14, no. 4, p. 145.
- Anderson, R.E., Longwell, C.R., Armstrong, R.L., and Marvin, R.F., 1972, Significance of K-Ar ages of Tertiary rocks from the Lake Mead region, Nevada-Arizona: Geological Society of America Bulletin, v. 83, p. 273-287.
- Angelier, Jacques, Colleta, Bernard, and Anderson, R.E., 1985, Neogene paleostress changes in the Basin and Range; a case study at Hoover Dam, Nevada-Arizona: Geological Society of America Bulletin, v. 96, p. 347-371.
- Ash, S.R., and Read, C.B., 1976, North American species of Tenskyia and their stratigraphic significance, with a section Stratigraphy and age of the Tenskyia-bearing rocks of southern Hidalgo County, New Mexico by R.A. Zeller, Jr.: U.S. Geological Survey Professional Paper 874, 42p.
- Baer, J.L., 1986, Reconnaissance gravity and magnetic survey of the northern Mesquite basin, Nevada-Utah: Utah Geological Association Publication 15, p. 109-118.
- Bell, J.W. and Smith, E.I., 1980, Geological map of the Henderson Quadrangle, Clark County, Nevada: Nevada Bureau of Mines and Geology Map 67, scale 1:24000.
- Bohannon, R.G., 1979, Strike-slip faults of the Lake Mead region of Nevada: in Armentrout, J.J., Cole, M.R., and Terbest, H., Cenozoic paleogeography of the western United States: Society of Economic Paleontologists and Mineralogists, Pacific Section, Pacific Coast Paleogeography Symposium 3, p. 129-139.
- _____ 1983a, Mesozoic and Cenozoic tectonic development of the Muddy, North Muddy, and northern Black Mountains, Clark County, Nevada, in Miller, D.M., Todd, V.R., and Howard, K.A., eds., Tectonic and Stratigraphic studies in the eastern Great Basin: Geological Society of America, Memoir 157, p. 125-148.
- _____ 1983b, Geologic map, tectonic map, and structure sections of the Muddy and northern Black Mountains, Clark County, Nevada: U.S. Geological Survey Miscellaneous Geologic Investigations Series Map I-1406, scale 1:62,500.
- _____ 1984, Nonmarine sedimentary rocks of Tertiary age in the Lake Mead Region, southeastern Nevada and northwestern Arizona: U.S. Geological Survey Professional Paper 1259, 72 p.
- Choukroune, Pierre and Smith, E.I., 1985, Detachment faulting and its relationship to older structural events on Saddle Island, River Mountains, Clark County, Nevada: Geology, v. 13, p. 421-424.
- Damon, P.E., Shafiqullah, M., and Scarborough, R.B., 1978, Revised chronology for critical stages in the evolution of the lower Colorado River: Geological Society of America, Abstracts with Programs, v. 10, no. 3, p. 101-102.
- Fleck, R.J., 1970, Tectonic style, magnitude and age of deformation in the Sevier orogenic belt in southern Nevada and eastern California: Geological Society of America Bulletin, v. 81, no. 6, p. 1705-1720.
- Frost, E.G., Cameron, T.E., and Martin, D.L., 1982, Comparisons of Mesozoic tectonics with mid-Tertiary detachment faulting in the Colorado River area, California, Arizona and Nevada: in Cooper, J.D., compiler, Geologic excursions in the California desert: Geological Society of America, Cordilleran Section meeting guidebook, p. 113-159.
- Glazner, A.F., Nielson, J.E., Howard, K.A., and Miller, D.M., 1986, Correlation of the Peach Springs Tuff, a large volume Miocene ignimbrite sheet in California and Arizona: Geology, v. 14, p. 840-843.
- Hintze, L.F., 1986, Stratigraphy and structure of the Beaver Dam Mountains, southwestern Utah: Utah Geological Association Publication 15, p. 1-36.
- Longwell, C.R., 1949, Structure of the Northern Muddy Mountain area, Nevada: Geological Society of America Bulletin, v. 60, p. 109-114.
- Longwell, C.R., Pampeyan, E.H., Bowyer, Ben and Roberts, R.J., 1965, Geology and mineral deposits of Clark County, Nevada: Nevada Bureau of Mines and Geology Bulletin 62, 218p.
- Lucchitta, Ivo, 1979, Late Cenozoic uplift of the southwestern Colorado Plateau and adjacent lower Colorado River region: Tectonophysics, v. 61, p. 63-95.
- Mills, J.G., 1985, The geology and geochemistry of volcanic and plutonic rocks in the Hoover Dam 7 1/2 quadrangle, Clark County, Nevada and Mohave County, Arizona (M.S. Thesis): Las Vegas, University of Nevada, 119 p.
- Olmore, S.D., 1971, Style and evolution of thrusts in the region of the Mormon Mountains, Nevada (Ph.D. Dissertation): Salt Lake City, University of Utah, 213 p.
- Royse, Frank, 1983, Magnitude of crustal extension in the southern Great Basin: comment: Geology, v. 11, no. 8, p. 495-496.
- Smith, E.I., 1982, Geology and geochemistry of the volcanic rocks in the River Mountains, Clark County, Nevada and comparisons with volcanic rocks in nearby areas, in Frost, E.G., and Martin, D.L., eds., Mesozoic-Cenozoic tectonic evolution of the Colorado River region, California, Arizona and Nevada: San Diego, California, Cordilleran Publishers, p. 41-54.
- _____ 1984, Geological map of the Boulder Beach Quadrangle, Nevada: Nevada Bureau of Mines and Geology Map 81, scale 1:24,000.

- Smith, E.I. and Howard, W.R., 1983, Chemical and mineralogical zonation in the late-Miocene Tuff of Bridge Spring, Eldorado Mountains, Nevada and comparison with ash-flow tuffs in nearby ranges: Geological Society of America Abstracts with Programs v. 15, no. 5, p. 391.
- Smith, E.I., Schmidt, C.S., and Weber, M.J., 1986, Mid-Tertiary volcanic rocks of the McCullough Range, Clark County, Nevada: Geological Society of America Abstracts with Programs v. 18, no. 2, p. 187.
- Spencer, J.E., 1985, Miocene low-angle normal faulting and dike emplacement, Homer Mountains and surrounding areas, southeastern California and southernmost Nevada: Geological Society of America Bulletin, v. 96, p. 1140-1155.
- Tschanz, C.M., and Pampeyan, E.H., 1970, Geology and mineral deposits of the Lincoln County, Nevada: Nevada Bureau of Mines and Geology Bulletin 73, 187 p.
- Weber, M.E. and Smith, E.I., 1986, Upper plate adjustments in the Eldorado-Saddle Island detachment structure, southern Nevada: Geological Society of America Abstracts with Programs v. 18, no. 2, p. 196.
- 1987, Structure and geochemistry; constraints on the reassembly of disrupted mid-Miocene stratovolcanoes in the Lake Mead-Eldorado Valley area of southern Nevada: Geology (in press).
- Wernicke, B.P., Guth, P.L., and Axen, G.J., 1984, Tertiary extensional tectonics in the Sevier thrust Belt, southern Nevada, in Lintz, J.P., ed., Western Geological Excursions: Guidebook, v. 4, MacKay School of Mines, Reno, Nevada, p. 473-510.
- Wernicke, B.P., Walker, J.D., and Beaufait, M.S., 1985, Structural discordance between Neogene detachments and frontal Sevier thrusts, Central Mormon Mountains, southern Nevada: Tectonics, v. 4, no. 2, p. 213-246.
- Young, R.A., and Brennan, W.J., 1974, Peach Springs Tuff: Its bearing on the structural evolution of the Colorado Plateau and development of Cenozoic drainage in Mohave County, Arizona: Geological Society of America Bulletin, v. 85, p. 83-90.

Crustal Transect: Colorado Plateau—Detachment Terrane—Salton Trough

Eric G. Frost
California Consortium for Crustal Studies
Department of Geological Sciences
University of California, Santa Barbara
Santa Barbara, California 93106

Thomas V. McEvelly
California Consortium for Crustal Studies
Earth Science Division
Lawrence Berkeley Laboratory
University of California
Berkeley, California 94720

Geoffrey S. Galvan
Phillips Petroleum Company
8055 East Tufts Avenue Parkway
Denver, Colorado 80237

Clay M. Conway
Pacific to Arizona Crustal Experiment
U.S. Geological Survey
2255 North Gemini Drive
Flagstaff, Arizona 86001

Thomas L. Heidrick
Chevron Oil Field Research Company
Post Office Box 446
La Habra, California 90633

David A. Okaya
California Consortium for Crustal Studies
Department of Geological Sciences
University of Southern California
Los Angeles, California 90089

Ernie C. Hauser
Consortium for Continental Crustal Profiling
Institute for the Study of the Continents
Snee Hall, Cornell University
Ithaca, New York 14853

Jill McCarthy and Gary S. Fuis
Pacific to Arizona Crustal Experiment
U.S. Geological Survey
345 Middlefield Road
Menlo Park, California 94025

Ronald G. Blom
Jet Propulsion Laboratory
4800 Oak Grove Drive
Pasadena, California 91109

INTRODUCTION

This trip is designed to provide its participants with an overview of the crustal-scale structure along a transect from the Colorado Plateau to the Salton Trough. Such a transect extends from stable North America across the Cordilleran orogenic belt and ends on the Pacific plate. This transect crosses multiple zones of Mesozoic deformation, magmatism, and metamorphism, all of which have been overprinted by Tertiary crustal extension. This extension and its disruption of the Mesozoic compressional deformation will be the primary focus of the field trip. As the trip crosses from the Colorado Plateau to the Transition Zone and into the detachment terrane, a crustal-scale view of detachment faulting and its relationship to the Plateau will be developed. A crustal-scale view of the continuation of this detachment terrane beneath the Mesozoic compressional deformation exposed in much of southern California will also be a primary topic of study and speculation.

This field trip is designed to integrate as many data sets as possible. The primary data sets include the field exposures of major crustal features, the CALCRUST and COCORP reflection profiles in western Arizona and southeastern California, the USGS PACE refraction surveys shot over these reflection lines, and the multitude of industry reflection lines in the Arizona and southern California regions. In addition, gravity and aeromagnetic studies, detailed studies of key outcrops, and thematic mapping satellite imagery

will be incorporated into the trip to set the stage for a three-dimensional view of the Cordilleran orogenic zone. By keying the geophysical data to outcrops and mountain ranges, the geologic reality as well as the possible ambiguity of the reflection and refraction profiles will be pursued. Such an integration of geology and geophysics seems to be one of the most promising techniques for understanding how large-scale, complex deformation actually takes place through geologic time. The authors hope that the understanding of crustal-scale geometries enhanced on this trip will, in turn, increase the understanding of complex orogenic zones elsewhere in the world.

From Phoenix, drive to Sedona for the first evening's lodging. A welcome to the field trip and introductory talks will be given at the pretrip dinner to set the stage for the transect. In the morning, begin vehicle mileage at the junction of US-89A and AZ-179, which is the main intersection in Sedona. Continue on US-89A toward West Sedona and Cottonwood. After 1.1 miles, turn left (south) onto Airport Road, then left onto Shrine Road after another 1.1 miles. Turn left into the parking lot of the Masonic temple and the Shrine of the Red Rock for an overview of the Mogollon Rim and the end of COCORP line 7.

DAY 1: COLORADO PLATEAU AND TRANSITION ZONE

Stop 1: Oak Creek Canyon Scenic Overlook

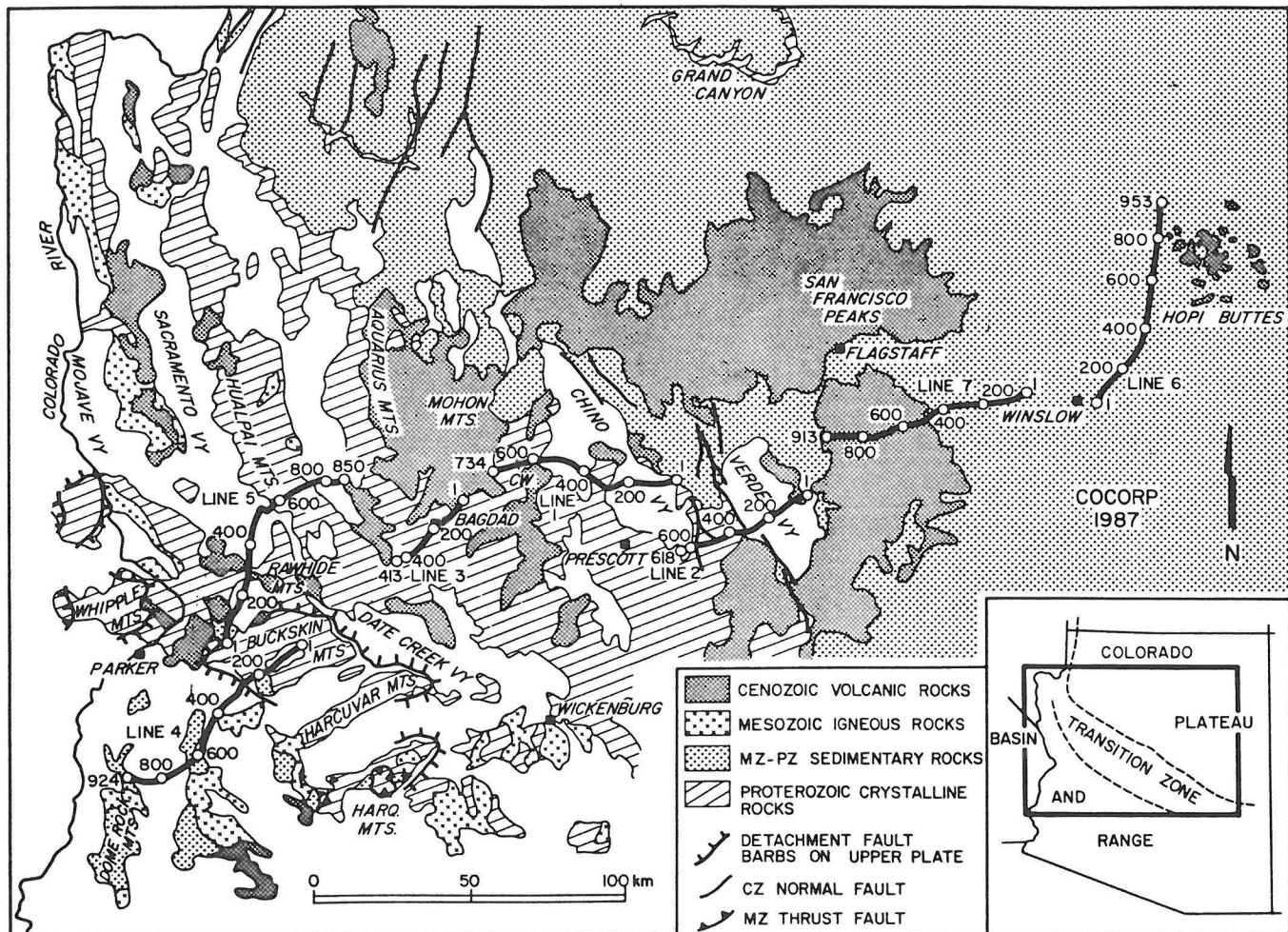


Figure 1. Shot-point and line-location map for the COCORP western Arizona survey. Area covered by the COCORP profile is also the region to be traversed on the first 2 days of this field trip. Geology generalized primarily from the Arizona state geologic map. From: Hauser and others (1987).

From this vantage point, the cliffs of the Mogollon Rim are strikingly visible, as they form the southern end of Oak Creek Canyon. The cliffs consist of the upper portion of the Paleozoic section with the Supai, Coconino, and Kaibab all prominently exposed on the northern skyline. These Paleozoic rocks were deposited on Precambrian supracrustal and granitic rocks, exposures of which can be seen on the western skyline near the town of Jerome. Above the Paleozoic cratonal section are late Tertiary black basalts, which crop out extensively on the southwestern edge of the Colorado Plateau. The nearly flat dips of the Paleozoic rocks and late Tertiary basalts exemplify the regional crustal stability of the Colorado Plateau for most of Phanerozoic time. The effects of vertical uplift are apparent from the altitude of the region, but little other deformation has visibly affected this area. The Colorado Plateau stands as the stable end member for both Mesozoic and Cenozoic deformation within this transect region.

The crustal structure of the immediate Plateau area is relatively unknown. The COCORP profile that was shot between Mormon Lake and Sedona (Figure 1) yielded little information (Hauser and others, 1986), perhaps because the Paleozoic rocks in this area are overlain by multiple basalt flows, which are visible on the cliff face just beyond the eastern edge of Sedona. Elsewhere, where industry data have been shot

in the Transition Zone, similarly poor results were commonly obtained when the vibration source was over multiple basalt flows. However, in some areas such as near Bagdad, excellent profiles were obtained by both industry and COCORP over thin accumulations of basalt.

From Stop 1, return to US-89A and continue west toward Cottonwood. At the junction with AZ-279 (after 18.7 miles from last stop), continue on US-89A. Follow the signs for US-89A through two left turns and out of Cottonwood toward Jerome. Turn right off US-89A near the edge of Jerome and follow the signs to the Jerome Historical Museum (28.5 miles from Stop 1).

Stop 2: Verde Valley, Mogollon Rim, and Precambrian Geology Overlook

As one looks east from the United Verde mine area at Jerome, the cliffs of Paleozoic rocks on the Colorado Plateau margin are clearly visible on the eastern skyline. Between these cliffs and Jerome is the Verde Valley, which formed in late Miocene time as a trap-doorlike half graben. Detailed study of some of the bounding faults for this half graben (Figure 2) has been possible because of the long-term mining-related development and mapping. The southwest boundary of the Verde Valley is composed of multiple faults that progressively drop the valley side downward. Offset on the individual faults is fairly well constrained,

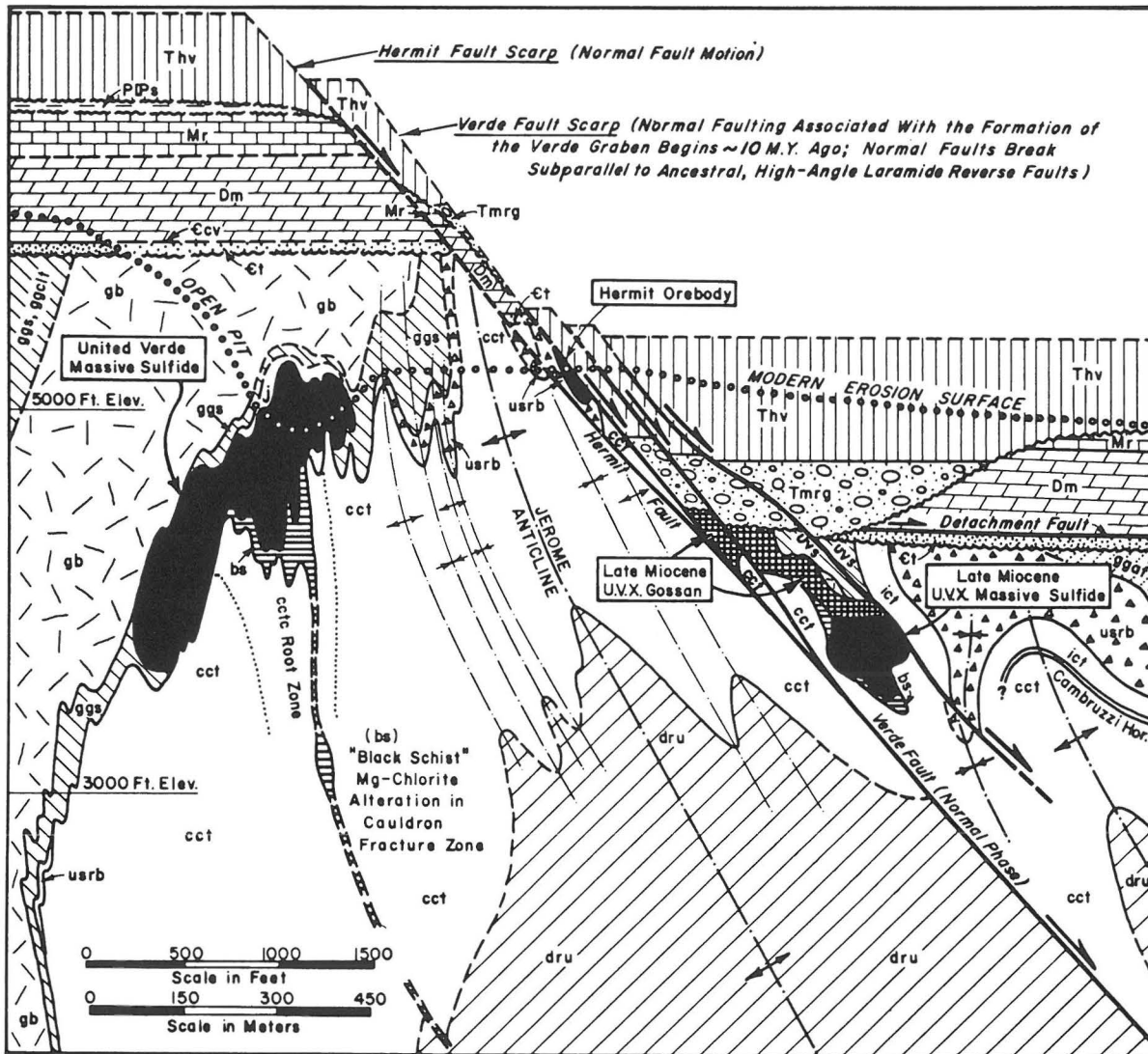


Figure 2. Cross section of the geologic relationships near Jerome, showing the steeply inclined foliation and compositional layering in the Precambrian rocks and nearly horizontal layering in the Paleozoic and Cenozoic rocks. The dip and multiple fault character of the valley-bounding structures is well known from the extensive mining and drilling in this region. From: Lindberg (1986).

with a normal fault throw of about 1900 feet on the main Verde fault. These normal faults appear to be subparallel to a Laramide-age reverse fault that lifted the eastern side up approximately 400 feet (Lindberg, 1986). One strand of the valley-bounding normal faults is visible at the southern margin of the United Verde mine and can be discontinuously traced through the town of Jerome. A model depicting the high-angle, curvilinear geometry of the faults has been constructed for the district and is displayed at the mining museum.

Seismic reflection profiles in the nearby Chino Valley help define the overall geometry of the several small basins present on the southwestern margin of the Colorado Plateau. These profiles, which were made available to CALCUST by Phillips Petroleum Company, suggest that the valleys are fairly simple half grabens in cross section, with reflections down to at least 5.0 secs. (TWT) dipping into the bounding normal faults. Late Tertiary valley fill is thickest near the present topographic lows. Reflections representing the base of the Tertiary valley fill, the Tertiary volcanic rocks, and the base of the Paleozoic

rocks are present, as are reflections within the Precambrian rocks. Offset of the middle to late Miocene (15-10 Ma) basalt flows along the normal faults has preserved the basalts below the Miocene and younger valley fill. Where the basalts can be interpreted to be present, data quality on the seismic lines is significantly reduced. COCORP profiles (Figure 1) cross directly over both Verde and Chino Valleys and show a number of reflections including subhorizontal reflections from deeper (below 5.0 secs.) in the crust (Hauser and others, 1986).

The identity of reflections below the Paleozoic-Precambrian unconformity is a source of major speculation. Exposures of Precambrian rocks, such as in the United Verde pit (Figure 2) indicate that many of the Precambrian structural and lithologic boundaries are very high angle. These boundaries would appear to be poor candidates for producing the subhorizontal reflections that characterize the region. One possibility for their identity is that they represent major low-angle thrust faults that were produced during Precambrian collisional events. Some of these imbricate thrusts are well exposed in outcrop in neighbor-

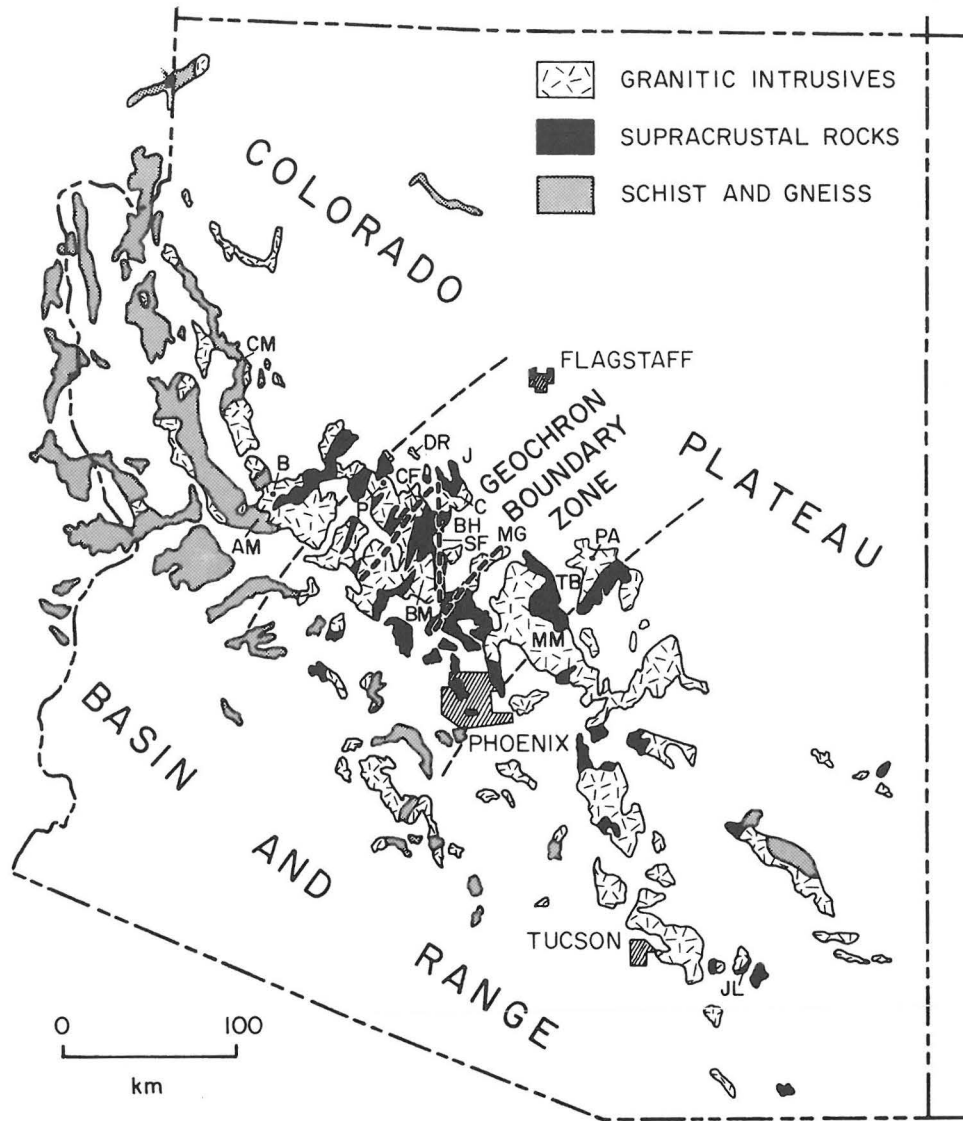


Figure 3. Map of Arizona showing 1.8 and 1.7 Ga Precambrian units into which younger (1.7 - 1.4 Ga) granitic rocks have intruded. Two age terranes, an older 1.8 - 1.7 Ga subprovince and a younger 1.7 - 1.6 Ga southern subprovince, are present and apparently traceable across most of the continent. A somewhat diffuse boundary zone separates the two terranes and may represent the boundary between a collage of Precambrian island-arc materials on the north and a terrane that is fundamentally cratonic on the south (Conway and Karlstrom, 1986). These Precambrian rocks are well exposed in the Transition Zone and probably extend for a significant distance under the Colorado Plateau as well as under the midcontinent. This combination of rock units represents the known surface geology for most of the first days traverse. This region has a distinctive seismic character as imaged on the many seismic lines in the Arizona Transition Zone. From: Conway and Karlstrom (1986).

ing ranges (Conway and Karlstrom, 1986). High-angle structures exposed in outcrop might then be the up-turned edges of some of these major thrust zones.

Another alternative is that the reflections represent the regional intrusive relationships of the many Precambrian granitic bodies into previously deformed gneiss and schist (Figure 3). The immense size of some of the exposed plutonic bodies is of sufficient magnitude to produce regionally extensive reflections. The homogeneous character and generally undeformed fabric of many of the plutonic rocks are also attractive for producing reflections when in contact with the lithologically and deformationally distinct country rocks of gneiss and schist. Intrusion of sill-like plutonic bodies into such country rocks could account for the multiple reflections with-

in the middle and upper crust of the region. Different age plutons characterize broad regions of the Transition Zone exposures, with the transect area falling along the somewhat diffuse boundary (Figure 3) between age terranes (Conway and Karlstrom, 1986). Multiple intrusion of regionally extensive plutonic bodies into a complexly layered Precambrian crust appears to be the most attractive overall cause for producing the reflections observed on seismic lines in the Transition Zone area.

From the mining museum, retrace the route back to US-89A and turn right (west) toward Prescott. If time permits on other trips, the United Verde open pit and bounding faults can be visited near the northwestern edge of town. For this trip, continue driving over the range, viewing the steeply inclined Precambrian

NW

3 KM

SE

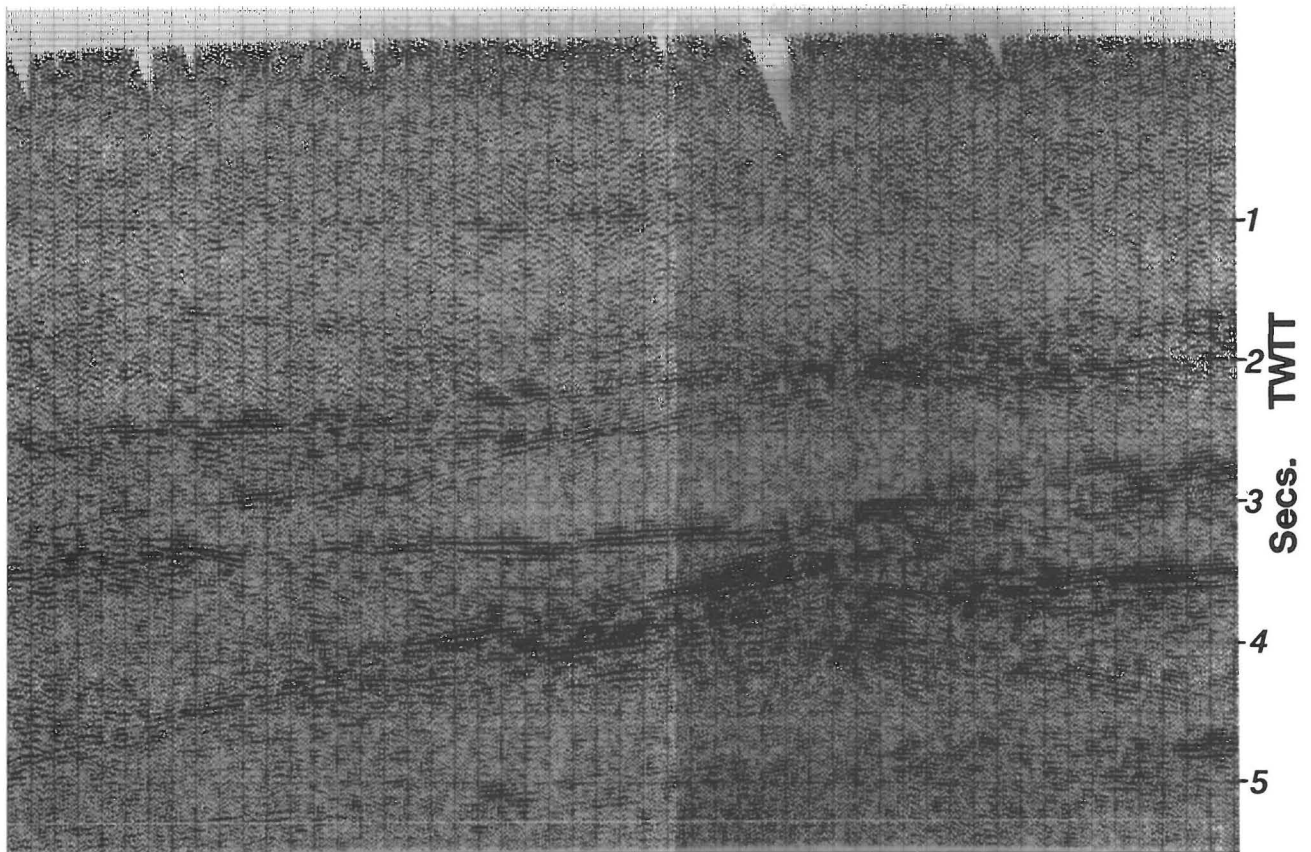


Figure 4. Industry seismic line (Phillips) northeast of Bagdad, Arizona, showing the upper-crustal structure of the Transition Zone along a NW-SE line parallel to the exposed length of the Transition Zone. The crust is composed of packages of highly reflective and nearly transparent rocks, which define broad zones that pinch and swell in three dimensions. The uppermost crust is characteristically nearly transparent, with only a few pronounced reflections. Highly reflective and transparent zones can be traced on the network of Phillips seismic lines throughout this portion of the Transition Zone. Similar reflections are imaged well on the COCORP transect in the same region.

rocks, the overlying Paleozoic sedimentary units, and capping late Tertiary basalts (Figure 2). Drive across Chino Valley to the intersection with US-89 at Entro (Granite Creek), which is 27.1 miles from Stop 2. Turn south onto US-89 toward Prescott. After 4.7 miles, turn left into Watson Lake State Park and drive to the top of the small hill to study the Precambrian granitic rocks and discuss the structure of Chino Valley.

Stop 3: Overview of Precambrian Granitic Rocks, Chino Valley, and Nearby Seismic Lines

One of the major plutonic bodies in the region crops out extensively near Prescott. This pluton is representative of the coarsely crystalline, homogeneous fabric of many of the Precambrian plutonic bodies. Intrusion of such large-scale plutonic units into already foliated gneiss and schist may be responsible for producing the alternating zones of nearly transparent fabric with highly reflective zones (Figure 4). This pattern of high-amplitude, subparallel reflections has been informally described as "railroad track" reflections, the Transition Zone reflective sequence (Galvan, 1987b), or the Bagdad reflective sequence (Hauser and others, 1987). The subparallel nature of reflections within this reflective sequence is pronounced, yet in three dimensions,

the reflections actually pinch and swell. The geometry of some of the nearly transparent zones, in particular, is suggestive of laccolithic-shaped bodies with wide centers and pinched ends in three dimensions.

From Watson Lake State Park, return to US-89 and follow it through Prescott toward Wickenburg. Precambrian granite and gneiss are visible in numerous roadcuts along the route. At the town of Kirkland Junction (27.7 miles from Stop 3), turn right (north) to Kirkland (4.4 miles). Continue north on AZ-96 for 11.7 miles to a major dirt road to the Mule Shoe and Indian Rock Ranches, a turnoff which is marked by a prominent red mailbox. The road makes a "Y" after 1.4 miles; bear left for 1.0 mile and stop at the small open field with a steel drill stem in the middle. This is the site of the Phillips Kirkland State A-1 well. The dirt road is the route along which Phillips line PW-48 (Figure 5) was shot.

Stop 4: Phillips Well Site and Network of Transition Zone Seismic Lines

The Kirkland State A-1 well was the last well drilled by Phillips Petroleum in their search for oil beneath crystalline rocks in Arizona. The exploration target for the several wells drilled by Phillips-Anchutz and partners was the interpreted presence of

NW

KIRKLAND STATE A-1 WELL

3 KM

SE

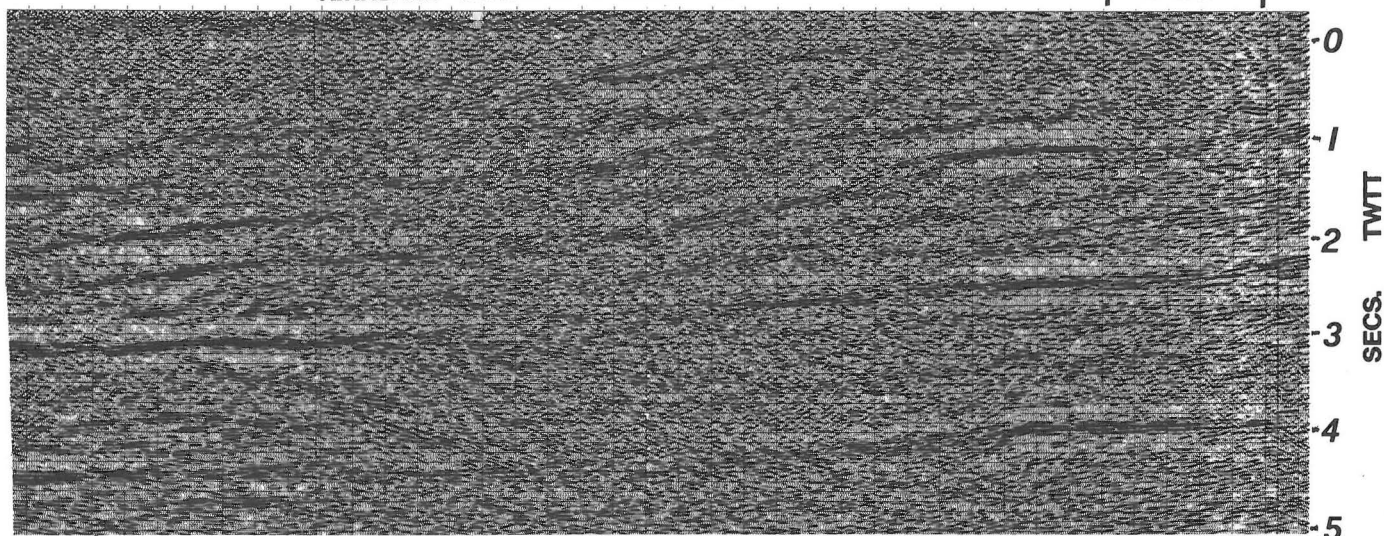


Figure 5. Migrated industry seismic line (Phillips) southeast of Bagdad, near Hillside and Kirkland, Arizona, showing the upper-crustal structure of the Arizona Transition Zone. The pronounced reflections have been informally referred to as "railroad track" reflections or the Transition Zone reflective sequence. The uppermost reflections were the target of the Kirkland State A-1 well, which was drilled by Phillips Petroleum in 1982. The well penetrated 6504 feet of granite, apparently crossing the upper two reflections before the well was abandoned. This seismic line images the structure parallel to the exposed length of the Transition Zone. A tie line oriented NE-SW images the same reflections (Galvan, 1986) dipping very gently to the northeast. These reflections continue over a very large area, forming a distinctive seismic character terrane. Extended correlation of these lines indicates the presence of lower reflections, as does the COCORP profile. Moho is sporadically imaged at about 11.0 secs. (TWT).

Paleozoic and Mesozoic sediments beneath the crystalline rocks of much of Arizona. Thrust-fault motion to displace the sedimentary rocks beneath the Precambrian rocks was interpreted to be Mesozoic in age on the basis of correlation to thrust terranes in Nevada and Utah. Precambrian rocks at the surface obviously correlated to the transparent uppermost portion of the seismic profiles. Packages of reflective rocks beneath the transparent Precambrian rocks were interpreted as imbricate stacks of Paleozoic and Mesozoic rocks. Coherent reflections between these packages (Figure 5) were then necessarily identified as thrust faults because of their older-on-younger geometry. The excellent reflections obtained in this area were interpreted as such thrust faults. Reflections in this immediate area may be of such high quality partly because the volcanic rocks are above the level of the road, and thus did not obstruct downgoing or upcoming seismic energy. Similarly good results were also obtained south of Phoenix (near Florence), where Phillips first tested the Anchutz overthrust model by drilling to a depth of 18,013 feet.

Much to the credit of Phillips Petroleum, their study of the drill core and ancillary data led to a radical reinterpretation (Reif and Robinson, 1981) of the original overthrust model for the Arizona A-1 well (Keith, 1980). Study of the seismic data, drill core, isotopic data, and regional geology led Reif and Robinson (1981) to interpret the upper-crustal geology as a stack of variably mylonitized and extended rock units. They identified compositional and age differences between the Precambrian units and matched the seismic reflections with these changes in composition and deformational fabric. Some of the reflections were interpreted as mid-Tertiary detachment faults produced by regional extension rather than compression.

The work of Reif and Robinson (1981) on the Arizona A-1 well near Florence was within the zone of metamorphic core complexes (e.g., Banks, 1980; Reynolds and Rehrig, 1980). A similar overthrust model was proposed for the Transition Zone between Kirkland and Bagdad, Arizona. The final well drilled by Phillips was spudded and completed in Precambrian granite (STOP 4) northeast of the small town of Hillside, and about 24 km southeast of Bagdad. The hole was drilled to a depth of 6504 feet (Figure 5) in an attempt to penetrate an antiformal reflection whose culmination was beneath the well site. The reflection was apparently crossed, with Precambrian rocks rather than Paleozoic and Mesozoic rocks beneath it. Drill core from near the interpreted area of the reflection, where the water was also lost, was chloritized and brittlely deformed with slickensides and striations reported from the drill cuttings (Galvan, 1986, 1987a, b).

Reinterpretation of the original model for the Transition Zone structure was done by Galvan (1986, 1987a, b). Besides reinterpreting the original seismic and well data, Galvan also tried to correlate the reflection profiles to the regional geology. Using the grid of lines shot for the Phillips-Anchutz exploration program, he was able to trace reflection packages over broad areas in the western Arizona Transition Zone. He pointed out that the identity of the reflections could be: 1) Precambrian crustal layering, 2) plutonic intrusions into previously metamorphosed Precambrian rocks, 3) Mesozoic thrust faults or related fabrics, 4) Tertiary detachment faults or related fabrics, or 5) a combination of two or more of these possibilities. Correlation of the seismic data to the local geology and the drill core suggests that many of the upper-crustal reflections represent laccolithic- or lens-shaped plutonic bodies intruded into

Precambrian gneiss and schist, which were all subsequently overprinted by Tertiary extensional deformation. Such a geologic history is suggested by exposures in the nearby Weaver Mountains, which project onto the seismic lines near the well site (Galvan and Frost, 1985; Galvan, 1986, 1987a, b). The overall coherence of the reflections in this area contrasts with the more discontinuous reflections in the detachment terrane, suggesting that the reflections are not solely, or perhaps even primarily, related to Tertiary extensional deformation.

After studying the granitic rocks in the vicinity of the well site, return to AZ-96 and turn right toward Bagdad. En route, a variety of Precambrian granitic and metamorphic rocks are exposed in the roadcuts, with a steeply dipping foliation fabric prominently exposed in many places just south of Bagdad. These well-foliated, steeply inclined rocks are mostly metamorphosed andesites, basalts, tuffs, and sediments of the older Precambrian Bridle Formation and Hillside Mica Schist (Anderson and others, 1955). At Bagdad (28.0 miles from Stop 4), turn right off AZ-96 (Main Street) onto North Lundahl Street (COCORP line 4). Follow this road for 3.1 miles, after which it becomes a dirt road. After an additional 0.8 mile, bear left at the fork and continue past the pumice mine workings for 0.3 mile to the top of the ridge. Walk out the ridge line to the clearing for an overview of COCORP line 4, Phillips line 31, and the local geologic relationships.

Stop 5: Seismic Profiles of the Transition Zone Near Bagdad and Their Relationship to the Exposed Geology

The road in the foreground was the route for the COCORP profile, on which some of the best reflections from entire western Arizona survey were obtained (Hauser and others, 1986, 1987). Similarly good results were obtained from the Phillips-Anchutz lines to the northeast of Bagdad (Figure 5) on Bozarth and Behm Mesas. These high-quality lines were obtained even though surface outcrops are of steeply dipping Precambrian gneiss, intruded by a variety of granitic rocks, and overlain by thin flows of late Tertiary basalt. The top of one of the major plutonic bodies, the 1.4 Ga Lawler Peak Granite, is exposed in the foreground with a gently undulating, subhorizontal contact exposed across much of the field of view. The possible identity and development of the multiple reflections and reflection packages in the Transition Zone will be discussed in detail here. The geometry and potential significance of apparent offsets in Moho as imaged on the COCORP lines will also be highlighted at this stop.

Return to Bagdad, then turn south back down AZ-96 for 4.3 miles to the junction with AZ-97. Turn southwest (right) onto AZ-97 and follow it for 11.3 miles to the intersection with US-93, across nearly continuous exposures of Precambrian granite. If time allows, turn northwest (right) onto US-93 and drive 3.3 miles. Watch for a dirt road that is present on both sides of the highway. Carefully turn left across US-93 onto the dirt road. Atop the small rise is a barbed wire gate. Stop here or continue past the gate for an additional 0.2 mile. The overlook stop is atop the nearby basalt-topped rise, which is about a 10-minute hike from the gate.

Stop 6: Overlook of the Transition Zone from the Edge of the Detachment Terrane

From this vantage point, a large area of the Transition Zone that has been the focus of the field trip to this point can be seen. The overall topography, composition, and crustal structure of the

region can be reviewed if one looks to the east; seismic lines such as those shown in Figures 5 and 6 are representative of the upper-crustal structure of the region. The area between this stop (along Highway 93) and Bagdad marks the change from Transition Zone structure to detachment-terrane crustal structure. On a crustal scale, the area beneath this stop can be characterized as part of the detachment terrane, whereas Bagdad (15 km to the northeast) is part of the Transition Zone. Between the two COCORP lines in this area (lines 3 and 5) and near the southern end of line 3 are two of the apparent Moho offsets suggested by Hauser and others (1986, 1987), which were studied in detail by a joint Stanford-PACE-CALCRUST-PASCAL experiment in the Spring of 1987 (Erik Goodwin, pers. commun., 1987). Preliminary results of this survey and the main PACE refraction survey over the COCORP lines and industry lines will be discussed at this stop (or the preceding one as time dictates). From this stop, drive south along US-93 to Wickenburg (47.6 miles) for the evening.

DAY TWO: DETACHMENT TERRANE

Depart from Wickenburg and drive west on US-60W toward Los Angeles. Begin the mileage at the center of Wickenburg (intersection of US-89 and US-60). Drive through upper-plate tilted volcanics of the Vulture Mountains extensional terrane (Rehrig and others, 1980) toward Aguila, which sits between the Harquahala Mountains to the south and Harcuvar Mountains to the north. In Aguila, turn north (right) onto Eagle Eye Road. After 2.1 miles, the pavement ends, although the dirt road is well maintained. The county line between Maricopa and Yavapai Counties is 1.9 miles down the dirt road. Turn left (west) at the county line and follow the road for 2.5 miles, then take a right turn to the north. At 3.0 miles, there is a fork in the road; continue straight. After another 2.9 miles (near the highest point on the road), turn off the main road onto a jeep trail to a mine shaft 0.2 mile off the main dirt road. Park and walk southeast to the crest of the ridge for an overview of the Harcuvar and adjoining mountain ranges. The distance from Wickenburg is 38.7 miles. An alternative first stop for other trips is the spectacular overview in morning light of the Transition Zone-detachment terrane boundary from the abandoned restaurant near the top of the Yarnell grade east of Congress.

Stop 1: Overview of Harcuvar Mountains, Bullard Detachment Fault, and Nearby Seismic Lines

The character of the light-colored, lower-plate gneisses and darker colored upper-plate rocks in the Harcuvar Mountains is visible for tens of kilometers before one reaches the area of the detachment fault for Stop 1. The detailed geology of the area is described by Rehrig and Reynolds (1980) and Reynolds and Spencer (1985). Looking down the valley to the southwest, one can see the long axis of one of the most prominent northeast-trending antiforms in the detachment terrane. Phillips seismic lines TR-6, CXP-3, and TR-2 traverse this valley from the Granite Wash Mountains along the entire length of the range and across the Date Creek Valley to an area near the Date Creek Mountains (Figure 6). These dynamite lines show a very pronounced, gently inclined to subhorizontal structure down to about 2.5 secs. (TWTT), where this fabric merges into nearly horizontal reflections (Frost and Okaya, 1986). The detachment fault would thus appear to form a wedge in two dimensions, with the Bullard fault as the upper edge of the wedge and the subhorizontal reflections as the lower edge. The lower reflections have the short, noncontinuous character

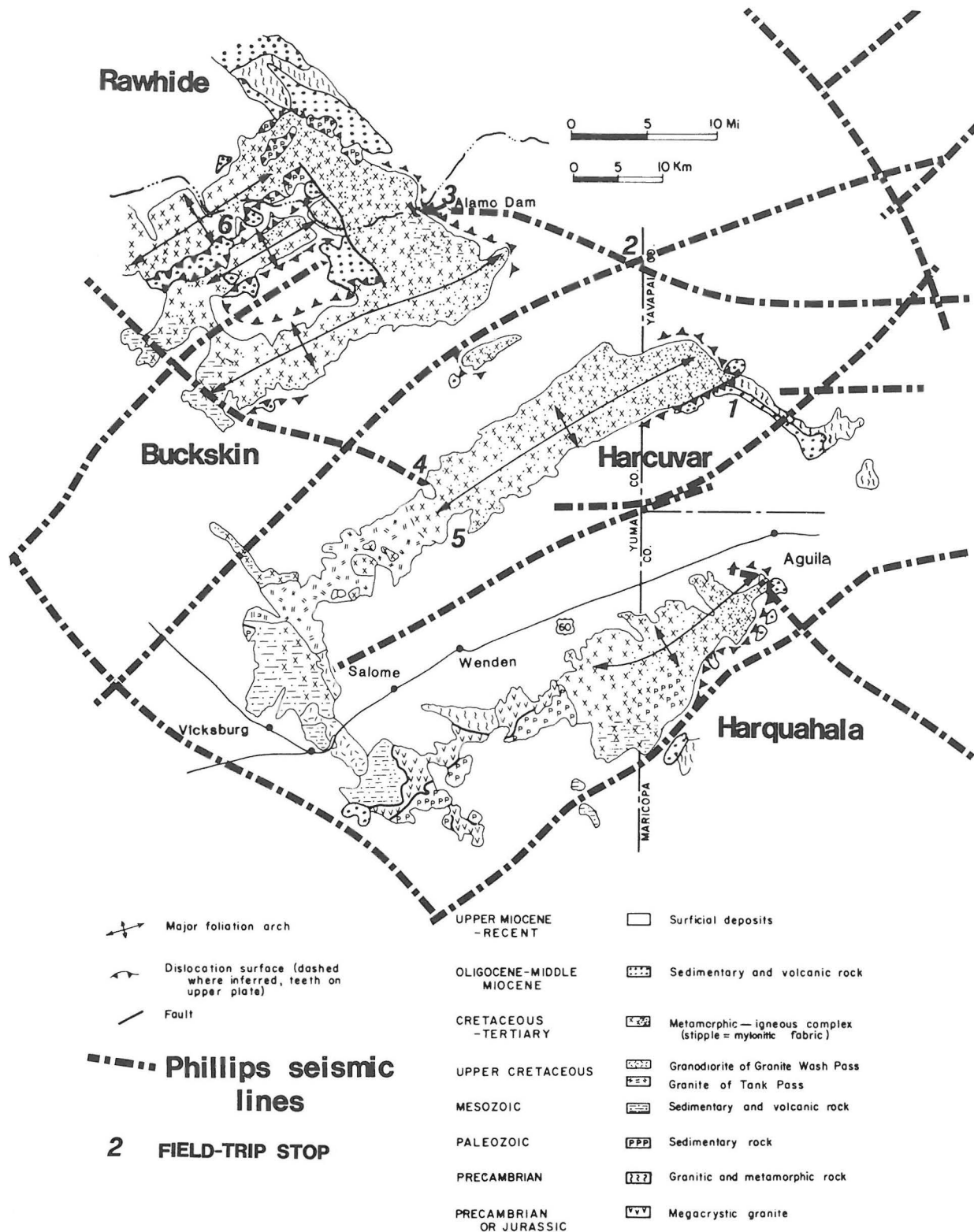


Figure 6. Line-location map of industry seismic lines (Phillips) in the Buckskin-Harcuvar-Harquahala Mountains region to be traversed during this trip. Most of these lines are dynamite lines and are therefore less useful than the Vibroseis lines that were shot in the Transition Zone. They do, however, provide a framework for tracing the surface geology of the detachment terrane between ranges and toward the Transition Zone. Base map showing the geology modified from Rehrig and Reynolds (1980).

typical of mylonitic rocks as interpreted from this and other regions (e.g., Hurich and others, 1985), as do many of the overlying, gently inclined reflections.

This geometry would seem to suggest that the detachment faults exposed in the core-complex region do not descend uniformly through the crust (Wernicke, 1985),

but descend into a middle-crustal, low-angle fabric that appears to record very low-angle, simple shear of the crust (Okaya and Frost, 1986a, b).

After discussing the relationship of the seismic lines to the geology of the Harcuvar Mountains, return to the main dirt road and proceed north (right) for 0.4 mile. Stop briefly to look at the mylonitic rocks, chlorite breccia zone, and associated structures along the road. Continue driving to the north, following the main dirt road to its intersection with the Alamo road (5.8 miles past Stop 1).

Stop 2: Overview of Ranges and Seismic Lines Tying Detachment Terrane to the Transition Zone

Two Phillips industry profiles intersect at this junction and image mostly lower-plate rocks; very little upper-plate material is imaged on the seismic profiles in the vicinity of this intersection. At this stop, the spatial arrangement of the Harcuvar, Buckskin, and Rawhide core complexes can be seen with respect to the Transition Zone on the eastern skyline. With seismic lines that cross at this road intersection (TR-1 and TRD-2), a three-dimensional picture can be obtained for the seismic structure in relation to the exposed ranges. Both these seismic lines show a pattern of short, discontinuous reflections, which are interpreted as the mylonitic rocks that crop out in the Harcuvar, Buckskin, and Rawhide Mountains. The antiformal-synformal nature of the ranges is visible on the lines, as is the pronounced subhorizontal fabric characteristic of most of the seismic lines in this region. Even though the upper detachment fault (Bullard detachment in the nomenclature of Reynolds and Spencer, 1985) has an antiformal-synformal shape, the pronounced reflections and reflection packages at depths of 2.0 or more secs. (TWTT) are nearly horizontal. This suggests that the upper-crustal shape of the detachment fault is not imaged as mirroring the deeper crustal geometry of the terrane.

Turn left (west) onto the Alamo road and drive 14.8 miles to the Wayside Trailer Park, taking the 45-degree left turn toward the Buckskin Mountains. After 2.9 miles, the dirt road intersects a paved road. Turn right (north) on the paved road and continue into the Alamo Lake State Park. Stop at the ranger station (22.2 miles from Stop 1 and 60.9 miles from Wickenburg).

Stop 3: Buckskin Detachment Fault and Lower-Plate Rocks

The detachment fault is exposed directly across the highway from the ranger station. The gentle dip of the fault is apparent as are the many normal faults that feed into the detachment fault. The red-green color contrast so typical of the alteration along detachment faults in the region is best displayed in afternoon light. The character of the complex deformation in the lower plate can be viewed by walking through the highly deformed gneisses to the dam overlook (0.8 mile from ranger station). Brittle overprinting of both high-angle and low-angle faults on the ductile fabric and intense chloritic alteration of the lower plate are especially well exposed in the many road cuts between the ranger station and dam. Several good exposures of multiple, anastomosing detachment faults that produce a lensoidal pattern of faulting can also be seen in the road cuts. The highly deformed character of these rocks and their apparent seismic expression on lines TRD-2 and TR-1 may provide a basis on which similar profiles can be evaluated as showing the same type of extensional deformation.

After having lunch and studying the character of the lower-plate deformation and its expression on the

seismic profiles, return down the paved road toward Cunningham Pass in the Harcuvar Mountains. The road traverses around the nose of the Buckskin Mountains through mylonitized schist and gneiss, then past the small antiformal exposure of lower-plate rocks (Butler Hills) in the valley and nearby circular hill of upper-plate rocks (mile 79.9). Stop at the light-dark contact on the eastern cliff face (mile 87.7), just as the road enters the Harcuvar Mountains (Cunningham Pass). Walk east to the major stream, where spectacular small-scale folding and boudinage of Mesozoic age are exposed (Rehrig and Reynolds, 1980), and up the side of the hill for a vantage point to look at Butler Valley and the adjoining ranges.

Stop 4: Butler Valley Overview; Mesozoic Versus Tertiary Structure

Phillips lines TR-1 and TRD-5 intersect (Figure 6) near the center of Butler Valley and provide a view of what lies between two core complexes. Although work on these dynamite lines has just begun, it appears that the valley fill is fairly shallow. The Mesozoic metamorphism and deformation that are so well displayed in outcrop here at Cunningham Pass (Rehrig and Reynolds, 1980) can be interpreted to descend downward toward the Buckskin Mountains. However, how this older structure is truncated or overprinted by the Tertiary fabric is not completely clear on line TRD-5. There is some suggestion, though, that the Mesozoic structure is truncated at depth by the short, discontinuous reflections thought to represent mylonitic rocks. Line TR-1 shows these same mylonitic reflections as well as some pronounced reflections between broader zones of reflection packages. The antiformal lower-plate hill on the northeastern end of the valley between the Harcuvar and Buckskin Mountains appears to be underlain by a pronounced reflection at 2.0 secs. (TWTT), providing what appears to be a cross-sectional view of a fault-bounded lens.

Continue driving south through Cunningham Pass to the broad turnout to the right just past the powerline towers (2.5 miles from Stop 4).

Stop 5: Harquahala Mountains, McMullen Valley, and Mesozoic Thrusting Overlook

This brief stop will provide a view across McMullen Valley to the northern Harquahala Mountains, where the Paleozoic cratonal section is exposed in thrust-fault contact with probable Precambrian and Mesozoic crystalline rocks (Reynolds and others, 1986). In afternoon light, the white color of some of the Paleozoic rocks can be seen on the flanks of the Harquahala Mountains. These outcrops are in a quarry that can be easily visited if there is time on other trips. The relationship of these thrusts to the seismic profiles in McMullen Valley and elsewhere in the region will be the topic of speculation here.

From Stop 5, return north to the area of Stop 4 and turn left onto the powerline road that goes north across Butler Valley (route of Phillips line TRD-5). Stop briefly (after 15-mile drive across the valley) at the first outcrops in the Buckskin Mountains and look back at the Harcuvar Mountains to compare rock fabrics on either side of Butler Valley and discuss their relationship to the seismic profile along this road. Continue driving through the low foothills of the Buckskin Mountains, where Paleozoic rocks sit just above the very gently inclined detachment fault. At mile 111.6, the powerline road intersects the Swansea road (two-lane, well-graded road), just past another well-graded road. COCORP line 4 is located on the first dirt road; two Phillips profiles intersect at the powerline-Swansea road join. Turn right and fol-

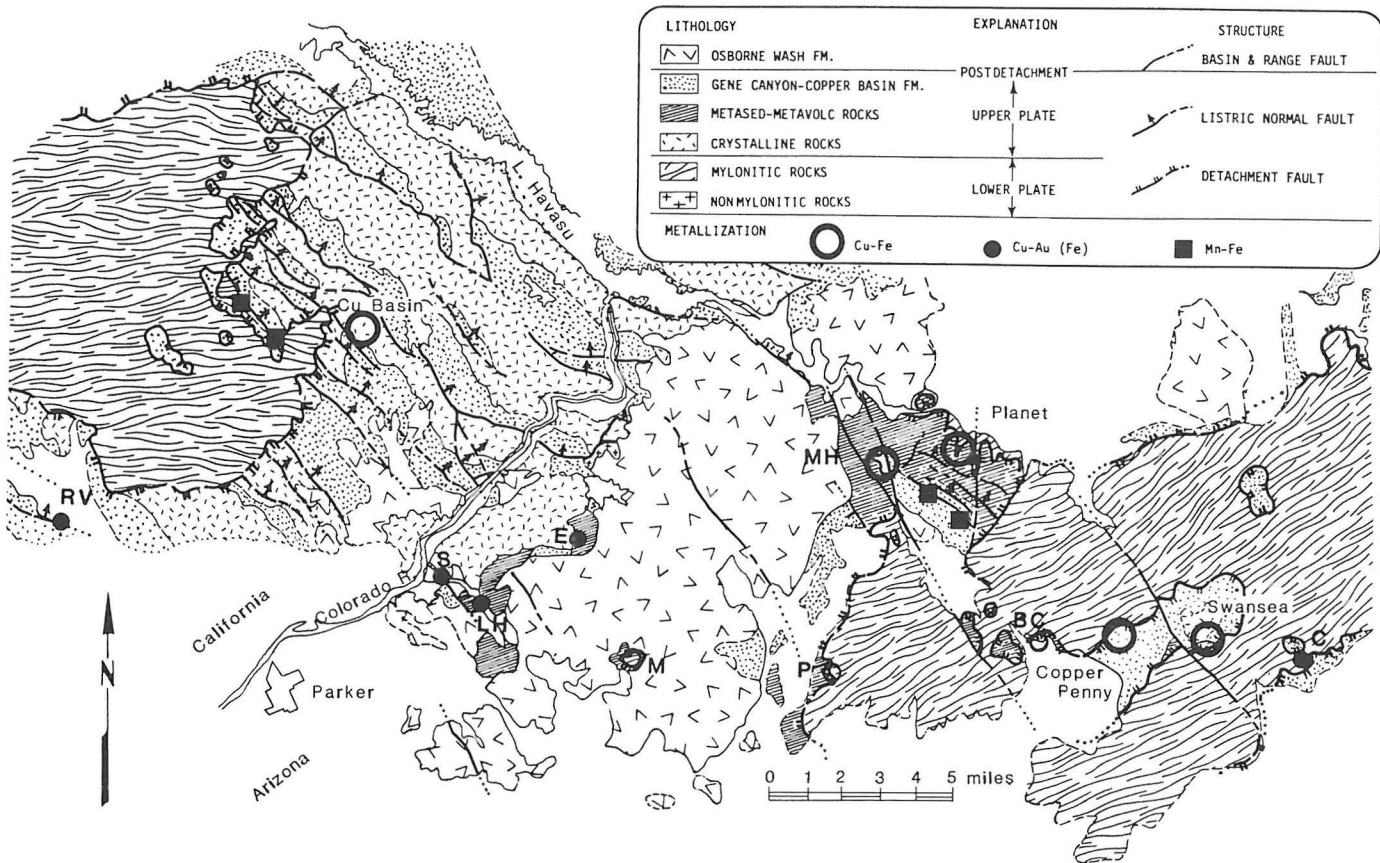


Figure 7. Regional geologic map of the Whipple - Buckskin Mountains area showing the general geology, structure, and major mineral deposits in the area from Wilkins and Heidrick (1982). The Copper Penny area is located in the Swansea synform, one of the numerous NE-SW-trending antiforms and synforms in the region produced during detachment faulting. Disruption of the major detachment fault by later, basin-and-range-style normal faults has produced a subhorizontal effective dip for the detachment fault on a large scale as measured in a NE-SW direction. COCORP and industry profiles traverse across the southeastern corner of the map area within predominantly lower-plate rocks. Prospects and mines designated by initials are: BC = BCC mine; C = Clara; E = Empire; LH = Lion Hill; M = Mammon; MH = Mineral Hill; P = Pride; RV = Riverview.

low the Swansea road for 5.0 miles to where it intersects the Planet road (on left). Continue on the Swansea road (bearing right) for 5.4 miles to a dirt road marked by a fallen chain gate. Turn off the Swansea road onto the Copper Penny access road (through chain gate), bearing right after 0.2 mile. Stay on this road for 2.8 miles to the Copper Penny mine.

Stop 6: Copper Penny Mine, Buckskin Detachment Fault, and Upper- and Lower-Plate Structures

The Copper Penny has been one the most intensively studied (Heidrick and Wilkins, 1980; Wilkins and Heidrick, 1982; Spencer and Welty, 1986; Lehman and others, 1987) portions of the detachment terrane because of the mineralization exposed here. Superb exposures of the detachment fault and microbreccia ledge are abundant in the Copper Penny area. Both upper- and lower-plate structures are also well displayed and were drilled by Gulf Minerals, providing a third dimension to our understanding of detachment faults (Figures 7 and 8). The relationship of these exposed structures to both the COCORP line and Phillips line (both shot on the same road) will be discussed. From this vantage point, the Rawhide detachment fault, where Shackelford (1976, 1980) first discerned the existence and many of the characteristics

of the detachment terrane in western Arizona, is very evident in afternoon light. The Transition Zone can be seen on the far eastern skyline, making possible a summary of the join of the detachment terrane to the Transition Zone. COCORP profile 4 and Phillips lines will be discussed in the context of the day's stops and the geometries of detachment faulting exposed near the Copper Penny mine. Drive to Parker for the night.

DAY THREE: DETACHMENT TERRANE AND MESOZOIC THRUSTS

Drive across the bridge at Parker to California and turn north (right) on US-95. Turn off the highway onto the small loop road on the left side of the highway just before entering the Colorado River Indian Tribes Reservation (4.1 miles from Colorado River bridge). The traverse along the road from Parker crosses through outcrops of the Miocene-Pliocene Bouse Formation (white tufa), flat-lying fanglomerates and volcanics of the Osborne Wash Formation, and tilted early Miocene volcanic and sedimentary rocks.

Stop 1: Geometry and Timing of Upper-Plate Tilting and Faulting

Tilting of upper-plate rocks during detachment-related deformation is one of the most characteristic attributes of mid-Tertiary extension in this region.

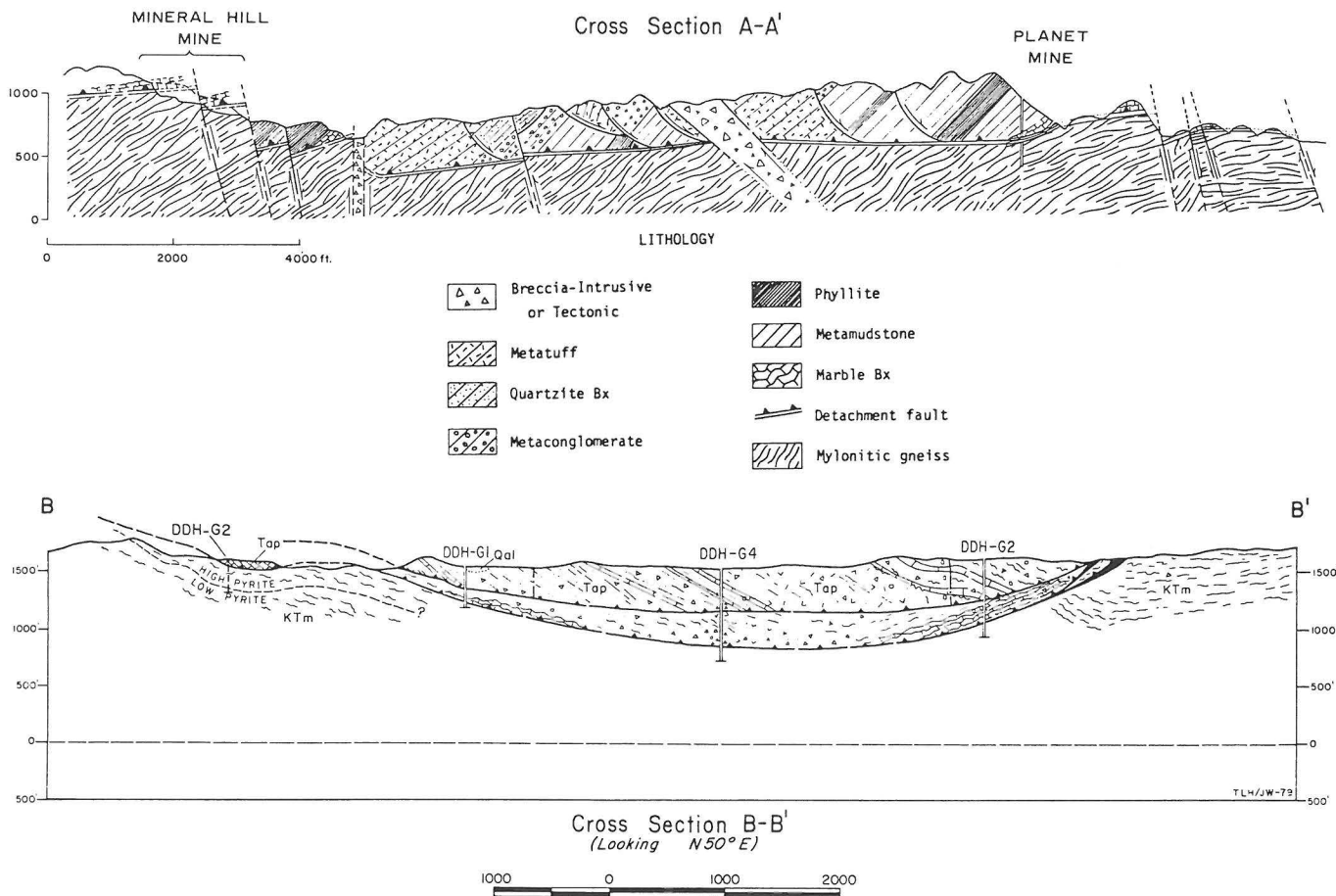


Figure 8. Cross sections through the detachment complex of the central Buckskin Mountains illustrating the outcrop-scale structure and providing a model for the overall style of extensional deformation in this region. Cross section A - A' is a NE-SW view through the Mineral Hill - Planet area northwest of the Copper Penny mine. The style of upper-plate faulting, truncation of the lower-plate mylonitic rocks, and offset of the detachment fault by later faulting are all evident. Offset and tilting of the Buckskin detachment fault produces an overall effective dip that is nearly horizontal, rather than the observed dip from outcrop. Structures at this scale should be interpretable on the seismic lines in the area. Cross section B - B' is a NW-SE view through the Copper Penny mine area showing the shallow keel of the synform, the truncation of lower-plate foliation in some areas and parallelism with it in others, and the truncation of upper-plate rocks. This was perhaps the first demonstrated area (Heidrick and Wilkins, 1980) for multiple detachment faults, many of which are visible in outcrop along the main detachment fault. From: Wilkins and Heidrick (1982).

Tilting of the sedimentary and volcanic rocks provides a tape-recording-like record of when deformation occurred and when it ended. This outcrop is a small-scale example of the style of tilting associated with detachment faulting in the Whipple Mountains region. The steeply tilted sedimentary and volcanic rocks are from the oldest part of the Tertiary section, the Gene Canyon Formation. Their southwest dip is characteristic of nearly all of the upper-plate rocks in the area, indicating large-scale relative motion of the upper plate to the northeast or of the lower plate to the southwest. Major normal faults that extend down to and join the detachment fault dip to the northeast, producing the southwest dip and back tilting of the Tertiary rocks. Many of the upper-plate Precambrian crystalline rocks on which the Tertiary section was deposited are tilted back to the southwest, suggesting that the foliation and general lithologic layering within these crystalline rocks were subhorizontal at

the onset of detachment faulting.

Tilting of the upper-plate rocks has also tilted the original normal faults. In this outcrop, the angular relationship between the faults and bedding appears to be similar to the 60° to 70° angle classically expected for normal faults. Tilting of the Tertiary section to a near-vertical orientation tilted the first-formed normal faults past the horizontal so that they now appear as reverse faults. Upper-plate faulting is also distributed on a multitude of small faults, effectively transforming the large-scale fault blocks into nonrigid bodies of rock. Such small-scale, intrablock faulting led Gross and Hillemeier (1982) to suggest using the term "fault-block complexes," a concept that helps make the difficulties of balancing sections and determining amounts of extension in these terranes more understandable.

Overlying these tilted and highly deformed rocks

SW

**CALCRUST Line
WM - 3**

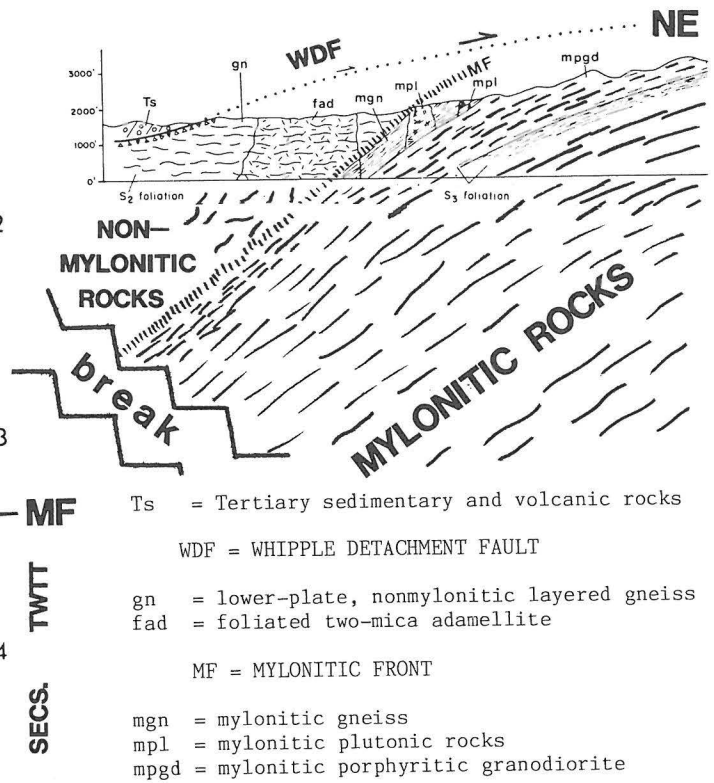
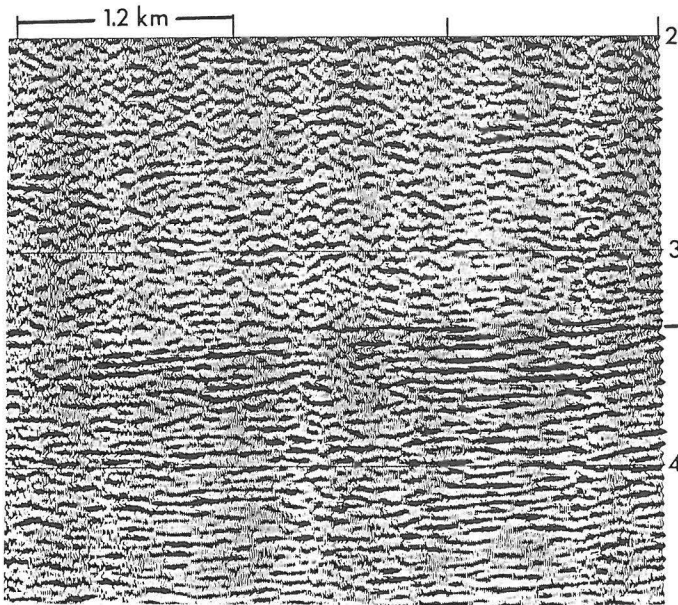


Figure 9. Schematic diagram showing the interpreted continuation of the mylonitic front exposed in the southwestern Whipple Mountains (Davis and others, 1980) with the top of the zone of highly reflective rocks imaged on the CALCRUST Whipple Mountains profiles. The change from the complex structure and fairly non-reflective character of the unmylonitized crystalline rocks to the higher velocity, much more reflective mylonitic rocks appears to image especially well on profile WM-3. Currently, a 9-km break exists between the outcrop of the mylonitic front and the nearest CALCRUST line, a break that will be profiled during the 1987-1988 field season to completely evaluate the interpreted equivalence of "mylonitic front" reflections to the exposed mylonitic front. Upward transport of the mylonites (Davis, 1986) during detachment faulting has exposed these middle-crustal rocks in the core-complex window, sampling what may be a regionally extensive middle-crustal zone of ductile deformation produced during very low-angle, crustal-scale simple shear.

are fanglomerates and basalt flows of the Osborne Wash Formation. Numerous ages on the flows have overlapping error brackets at about 12 Ma for the oldest flows. Similar dark basaltic rocks occur along the entire length of this transect from the Colorado Plateau to the San Andreas fault and have similar chemistries and age spans. This fundamental change from detachment-related extension to minor basin-and-range style faulting, and change from arc-related andesitic volcanism to basalts derived from the mantle or lower crust seem to coincide well with the 12 Ma initiation of major faulting within the San Andreas transform system as indicated by motion on the San Gabriel fault (Crowell, 1981). A fundamental plate-tectonic cause for both this intra-arc detachment faulting and its cessation seems to be required, given such a regional coordination of deformation and magmatism.

Continue north along the river to the Parker Dam settlement just south of Parker Dam and reset mileage. Follow the left branch of the "Y" in the road just north of the town and traverse through the Tertiary section, then along strike of one of the major fault blocks into the interior of the Whipple Mountains. Follow the main paved road, which turns into a graded road, toward Black Meadow Landing. Turn off this road at the Havasu Palms resort road (mile 6.2), which is marked by an Exxon sign. Turn left onto the main powerline road (mile 8.4), where the Havasu Palms road turns east. Continue on the powerline road to the top of the last hill overlooking

Whipple Wash (mile 9.5), next to a powerline pole on the right and a small turnout on the left.

Stop 2: Whipple Detachment Fault Near Whipple Wash

From this overview, the Whipple detachment fault is strikingly visible to the north in morning light. The gentle dip of the fault, its antiformal-synformal character, and its associated upper- (red) and lower- (green) plate alteration are very well displayed. Also visible are several of the surrounding ranges, including the Chemehuevi Mountains to the north and Mohave Mountains to the northeast. The spatial and geologic relationships of these ranges to the Whipple Mountains during the continuum of the three-dimensional progressive deformation of detachment faulting will be among the major topics of the discussion held here.

One element of the development of crustal-scale extensional deformation is the tilting of upper-crustal blocks, much like the tilting of individual fault blocks within the upper plate. Within the Whipple Mountains, the highest structural level within the lower plate is in the westernmost part of the range where the rocks are nonmylonitic. The boundary separating these nonmylonitic rocks from the underlying mylonites (Figures 9 and 10) of the central and eastern Whipple Mountains is the mylonitic front (Davis and others, 1980). The westward tilt of the mylonitic front is one indication of the westward tilt

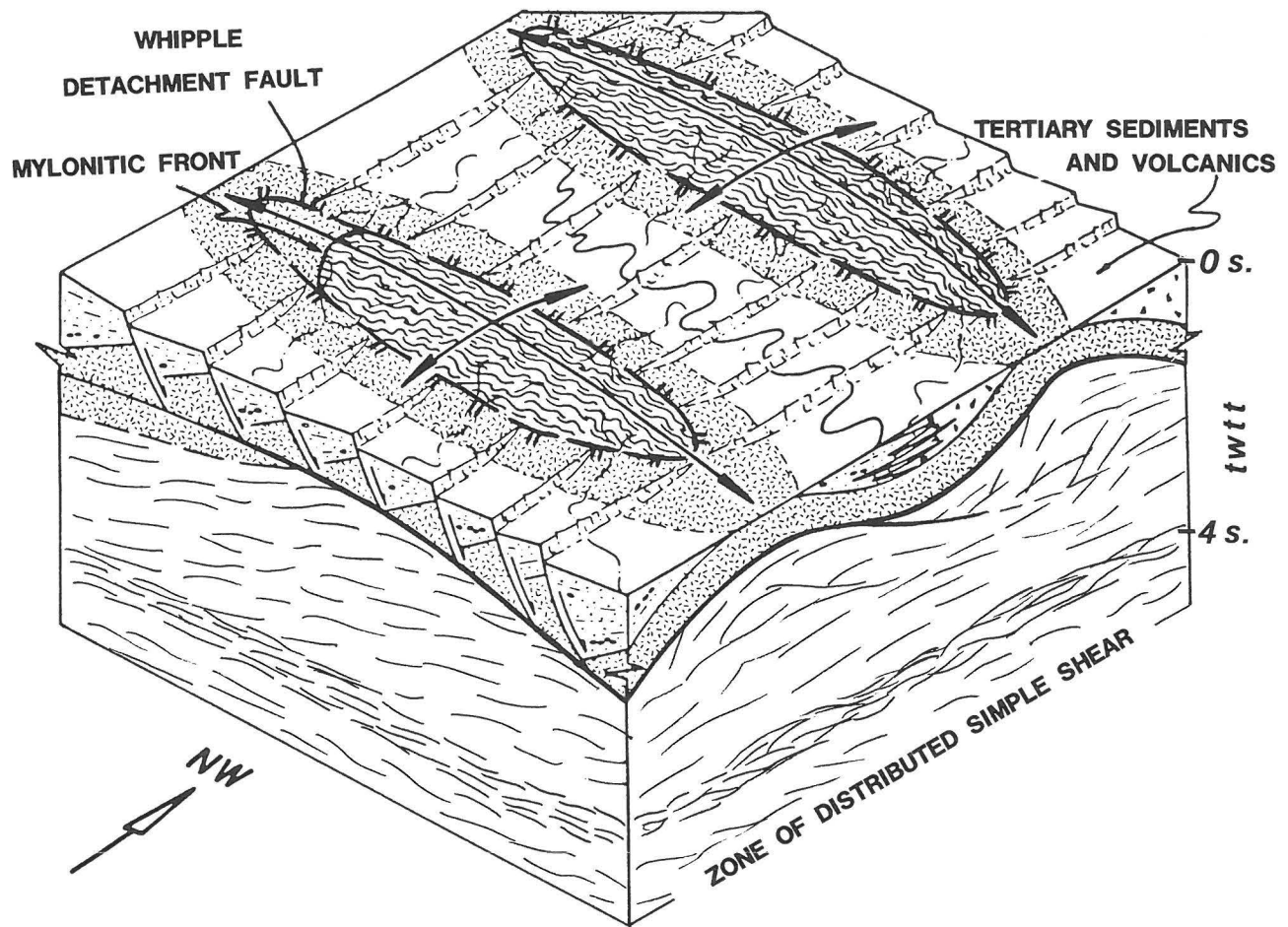


Figure 10. Block diagram of the interpreted relationships in the Whipple Mountains area on the basis of the exposed surface geology and the interpretation of the CALCRUST and industry seismic lines. The mylonitic front dips to the west away from the Whipple Mountains for an unknown distance. The mylonitic front is cut by the Whipple detachment fault, which progressively cuts down section to the northeast. Reflections appear to become subhorizontal at about 3.5-4.0 secs. (TWT) over a very broad region on the basis of the network of industry seismic lines. Tilting of the probably once subhorizontal mylonitic rocks to their current dips appears to have been caused by progressive simple shear of the crust, which produced detachment faults that penetrated to the surface and tilted the upper portion of the regional mylonitic zone.

of the entire upper crust, including that below the Whipple detachment fault. The lower-plate mylonitic rocks are clearly domed within the range, so that the lower plate is not simply a southwest-tilted fault block, but an elongate dome with mylonitic rocks and the mylonitic front truncated by the Whipple detachment fault. This truncation suggests that formation of the exposed mylonitic rocks occurred at lower angles, with subsequent tilting of the mylonitic foliation by progressive deformation within a very low-angle, crustal-scale shear zone (Okaya and Frost, 1986a, b). Truncation of southwest-tilted mylonitic rocks by the Whipple detachment fault is well displayed within the lower-plate rocks beneath the small klippe visible from this stop.

Return to the Colorado River by the same route, past Earp and toward Vidal Junction on California Highway 92. On the drive to the southwestern edge of the Whipple Mountains, the Whipple detachment fault is visible as the light-dark contact around the margins of the range. In afternoon light, the western side of the high klippe shows the shape of the synformal depression between the Whipple Peak and Bowmans Wash antiforms. If time permits on other trips (half day), the mylonitic front can be visited, following the directions from Anderson and others (1979). On this

trip, continue past the Chambers Well road, which leads to the mylonitic front, and turn north on the Savahia Peak road (9.4 miles from Earp), which is marked by two wooden posts and a sign describing the Savahia mine. Stop at the water tower and walk to the mine portal area.

Stop 3: Whipple Detachment Fault at Savahia Peak

In this western portion of the Whipple Mountains, the detachment fault is distinctly different from the detachment fault where the lower-plate rocks lie beneath the mylonitic front. No well-developed micro-breccia or chlorite breccia zone is present. Instead, where the Tertiary rocks form the upper plate, they are truncated against lower-plate, nonmylonitic rocks along a poorly exposed fault zone. Lower-plate gneissic rocks are shattered and show abundant small-scale normal faults. Upper-plate, nonmylonitic crystalline rocks also show evidence of brittle deformation, but exposures are relatively poor, especially compared with other parts of the Whipple Mountains, making the upper-plate deformation difficult to study in any detail.

The juxtaposition of nonmylonitic crystalline rocks in the upper plate against nonmylonitic crys-

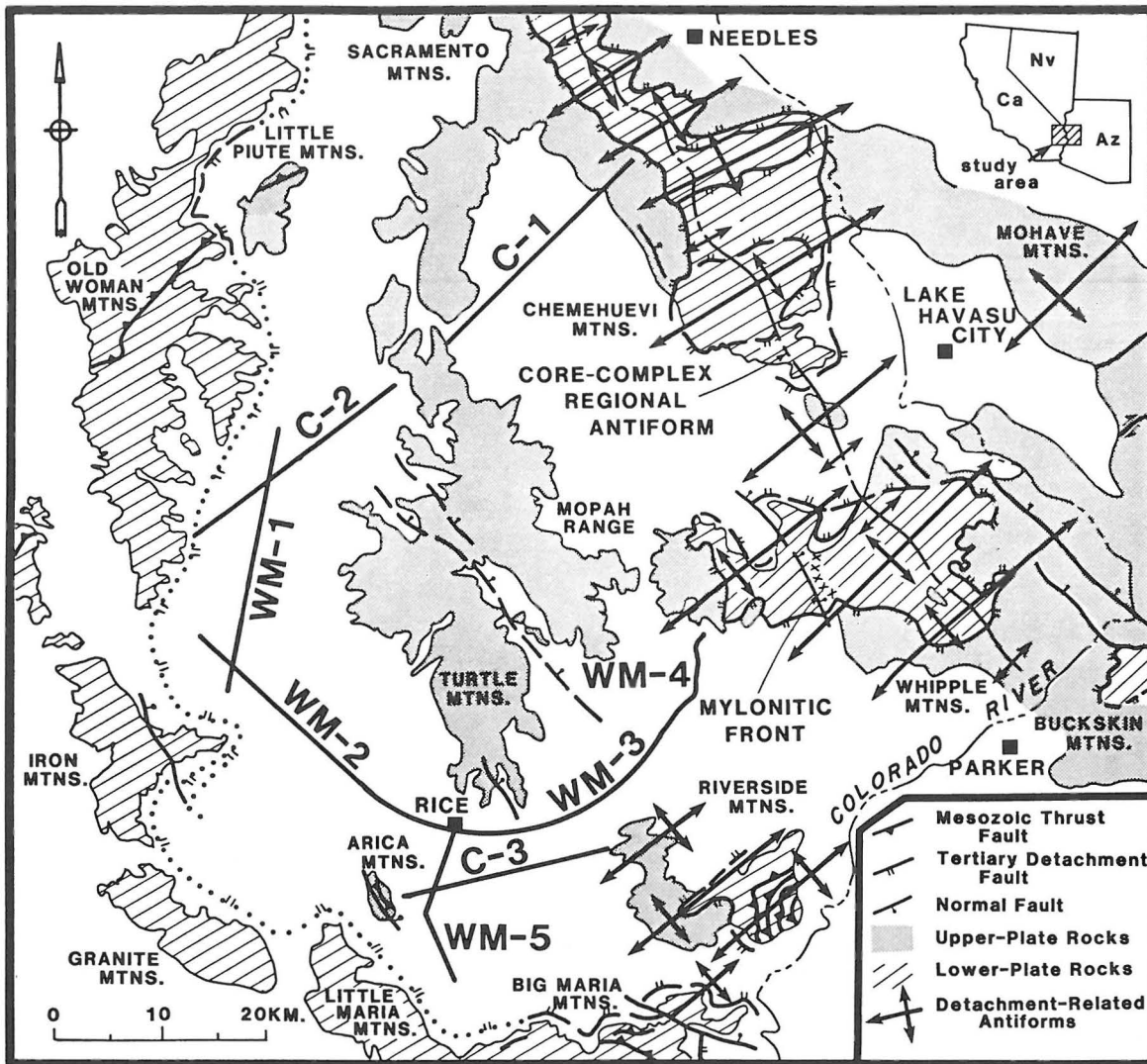


Figure 11. Line location map for the CALCRUST Whipple Mountains profiles and CCG industry profiles C-1, C-2, and C-3. Base map shows upper- and lower-plate terranes in a simplified fashion. Antiforms (synforms not shown for clarity) within the regional core-complex antiform are also shown. Middle-crustal mylonitic rocks exposed in this major antiform appear to underlie the entire area, not just the region to the northeast toward the Colorado Plateau.

talline rocks in the lower plate makes it difficult to image seismically the detachment fault, except where the fault separates Tertiary rocks from lower-plate crystalline rocks. Similar juxtaposition of dissimilar rock types, but between different types of crystalline rocks, such as appears to be the case along CCG line C-1 (Figure 11) in the Chemehuevi Mountains, seems to produce reflections that can be interpreted as the detachment fault. Within such rocks, however, there is a tendency for the reflections to be sporadically developed, probably because of the irregular juxtaposition of units and the differences in data quality. Identification of a subhorizontal reflection as a detachment fault is easiest where the reflection can be traced to the surface or projected across a short distance to an exposure of a detachment fault. Alternatively, a subhorizontal or gently inclined reflection can be interpreted as a detachment fault by the truncation of the normal faults that feed into it. These normal faults are well defined by the half grabens containing Tertiary sedimentary and volcanic rocks, which image quite well on both the CALCRUST and industry profiles

in the region. CALCRUST line WM-4, which is a crooked line stopping about 1 km from Savahia Peak (Figure 11), will be studied in detail here as will its correlation to the surface geology. The two PACE refraction lines, which were shot in the form of a large cross whose intersection is just to the east, will also be discussed and compared with the reflection lines (McCarthy and others, 1986).

Much more apparent on the seismic lines than the detachment fault is the change from mylonitic rocks to nonmylonitic rocks (Figure 9). CALCRUST line WM-3 (Vidal Junction to Rice) shows a well-developed reflection package consisting of short, discontinuous reflections across the entire length of the profile. These reflections climb gently toward the surface on the eastern end of the profile and project to within about 1 km of the exposed mylonitic front in the southwestern Whipple Mountains. A detailed wide-angle reflection survey shot as a piggyback to the CALCRUST experiment (Fleuh and Okaya, 1987) shows the three-dimensional form of the mylonitic front and images the front substantially better than the main CALCRUST survey. Seismic velocity studies on mylonitic and

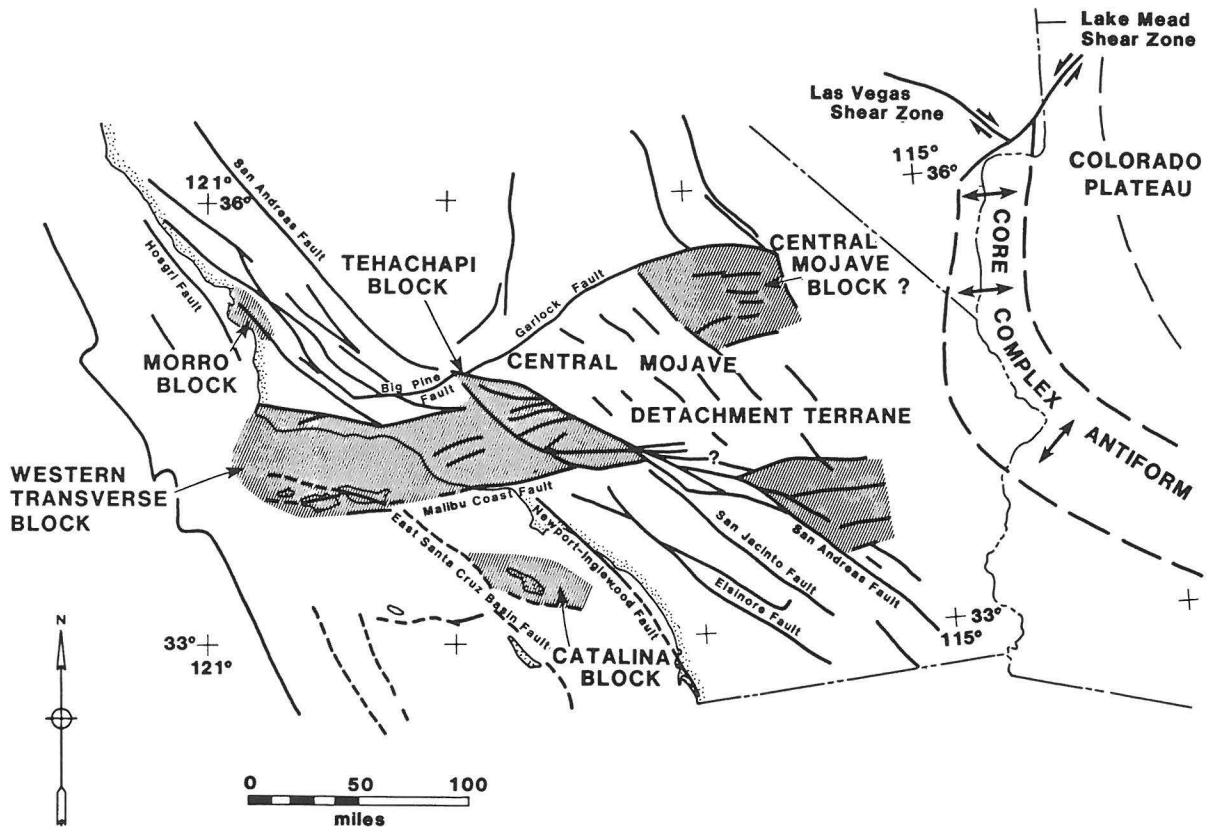


Figure 12. Map of some of the major Tertiary structural features of southern California and western Arizona. Middle-crustal rocks exposed in the core-complex regional antiform may extend beneath the central Mojave detachment terrane of Dokka (1986) and the southeasternmost portion of California on the basis of numerous reprocessed industry seismic lines. The Tertiary ductile reworking of the crust documented in the core-complex windows may thus be present under this entire region. Microplatelike rotation of the upper crust (shaded areas) during the middle Miocene (Luyendyk and others, 1980, 1985) may have taken place as a passive result of an actively moving middle and lower crust. Offset of this middle- and lower-crustal fabric should have occurred along the San Andreas fault system. Base map from Carter and others (1987).

nonmylonitic rocks from the western portion of the range suggest that the change from mylonitic to nonmylonitic rocks is sufficient to have produced the observed reflections (Ruppert and others, 1986). Continuation of mylonitic rocks west of the Whipple Mountains for at least several tens of kilometers indicates that the mylonitic rocks are not just the ductile equivalents of detachment faults tilted beneath the Colorado Plateau, but are instead an exposed portion of a large-scale, very low-angle shear zone that was brought to the surface during three-dimensional, progressive deformation associated with crustal-scale extension. The Whipple Mountains appear to be simply a window into the middle crust, exposing mylonitic rocks that may underlie a major portion of Arizona and southern California.

Return to the paved highway and continue west past Vidal Junction, where CALCRUST line WM-4 extends toward the Whipple Mountains and line 3 toward Rice. Drive to Rice and turn south on the Rice-Blythe road, stopping about a mile south of the town.

Stop 4: Intersection of Seismic Lines and Dip of Middle-Crustal Mylonitic Rocks

From Rice it is possible to see some of the high-angle faults in the Turtle Mountains that offset Tertiary volcanic rocks and the underlying Precambrian crystalline rocks, which compose most of the southern portion of the range. At Rice, CALCRUST profile WM-2

extends to the west-northwest toward the southern end of the Old Woman Mountains (Figure 11) and line WM-5 extends to the south toward the Big Maria-Little Maria Mountains. From the intersection of lines WM-2, 3, and 5, one can infer that the mylonitic rocks dip very gently to the southwest. Continue driving south toward Blythe along the Rice road (WM-5), crossing in front of the Arica Mountains, where Mesozoic thrust faults are cut by normal faults that are interpreted to be upper plate to the major Old Woman-Iron-Granite-Little Maria-Big Maria detachment fault. Continue to the top of the pass and take the jeep trail to the left (east), which leads to the top of the low ridge separating the Big Maria and Little Maria Mountains for a view back toward the portion of the detachment complex just traversed.

Stop 5: Mesozoic Thrust and Nappe Structure and Their Tertiary Overprint

From this vantage point, much of the area profiled during the first CALCRUST experiment is visible. The footwall to the Old Woman-Iron-Granite-Little Maria-Big Maria detachment fault makes a broad arcuate turn from the north down to the alluvial foreground in front of this stop and then into Arizona. According to some models (e.g., Howard and John, 1987), this is the headwall for the detachment terrane in this region. The mylonitic rocks would appear to extend down and beneath at least some of these ranges, suggesting

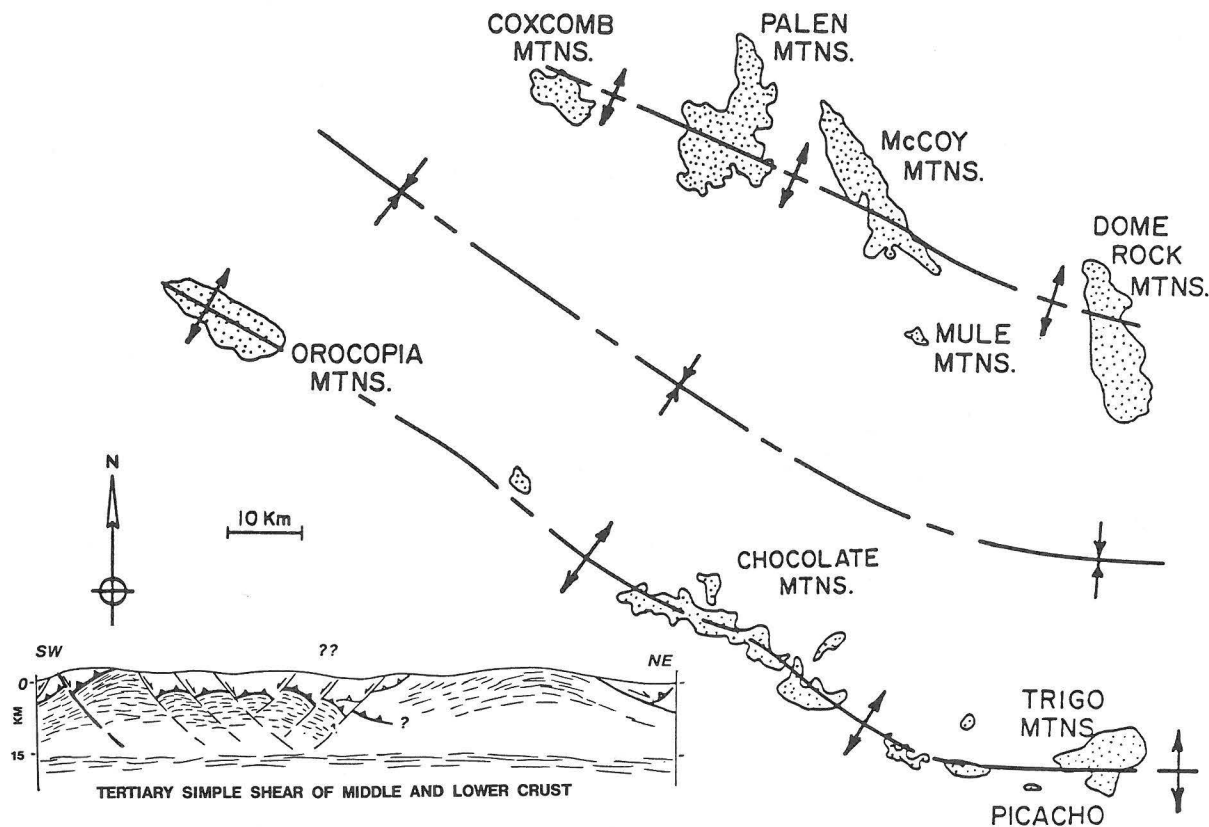


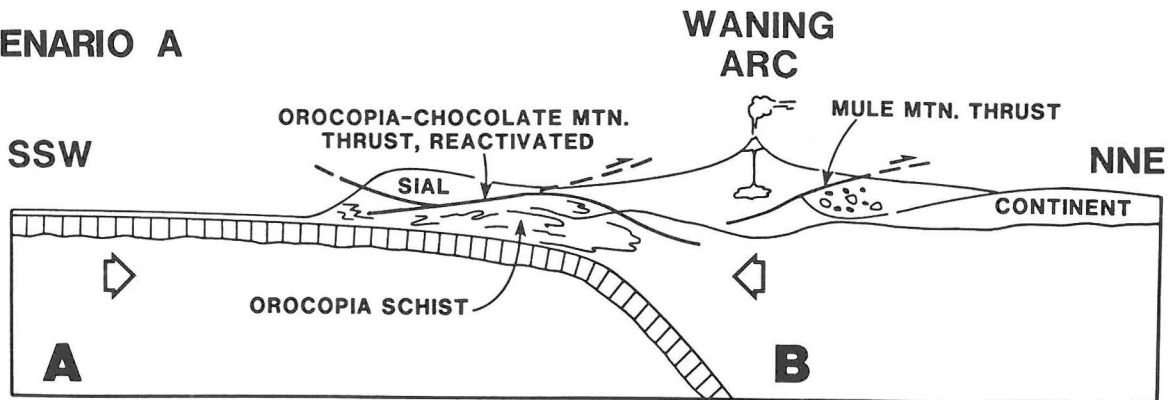
Figure 13. Diagrammatic map and cross section of some of the principal mountain ranges in southern California and western Arizona that contain thick sections of Mesozoic metaclastic rocks. Ranges on the north expose rocks considered to be the Jurassic-Cretaceous McCoy Mountains Formation. Ranges to the south expose the mostly Jurassic Orocopia Schist and Winterhaven Formation, whose relationship to the McCoy Mountains Formation is still unresolved. Seismic lines in the area indicate that the Mesozoic thrust sequence has been both extended and tilted, producing the large-scale antiforms and synforms. Prior to extension, these Mesozoic sections and their bounding thrust faults were closer together and would seem to have had a close spatial, if not genetic, relationship to each other. Near-horizontal middle- and lower-crustal reflections are thought to extend under the entire area on the basis of reprocessed industry seismic lines along portions of the cross section.

that crustal extension continued to the west of the "headwall," even if distinct detachment faults are not exposed around the flanks of these ranges as they are in the Whipple and Chemehuevi Mountains. Based on reprocessed industry lines (Exxon) west of the Old Woman Mountains, one can infer that the mylonitic rocks exposed in the Whipple and Chemehuevi Mountains extend at least as far west as the Sheep Hole-Calumet-Bristol Mountains. How far west Tertiary extensional fabrics continue is currently unknown. An intriguing consideration is the middle-crustal join of the Colorado River detachment terrane to the central and western Mojave detachment terrane (Figure 12) described by Dokka (1986), Dokka and Woodburne (1986), and Glazner and others (1987). Dokka (1986) has continued his detachment terrane to the Calumet Mountains, which can be joined to the Colorado River detachment terrane. If the interpretation of Spongberg and Henyey (1987) of reprocessed industry lines (Texaco and SeisData) in much of the northwestern Mojave (Figure 12) is correct, then this mylonitic fabric underlies most of the western Mojave Desert. Reflections imaged by COCORP in the western Mojave (Cheadle and others, 1986) could thus be interpreted as a continuation of the mylonitic fabric exposed in middle-crustal windows such as the Whipple Mountains. Similar reflections are also present in the southeasternmost portion of California near Yuma, Arizona on reprocessed industry (Exxon) profiles (Morris and Okaya, 1986; Morris, 1987), fur-

ther suggesting that much of southern California may be underlain by this mylonitic fabric. Major Tertiary reworking of the lower crust is thus indicated for the entire region. Such Tertiary reworking of the middle and lower crust may also underlie many of the rotated terranes of southern California (Figure 12) and could help explain how the upper crust has been able to move about a vertical axis in response to North America-Pacific plate motions.

Besides the Tertiary extensional deformation that is visible to the north and east, this region has been fundamentally affected by Mesozoic thrust faulting and nappe formation (Hamilton, 1982). The Grand Canyon cratonal section, much like that visible at Oak Creek Canyon, has been folded and faulted in the Big Maria-Little Maria Mountains area. Both Jurassic and Late Cretaceous plutonic rocks are present in the ranges and help define a complex history of deformation, intrusion, and metamorphism. Metamorphism was accompanied by massive fluid influx in some areas, as delineated by the detailed studies of Hoisch (1987). Hoisch suggests that deep penetrative structures within the crust may serve to channel fluids to the upper crust, perhaps making such fluid-weakened zones susceptible to compressive deformation. This may account for the common association of intense deformation with the presence of Paleozoic rocks in the region. Such a relationship could help define large-scale crustal structure if the seismic-reflection character of the

SCENARIO A



SCENARIO B

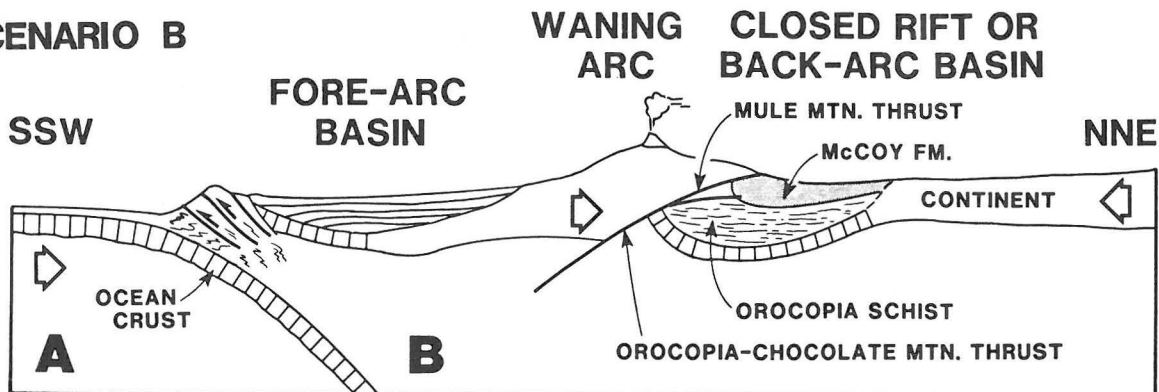


Figure 14. Interpreted plate-tectonic setting of the McCoy Mountains Formation and Orocofia Schist terranes as suggested by Crowell (1981). The McCoy Mountains terrane would appear to have been shed off both the North American continent and an arc active in Jurassic - Cretaceous time. The Orocofia Schist could be part of this same system and laterally equivalent, in part, or lower in the same tectonostratigraphic sequence as the McCoy Mountains Formation. Alternatively, the Orocofia Schist may have formed in a fore-arc position and then accreted onto North America or deformed as part of North America. The amount of strike-slip motion involved in this deformation is unknown and could easily disrupt or alter these suggested geometries. These are two of many possible scenarios and illustrate two end members for the relationship between the Chocolate Mountains thrust and the Mule Mountains thrust. Redrawn from Crowell (1981).

Paleozoic rocks can be determined.

Foliation within the interleaved Paleozoic meta-sedimentary rocks, Precambrian gneiss, and Mesozoic intrusive rocks dips to the north along most of the the northern end of the Big Maria-Little Maria Mountains and appears to continue down to middle-crustal depths. As imaged on WM-5, this Mesozoic compressional fabric is truncated at middle-crustal depths by the short, discontinuous reflections interpreted as the Tertiary mylonitic rocks. Offset of portions of the Paleozoic or Mesozoic metasedimentary sequences during northeast-directed crustal extension could help account for the middle-crustal low-velocity zone discerned in the region by the PACE refraction survey (McCarthy and others, 1986).

Continue south on the Rice-Blythe road to Blythe for the night. The overturned syncline of Paleozoic rocks whose upper limb is attenuated to 1% of its original thickness (Hamilton, 1982) is dramatically visible in afternoon light along this road.

DAY 4: MESOZOIC CLASTIC SECTIONS AND THRUSTS AS OVERPRINTED BY TERTIARY EXTENSION AND TRANSFORM TECTONICS

Drive west on Interstate 10 from Blythe to the Mesa Drive - Airport exit (Union 76 truck stop) west of town. At the offramp, turn onto the graded dirt road (Black Rock Road) just north of the freeway fence leading west toward the southern end of the McCoy Mountains. Follow the main dirt road to the foot of

the prominent hill with several microwave towers (4.0 miles) and park the vehicles. Walk up the road (past gate) to the large flat area at the last turn before the microwave installation.

Stop 1: McCoy Mountains Formation, Mule Mountains Thrust, and Buckhorn Seismic Lines

From this vantage point, the Paleozoic cratonal rocks in the Big Maria-Little Maria-Dome Rock Mountains can be seen, although they stand out best in afternoon light. These Paleozoic rocks and their underlying Precambrian crystalline rocks represent the southward extent of unequivocal North American rocks. Although much of the terrane south of the Big Maria Mountains is probably also autochthonous or para-autochthonous to North America, the possibility exists that much of this region has been accreted to North America (e.g., Vedder and others, 1983). The McCoy Mountains Formation, with an exposed thickness of greater than 7,000 m, is the obvious southern boundary to North America on a map view. In the third dimension, the McCoy Mountains Formation metaclastic and metavolcanic rocks sit depositionally on the cratonal Paleozoic rocks in the nearby Plomosa Mountains (Robison, 1980). The Paleozoic and Precambrian rocks would thus appear to extend beneath the McCoy Mountains Formation for an unknown distance to the southwest. Because it has not yet been possible to demonstrate how far North American rocks continue beneath the

McCoy Mountains Formation, this thick metaclastic section has been the source of much controversy about its age, origin, subsequent deformation, and relationship to other thick Mesozoic clastic sections in the region. A key question that will be examined is the possible equivalence of part of the McCoy Mountains Formation with part of the Orocopia Schist, another equally thick Mesozoic clastic section, which is exposed to the south and west of the regional antiform defined by the McCoy Mountains Formation (Figure 13).

In the McCoy Mountains and neighboring Dome Rock, Palen, Mule, and Coxcomb Mountains, the McCoy Mountains Formation dips to the south at the southern end of the ranges. As currently defined by most workers, this 7,000-m-thick section is not seen again to the southwest, unless units such as the Winterhaven Formation (Haxel and others, 1985) or the Orocopia Schist are lateral equivalents of the McCoy Mountains Formation. To the south and west, exposures of the Orocopia Schist in the Chocolate and Orocopia Mountains dip to the northeast beneath the Chuckwalla, Palo Verde, and Little Mule Mountains, but are not recognized as being exposed anywhere to the north of the Chocolate Mountains regional antiform (Figure 13).

Industry seismic lines (Buckhorn) in the McCoy-Palen Mountains area do not appear to shed light on this problem (Sanborn and others, 1986; J. McCarthy, pers. commun., 1987), but do appear to suggest that Tertiary extensional deformation has overprinted the Mesozoic structure. Reprocessing of the Buckhorn data suggests that the McCoy Mountains area may be underlain by reflections that are continuations of the reflections interpreted as mylonitic rocks on the CALCRUST Whipple Mountains profiles (J. McCarthy and D. Okaya, work in progress). If this is so, then the exposed Mesozoic structure has simply been reworked in Tertiary time at middle-crustal depths.

Seismic lines south of the Palo Verde Mountains in Milpitas Wash image this Tertiary extension very nicely. These lines suggest that individual ranges have been tilted to the southwest or northeast as half grabens, disrupting and extending the Mesozoic compressional tectonic fabric recorded in the Orocopia Schist, Chocolate Mountains thrust, and Mule Mountains thrust (Morris and Okaya, 1986; Morris, 1987). As such, the probability that the McCoy Mountains Formation and Orocopia Schist represent offset pieces of a once more continuous and genetically related terrane seems to be strongly indicated. Various geometric and geochronologic constraints and possible models for the origin and deformation of these terranes will be discussed, as will the proposed CALCRUST-PACE profiling work across these terranes.

Return to the vehicles and the freeway, heading east to the Highway 78 - Neighbours Boulevard offramp (first exit). Turn south along Highway 78 and drive through the towns of Ripley and Palo Verde. Where the highway heads west, the Mule Mountains thrust can be identified in the nearby Mule Mountains to the west as the somewhat subtle contact dipping to the south, which separates the foliated McCoy Mountains Formation (on the north) from more massive Jurassic granitic rocks (Tosdal, 1982, 1986) that overlie them. This thrust and its continuation into Arizona have been studied by Tosdal (1982, 1986), who has described its southwest-dipping geometry and northeast-directed transport. In the Big Maria terrane, fabrics that indicate this transport direction are overprinted on the large-scale, southwest-directed nappe structures. The presence of multiple Mesozoic deformations makes understanding the complex geometries of the terrane much more straightforward. Subsequent, crustal-scale extensional deformation of these Mesozoic fabrics has produced the current geometries, making most exposures in the region a product

of at least three deformational episodes.

Continue south past Palo Verde along Highway 78, over the flank of the Palo Verde Mountains, and through Milpitas Wash. Stop alongside the highway at the large turnout just south (0.8 mile) of Milpitas Wash (29.8 miles south of Interstate 10). From this vantage point on the terrace top, the Palo Verde, Midway, Trigo, Dome Rock, Little Mule, and Chocolate Mountains can be seen. The bright white tufa deposits ringing the low areas of the Palo Verde Mountains and Trigo Mountains across the Colorado River are remnants of the Bouse Formation, which records the late Miocene-Pliocene incursion of the Gulf of California into this region. It also demonstrates that the current level of exposure is similar to that of late Miocene time, so that much of the current topography is a reflection of Miocene extensional tectonics.

Stop 2: Milpitas Wash Seismic Lines, Palo Verde Antiform, Chocolate Mountains Thrust, and Regional Detachment Faults

Portions of the two thick Mesozoic clastic sections can be seen from this vantage point, where the possible relations between these sections and the Chocolate Mountains thrust and Mule Mountains thrust will be discussed (Figure 14). Numerous possibilities exist for connecting these rocks and structural features (Figure 14); a solution to the problem could be found by the CALCRUST survey that will be shot here during the 1987-1988 field season.

Four industry seismic lines (Exxon) in Milpitas Wash, which is in the foreground between the Palo Verde and Chocolate Mountains, have been reprocessed by David Okaya and Rebecca Morris and show a profound Tertiary extensional overprint on the Mesozoic Orocopia Schist and Chocolate Mountains thrust (Morris and others, 1986a). The Orocopia Schist crops out near the western edge of the seismic lines, making the identification of the thrust on the seismic lines possible. The thrust, which crops out on the southwestern margin of the basin, can be fairly accurately projected to the seismic lines, but appears to have a fairly subtle image. The thrust is marked more by a change in reflective packages than by an individual reflection. Even though the thrust is a major tectonic feature within southern California, its juxtaposition of rocks with similar densities and general composition across a thin mylonitic horizon does not lend itself to producing a major reflection at the thrust contact. Rather, the more complex and irregular structure in the upper-plate gneisses seems to contrast with the very regular and well-foliated character of the lower-plate Orocopia Schist. Two-and-a-half to three seconds (TWTT) below the interpreted location of the thrust, however, is a set of booming reflections (Figure 15). These reflections separate the Orocopia Schist from a package of even more highly reflective rocks underneath the schist. Although the identity of these lower rocks is currently impossible to determine, an obvious interpretation of the reflections separating these rocks from the Orocopia Schist is that they represent the base of the Orocopia Schist (Morris and others, 1986b). These reflections are very similar to those imaged beneath the Sierra Pelona antiform (Figure 12) by May and others (1982) in the eastern Transverse Ranges on the west side of the San Andreas fault. They are also much like the similarly interpreted reflections in the northwestern Mojave as imaged on reprocessed industry lines (Texaco and SeisData) by Spongberg and Henyey (1987). These same reflections are present on the COCORP Mojave lines (Cheadle and others, 1986), although they were not interpreted as the base of the schist.

Overprinted on the Orocopia Schist, the Chocolate

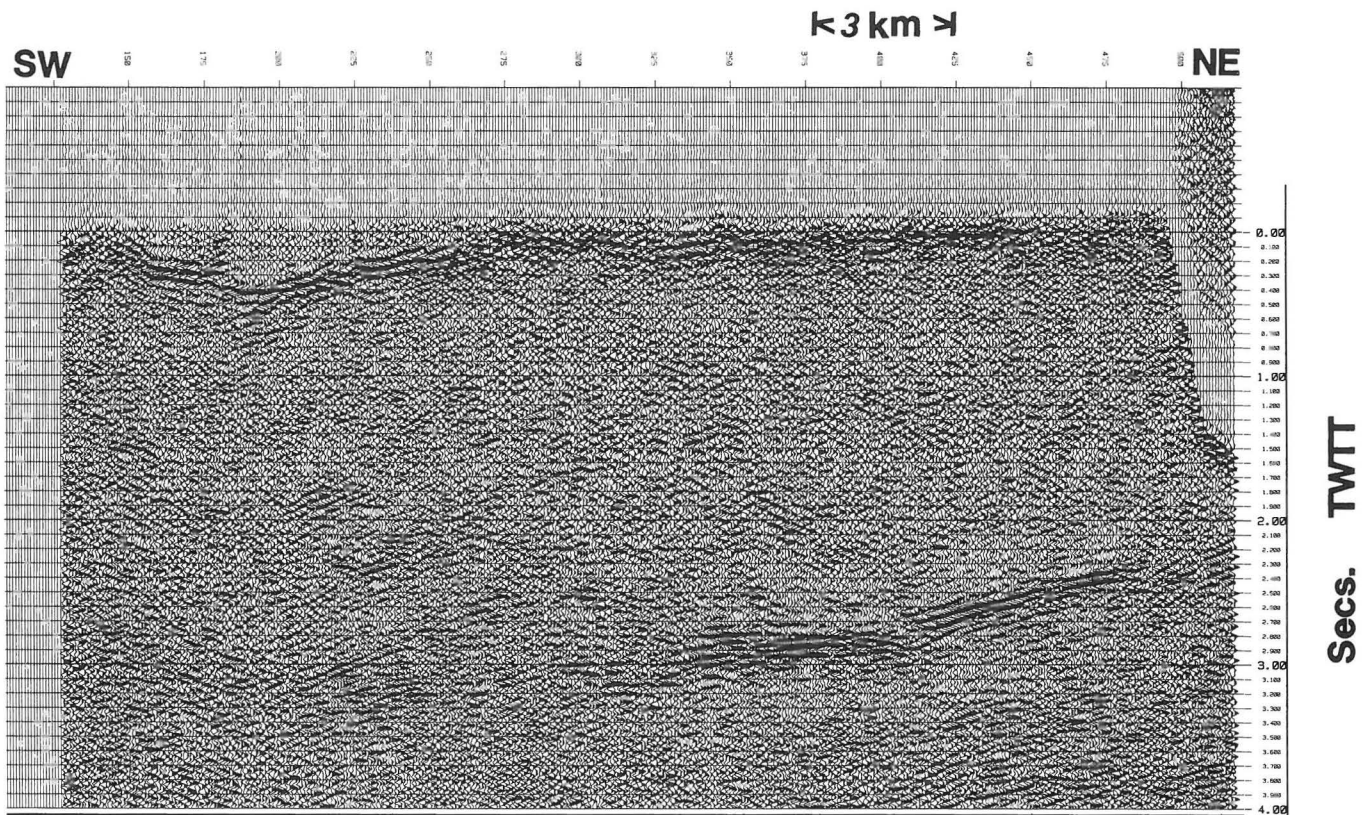


Figure 15. Reprocessed Exxon seismic line that extends southwestward from just north of the Cargo Muchacho Mountains, which are south of the Chocolate Mountains. Booming reflections are interpreted to represent the base of the Orocochia Schist. Outcrops of the schist are present just to the north in the Gavilan Hills. The Chocolate Mountains thrust can be projected to the uppermost part of the section where a subtle reflection is present. Orocochia Schist appears to have an identifiable reflective character, which is more highly reflective than the mostly Jurassic gneisses that overlie the schist. Rocks below the interpreted base of the Orocochia Schist are much more highly reflective than the schist and may represent highly deformed North America, highly deformed oceanic rocks that originally formed the base of the schist, or some unknown terrane. Tying these reflections back to known surface geology or known reflections may be the most direct way of identifying the subschist reflections. Similar reflections also appear to underlie much of the northwestern Mojave as well as areas on the west side of the San Andreas.

Mountains thrust, and the base-of-the-schist reflections are high-angle and low-angle normal faults that record major Tertiary extension in the region. Numerous half grabens are visible on the Exxon seismic lines and are filled with Tertiary sedimentary and volcanic rocks. These sedimentary and volcanic rocks are well exposed around the margins of the basin in the Midway, Palo Verde, and Chocolate Mountains. Tilting of the upper plate to the southwest in the Chocolate Mountains and to the northeast in the Trigo and part of the Palo Verde Mountains defines a large-scale anticline as a product of motion above a middle-crustal detachment fault. This anticline is difficult to see in the field because of the low relief and homogeneous color of the rocks. On thematic mapping satellite images, however, the anticline is spectacularly displayed, powerfully demonstrating the value of the technique for regional tectonic analysis (Blom and others, 1987).

The half-graben basins appear to have formed as an upper-crustal, brittle response to more ductile motion of the middle and lower crust (Morris and others, 1986a; Morris, 1987). Below about 5.0 secs. (TWTT), the short, discontinuous reflections similar to those imaged on the CALCRUST Whipple profile pervade the seismic lines. If this mylonitic fabric, as these reflections are interpreted to represent, is continuous from its surface exposure in the Whipple Mountains to this area of southeasternmost California,

then the Tertiary reworking of the middle and lower crust would have affected nearly the whole area of the Colorado Plateau to Salton Trough transect. If these reflections are also continuous with those in the northwestern Mojave that have been interpreted as representing the same mylonitic fabric (Sponberg and Henyey, 1987), then most of southern California may be underlain by this ductile fabric.

Stop 3: Salton Trough, San Andreas Fault System, Chocolate Mountains Antiform and Thrust System, and Mesquite Mine Overlook

After leaving the Milpitas Wash area, continue south along Highway SH 78 past the Ogilby Road turn-off to the entrance of the Mesquite gold mine. Stop at the gate for an escort, then continue to the overlook stop at the top of the large rounded hill west of the mine (Brownie Mountain). From this vantage point, the antiformal structure of the Chocolate Mountains with the Orocochia Schist at its core is evident on the eastern skyline. Structurally above the schist and forming most of the low, calico-colored hills on the western edge of the range, is a complex mixture of mostly Jurassic gneisses, with lesser amounts of Triassic and Cretaceous plutonic and metamorphic rocks. These rocks may represent a terrane accreted (Figure 16) to North America (Vedder and others, 1983), or simply a complexly formed and de-

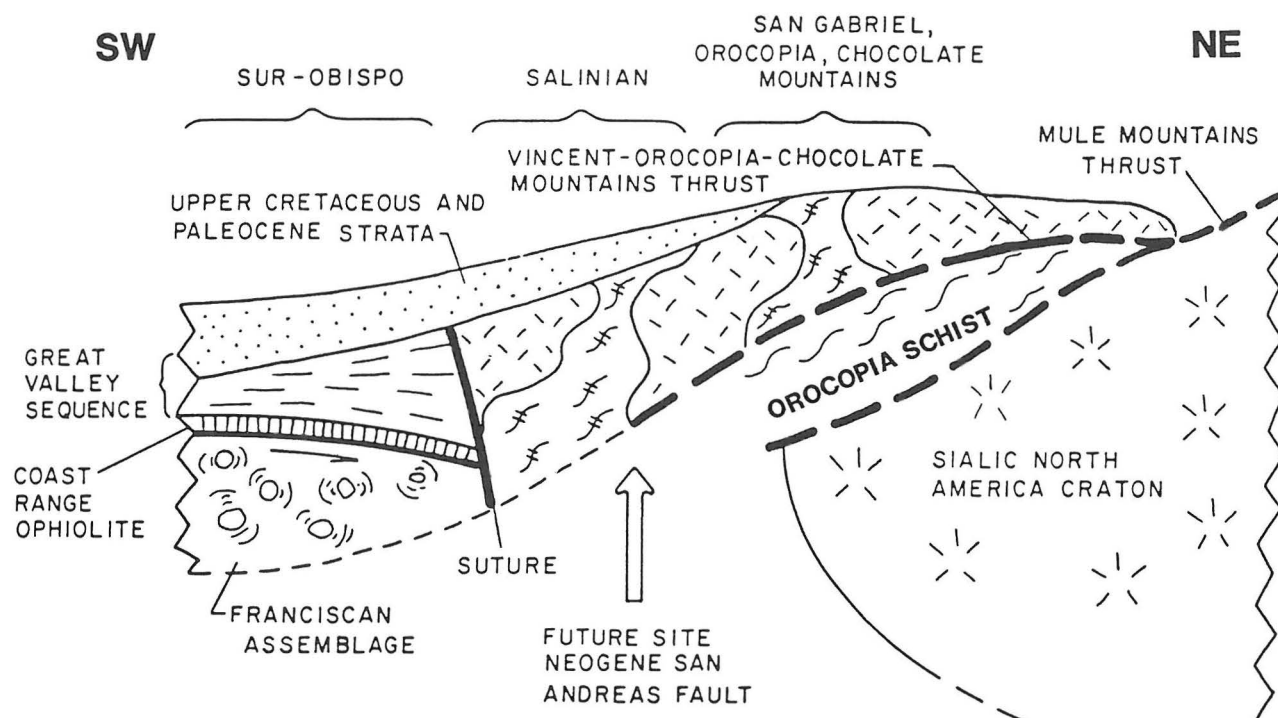


Figure 16. Diagrammatic cross section from Vedder and others (1983) showing the possible early Eocene crustal structure of the Santa Lucia - Orocofia allochthon and its terrane elements. According to this model, the Orocofia Schist is sandwiched between autochthonous North America and the mostly crystalline rocks that sit structurally above the schist. Continuation of the base of the Orocofia Schist to the southwest would supposedly put it on oceanic rocks. The reflections interpreted as the base of the schist could represent the contact of the schist with underlying North American rocks, underlying oceanic crust, or something else. Tracing these reflections to the northeast is one of the goals of the 1987-1988 CALCRUST program.

formed portion of North America. Ongoing work by Gordon Haxel and Dick Tosdal of the USGS (e.g., Haxel and others, 1985; Haxel and Tosdal, 1986) has shed much light on the overall geologic history of the region. Detailed studies of the world-class mineralization at Mesquite, which appears to be Tertiary in age and localized in a complex extensional fault system, are in progress by Scott Manske as a Stanford Ph.D. thesis (Manske and others, 1987). Detailed U/Pb and Ar/Ar studies of the mine area and related rocks by Donna Frost are in progress as part of a UCSB dissertation (Frost, 1987). The regional implications of the preliminary results of both these studies will be discussed here. The USGS refraction studies (Figure 17) in the Salton Trough area (Fuis and others, 1982) and their implications for the crustal structure of the Salton Trough and San Andreas fault system will also be discussed here.

The seismic reflection character that typifies the region of the transect thus far changes radically to the west of the Mesquite mine overlook. The prominent middle- and lower-crustal reflections disappear, as does an identifiable Moho. Extended correlation of Exxon and Chevron seismic lines by Lupe Severson (Severson, 1987; Severson and McEvilly, 1987) indicates that almost no reflections occur below the Pliocene-basement contact where basement can be identified from drilling records or projected from surface exposures (Figure 18). Near Glamis the Pliocene-basement contact is at a depth of as much as 13,500 feet on the basis of Shell line 82-147 787, which is described by Smith and others (1984). Numerous half-graben basins appear to underlie the Algodones dunes and may represent the western margin of North America. Alternatively, these normal faults could represent the collapse of the edge of North America, with the actual

margin being further west in the Salton Trough proper. Elsewhere, especially in the eastern Salton Trough, the lowest reflections that are imaged may still be Pliocene-Pliocene contacts. Where regions of high heat flow occur, as in the known geothermal resource areas, even these Pliocene reflections are destroyed. The cumulative effect of high heat flow, young crust, and abundant fluids combine to make the seismic reflection technique of limited value for discerning the details of crustal structure.

Away from the known geothermal areas, flower structures and rhombochasmlike extensional basins delineate many of the major strike-slip faults, which correlate well with the known surface geology (Severson, 1987). Detachment faults have been interpreted to be present between the Pliocene basin fill and the underlying basement (Figure 19) in portions of the western Salton Trough (Severson, 1987) because of the angular relationship of the Pliocene to the underlying crystalline rocks and correlation to exposed detachment faults in the southern Santa Rosa Mountains (Wallace and English, 1982) and Yaqui Ridge area (Schultheiss, 1984).

Across the transect area, the seismic reflection profiles seem to image numerous terranes marked by distinct seismic reflection characteristics. Having crossed from the Colorado Plateau through the Transition Zone with its "railroad track" reflections, most of the transect area is actually composed of rocks affected by Tertiary extensional deformation. The unmylonitized rocks appear to produce a characteristic "transparent" reflectivity, perhaps largely because of their complex structure and composition. Structurally below these rocks are the Tertiary mylonitic rocks with their typically short, discontinuous reflections. Mesozoic deformational and compositional boundaries

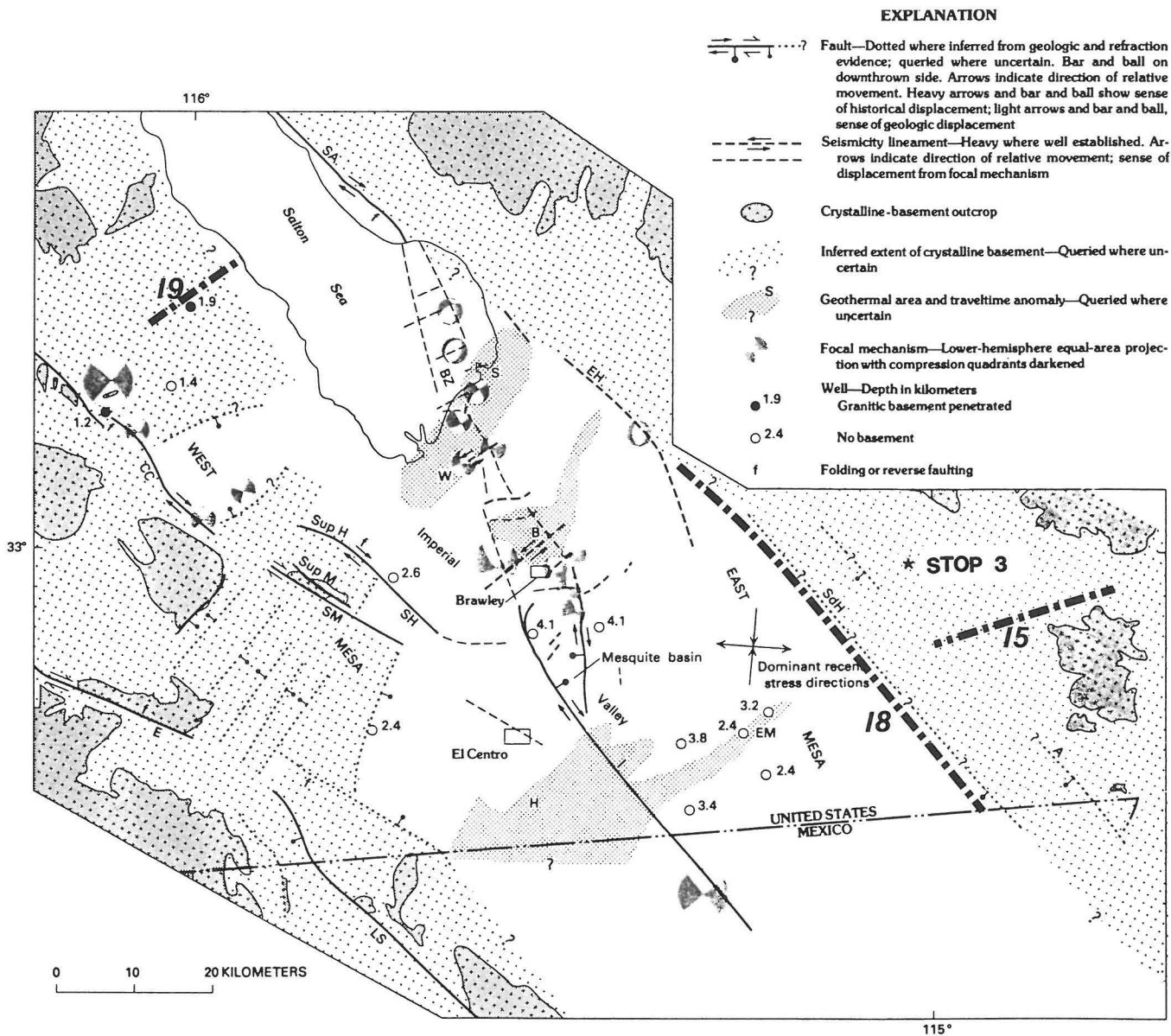


Figure 17. Regional structural map of the Imperial Valley region showing the last field trip stop and the location of the seismic lines of Figures 15, 18, and 19. How far North America continues into the southern Salton Trough is not well known, although the active transform margin is near Brawley and El Centro rather than along the eastern margin of the trough where the trace of the San Andreas is typically drawn. In the area of the Sand Hills Fault (SdH), Exxon and Shell seismic lines image multiple half-graben-appearing basins, suggesting that the upper crust in the southeastern Salton Trough is collapsing into the central trough. The amount of strike-slip offset on these faults, however, is nearly impossible to evaluate.

appear to have their own, more coherent reflections and reflection packages than the Tertiary fabric. Overprinted on these fabrics is the San Andreas-Salton Trough transform deformation, which seems to eventually destroy all previous fabrics. The geologic history recorded in the rocks across the transect region seems to be imaged also on the seismic lines that cross different portions of the Colorado Plateau to the Salton Trough region. Completion of the transect by a combination of CALCRUST, COCORP, PACE, and industry reflection and refraction surveys should make this one of the most instructive crustal transects yet done across an orogenic zone. (Return to Phoenix for the GSA meeting.)

ACKNOWLEDGMENTS

We would like to thank George Davis and Evelyn VandenDolder for their patience and assistance. Without their help, this field guide would never have been assembled. We would also like to thank the Geophysics Division of GSA and its president, Mary Lou Zoback, for sponsoring this field trip. We are indebted to Scott Fenby for drafting many of the figures. We would like to thank the many, many geoscientists who have helped in the data acquisition, processing, and interpretation of the seismic lines that form the basis of this trip. Perhaps most importantly, we would like to express our sincere appreciation to

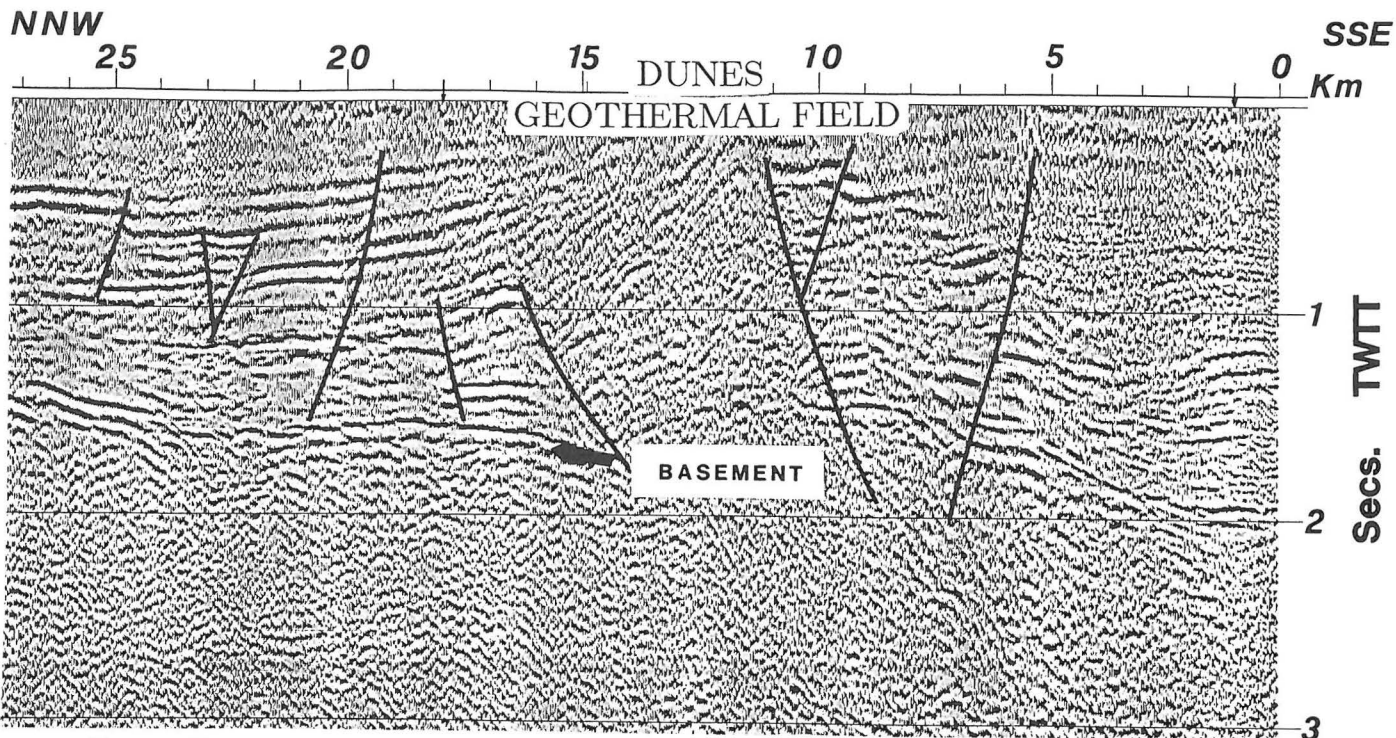


Figure 18. Reprocessed industry (Exxon) seismic line along the All-American Canal in southeastern California showing reflections within the Pliocene basin fill and a major reflection at the Pliocene-basement contact. The Dunes geothermal field is delineated by a "fading" of the reflections and higher velocities. Even though numerous record sections were recorrelated and processed to yield 12.0 sec. (TWTT) profiles, almost no reflections are present beneath the Pliocene - basement contact. From: Severson (1987).

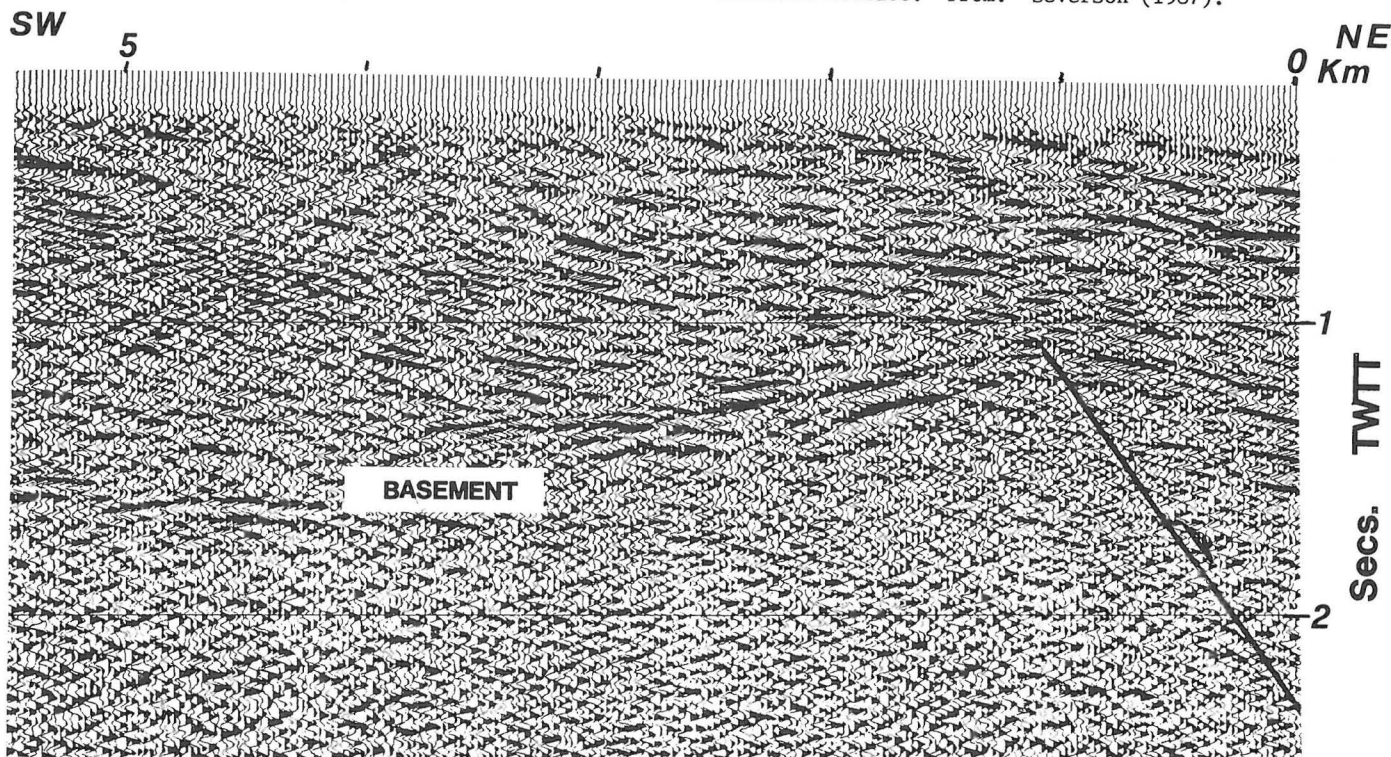


Figure 19. Reprocessed industry (Chevron) seismic line south of the Santa Rosa Mountains in the western Salton Trough showing a truncation of the reflections produced by the tilted and folded sedimentary section against the underlying basement rocks. Where exposed, this contact is a detachment fault, although its present-day activity is thought to be related to motion of the crystalline rocks beneath the sediments during composite motion on the San Andreas system. Major escarpment into the deep portion of the Salton Trough offsets the Pliocene-basement contact an unknown amount. Extended correlation of this profile did not show deeper reflections. From: Severson (1987).

Phillips, Exxon, Chevron, Texaco, Amoco, Arco, CGG, and Buckhorn for providing the resources and original seismic tapes that have opened up the third dimension to this region. Their generosity in providing these data to the academic world has enormously increased our understanding of this complex orogenic zone. We also deeply appreciate the support of the National Science Foundation, the primary funding agency for both COCORP and CALCRUST.

REFERENCES

- Anderson, C. A., Scholz, E. A., and Strobell, J. D., Jr., 1955, Geology and ore deposits of the Bagdad area, Yavapai County, Arizona: U. S. Geological Survey Professional Paper 278, 103 p.
- Anderson, J. L., Davis, G. A., and Frost, E. G., 1979, Field guide to regional Miocene detachment faulting and early Tertiary(?) mylonitic terranes in the Colorado River trough, southeastern California and western Arizona, *in* Abbott, P. L., ed., Geological excursions in the southern California area: Department of Geological Sciences, San Diego State University, Geological Society of America Field-Trip Guidebook, p. 109-133.
- Banks, N. G., 1980, Geology of a zone of metamorphic core complexes in southeastern Arizona, *in* Crittenden, M. D., Jr., and others, eds., Tectonic significance of metamorphic core complexes of the North American Cordillera: Geological Society of America Memoir 153, p. 177-215.
- Blom, R. G., Morris, R. S., Okaya, D. A., and Frost, E. G., 1987, An anticline in the Palo Verde Mountains revealed on Landsat thematic mapper images and CALCRUST seismic reflection data: Geological Society of America Abstracts with Programs, v. 19 (in press).
- Carter, J. N., Luyendyk, B. P., and Terres, R. R., 1987, Neogene clockwise tectonic rotation of the eastern Transverse Ranges, California, suggested by paleomagnetic vectors: Geological Society of America Bulletin, v. 98, p. 199-206.
- Cheadle, M. J., Csuchra, B. L., Byrne, T., Ando, C. J., Oliver, J. E., Brown, L. D., Kaufman, S., Malin, P. E., and Phinney, R. A., 1986, The deep crustal structure of the Mojave Desert, California, from COCORP seismic reflection data: Tectonics, v. 5, p. 293-320.
- Conway, C. M., and Karlstrom, K. E., 1986, Early Proterozoic geology of Arizona: EOS (American Geophysical Union Transactions), v. 67, p. 681-682.
- Crowell, J. C., 1981, An outline of the tectonic history of southeastern California, *in* Ernst, W. G., ed., The geotectonic development of California: Englewood Cliffs, N.J., Prentice-Hall, Inc., p. 583-600.
- Davis, G. A., 1986, Upward transport of mid-crustal mylonitic gneisses in the footwall of a Miocene detachment fault, Whipple Mountains, southeastern California: Geological Society of America Abstracts with Programs, v. 18, p. 98.
- Davis, G. A., Anderson, J. L., Frost, E. G., and Shackelford, T. J., 1980, Mylonitization and detachment faulting in the Whipple-Buckskin-Rawhide Mountains terrane, southeastern California and western Arizona, *in* Crittenden, M. D., Jr., and others, eds., Tectonic significance of metamorphic core complexes of the North American Cordillera: Geological Society of America Memoir 153, p. 79-129.
- Dokka, R. K., 1986, Patterns and modes of early Miocene crustal extension, central Mojave Desert, California: Geological Society of America Special Paper 208, p. 75-95.
- Dokka, R. K., and Woodburne, M. O., 1986, Mid-Tertiary extensional tectonics and sedimentation, central Mojave Desert, California: Louisiana State University Publications in Geology and Geophysics, v. 1, p. 11-55.
- Flueh, E. R., and Okaya, D. A., 1987, Geometry and nature of reflections beneath the mylonitic front in the Whipple Mountains, SE California: Geological Society of America Abstracts with Programs, v. 19, p. 337-338.
- Frost, D. M., 1987, Pb and Ar isotopic studies on gold mineralization in the Mesquite mine and adjoining regions, southeastern California: a progress report: Society of Economic Geologists Abstracts with Programs (in press).
- Frost, E. G., and Okaya, D. A., 1986, Crustal geometries of detachment faulting in the Colorado River extensional terrane as displayed on reprocessed industry seismic reflection data: Geological Society of America Abstracts with Programs, v. 18, p. 356.
- Fuis, G. S., Mooney, W. D., Healey, J. H., McMechan, G. A., and Lutter, W. J., 1982, Crustal structure of the Imperial Valley region: U. S. Geological Survey Professional Paper 1254, p. 25-49.
- Galvan, G. S., 1986, Seismic reflection evaluation of detachment-related crustal extension in the Transition Zone, Yavapai County, Arizona (M.S. thesis): San Diego, San Diego State University, 76 p.
- _____ 1987a, Geometric description and interpretation of seismic profiles in west-central Arizona: Geological Society of America Abstracts with Programs, v. 19, p. 380.
- _____ 1987b, A seismic interpretation of the crustal structure beneath the Transition Zone, west-central Arizona: Geology (in press).
- Galvan, G. S., and Frost, E. G., 1985, Seismic reflection evaluation of detachment-related deformation in the Transition Zone, west-central Arizona: EOS (American Geophysical Union Transactions), v. 66, p. 978.
- Glazner, A. F., Dent, S. B., and Bartley, J. M., 1987, Miocene detachment fault in the Waterman Hills, central Mojave Desert, California: Geological Society of America Abstracts with Programs, v. 19, p. 381-382.
- Gross, W. W., and Hillemeier, F. L., 1982, Geometric analysis of upper-plate fault patterns in the Whipple-Buckskin detachment terrane, *in* Frost, E. G., and Martin, D. L., eds., Mesozoic-Cenozoic tectonic evolution of the Colorado River region, California, Arizona, and Nevada: San Diego, Cordilleran Publishers, p. 256-266.
- Hamilton, W., 1982, Structural evolution of the Big Maria Mountains, northeastern Riverside County, California, *in* Frost, E. G., and Martin, D. L., eds., Mesozoic-Cenozoic tectonic evolution of the Colorado River region, California, Arizona, and Nevada: San Diego, Cordilleran Publishers, p. 1-28.
- Hauser, E. C., Barnes, A., Gephart, J., Latham, T., Lundy, J., Brown, L., and Oliver, J., 1986, COCORP deep reflection transect in Arizona; across the Transition Zone from Colorado Plateau to core complexes: EOS (American Geophysical Union Transactions), v. 67, p. 1096.
- Hauser, E. C., Gephart, J., Latham, T., Oliver, J., Kaufman, S., Brown, L., and Lucchitta, I., 1987, COCORP deep seismic reflection traverse of central Arizona from the Colorado Plateau to the core complexes: strong crustal reflectors and evidence for Moho offset: Geology (in press).

- Haxel, G. B., and Tosdal, R. M., 1986, Significance of the Orocochia Schist and Chocolate Mountains thrust in the late Mesozoic tectonic evolution of the southeastern California-southwestern Arizona region-extended abstract, *in* Beatty, B., and Wilkinson, P. A. K., eds., *Frontiers in geology and ore deposits of Arizona and the Southwest: Arizona Geological Society Digest*, v. 16, p. 52-61.
- Haxel, G. B., Tosdal, R. M., and Dillon, J. T., 1985, Tectonic setting and lithology of the Winterhaven Formation, a new Mesozoic stratigraphic unit in southeasternmost California and southwestern Arizona: *U. S. Geological Survey Bulletin* 1599, 19 p.
- Heidrick, T. L., and Wilkins, J., Jr., 1980, Mylonitization, detachment faulting, and associated mineralization, Whipple Mountains, California, and Buckskin Mountains, Arizona: *Arizona Geological Society, Guidebook*, p. 31-55.
- Hoisch, T. D., 1987, Heat transport by fluids during Late Cretaceous regional metamorphism in the Big Maria Mountains, southeastern California: *Geological Society of America Bulletin*, v. 98, p. 549-553.
- Howard, K. A., and John, B. E., 1987, Crustal extension along a rooted system of imbricate low-angle faults: Colorado River extensional corridor, California and Arizona, *in* Coward, M. D., and others, eds., *Continental extensional tectonics: Geological Society of London Special Publication*, p. 299-311.
- Hurich, C. A., Smithson, S. B., Fountain, D. M., and Humphreys, M. C., 1985, Seismic evidence of mylonite reflectivity and deep structure in the Kettle Dome metamorphic core complex, Washington: *Geology*, v. 13, p. 577-580.
- Keith, S. B., 1980, The great southwestern Arizona oil and gas play; drilling commences: *Arizona Bureau of Geology and Mineral Technology Fieldnotes*, v. 10, no. 1, p. 1-3, 6-8.
- Lehman, N. E., Spencer, J. E., and Welty, J. W., 1987, Middle Tertiary mineralization related to metamorphic core complexes and detachment faults in Arizona and California: *Society of Mining Engineers Preprint* 87-21, 9 p.
- Lindberg, P. A., 1986, A brief geologic history and field guide to the Jerome district, Arizona, *in* Nations, J. D., and others, eds., *Geology of central and northern Arizona: Geological Society of America Rocky Mountain Section Meeting, Guidebook*, p. 127-139.
- Luyendyk, B. P., Kamerling, M. J., and Terres, R. R., 1980, Geometric model for Neogene crustal rotations in southern California: *Geological Society of America Bulletin*, v. 91, p. 211-217.
- Luyendyk, B. P., Kamerling, M. J., Terres, R. R., and Hornafius, J. S., 1985, Simple shear of southern California during Neogene time suggested by paleomagnetic declinations: *Journal of Geophysical Research*, v. 90, p. 12,454-12,466.
- McCarthy, J., Fuis, G. S., and Howard, K., 1986, A seismic-refraction survey of the Whipple Mountains metamorphic core complex, southeastern California; a progress report from PACE: *Geological Society of America Abstracts with Programs*, v. 18, p. 356.
- Manske, S. L., Matlack, W. F., Springett, M. W., Strakele, A. E., Jr., Watowich, S. N., Yeomans, B., and Yeomans, E., 1987, *Geology of the Mesquite deposit, Imperial County, California: Society of Mining Engineers Preprint* 87-107, 9 p.
- May, D., Malin, P. E., Henyey, T. L., and Applegate, J., 1982, Seismic reflection profile across the Vincent thrust and Pelona Schist, Sierra Pelona, California: *EOS (American Geophysical Union Transactions)*, v. 63, p. 1033.
- Morris, R. S., 1987, Tertiary basin formation above middle-crustal shear zones in southern Chocolate Mountains, SE California: *Geological Society of America Abstracts with Programs*, v. 19, p. 434.
- Morris, R. S., Frost, E. G., and Okaya, D. A., 1986a, Preliminary seismic reflection interpretation of the overprint of Tertiary detachment faulting on the Orocochia Schist-Chocolate Mountains thrust system, Milpitas Wash area of southeastern California, *in* Cenozoic stratigraphy, structure, and mineralization in the Mojave Desert: *Geological Society of America Cordilleran Section Meeting, Guidebook and Volume for Field Trips 5 and 6*, p. 122-126.
- Morris, R. S., and Okaya, D. A., 1986, Crustal geometry of detachment faulting - structural analysis of seismic reflection data in SE California: *Geological Society of America Abstracts with Programs*, v. 18, p. 160.
- Morris, R. S., Okaya, D. A., Frost, E. G., and Malin, P. E., 1986b, Base of the Orocochia Schist as imaged on seismic reflection data in the Chocolate and Cargo Muchacho Mountains region of southeasternmost California and the Sierra Pelona: *Geological Society of America Abstracts with Programs*, v. 18, p. 160.
- Okaya, D. A., and Frost, E. G., 1986a, Seismic reflection imaging of detachment faults and mylonites in the Whipple detachment terrane, SE California: *Geological Society of America Abstracts with Programs*, v. 18, p. 400.
- 1986b, Regional tectonic implications of the CALCRUST seismic profiling southwest of the Whipple Mountains, SE California: *EOS (American Geophysical Union Transactions)*, v. 67, p. 1109.
- Rehrig, W. A., and Reynolds, S. J., 1980, Geologic and geochronologic reconnaissance of a northwest-trending zone of metamorphic core complexes in southern and western Arizona, *in* Crittenden, M. D., Jr., and others, eds., *Tectonic significance of metamorphic core complexes of the North American Cordillera: Geological Society of America Memoir* 153, p. 131-157.
- Rehrig, W. A., Shafiqullah, M., and Damon, P. E., 1980, Geochronology, geology, and listric normal faulting of the Vulture Mountains, Maricopa County, Arizona, *in* Jenney, J. P., and Stone, C., eds., *Studies in western Arizona: Arizona Geological Society Digest*, v. 12, p. 89-110.
- Reif, D. M., and Robinson, J. P., 1981, Geophysical, geochemical, and petrographic data and regional correlation from the Arizona State A-1 well, Pinal County, Arizona: *Arizona Geological Society Digest*, v. 13, p. 99-109.
- Reynolds, S. J., and Rehrig, W. A., 1980, Mid-Tertiary plutonism and mylonitization, South Mountains, central Arizona, *in* Crittenden, M. D., Jr., and others, eds., *Tectonic significance of metamorphic core complexes of the North American Cordillera: Geological Society of America Memoir* 153, p. 159-175.
- Reynolds, S. J., and Spencer, J. E., 1985, Evidence for large-scale transport on the Bullard detachment fault, west-central Arizona: *Geology*, v. 13, p. 353-356.
- Reynolds, S. J., Spencer, J. E., Richard, S. M., and Laubach, S. E., 1986, Mesozoic structures in west-central Arizona, *in* Beatty, B., and Wilkinson, P. A. K., eds., *Frontiers in geology and ore deposits of Arizona and the Southwest: Arizona Geological Society Digest*, v. 16, p. 35-51.

- Robison, B. A., 1980, Description and analysis of Mesozoic "red beds," western Arizona and southeastern California, *in* Jenney, J. P., and Stone, C., eds., *Studies in western Arizona: Arizona Geological Society Digest*, v. 12, p. 147-154.
- Ruppert, C., Wang, C. Y., and Davis, G. A., 1986, Velocity structure and anisotropy of the Whipple Mountains shear zone in southern California: *EOS (American Geophysical Union Transactions)*, v. 67, p. 1109.
- Sanborn, A. F., Frost, E. G., and Okaya, D. A., 1986, Structure of the Chuckwalla Valley region of SE California from seismic reflection and gravity data; overprint of Tertiary detachment tectonics on Mesozoic structure: *Geological Society of America Abstracts with Programs*, v. 18, p. 180.
- Schultejann, P. A., 1984, The Yaqui Ridge antiform and detachment fault; mid-Cenozoic extensional terrane west of the San Andreas fault: *Tectonics*, v. 3, p. 677-691.
- Severson, L. K., 1987, Interpretation of the shallow-crustal structure of the Imperial Valley, California, from seismic reflection profiles (M.S. thesis): Berkeley, University of California, 68 p.
- Severson, L. K., and McEvilly, T. V., 1987, Analysis of seismic reflection data from the Imperial Valley California: *Geological Society of America Abstracts with Programs*, v. 19, p. 449.
- Shackelford, T. J., 1976, Structural geology of the Rawhide Mountains, Mohave County, Arizona (Ph.D. thesis): Los Angeles, University of Southern California, 175 p.
- _____, 1980, Tertiary tectonic denudation of a Mesozoic-early Tertiary(?) gneiss complex, Rawhide Mountains, western Arizona: *Geology*, v. 8, p. 190-194.
- Smith, R. S. U., Yeend, W., Dohrenwend, J. C., and Gese, D. D., 1984, Mineral resources of the north Algodones Dunes wilderness study area (CDCA-360), Imperial County, California: U. S. Geological Survey Open-File Report 84-630, 11 p.
- Spencer, J. E., and Welty, J. W., 1986, Possible controls of base- and precious-metal mineralization associated with Tertiary detachment faults in the lower Colorado River trough, Arizona and California: *Geology*, v. 14, p. 195-198.
- Spongberg, M. E., and Henyey, T. L., 1987, Crustal reflection profiling in the western Mojave Desert, California: *Geological Society of America Abstracts with Programs*, v. 19, p. 454.
- Tosdal, R. M., 1982, The Mule Mountains thrust in the Mule Mountains, California and its probable extension in the southern Dome Rock Mountains: a preliminary report, *in* Frost, E. G., and Martin, D. L., eds., *Mesozoic-Cenozoic tectonic evolution of the Colorado River region, California, Arizona, and Nevada: San Diego, Cordilleran Publishers*, p. 55-60.
- _____, 1986, Mesozoic ductile deformations in the southern Dome Rock Mountains, northern Trigo Mountains, Trigo Peak and Livingston Hills, southwestern Arizona, and Mule Mountains, southeastern California, *in* Beatty, B., and Wilkinson, P. A. K., eds., *Frontiers in geology and ore deposits of Arizona and the Southwest: Arizona Geological Society Digest*, v. 16, p. 62-71.
- Vedder, J. G., Howell, D. G., and McLean, H., 1983, Stratigraphy, sedimentation, and tectonic accretion of exotic terranes, southern Coast Ranges, California, *in* Watkins, J. S., and Drake, C. L., eds., *Studies in continental margin geology: American Association of Petroleum Geologists Memoir 34*, p. 471-498.
- Wallace, R. D., and English, D. J., 1982, Evaluation of possible detachment faulting west of the San Andreas, southern Santa Rosa Mountains, California, *in* Frost, E. G., and Martin, D. L., eds., *Mesozoic-Cenozoic tectonic evolution of the Colorado River region, California, Arizona, and Nevada: San Diego, Cordilleran Publishers*, p. 502-510.
- Wernicke, B., 1985, Uniform-sense normal simple shear of the continental lithosphere: *Canadian Journal of Earth Science*, v. 22, p. 108-125.
- Wilkins, J., Jr., and Heidrick, T. L., 1982, Base and precious metal mineralization related to low-angle tectonic features in the Whipple Mountains, California and Buckskin Mountains, Arizona, *in* Frost, E. G., and Martin, D. L., eds., *Mesozoic-Cenozoic tectonic evolution of the Colorado River region, California, Arizona, and Nevada: San Diego, Cordilleran Publishers*, p. 182-204.